Stratigraphy and sedimentology of Pliocene limestones, Wairoa district, northern Hawke's Bay

A thesis submitted in partial fulfilment

of the requirements for the degree

of

Master of Science

in Earth Sciences

at

The University of Waikato

by

Jared Jiang

The University of Waikato
2011

Abstract

This project documents the sedimentary geology of a shallow-marine, limestone-bearing Pliocene succession (Mangaheia Group; up to 1.5 km thick) within the Wairoa Syncline, northern Hawke's Bay. The primary focus is three cool-water "Te Aute type" limestone units in the succession – the early Opoitian age Opoiti Limestone (5-10 m thick), the late Opoitian age Whakapunake Limestone (30-100 m thick) and the Waipipian age Tahaenui Limestone (10-30 m thick) – that form locally spectacular outcrops in the Wairoa district. Lithostratigraphically, the limestones are given formational status while the encasing siliciclastic sandstones and mudstones are lumped into a newly defined Wairoa Formation which can be informally classified as A, B, C or D depending on position with respect to the three limestone formations. Three field lithofacies groups – limestone (L), sandstone (S) and mudstone (M) – are erected, and variability within these groups is recognised by subdivision into three lithofacies types, L1-3, S1-3 and M1-3. The massive Opoiti Limestone (35-65% $CaCO_3$; L3 and S2) comprises poorly sorted, variably sandy, barnacle, epifaunal bivalve and locally brachiopod debris well-cemented by low-Mg calcite (LMC) (micro)sparite and micrite. Opoiti Limestone is a bioclastic quartzofeldspathic arenite to biosparrudite, occasionally dolomite-bearing. Occasional calcite infilled biomoulds are testament to former aragonite molluscan skeletons. Opoiti Limestone unconformably overlies Wairoa Formation A (2-200 m thick), and grades up into differentially cemented mudstone of Wairoa Formation B (700-800 m thick) which is unconformably overlain by Whakapunake Limestone. The late Opoitian Whakapunake Limestone (up to 85% $CaCO_3$; L1, L2 and S1) comprises (cross) bedded and differentially cemented interbeds of fossiliferous and more siliciclastic-rich facies. The limestones are typically poorly sorted bivalve-barnacle biomicrite to biosparrudite cemented by variable amounts of fringe and later equant LMC (micro)spar, sometimes including abundant zoned stoichiometric dolomite rhombohedra. Fabrics are moderately open to tight with some conspicuous limonitised glauconite. Whakapunake Limestone passes conformably up into massive calcareous mudstone of Wairoa Formation C (latest Opoitian; >10 m thick). A shallow angular unconformity separates the Whakapunake Limestone and/or

Wairoa Formation C from the overlying well-cemented flaggy Tahaenui Limestone (50-80% $CaCO_3$; L1), a bivalve-barnacle biosparite to biosparrudite with some neomorphosed former aragonite skeletons and a moderately open fabric. In this limestone early formed dull luminescent isopachous fringing cements (host specific) precede variable pore occlusion by dirty LMC (micro)spar and/or micrite.

The three limestone formations accumulated on the eastern side of a narrow forearc basin seaway (Ruataniwha Strait) within the Hikurangi subduction complex atop and about antiform upthrust ridges in an active convergent margin setting. Tectonics was the main control on the location and mainly lensoidal geometry of the limestone units, while Pliocene glacioeustatic sea-level fluctuations played a secondary role. Cross-bedded and interbedded limestone-sandstone facies attest to deposition under the influence of strong tidal flows and repeated storm events that produced high-energy hydraulic conditions and reworking of variably mixed terrigenous-skeletal sands in the shallow (<30 m) seaway during Pliocene. Redeposition down flank from antiform summits provided accommodation space for sediment build-up.

The calcite dominated cool-water skeletal make-up of these limestones, combined with their relatively shallow burial depths (150-700 m), has resulted in them retaining significant macroporosity (up to 20%). Consequently, as well as having application as a lime or hard rock resource they also have reservoir potential for hydrocarbons in the subsurface.

Acknowledgements

First and foremost, thanks to my parents for all the financial support given me during my years at university, and especially my mum whose help has been imperative.

I am most appreciative of Professor Cam Nelson for his tremendous amount of supervisory input in the course of my study, and especially for the thorough reviews, editing, and constructive criticism of thesis chapter drafts. I also express my sincere appreciation to Dr. Steve Hood for his supervisory support the last two years at Waikato, and especially for his tremendous help with my petrography and stable isotopic analyses. Additionally, Professor Peter Kamp is acknowledged for research funding support and encouragement to complete this thesis. The Broad Memorial Fund kindly provided some funds for field support.

Thank you to Jacinta Parenzee, Renat Radosinsky, Chris McKinnon and Annette Rodgers for their technical advice and support during lab work. Many thanks to Kyle Bland and Julie Lee (GNS) for providing some relevant field-related information, and to Dave Francis (Geological Research Ltd) and Bill Leask (Ian R. Brown Associates Ltd) for constructive advice and willingness to help about Wairoa district geology. Sincere thanks to Leigh Aitken from QRS Wairoa for allowing me to examine and sample some inhouse limestone cores.

Also, special thanks to the farm and landowners in the northern Wairoa district for their warm hospitality, land access and useful local knowledge. In particular, I thank Snow Brownlie for offering comfortable shearer’s quarters for accommodation during my time in the field. Thanks to Darton King for allowing me to access the Whakapunake Plateau, and to Sam Hiko for escorting me to some other wonderful limestone outcrops in the area.

Lastly, Michele Drinnan, April Gibson and Riki Lewis, thank you for being great friends and being there for me during the last couple of years. And thank you to all my friends for sharing with me a great time over these years in Hamilton – you have made my life great.

Table of contents

List of figures

List of tables

1 Chapter One

Introduction

1.1 Study area

The study area is located in the wider Wairoa district, northern Hawke's Bay (Fig. 1.1). It covers an area of approximately 300 km^2 on either side of the NNE-SSW trending, plunging asymmetrical Wairoa Syncline (Fig. 1.2). SH 36/Tiniroto Road closely follows the syncline axis, and divides the study area into eastern and western halves. The shape of the study area (outlined in pale yellow in Fig. 1.2) is defined roughly by the chronostratigraphic boundary between the Miocene and Pliocene sedimentary sequences. In this study, all grid references are given in New Zealand Map Grid (NZMG 1949), which are covered by topomap X18 and X19 of NZ260 series produced by the Department of Survey and Land Information (now Land Information New Zealand (LINZ)).

Large portions of the land area are mainly used for sheep and beef farming, with localised forestry operations. The topography comprises rolling-hill and steep-hill country with deeply entrenched river valleys, typical of the wider Hawke's Bay region. The geology has a strong influence on shaping the local landscape. The region is covered mostly by upper Tertiary sediments (Kann 1960). The country in general is rugged, the soft younger Tertiary sediments being easily eroded and deeply incised by rivers and streams. The majority of the Pliocene rocks are sandy mudstone (often tuffaceous), interbedded sandstone and mudstone (flysch), lens-like sandstone and occasional sandy to coquina limestone (Edwards 1987). These strata often form scarps and they dip stronger (up to 30º) on the eastern side of the syncline axis than on the western side.

1.1.1 Mangapoike River section

The Mangapoike River section (showing as the red star in Fig. 1 2) on the eastern limb of the Wairoa Syncline is selected as a key section in this study. It has been reported on by a number of geologists in the past (e.g. Kennett & Watkins 1974; Hornibrook 1984; Wright & Walcott 1986; Edwards 1987). The section provides a reasonably complete biostratigraphic record for the Pliocene time period back to the early Miocene, and has been informally divided into the lower and upper Mangapoike section by the poorly exposed Miocene-Pliocene boundary (X19/970086; Wright & Walcott 1986; Edwards 1987). This particular section along with the Blind River section, in Marlborough in the northern South Island, has been regarded as providing evidence for cool subtropical (warm temperate) paleotemperature oscillations during the late Miocene-early Pliocene, with perhaps one subantarctic interval during the latest Miocene time (Edwards 1987).

1.1.2 Whakapunake Plateau

The Whakapunake Trig, named after the Whakapunake Plateau, is the point of highest elevation in the area, at an altitude of almost 1000 m amsl (Fig. 1.2). The plateau is a major topographic feature in the study area. It is formed on a large, localised limestone sheet, which is gently dipping westwards at about 8°, and occupies the deeply cut Mangapoike River valley as a limestone gorge, the Haupatanga Gorge on the eastern limb of the Wairoa Syncline. The prominent limestone cliff (shown by bold red line in Fig. 1.2) on the eastern side of the plateau runs almost parallel to the syncline axis (Wairoa Syncline) for 15 km from the trig to Hereheretau Road (Fig. 1.2).

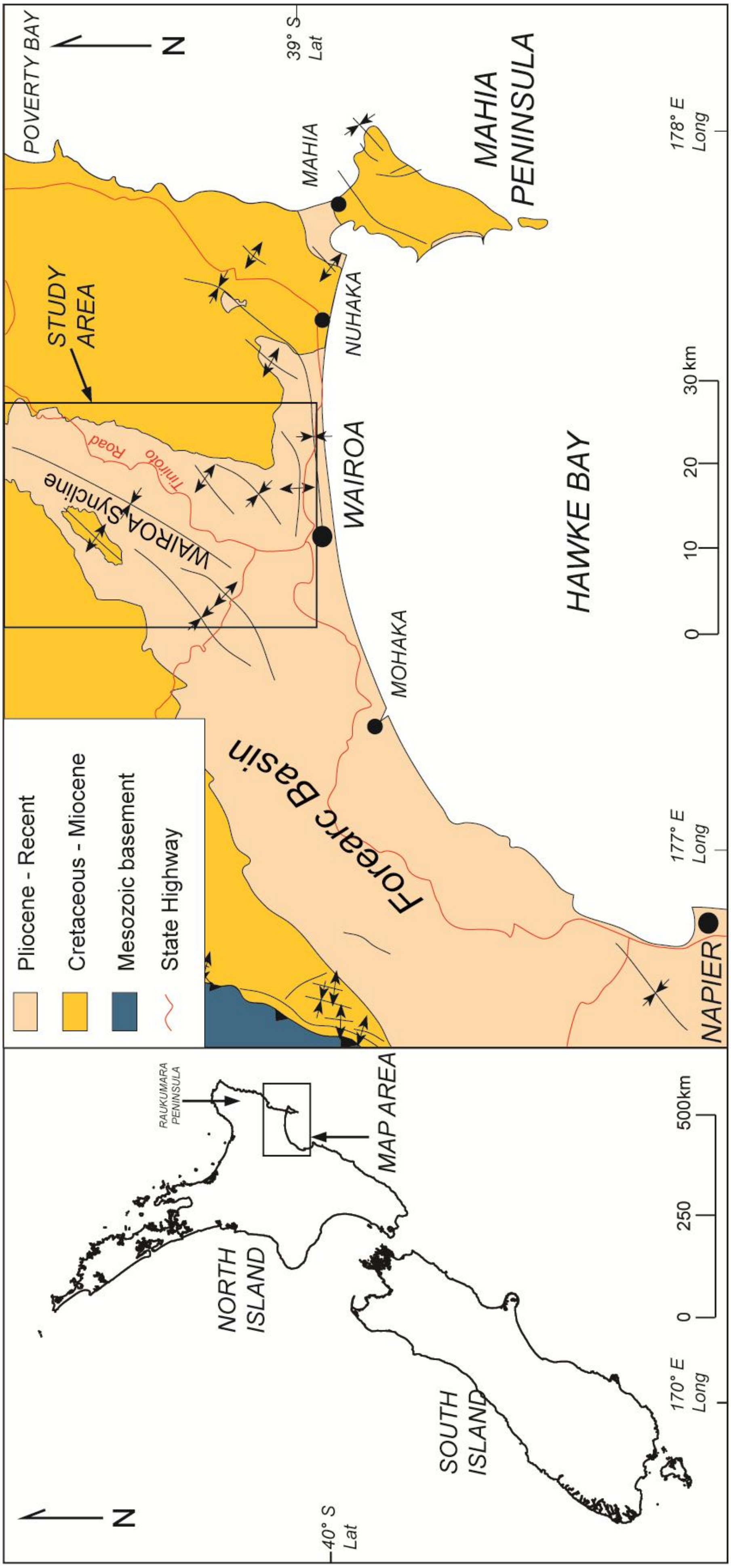

Figure 1.1: Simplified geological and some structural information for the study area. Adapted from Barnes *et al*. (2002).

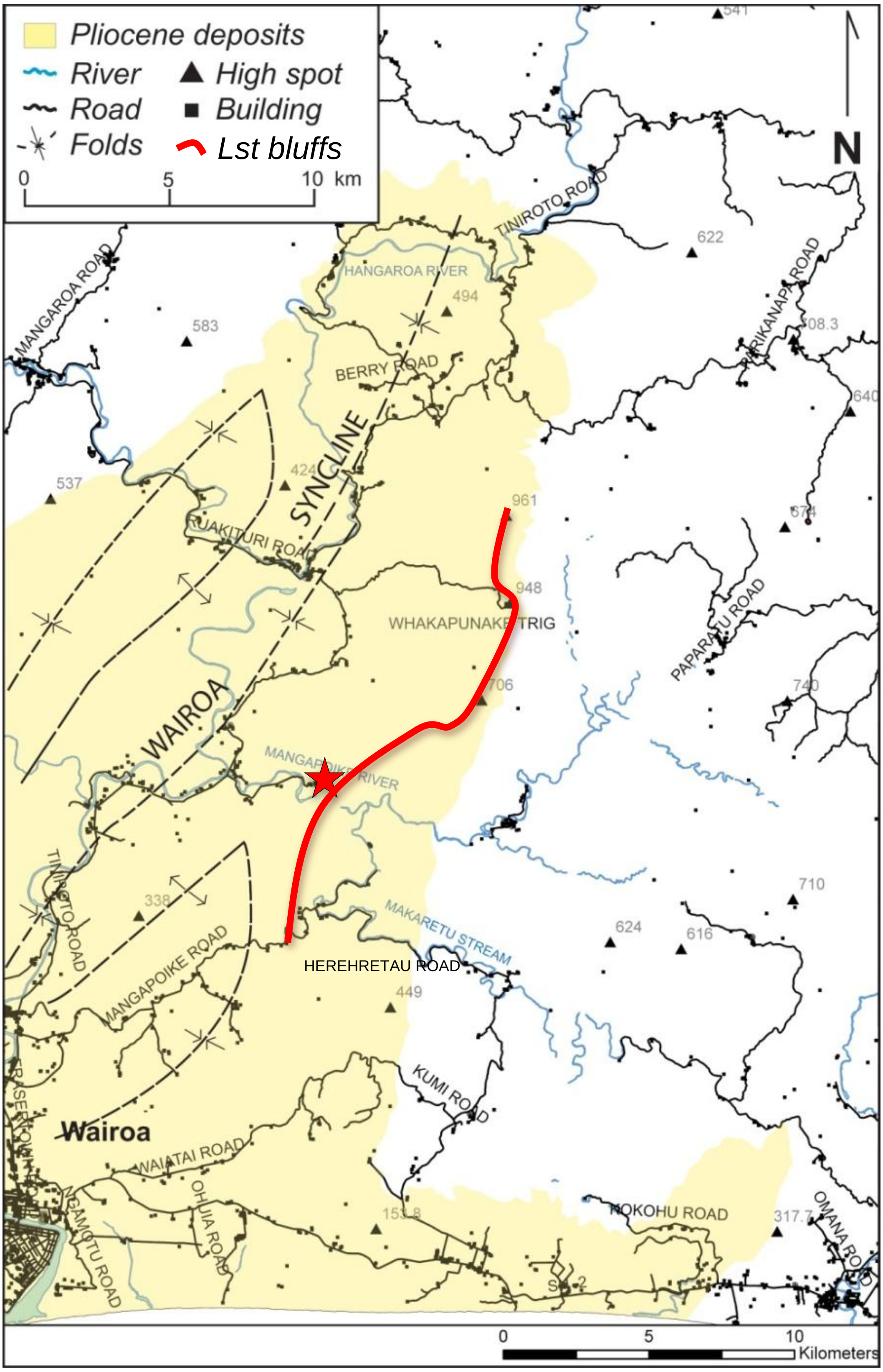

Figure 1.2: Simplified map of the field area showing the distribution of the Pliocene deposits, including the limestone bluffs on the eastern side of the Whakapunake Plateau, and the position of the Wairoa Syncline axis.

1.2 Neogene stratigraphy of study area

The Neogene (Miocene-Pliocene) sedimentary record in northern Hawke's Bay has been divided into two lithostratigraphic groups: the Tolaga Group and Mangaheia Group (Bland *et al.* 2007). The stratigraphic focus in this study is the Mangaheia Group, involving Early Pliocene (earliest Opoitian) to Late Pliocene (Waipipian) siliciclastic deposits that include three cool-water carbonate-enriched units that crop out about the Wairoa Syncline. The general stratigraphy for the Late Neogene strata in Hawke's Bay is summarised in Fig. 1.3. The stratigraphic nomenclature for the Pliocene deposits in particular in northern Hawke's Bay is poorly defined by previous studies. One of the aims of this study is to improve the current stratigraphic nomenclature for the region into a simpler one. A revised version is provided in Chapter 4.

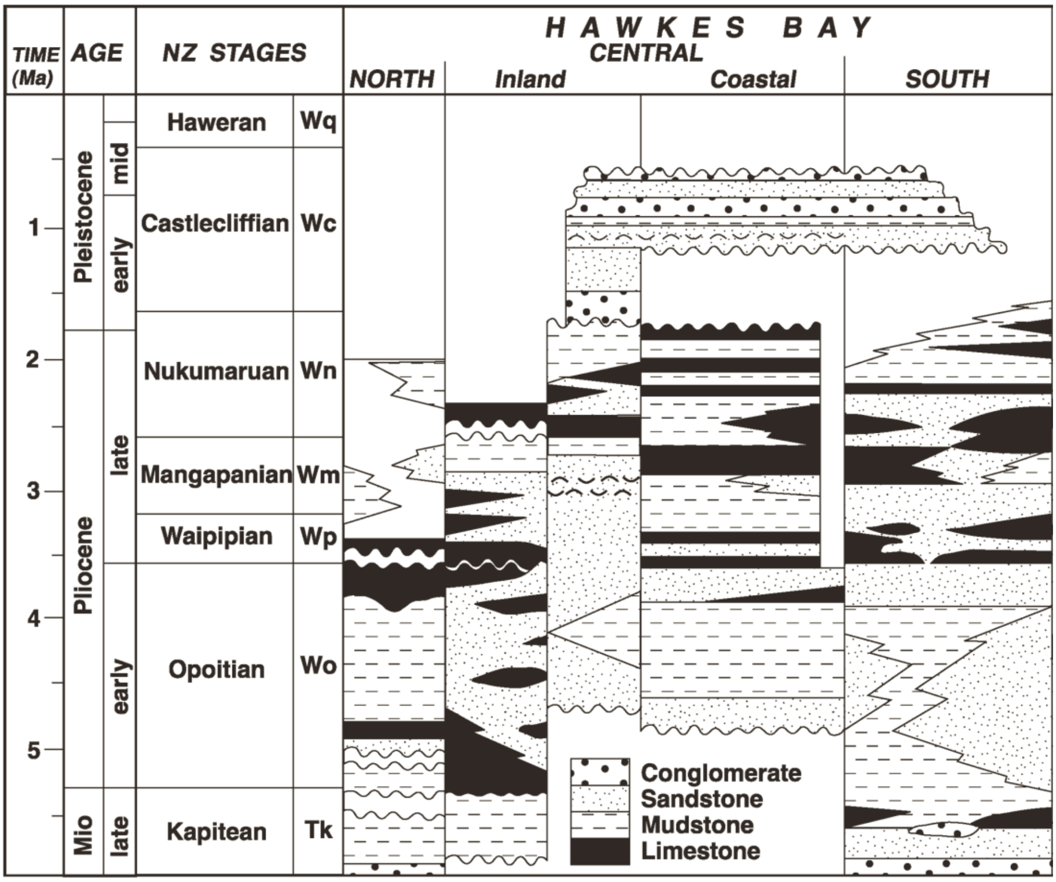

Figure 1.3: Chronostratigraphic panel showing the complex distribution of some of the main Pliocene Te Aute limestone occurrences from north to south in central North Island (Nelson *et al.* 2003). The present study area is contained in the NORTH column.

1.2.1 Tolaga Group

The name Tolaga Group is derived from the Tolaga Bay, NE of Gisborne. The Tolaga Group encompasses Miocene age sedimentary rocks (Waitakian to Upper Tongaporutuan) in the Tauwhareparae area inland from Tolaga Bay (Fig. 1.6), (Mazengarb *et al.* 1991; Bland *et al.* 2007).

As in the Tolaga Group of Mazengarb *et al.* (1991), shallow-water beds of Early to Late Miocene age are limited in extent in central Hawke's Bay, and the succession is dominated by massive deep-water mudstones and redeposited sandstones. Mazengarb and Speden (2000) extended the definition of the Tolaga Group to include all rocks of Early to Late Miocene age cropping out in the area of the Raukumara QMAP sheet. Bland *et al.* (2007) have included beds of similar age, lithology and inferred depositional environments to Tolaga Group that crop out widely throughout the northern parts of central Hawke's Bay.

1.2.2 Mangaheia Group

The name Mangaheia Group is derived from the Mangaheia River, NE of Gisborne. Steineke (1934) first named the Mangaheia Formation that occurred immediately south of the Tauwhareparae area. Mazengarb *et al.* (1991) redefined the succession at Tauwhareparae in the vicinity of East Cape as the Mangaheia Group, which encompasses mainly shallow-marine sandstone and limestone facies from Late Miocene (Kapitean)–Pliocene (Bland *et al.* 2007).

Later, Mazengarb and Speeden (2000) broadened the definition and occurrence of the Mangaheia Group from areas south of Tauwhareparae to encompass rocks of similar age and facies in the Wairoa and Mahia regions (Bland *et al.* 2007). In this study, the Mangaheia Group refers to rocks of entirely Pliocene age within the Wairoa Syncline.

1.3 Significance of Limestones

Limestones represent a significant (c. 20%) part in the Earth's sedimentary rock record (Moore 1989). Understanding both physical and chemical characteristics of limestone deposits are vital to unraveling paleoenvironmental conditions and depositional processes. Textural and structural properties of limestones can indicate the environmental energy conditions. A range of geochemical properties reflects physio-chemical conditions acted upon the sediments at the time of formation and diagenesis, which include major elements, cathodoluminescence, oxygen and carbon isotope values (Hood 1993). Modern carbonate sediments deposited around the world's oceans are analogues form of many ancient limestone deposits. Close studies of these modern carbonate deposits can also help interpret depositional environments of their ancient relatives (James & Clark 1997). Limestone deposits have much practical and economical significance. The porosity in limestones acts as aquifers, and as reservoirs for hydrocarbons. They are also an important source of CaO in the chemical industry, as an essential element in cement manufacture. Purer limestones are required for agricultural lime and smelting (Hood 1993).

1.4 Cool-water carbonates and New Zealand equivalent

Carbonate sediments are fundamental building blocks of all limestone deposits around the globe. The modern carbonate sediments are found in both marine and terrestrial settings, but the place of greatest abundance is on the shelf segment or deeper on the sea floor, in tropical and temperate regions (Fig. 1.4) (Hood 1993). The traditional view of shelf carbonate sedimentation saw it as a (sub)tropical phenomenon. It is almost 45 years ago since Chave (1967) suggested otherwise by turning attention to carbonate formations on modern shelves beyond the tropics. He argued that the condition for carbonate sedimentation is not just climate itself, but is fundamentally related to locally low rates of siliciclastic sedimentation. Consequently, the occurrences of shallow marine carbonate sediments are primarily depended on the overall tectonic setting and its control on the introduction and sea-floor dispersal routes of siliciclastic materials. Since Chave's (1967) unconventional views on carbonate sedimentation were acknowledged, there has been a growing appreciation about the occurrence of modern and ancient carbonate sediments in temperate to higher latitudes (Fig. 1.4). Many researchers started to slowly expand towards a more realistic picture of the global distribution patterns of modern shallow-marine carbonate facies.

Lees & Buller (1972) analysed attributes of modern carbonate sands and gravels from shelves between 60°N and 60°S latitudes, and to hopefully determine some distinctive features between low-latitude and mid-latitude carbonate sediments that would help distinguish the two in the rock record. They recognised the 'cool-water' carbonates comprised mainly of molluscs and foraminifers, and with associated skeletal grains of echinoderms, bryozoans, barnacles, ostracods, sponges, worms, ahermatypic corals and coralline algae. Since then, well over a dozen researchers (e.g. Lees 1975; Nelson 1978; Alexandersson 1978, 1979; Leonard *et al.* 1981; Rao 1981; Nelson & Bornhold 1984; Nelson & Hancock 1984) compiled the basic facies characteristics of cool-water carbonates, and drew attention to many other distinctive differences between the carbonates of warm (sub)tropical latitudes and those of temperate origin (Table 1.1). The term cool-water or non-tropical was then introduced to define limestones that formed at shelf regions polewards of about 30° latitude and at water depths less than 200 m (Nelson 1988c). More recently, Kamp & Nelson (1987), Kamp *et al.* (1988), Nelson *et al.* (1988a, 1988b); Hayton *et al.* (1995), Nelson *et al.* (2003), Bland *et al.* (2004a), amongst others, have further expanded the cool-water carbonate concept in relation to the active margin setting of the New Zealand sub-continent. The dynamic depositional and tectonic setting strongly influenced both the style and subsequent diagenetic evolution of the limestones (Nelson *et al.* 2003).

Around 50,000 km^2 of shallow-marine (<200 m) platforms off northern (34°S) and southern (48°S) New Zealand are covered by modern skeletal carbonate sediments, despite the geographic of these regions being close to an active plate boundary (Nelson *et al.* 1988a). These carbonate sediments are exclusively cool-water in origin, dominated by skeletal assemblages such as foramol and bryomol, with lacking tropical chlorozoan facies (Hood 1993).

Cool-water shelf limestones are widely distributed in the New Zealand Cenozoic rock record, and well developed in the Oligocene (Nelson 1978). They formed between latitudes 35°S and 60°S under cool-temperate to warm-temperate conditions. The skeletal facies distributions of these limestones are best illustrated by a cool-water shelf carbonate model (Fig. 1.5).

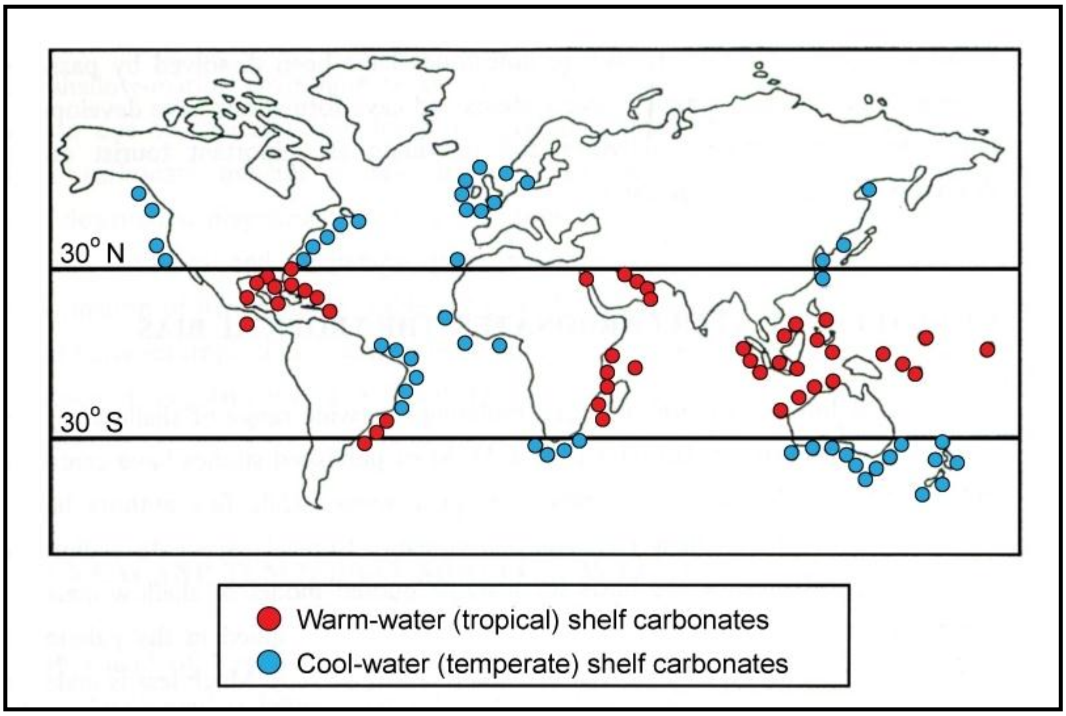

Figure 1.4: The global distribution of modern (sub)tropical and temperate shelf carbonate sediments (adapted from Nelson 1988).

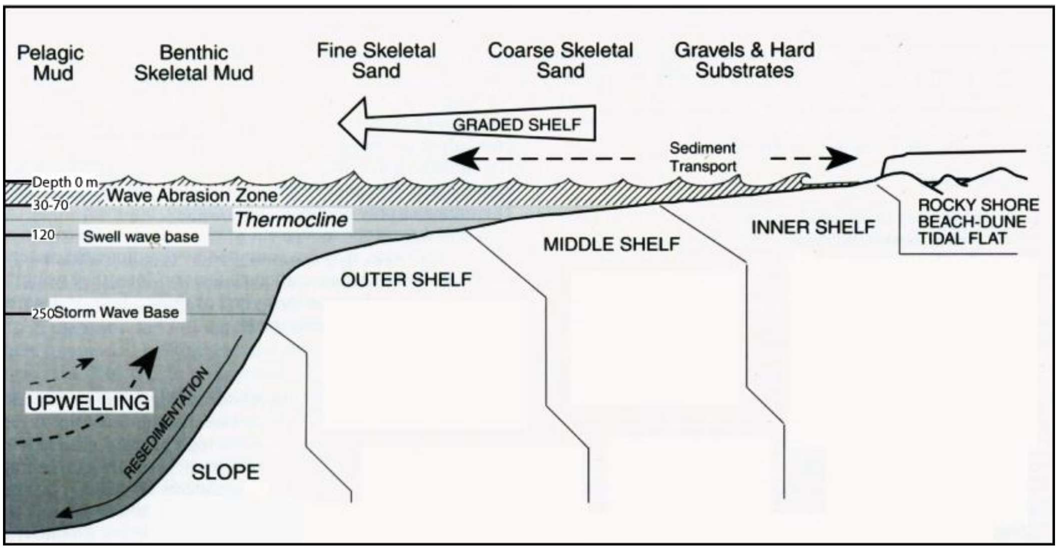

Figure 1.5: Hydrodynamic zones on a cool-water carbonate shelf showing skeletal facies distribution (adapted from James & Clarke 1997).

Table 1.1: Summary of typical tropical vs. non-tropical shelf carbonate systems (Nelson *et al.* 2003).

Tropical shelf carbonates	Non-tropical shelf carbonates
Warm water >20°C Saturated to supersaturated	Cool water <20°C Saturated to undersaturated
Rimmed and unrimmed shelf High to low energy	Unrimmed shelf High energy
Hermatypic coral reefs from 30°N to 30°S	No hermatypic reefs beyond 30°N and S
Non-skeletal grains (ooids, aggregates)	No non-skeletal grains
Bioclastic sediments: coral-calcareous green algal- molluscan-benthic foram	Bioclastic sediments: bryozoan-echinoderm-bivalve molluscan-benthic-planktic
Photozoan grain association	Heterozoan grain association
Sand and mud textures dominate, or *in situ* framework	Gravel and sand texture
Constructive marine diagenesis	Destructive marine diagenesis
Aragonite and high-Mg calcite mineralogy	Low- and intermediate-Mg calcite mineralogy
Typically high (>10 cm/ka) accumulation rates	Typically low (<10 cm/ka) accumulation rates

1.5 Neogene active margin limestones

Miocene-Pliocene age limestones are a volumetrically small but nevertheless significant part of the Neogene marine sequences now exposed onland in eastern North Island, New Zealand (Nelson *et al.* 2003). These limestones consist exclusively of skeletal hashes, dominated by bryozoans, bivalves, barnacles and foraminifers, typical of cool-water carbonates (Kamp & Nelson 1987). They are locally thick (up to a few hundred metres) and form typically as isolated pods and sheets within siliciclastic-rich deep-water facies. The tectonic uplift and subsidence of the sea floor resulted formation of imbricate thrust ridges and fault-bounded platforms provided depositional settings of these localised cool-water carbonates. There are some major differences between the Miocene and Pliocene limestones in respect of their distribution, geometry, thickness and components (Kamp & Nelson 1988), as noted below.

Miocene limestones

The onshore sequence within the northern part of the forearc basin contains many Miocene age limestone pods or lenses ranging from a few hundred square metres in extent and 5-10 m thick, up to 4 km^2 in area and over 100 m thick (Kamp & Nelson 1988). Those Miocene limestones are outer shelf to upper slope channel-fill deposits based on their geometry and facies characteristics and components. Most of the limestones crop out within very thick and massive mudstones and sandstones. Some smaller limestone bodies are separated by a channellised contact from the underlying lithologies. They are usually poorly bedded and internally massive, and consist of whole or fine-grained shell hash in an argillaceous, often micritic matrix, and some inverse grading and internal laminations (Kamp & Nelson 1988). All the features above suggest the limestones represent redeposited facies.

Pliocene limestones (Te Aute lithofacies)

The limestones of Pliocene age occur quite extensively within the central and southern parts of the Ruataniwha Strait, in part of the forearc basin (Fig. 1.6).

They often form locally spectacular scarps and dip slopes in eastern North Island (Fig. 1.7). Their distinctive lithology, loosely cemented barnacle coquina, and scarp-forming character mean the limestones can be expressed in the topography continuously over long distances, while others vary in thickness dramatically over only a few kilometres. The Pliocene limestones are quite similar in their lithological characteristics, suggesting that the same depositional setting was repeated in time. They are characterised by an unusually high content of barnacle plates, and more broadly a typical cool-water skeletal association involving barnacles, epifaunal calcitic bivalves, and locally rich brachiopod materials (Kamp *et al.* 1988; Beu 1995; Hayton *et al.* 1995). The limestones are typically well-bedded, locally tabular and/or trough cross-stratified and show varying but generally small degrees of cementation (Kamp & Nelson 1988). The shallow-water skeletal carbonate deposits are a particular indicator of the position of the marginal facies of the N-S seaway that formerly occupied the region during the Pliocene, named the Ruataniwha Strait (Beu *et al.* 1980). The faunal assemblages and bedding characteristics also indicate that the barnacle-dominated limestones formed in high-energy settings dominated by tidal and subtidal currents (Nelson *et al*. 2003).

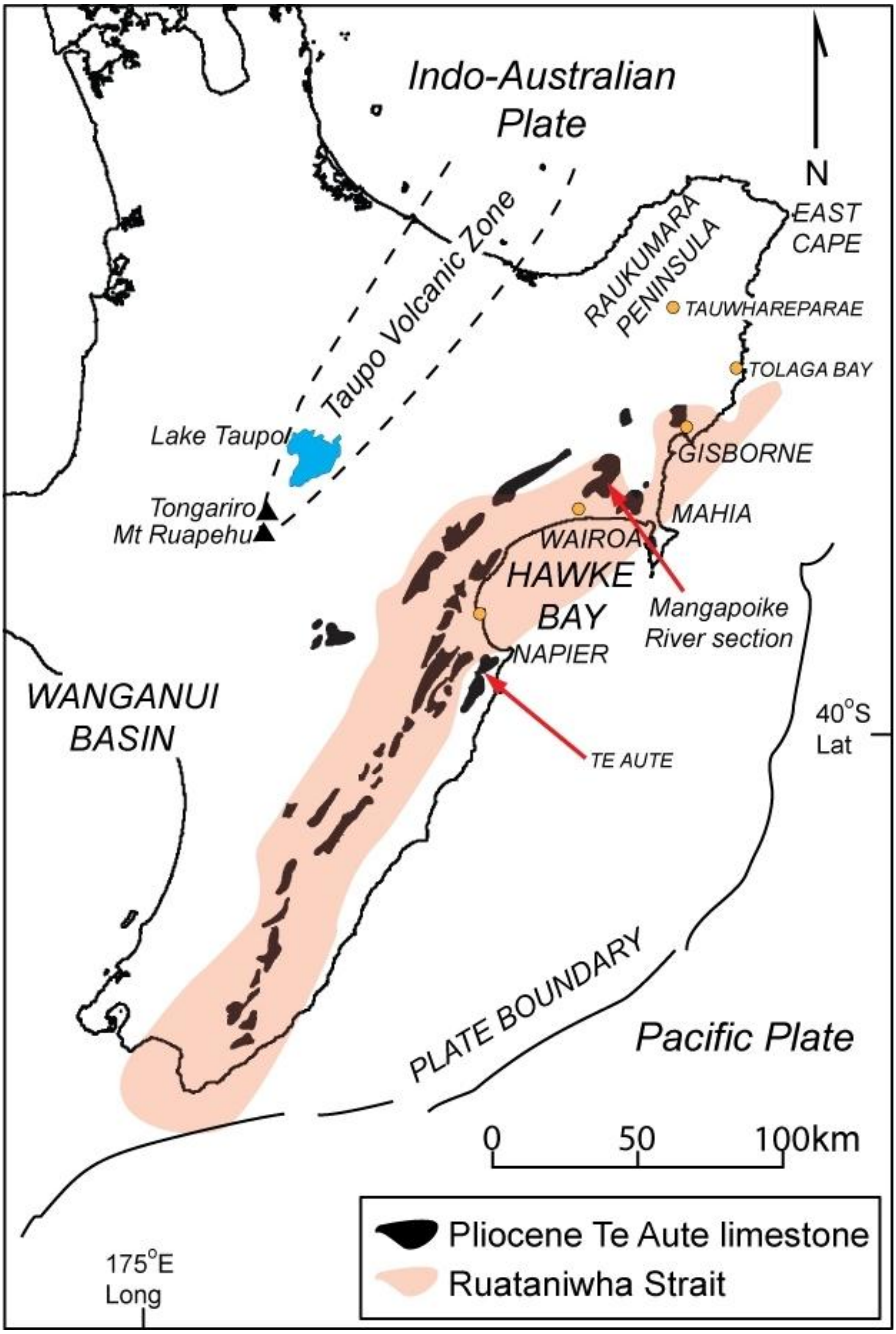

Figure 1.6: General distribution of Pliocene limestones, eastern North Island. Modified from Nelson *et al.* (2003).

Figure 1.7: Spectacular dipping late Opoitian Whakapunake Limestone in the Haupatanga Gorge, Mangapoike River, northern Wairoa district. A sheep is circled in red in the background for scale.

The Pliocene limestones in the East Coast Basin are referred to as Te Aute type limestones. The name is derived from the village of Te Aute (V22/210458, Fig. 1.6) at the foot of the Ruakawa Range. The Te Aute limestones were first mentioned by Hector (1887) and formally defined as Te Aute Formation by Lillie (1953). The name was once given to all the Pliocene marine sediments overlying the regional, mostly angular, unconformity on uppermost Miocene section (Harmsen 1985).

The Te Aute limestones formed at paleolatitudes near 40–42°S, where the rate and extent of terrigenous sediment accumulation was highly variable as a result of the thrust faulting and folding in an active plate margin setting during the Pliocene-Pleistocene (Nelson 1988c; Nelson *et al.* 2003). Beu (1995) summarised the history of stratigraphic nomenclature for the Te Aute limestones in the East Coast Basin based on a detailed study of the pectinid lineages of the limestones. He suggested abandoning the formal lithostratigraphic name Te Aute, and instead subdivided the limestones into 6 groups, 45 formations, and 12 members based on their pectinid age, outcrop distribution and lithology. The majority of the Te Aute limestones scattered over eastern North Island have roughly similar lithological characteristics, being coarse skeletal calcarenites, skeletal calcirudites and coquinas with variable amounts of siliciclastic materials (Fig. 1.8) (Nelson *et al.* 2003). Their colours are mostly cream to yellow or yellowish brown, and they commonly occur in a cyclic fashion in between mudstone or sandstone (Haywick 1992, 2000). In general, these non-tropical limestones are horizontally bedded and cross-bedded on a wide range of scales. The spectrum of cross-bedded structures often shows bi-directional foreset orientations (Kamp & Nelson 1988).

The three limestones in northern Hawke's Bay study area, named the Opoiti, Whakapunake, and Tahaenui Limestones, are unconformity-bound and separated by thick sections of soft, siliciclastic sandstone and mudstone, all variably fossiliferous and locally tuffaceous. The limestones typically form prominent cliffs in outcrop and extend also into the subsurface. The limestones are typical non-tropical skeletal carbonate deposits that formed under the influence of commonly strong tidal flows along an actively deforming and differentially uplifting forearc basin seaway, near inboard of the Pacific-Australian subduction plate boundary during the Pliocene (Nelson *et al.* 2003). The two younger limestone formations thicken and thin dramatically from place to place. The Opoiti limestone is a relatively thin unit (c. 12 m), with rather consistent thickness throughout the field area. All three limestones are composed of much coarse broken shell material and coquina (whole shells), especially barnacles, pectinids (*Phialopecten marwicki, and Towaipecten ongleyi*, Table 1.2), oysters (*Crassostrea ingens*), and include variable amounts of siliciclastic material. They show significant differences in their degree of cementation in different areas (Beu 1995). The latter characteristic means they can have high porosities (and permeabilities), and so they afford clear targets as potential petroleum oil and gas reservoirs in the subsurface.

Table 1.2: Summary of age diagnostic pectinids in the limestones in northern Hawke's Bay (Beu 1995). See New Zealand Stage names in Fig. 1.3.

Age	Family pectinidae
Late Opoitian-Waipipian	*Phialopecten marwicki*
Early Opoitian	*Towaipecten ongleyi*

The skeletal composition of some of the Te Aute lithofacies limestones was summarised by Kamp *et al.* (1988) and noted that the most unusual characteristic was their predominance of barnacle fragments (Fig. 1.8). Barnacle plates are fragile and easily abraded, and will not survive transport over distance of tens of metres, so their presence is suggestive deposition near their living site (Beu 1995). This distinctive character, along with the barnacle taxa, have been recognised as important clues in determining the environment of deposition.

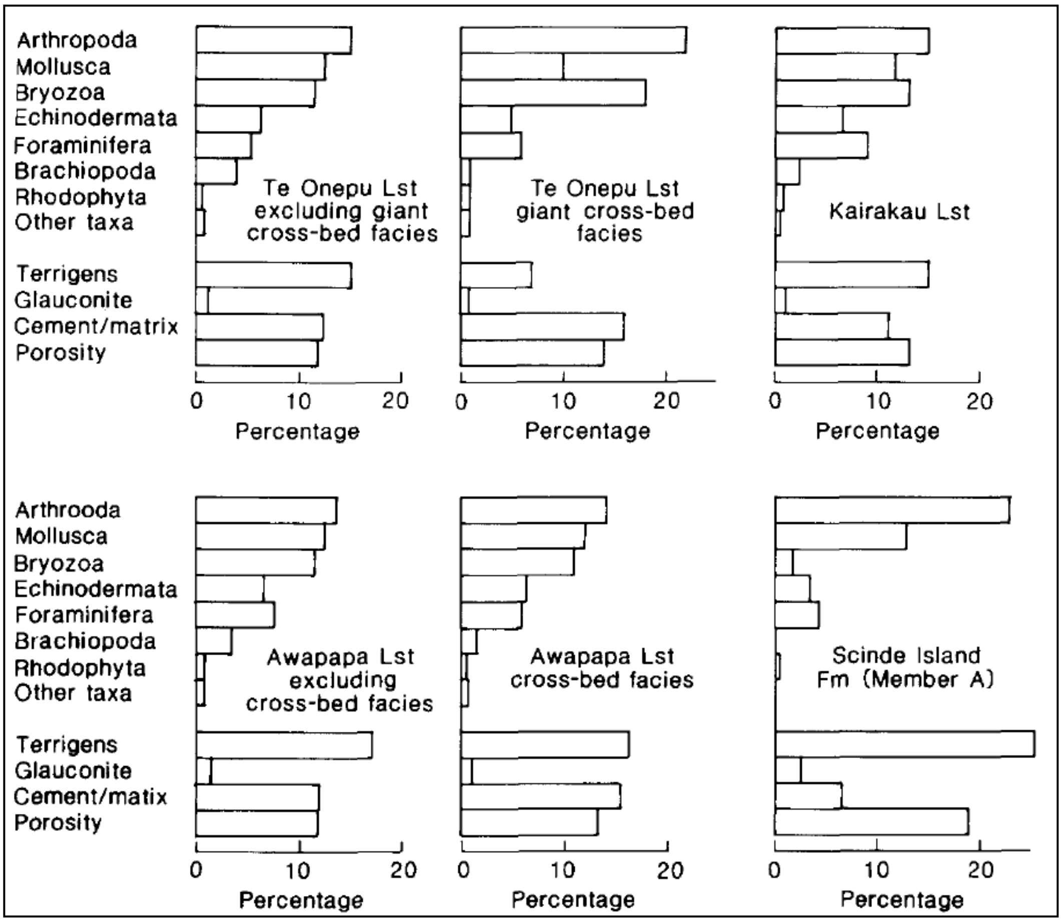

Figure 1.8: Composition of central Hawke's Bay Te Aute facies limestone formations, from Kamp *et al.* (1988).

1.6 Objectives of study

The primary aim of this project was to unravel the sedimentary and diagenetic history and origin of the three Pliocene limestone units within the otherwise siliciclastic-dominated Pliocene succession in the wider Wairoa district of northern Hawke's Bay. The project involved considerable fieldwork with descriptions and local mapping of outcrops and the construction of stratigraphic logs to show the main sedimentological features of the three carbonate units in the field. The encasing siliciclastic sandstones and mudstones were also noted in a more general way. Together these records help in unravelling the main external (tectonic, sea-level and climate changes) and internal (sedimentary environment) controls on the development of this mixed carbonate-siliciclastic succession during the Pliocene.

In the laboratory, texture and composition of samples were analysed using both standard and cathodoluminescence petrography, while calcium carbonate percentage and grain size data were determined using standard methods. Geochemical analyses were taken to determine the bulk elemental composition of all three limestones facies and subsequently some sandstone and mudstone facies. These data will provide further understanding of the Te Aute limestones and other sedimentary deposits in northern Hawke's Bay.

1.7 Historical studies

Geological research in the northern Hawke's Bay region has involved studies of lithostratigraphy, biostratigraphy, magnetostratigraphy and zircon fission-track analyses in the past. The study area was mapped previously by Quennell (1940), Haw (1958) and Francis (1993), mostly for the purpose of petroleum exploration. Smith (1876) and McKay (1887) were some the first geologists to carry out studies of the sedimentary facies in the northern Hawke's Bay region.

Some more recent studies involved detailed geological investigation that focused on the distribution of sedimentary facies and geologic structures from Gisborne to Wairoa as part of the petroleum-related projects. Moore & Hatton (1985) carried out an investigation on the limestone resources in the northern and central Hawke's Bay region, which included the study area. Lithostratigraphic studies of the Pliocene deposits were carried out by Ongley (1930) and Kennett & Watkins (1974) in the study area. McInnes (1964), Scott (1978), Beu (1978), Hornibrook (1984) and Edwards (1987) have published studies of the biostratigraphy of the Pliocene sections in the study area. Hornibrook (1984) and Kamp & Xu (2002) carried out zircon fission-track studies to unravel the Neogene thermal history of the Hawke's Bay Basin.

Regarding the limestones, Ongley (1928), Marwick (1965), Beu *et al.* (1980) and Beu (1995) carried out some specific studies (Table 1.3), and assigned different ages to each of the three limestones based on their *Phialopecten* lineage. Past studies gave many different names to the same limestones and their lateral equivalents. Table 1.3 is a summary of the limestones occurring in the wider northern Hawke's Bay region. Kamp & Nelson (1987, 1988), Kamp *et al.* (1988), Nelson *et al.* (2003) and Bland *et al.* (2008) have also published studies that include mention of the limestones in the area. A revised stratigraphic nomenclature for the Pliocene limestones will be mentioned later, in Chapter 4.

Table 1.3: Previously published names for the various Pliocene limestones in northern Hawke's Bay.

Name	Author	Distribution	Age
Tahaenui Limestone	Moore & Hatton 1985 (informal), Edwards 1988, Kamp *et al.* 1988, Beu 1995 (formal)	Northern Hawke's Bay	Waipipian
Long Point Limestone/Tahaenui Limestone	McKay 1887	Long Point (Mahia Peninsula), Tahaenui	Waipipian
Waihua beds (basal part)/Tahaenui Limestone	Ongley 1928	Wairoa-Tiniroto	Waipipian
Whakapunake Limestone	Beu *et al.* 1980, Kamp *et al.* 1988, Beu 1995	Northern Hawke's Bay	Opoitian
Maungaharuru Limestone/Whakapunake Limestone	Smith 1870, Beu *et al.* 1980	Northern Hawke's Bay-Mahia Peninsula	Opoitian
Opoiti Series/Limestone	Ongley 1928, 1930	Wairoa-Tiniroto	Opoitian
Opoiti Limestone (Mbr)	Beu *et al*. 1980 (informal), Beu 1995 (formal)	Northern Hawke's Bay	Opoitian

2 Chapter Two

Geological setting and structural overview

2.1 Introduction

The three Pliocene limestones in the northern Hawke's Bay formed at paleolatitudes near 40°S in a tidal current dominated ancient forearc seaway, part of the modern day East Coast Basin, eastern North Island, New Zealand (Nelson *et al.* 2003). The tectonic elements associated with this dynamic depositional setting have been important controls on the distribution, character and subsequent diagenetic evolution of these limestones. This chapter briefly summarises the present broad tectonic setting of the East Coast Basin and the controlling elements that influenced deposition of the Pliocene sedimentary facies in the study area.

2.2 Present day tectonic setting

The modern Indo-Australian plate boundary transecting the New Zealand sub-continent comprises northern, central and southern segments (Fig. 2.1): (1) Hikurangi margin, eastern North Island; (2) continental transform system through most of the South Island; and (3) Puysegur active continental margin in southernmost South Island and offshore (Kamp & Nelson 1988). The northern part of this modern plate boundary, the Hikurangi margin where the oceanic crust of the Pacific Plate subducts obliquely beneath the eastern North Island, partially transforms at northernmost South Island. The continental transform system between the two subduction systems is mostly represented by the Alpine Fault of the western South Island. Here the continental crust of the Pacific Plate obliquely overthrusts continental crust of the Indo-Australian Plate, and relative plate motion is taken up by dextral strike-slip movement (Cole & Lewis 1981). Further south, the oceanic crust of the Indo-Australian Plate is being obliquely subducted beneath the continental crust of the Pacific Plate at the Puysegur Trench and beneath Fiordland in southernmost South Island, in the opposite direction to that occurring in the Hikurangi margin to the north (Sutherland *et al.* 2006).

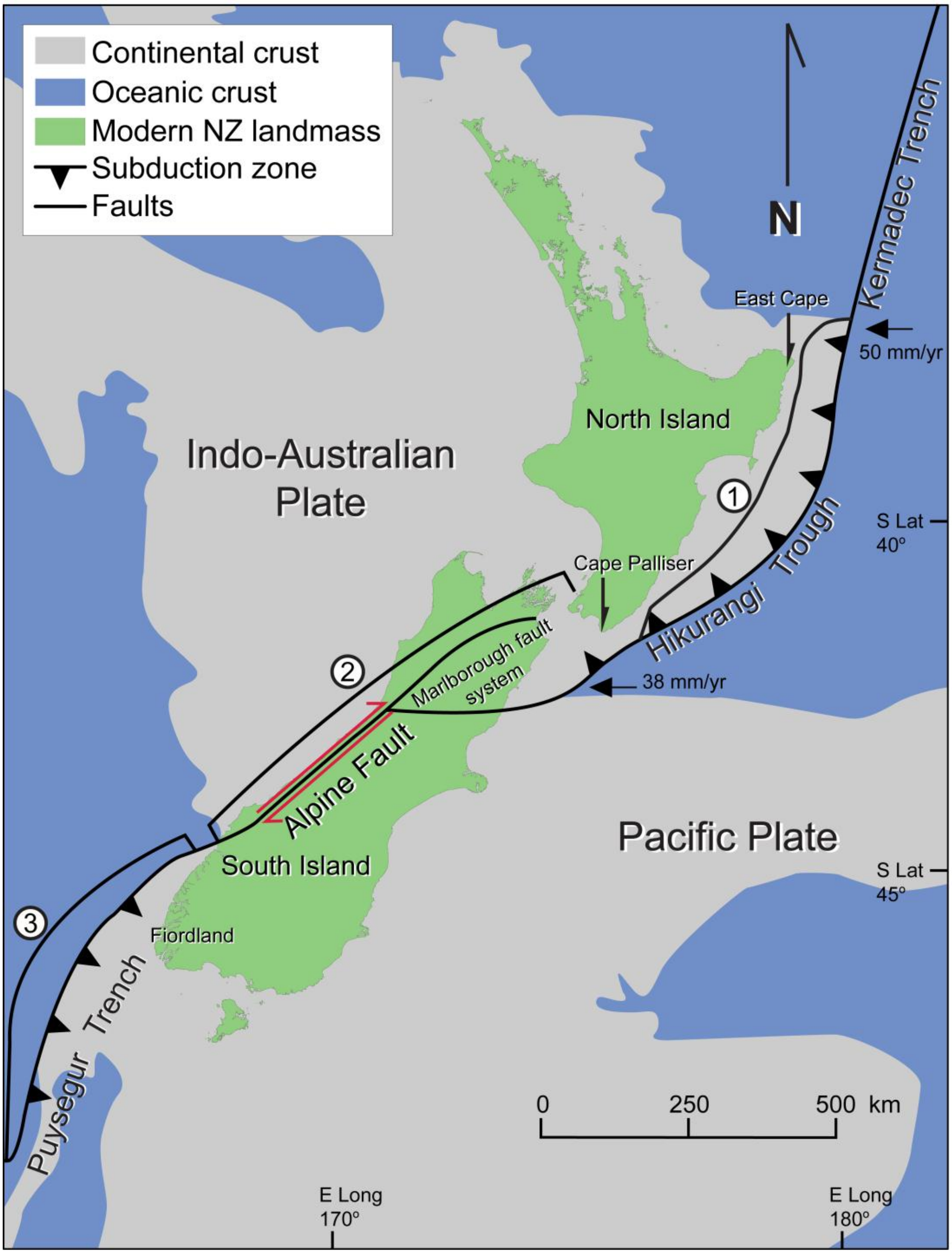

Figure 2.1: Plate tectonic setting of the New Zealand continental block. Adapted from Beu (1995). (1) Hikurangi margin, (2) Alpine Fault (continental transform boundary) and (3) Puysegur active continental margin.

2.3 East Coast Basin

The East Coast Basin (Fig. 2.2) lies along the NE margin of the New Zealand sub-continent of the Indo-Australian Plate. It marks the southern end of the Tonga–Kermadec subduction system that stretches for over 3000 km, where the Pacific Plate is being subducted obliquely westwards beneath the North Island, New Zealand at a rate of about 43 mm/year (Fig. 2.1) (Lewis & Pettinga 1993; Campbell *et al.* 2008). The basin is orientated in a NNE-SSW direction, parallel to the subduction system. It has an area of approximately 70,000 km^2, extending 650 km from East Cape to Cape Palliser in eastern North Island, and also includes the northeastern part of the South Island, encompassing the regions of Raukumara, Hawke's Bay, Wairarapa and eastern Marlborough (Rogers *et al.* 1999; Campbell *et al.* 2008). In this study we restrict our attention to the northern part of the Hawke's Bay region.

The East Coast Basin is bounded to the west by the North Island axial ranges, and continues offshore across the continental shelf and slope to the east, into the Hikurangi subduction complex. The width of the basin varies from 60 to 110 km, about a half of which is off shore (Field *et al.* 1997).

2.4 Hawke Bay

Hawke Bay is the large embayment of sea partly enclosed by Mahia Peninsula and Cape Kidnappers (Fig. 2.2). Water depths in Hawke Bay are on average less than 120 m, and the sea floor is smooth and gently dips towards the east at less than 1°. Further eastwards, the continental shelf includes Hawke Bay itself and has a total width of 70 km (Field *et al.* 1997).

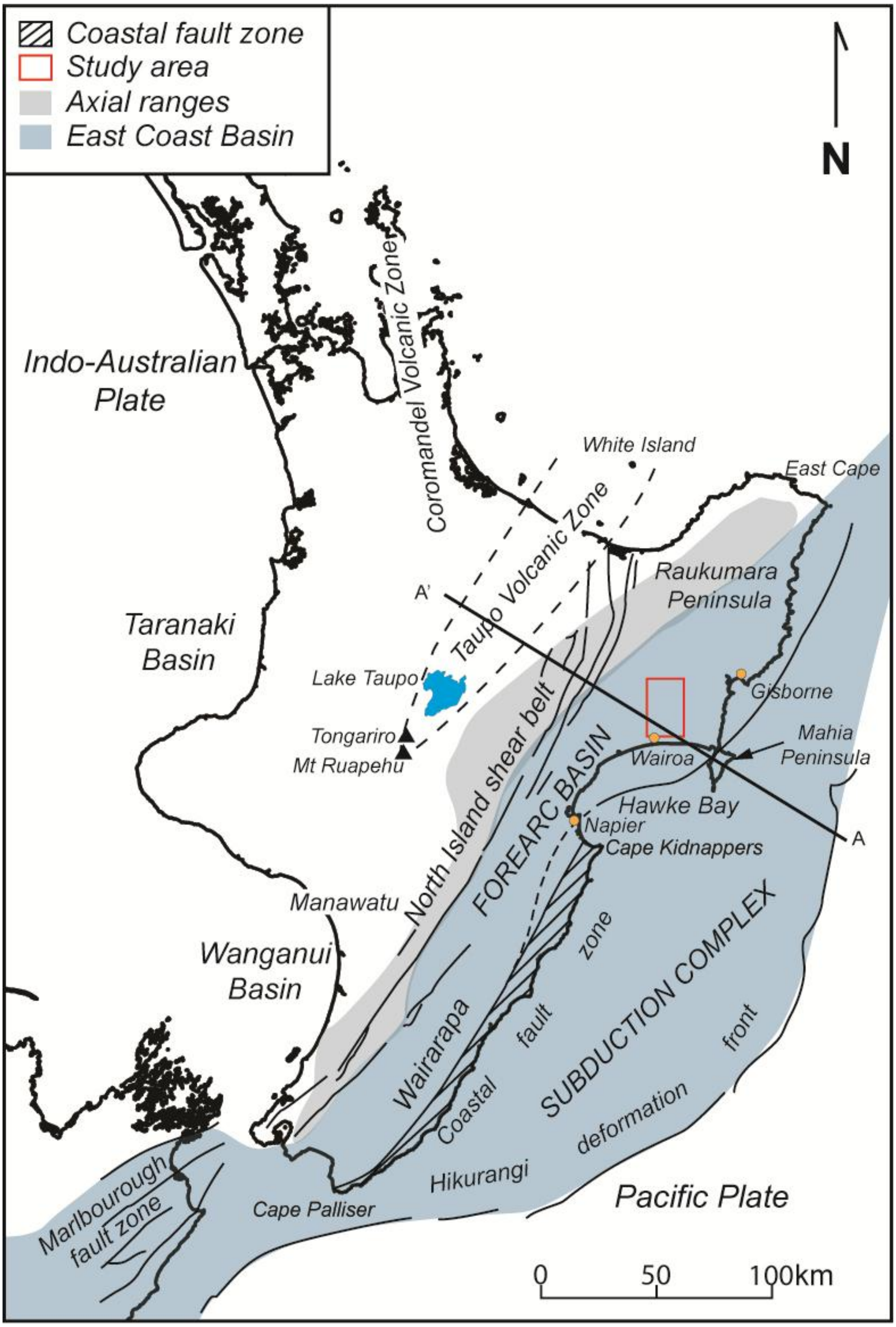

Figure 2.2: Tectonic elements of the East Coast Basin. Adapted from Beanland (1995).

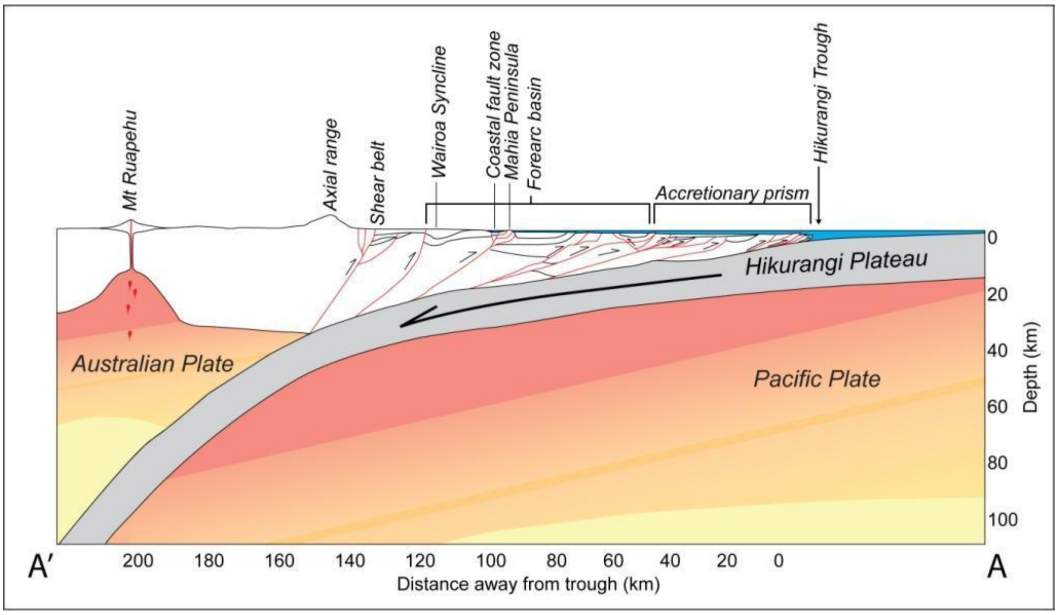

Figure 2.3: Cross-section A'-A in Fig. 2.2. Modified from Barnes *et al.* (2002).

2.5 Tectonic elements across the Hikurangi margin

The Hikurangi margin is 500 km long by 480 km wide, and is a region of transition between the ocean-ocean subduction at the Kermadec Trench and continental-continental strike-slip collision in the northern and central South Island (Nicol & Wallace 2007). Off eastern North Island, the Pacific Plate is subducting obliquely at a rate of about 40-50 mm/yr beneath the Indo-Australia Plate (Fig. 2.1) (Nelson *et al.* 2003). At a large tectonic scale the Hikurangi margin includes five tectono-geomorphic elements from E-W across the convergent margin: (1) Backarc region, (2) Taupo Volcanic Zone (volcanic arc), (3) North Island Axial Ranges, (4) Hikurangi Forearc Basin, and (5) Hikurangi Subduction Complex. The axial ranges, forearc basin and subduction complex are all within the East Coast region (Fig. 2.2, 2.3). The subsequent development of the Hikurangi margin had more direct influences to the evolution of the East Coast Basin since the Early Miocene, compared to other basins around New Zealand (Field *et al.* 1997).

The margin exhibits complex tectonic structure and stratigraphic evolution (e.g., Lewis & Pettinga 1993; Collot *et al.* 1996; Field *et al.* 1997; Barnes *et al.* 2002;

Barnes & Nicol 2004; Henrys *et al.* 2006; Nicol *et al.* 2007). The northern margin off Raukumara Peninsula is characterized by non-accretion and tectonic erosion associated with seamount impact scars (Lewis *et al.* 1997, 1998, 2004; Collot *et al.* 2001). To the south off the Wairarapa coast exists a more classical example of an imbricated thrust wedge dominated by accretion (Davey *et al.* 1986; Lewis & Pettinga 1993; Collot *et al.* 1996; Barnes & Mercier de Lépinay 1997; Lewis *et al.* 1997). The very southern end of the margin is relatively narrow and lies in the transition from oblique subduction to continental strike-slip deformation, where it is incised by Cook Strait Canyon (Holt & Haines 1995; Barnes *et al.* 1998; Barnes & Audru 1999; Mountjoy *et al.* 2009).

Backarc region

The backarc region is a continental segment extension of the nearly 2700 km long Tonga-New Zealand offshore backarc system (Gamble & Wright 1995). It lies 140-400 km to the W and NW of the current frontal volcanic arc. It is characterised by a much-faulted basin-and-range topography involving Mesozoic basement rocks, Cenozoic sedimentary deposits and basic Quaternary mafic volcanics, the latter in five main fields: Alexandra, South Auckland, Auckland, Whangarei, and Kaikohe-Bay of Islands (Cole & Lewis 1981).

Volcanic arc

The modern arc, Taupo Volcanic Zone (or TVZ), is one of the most volcanically active regions on Earth. It is a volcano-tectonic depression that lies between the frontal ridge and the backarc region of the subduction margin in central North Island. The subducting oceanic lithosphere melts beneath the continental crust at a depth of 80-100 km, and throughout the Quaternary has fuelled a wide range of volcanic activity stretching from Ruapehu volcano in the south to offshore White Island in the Bay of Plenty. This zone of Quaternary volcanism sites parallel to the subduction margin (Fig. 2.2), is 30-70 km wide, and filled with 2-4 km of mostly rhyolitic pyroclastic deposits (Cole & Lewis 1981; Healy 1992).

North Island axial ranges

The axial ranges of the North Island (frontal ridge) have been defined variously on geographical, lithological, structural and tectonic grounds (Field *et al.* 1997). The ranges extend nearly continuously from Cape Palliser in the south to East Cape in the north, and are disrupted only by structural sags at the Manawatu Gorge, and at two localities in Hawke's Bay now occupied by the Napier-Taihape and Napier–Taupo highways. The Kaimanawa and Raukumara Ranges in the north are broad and strike northeast, in contrast to the Tararua and Ruahine Ranges in the south which are narrow and strike north-northeast (Kamp 1988). The NE-SW-trending axial ranges consist of highly tectonised Triassic to Early Cretaceous greywackes and argillites belonging to the Torless Terrane (Field *et al.* 1997). The uplift history of the axial ranges has been long and varied, starting perhaps in late Early Miocene time and increasing in intensity during the Plio-Pleistocene through to the present day (Field *et al.* 1997).

Forearc basin

The Pliocene deposits investigated in this study in the northern Hawke's Bay region are located within the forearc basin of the Hikurangi margin. The forearc basin comprises two parts: an inner and an outer forearc separated by a coastal fault zone which runs in a NNE-SSW direction from offshore Raukumara, through part of Mahia Peninsula, and continuously out onto the Wairarapa shelf (Fig. 2.2) (Field *et al.* 1997).

The forearc basin is a major topographic and structural depression that is bounded by the structural ridge of axial ranges to the west and the deformation front offshore to the east (Kamp 1992). The Hikurangi forearc was formed in response to the inception and development of the Pacific and Indo-Australian subduction plate boundary since the end of Oligocene (Ballance 1993). It stretches from the southern terminus of the Tonga-Kermadec Trench to Cook Strait. The inner forearc is mostly exposed above sea-level. The outer forearc is completely submerged and extends eastwards towards the deformation front (Field *et al.* 1997). Most of the Tertiary marine sediments in the Hikurangi forearc are best exposed subaerially along the present day East Coast region, the region having been uplifted in the late Neogene (Kelsey *et al.* 1995).

Hikurangi subduction complex

The Hikurangi subduction complex comprises the structural trench and the accretionary prism/slope. The structural trench, named the Hikurangi Trough, marks the modern subduction plate boundary. It is a regional structural low (c. 3000 m deep) located at the base of the continental slope offshore eastern North Island (Fig. 2.2) (Cole & Lewis 1981). Compared to the Kermadec Trench (c. 9000), the Hikurangi Trough is shallower, and the plate interface here dips at a gentle angle of about 3° for at least 100 km beneath the subduction margin before steepening under the North Island (Davey *et al.* 1986; Henrys *et al.* 2006; Barker *et al.* 2009). The subduction front curls around the eastern North Island and comes onshore near Marlborough. It nevertheless marks the position where the Pacific oceanic lithosphere starts to subduct beneath the North Island (Kamp 1992). A complex series of low-angle thrust fault-controlled anticlinical ridges and slope-parallel basins have developed since the late Neogene (Lewis & Pettinga 1993). These structures are oriented NE-SW, parallel to the Hikurangi Trough. The slope-parallel basins are typically 5-30 km wide and 10-60 km long (Nelson *et al.* 2003).

2.6 East Coast Basin evolution

The East Coast Basin consists of a broadly fining-upwards, transgressive, passive margin Early Cretaceous to Paleogene succession of marine shelf to slope-basin conglomerates, breccias, sandstone, mudstone and flysch, which is overlain by a thick Neogene convergent margin sequence. Like most sedimentary basins in New Zealand, the East Coast Basin is a composite basin showing several stages of structural evolution and depositional fill. The basin evolution reflects the broad tectonic development of the New Zealand sub-continent through the last 110 my (King *et al.* 1999). The complex geological history of the basin has created an up to 10 km thickness of mostly fine-grained marine sediments associated with three distinctive tectonic intervals from the Middle Cretaceous to present (Field *et al.*

1997). Onshore, within the forearc basin, a series of deformed Cretaceous to Paleogene sedimentary rocks deposited in a passive margin setting prior to subduction are overlain by less deformed Neogene marine sediments formed after the onset subduction. This was followed by sedimentation that was driven by eustatic oscillations of sea-level, evident also in other basins in New Zealand (Field *et al.* 1997).

The basement rocks of the East Coast Basin are highly tectonised, indurated metagreywackes of Triassic-early Cretaceous age belong in the Torlesse Terrane (Mortimer 1995). They originally formed part of a paleo-frontal accretion along the edge of the Gondwana landmass (Lewis & Pettinga 1993). These are onlapped by Early Cretaceous shelf sandstones, and succeeded by a thick interval of Late Cretaceous through to Paleogene deep-water sandstones and mudstones formed in a passive margin setting (Field *et al.* 1997).

The transgressive sedimentation in the basin during the Cretaceous began about 15 Ma earlier than in Taranaki Basin on the western side of North Island (Fig. 2.2). The deposits consist of conglomerate and shallow-marine sandstone in Marlborough, followed by deeper water flysch or mudstone (Field *et al.* 1997). Passive margin sedimentation and subsidence through the Paleogene involved limited sediment sources within East Coast Basin, and relatively low depositional rates (Field *et al.* 1997; King *et al.* 1999). Siliceous mudstone (Whangai Formation) and organic-rich mudstone (Waipawa Black Shale) succeeded Late Cretaceous shelf sandstones. Bentonitic mudstone of Eocene age (Wanstead Formation) and marl of Oligocene age (Weber Formation) complete the passive margin depositional sequence (Field *et al.* 1997). The Cretaceous and Paleocene sediments contain known hydrocarbon source rocks, in particular the Whangai Formation and Waipawa Black Shale, both of which source onshore active oil and gas seeps at the present day (Rogers *et al.* 1999).

2.7 Structures in the study area

In most of the area, structure is dominated by combination of reverse faults and anticlines folds. Main folds from west to east, the main fold structures are Clyde Syncline (part of the Wairoa Synclinorium), Mangone Anticline (to the east of the study area), Nuhaka Syncline, and Morere Anticline, with the associated Opoutama Anticline (Fig. 2.4). The plunge of these folds is gentle except near the Tahaenui Fault Zone, where south plunge on the Mangaone Anticline increases abruptly. The Nuhaka Syncline is divided into two parts; the main fold trends generally northeast, the continuation southward swings towards an east-west orientation before trending southwestly into Hawke Bay (Francis 1993).

There are three major fault zones that associated with the major folds across the region (Fig. 2.4). The N to NNE trending Opoutama Fault Zone runs through Opoutama, to the east of the Mangaone Anticline, near Mahia. The main eastern fault is located by foraminiferal dates, and overlain by late Quaternary sands (Haw 1958). Several minor faults are detectable from both surface and petroleum well (Opoutama-1). Local outcrop pattern from Opoutama-Morere suggests reverse faulting (Francis 1993).

The Mangaone Fault Zone is recognized from the displacement of the Tahaenui Limestone, and extends into Tangihau Mudstone on the eastern limb of the Mangaone Anticline. The eastern limb of the syncline is much thinner than the west, Francis (1993) suggests the difference in thickness of either limbs of the syncline is the result of a reverse faulting.

The Tahaenui Fault Zone trends ESE, displaces upper Miocene (Tunanui Sandstone and younger) and possibly Pliocene strata (Tahaenui Limestone and Wairoa Formation to some extent westwards) (Haw 1958).

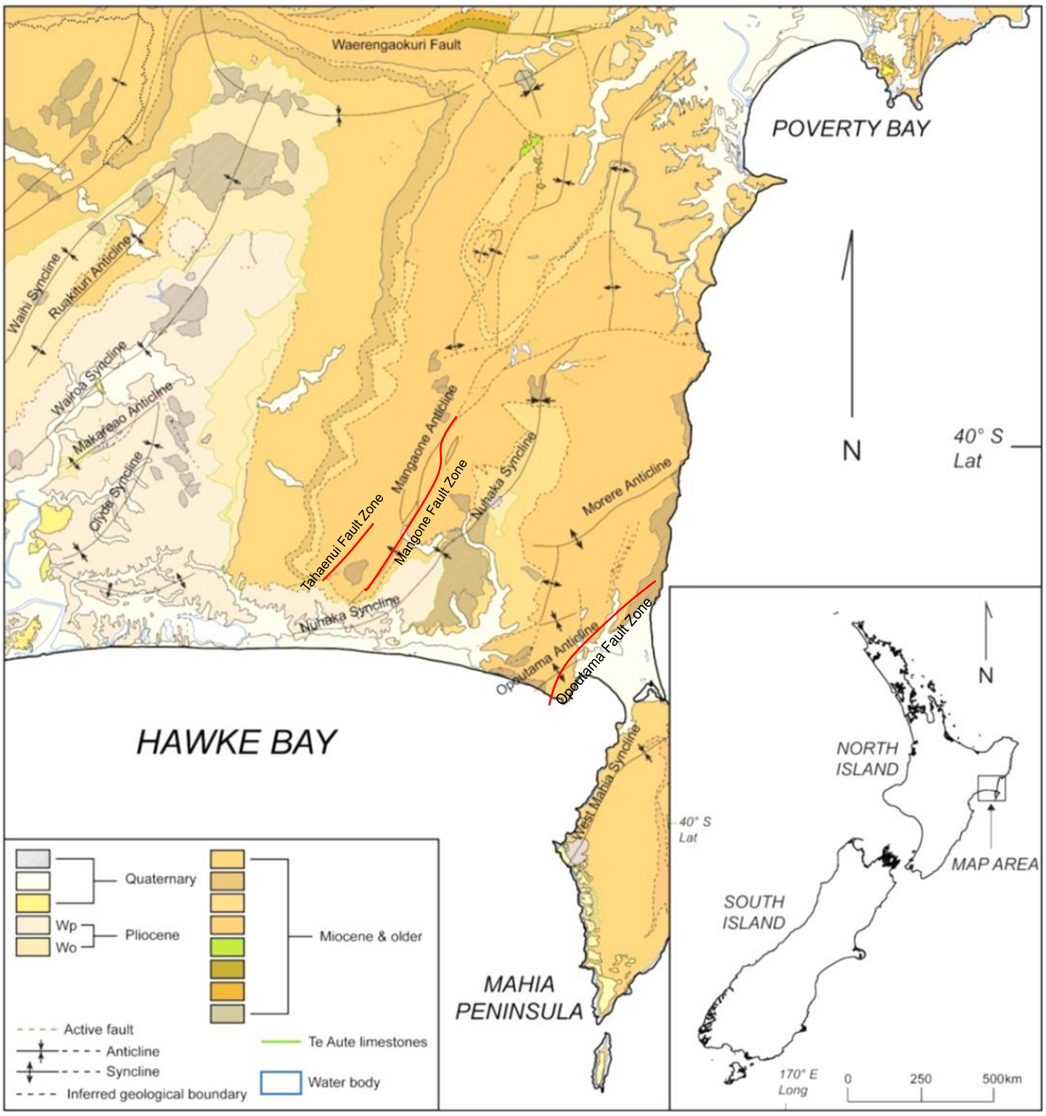

Figure 2.4: Structural setting of the study area (QMAP).

3 Chapter Three

Methods

3.1 Introduction

This chapter outlines both field and laboratory techniques used in this study to unravel the stratigraphy and petrology of the Pliocene limestones and associated siliciclastic rocks in the study area. The main laboratory techniques employed include standard and cathodoluminescence petrography, powder x-ray diffraction, grain texture analysis, $CaCO_3$ analysis, and stable oxygen and carbon isotopes.

3.2 Field work

A reconnaissance trip to the northern Hawke's Bay was made by Prof. Cam Nelson and Michele Drinnan in September 2009. Field work was done largely on foot, in the early part of the 2010. Sample locations and stratigraphic columns were recorded with the assistance of a GPS instrument (Garmin) using the New Zealand Map Grid, and the accompanying maps of the NZMG 260 Topo Series, sheets X18 (Tiniroto) and X19 (Wairoa). Sample and lithological information is shown on stratigraphic columns using a template modified from those used by Bland (2001), and are presented separately in Appendix I. Photographs of outcrop stratigraphic characteristics are included in each chapter. Scales in these photographs are often represented by a geological hammer or a 5 cm scale bar from Geological Society of New Zealand Field Wallet.

Rock slabs of all three Pliocene limestones were cut and scanned using a colour scanner for closer lithological analysis. The scanned images are presented for each limestone in the relevant chapter.

3.3 Bulk sample mineralogy

Both x-ray diffraction and $CaCO_3$ analysis were done to provide semi-quantitative bulk sample mineralogic characteristics.

X-ray diffraction

Fresh unweathered rock samples were selected and powdered using a ring mill. Samples generally required about 25 seconds of milling to achieve a suitably fine powder, although some more indurated samples required up to 30 seconds of milling. The bulk XRD analysis was performed on un-orientated powder mounts using a Philips analytical x-ray diffractometer with a PW 1729 X-ray generator and a PW 1840 diffractometer control. A scan range of 2-40 degrees 2θ was used, at a scan speed of 0.02º per second. Bulk XRD data are included in Appendix III and are depicted in graphical form in Chapters 5 to 8. Bulk mineralogy of the samples was then determined from peak positions. The intensity of each peak is related broadly to the relative abundance of each mineral present in the sample. This allows for a semi-quantitative estimate of the abundance of the minerals present in each sample.

$CaCO_3$ content

The content of $CaCO_3$ in a sedimentary rock is particularly important for helping classify different lithofacies. The term limestone is given to a sample that has a $CaCO_3$ content ≥ 50%. For this analysis, representative samples were powdered so as to ensure their rapid digestion in acid. Both sample and filter paper (Whatman No.2 18.5 cm) were first dried over night at 25ºC. The samples were then left in a well aerated environment (i.e. the fume hood) for at least 1 hour before beginning acid digestion. The filter papers were pre-weighed on a microbalance. 5 grams of sample was placed in a 250 ml beaker and mixed with 1 $molL^{-1}$ HCl in the digestion process. The HCl solution fully covered each sample to ensure a full reaction. The residue from the digestion was filtered and washed down with distilled water. The residue and filter paper were then dried in an oven at less than 60ºC over night and weighed the next day.

To classify samples, the $CaCO_3$ data were plotted together with the terrigenous mud and sand contents in a ternary diagram developed for this study (Fig. 3.1). This gave the samples an appropriate lithological name. Samples containing 50-100% $CaCO_3$ are termed limestone. The relative proportions of terrigenous mud (clay and silt), terrigenous sand and $CaCO_3$ content provide definitions for mudstone and sandstone (Fig. 3.1). Sand size ranges from 63 to 2000 µm and mud size is < 63 µm.

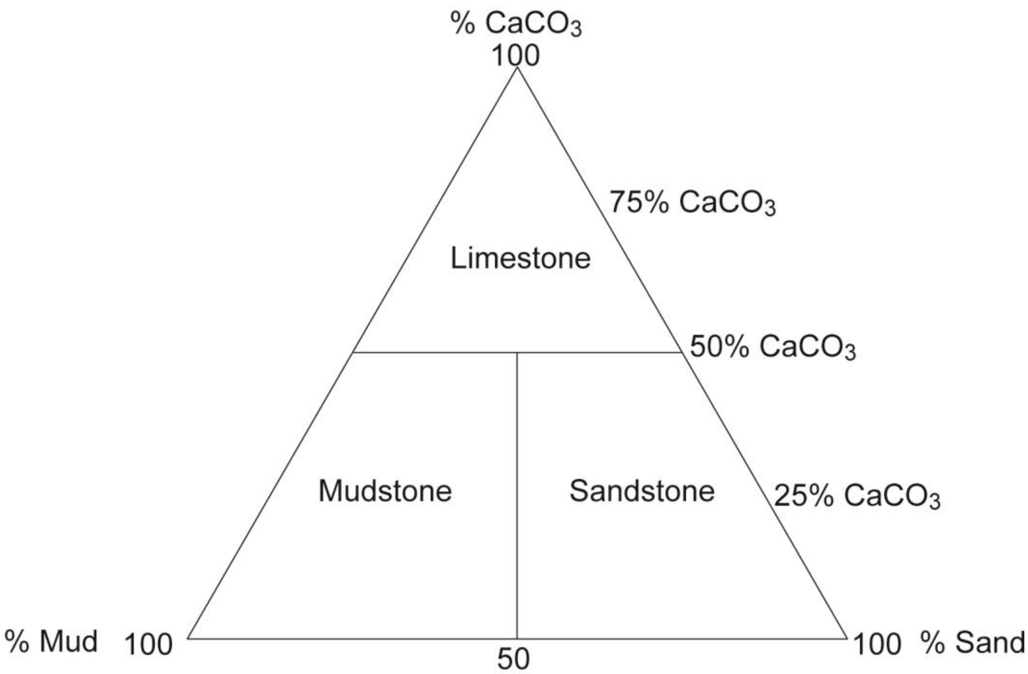

Figure 3.1: Ternary plot developed for field samples uses the $CaCO_3$, terrigenous sand and terrigenous mud content to determine lithological names.

3.4 Grain texture

The texture of non-carbonate (terrigenous) grains was examined in order to assist the lithological description and naming of the Pliocene rocks (Fig. 3.1).

The texture of non-carbonate grains was analysed using a Malvern Mastersizer-S laser particle sizer at the University of Waikato. This analysis used a 300RF mm range lens (0.05 µm-880 µm). All samples were broken down to pea-size chips instead of using the powder which was prepared for $CaCO_3$ analysis which would not have preserved the original grain texture of the rocks. All samples were digested in 1 molL^{-1} HCl acid. The grade scale of particle size proposed by Wentworth (1922) was used here to define the particle sizes. The normally accepted size classes are showing in Table 3.2. The non-carbonate particle-size data were plotted onto a ternary sand-silt-clay diagram (Fig. 3.2) adopted from Boggs (2004).

Table 3.1: Table of Wentworth scale of particle size ranges showing the clay, silt and sand sizes in µm (Wentworth 1922).

Clay	< 3.9 µm
Silt	3.9-63 µm
Sand	63-2000 µm

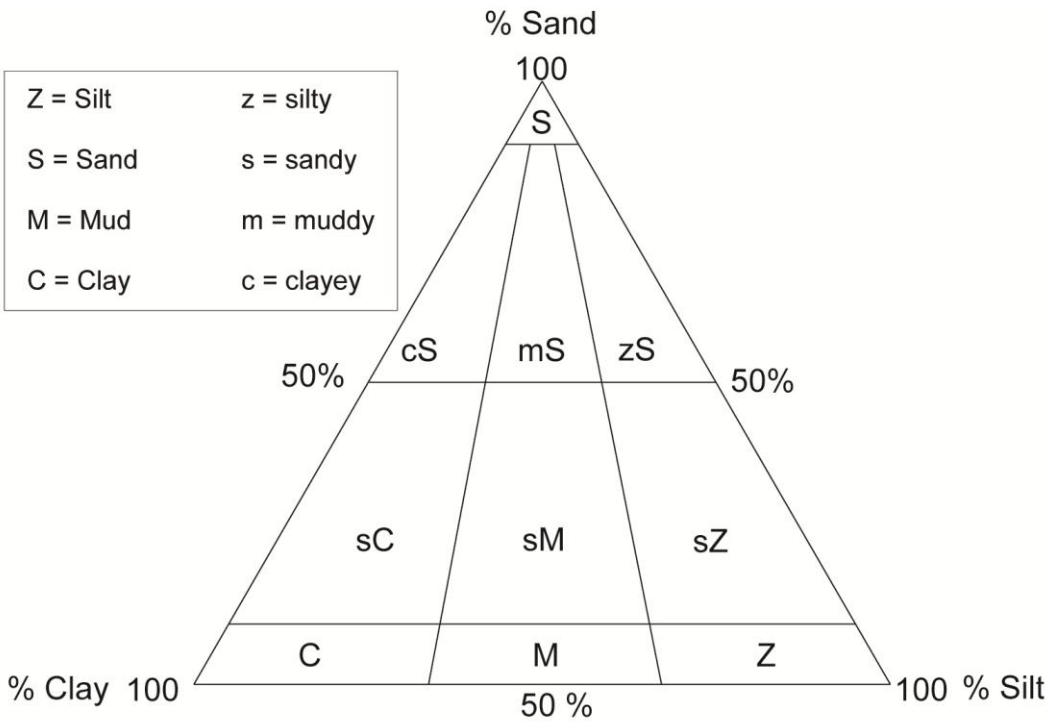

Figure 3.2: Ternary diagram showing terrigenous sample names based on their clay, silt and sand-size particle content (Boggs 2004).

3.5 Stable oxygen and carbon isotopes

The stable isotope composition of carbonate deposits can reflect the composition, salinity and temperature of the host fluids from the environment in which they formed, and the origin of the carbonate source fluids (Nelson & Smith 1996). 21 samples of limestone/calcareous sandstone, including some fossil shell, were analysed for stable oxygen and carbon isotope composition of their carbonate fraction at NIWA in Wellington. The isotope results, along with calculated burial temperatures and depths, are presented in Appendix IV. Five to seven samples from each limestone were selected and powdered, and also one sample from each age diagnostic pectinid fossil (early Opoitian, late Opoitian and Waipipian). Samples were reacted with 3 drops of H_3PO_4 at 75°C in an automated individual-carbonate reaction (Kiel IV) device coupled with a Finnigan MAT253 mass spectrometer. Internal precision of measurements is 0.02-0.08‰ for $\delta^{18}O$ and 0.01-0.06‰ for $\delta^{13}C$, and external precision is 0.03‰ for $\delta^{18}O$ and 0.02‰ for $\delta^{13}C$, relative to vPDB (Pee Dee Belemnite of Cretaceous age). All values are reported relative to vPDB, where $\delta^{13}C$ has a value of +1.95‰ and $\delta^{18}O$ has a value of -2.20‰ for the standard NBS19 calcite. The NBS18 standard was additionally run, due to the material submitted, where $\delta^{13}C$ has a value of -5.014‰ and $\delta^{18}O$ has a value of -23.20‰.

Burial temperatures have been estimated from the bulk $\delta^{18}O$ values using a mean $\delta^{18}O$ value of seawater (VSMOW) of -0.37 for Opoiti Limestone, and -0.02 for Whakapunake and Tahaenui limestones (Cooke *et al.* 2008). The paleo-temperature equation from Shackleton (1967) was used:

$$T\ (°C)=16.9-4.38(^{18}O_{c\text{-}w})+0.1(^{18}O_{c\text{-}w})^2$$

where $^{18}O_{c\text{-}w}$ is the isotope composition of the calcite cement ($^{18}O_{c=bulk\text{-}pectinid}$) minus that of water. Burial depths of the rocks have been derived assuming a starting depositional bottom-water temperature of 12°C. An average geothermal gradient of 24°C/km depth is used, the same as that presented in the Raukumara Basin fact file (NZ Petroleum & Minerals 2011). The results also include the data from Drinnan (2011).

The raw data of both $\delta^{13}C$ and $\delta^{18}O$ were plotted against each other (raw data see Appendix IV). All cross-plot of oxygen and carbon isotope values plots are used to provide clues about the diagenetic environments of alteration of the limestones, such as being meteorically or burial influenced (Nelson & Smith 1996). All cross-plots include also the raw data from Drinnan (2011).

3.6 Thin section preparation

Thin sections were prepared for rock samples using standard procedures. Due to the often poorly cemented and rather friable nature of most of the limestones they were impregnated using araldite to assist thin-section production and to prevent the loss of any pore-lining carbonate cement.

Thin sections were examined under plane polarised light (PPL) and some were also examined under cathodoluminescent light (CL). The usual technique of finishing thin sections on a glass plate with fine carborundum powder was employed for the standard petrography work. For CL petrography, some of the samples were finished on a Buehler Metaserv grinder-polisher, initially using fine grit metallographic paper and then a polishing cloth so that any obvious surface imperfections were removed. All thin sections are stored in labeled boxes and kept in the Advanced Microscope Facility, in the Department of Earth and Ocean Sciences, University of Waikato.

3.7 Petrography

The petrographic work was done at the University of Waikato. Standard PPL and CL petrographic techniques were employed for the determination of the basic textural and compositional properties of the Pliocene limestones. Petrographic observations were made using an Olympus AX70 petrographic microscope, and thin section photomicrographs were taken with a Nikon DXM 1200 digital camera under both plane polarised light (PPL) and cross polarised light (XPL). Skeletal grain identification was aided by the images contained in Scholle and Ulmer-Scholle (2003). Basic petrographic data were recorded on petrographic data sheets (Fig. 3.3) adapted from those used by Nelson (1973), and pictorially summarised in pie/histogram diagrams in Chapters 5 to 7.

Percentage abundance determination of total skeletal grains, total siliciclasts, and cement-matrix were estimated with the aid of the comparator charts published in Scholle & Ulmer-Scholle (2003). Individual skeletal grain and siliciclastic grain type abundances were determined as part of the whole rock composition, and are indicated using a series of abbreviated letters (Fig. 3.4). Grain size was measured using an internal graduated bar scale in the eyepiece, while grain sorting and grain roundness properties were determined with the aid of the comparator charts also published in Scholle & Ulmer-Scholle (2003). Any diagenetic features of note were recorded on the data sheets (see Appendix V).

Petrographic terminology

The term bioclasts refers to the fragmented carbonate shells of marine life forms. The terrigenous components include any non-carbonate, detrital materials, such as quartz, feldspar and rock fragments that survive weathering and are transported to the depositional site as clast. Authigenic materials are those of non-detritus, such as glauconite and pyrite that form *in situ* within the depositional site in response to geochemical processes. Porosity refers to any void between and within in the clastic grains.

Matrix refers to any fine-grained sedimentary materials that are transported to the depositional site; include clay, silt and microbioclasts, in which larger grains are embedded. Cements are calcitic materials that are precipitated around or within carbonate skeletal grains. The dominant cement types are sparite and micrite. Sparite is commonly a diagenetic product that precipitated around or within carbonate skeletal grains from $CaCO_3$ supersaturated pore fluids within rock or sediment. This type of cement can form from both burial and meteoric fluids, and is typically seen in the Pliocene limestones. Micrite cements are often made up from microbioclasts, in which large quantity of highly fragmented shell remains indiscriminately mixed in carbonate mud. Micrite is often associated with low-energy depositional environments that allow time for the very fine-grained materials to settle. Intrinsic fills refer to any materials that infilled pore spaces between grains, while extrinsic fills are materials infill the space within mainly skeletal chambers and borings.

Cathodoluminescent light (CL) petrography

Cathodoluminescence microscopy has become a common tool in petrology studies, revealing diagenetic features that are invisible under conventional transmitted light microscopy. The CL technique is especially useful studying limestones where one may observe the residue radiation emitted by carbonate crystals after excitation by an electron beam. As the cements emit a stable luminescence during the electron bombardment, the conditions of observation can be reproduced. The technique is sensitive to subtle changes in chemical composition and structure of the host crystals, in particular sparite. The colour and intensity of the luminescence are related to the mineralogy of the crystals and the geochemistry of the trace elements incorporated in the crystal lattice, either in interstitial or in substitution positions. These changes are commonly controlled by changes in pore-fluid chemistry. This technique is widely used for elucidating both the growth patterns of cement precipitates and the different stages of cementation (Caron 2002).

Cathodoluminescence petrography was carried out using a CITL (Cambridge Image Technology Limited) cathodoluminescence Mk5-1 instrument, and photomicrographs were taken by Dr Steve Hood using a Nikon D5-5Mc camera. The electron gun current was set at 350 mA and 16 kV.

	Strat Col No.					
	Sample No.					
Bioclasts	**Tot Bioclasts %**					
	Bivalves					
	Barnacles					
	Brachiopods					
	Bryozoans					
	Echinoderms					
	Calc red algae					
	Benthic forams					
	Planktic forams					
	Size: Max					
	Mode 1					
	Mode 2					
	Sorting					
	Abrasion					
Siliciclasts	**Tot Terrigenous %**					
	Quartz					
	Feldspar					
	Rock fragments					
	Mica					
	Clay					
	Size: Max					
	Mode 1					
	Mode 2					
	Sorting					
	Shape					
Authigenic	**Tot Authigenic %**					
	Glauconite pellets					
	Size (av.)					
	Glauconite infills					
	Pyrite grains					
	Size (av.)					
	Pyrite infills					
Diagenetic	**Matrix-Cement %**					
	Intrinsic material					
	Extrinsic material					
	Spar cement					
	Micrite					
	Porosity %					
	Other features					

Figure 3.3: Petrographic data sheet used in this study for recording thin section observations.

Data sheets

Keys used in petrographic analysis

Semi-quantitative abundance limits:

Abbreviation	Description	Percentage
VA	Very abundant	>75
A	Abundant	50 – 75
VC	Very common	25 – 50
C	Common	15 – 25
M	Many	5 – 15
S	Some	1 – 5
R	Rare	< 1
–	Absence	0

Sorting:

EW	Extremely well sorted
W	Well sorted
MW	Moderately – well sorted
M	Moderately sorted
MP	Moderately – poorly sorted
P	Poorly sorted

Shape:

Bioclasts:

UA	Unabraded
U-MA	Unabraded – moderately abraded
MA	Moderately abraded
M-WA	Moderately abraded – well abraded
WA	Well abraded

Siliciclasts:

A	Angular
SA	Sub-angular
SR	Sub-rounded
R	Rounded

Intrinsic and extrinsic cements:

M	Micrite
S	Sparite

Diagenetic features:

NEO	Neomorphic feature
PD	Pressure dissolution
MB	Micro-boring
L	Limonitisation
ISO	Isopachous rind
BIOM	Biomold

Figure 3.4: Abbreviation letters used on petrographic data sheets (Fig. 3.3) include semi-quantitative abundance limits, sorting and shape of both bio- and siliciclastic-grains, content of both intrinsic and extrinsic cement, and additional diagenetic features in samples.

3.8 Petrographic classification for limestones

There is a need for both carbonate and non-carbonate rock classification schemes to satisfy a comprehensive description of the samples in this study. Consistent classification and concise naming of rocks are absolutely essential for effective communication throughout the international scientific community. An ideal classification scheme combines objective, quantifiable description of readily observable features that are grouped into named categories (Scholle & Ulmer-Scholle 2003). The name will reflect the mechanisms of formation, environments of deposition, and the like. There have been a number of carbonate rock classification schemes developed over the last 50 years.

The schemes developed for carbonate rocks have divided them into many classes according to the kind and proportion of skeletons and other allochems, and their texture and cement fabrics. Despite the number of classifications proposed for carbonate rocks, only two, those of Folk (1962) and Dunham (1962), have successfully met the test of time. In this study Folk's (1962) classification is better suited for describing the carbonate rocks in thin sections. It uses multiple descriptive terms with eleven basic names which are generated based on the nature of the grains and the relative abundance of micrite matrix versus open pore spaces (or sparry calcite cement infilling such pores). The ratio of micrite to sparite is deemed to indicate the degree of hydraulic energy of the depositional environment (Fig. 3.5). Another component of the Folk (1959, 1962) classification is based on the textural maturity of samples which considers also the roundness and sorting of the carbonate grains (Fig. 3.6). A third component of the full Folk name relates to the average grain size of the carbonate grains in the rock (Fig. 3.7).

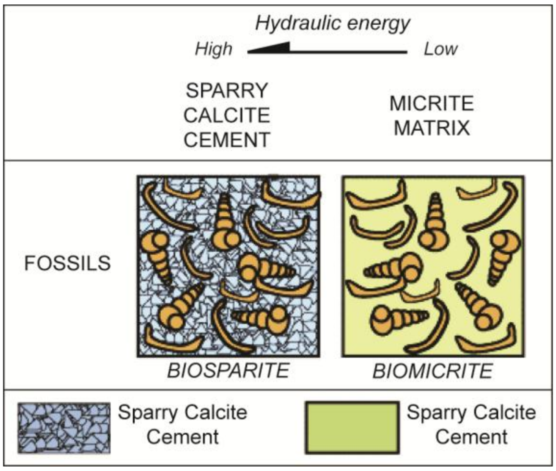

Figure 3.5: Folk’s (1959) classification for fossiliferous carbonate rocks. From Kendall (2005).

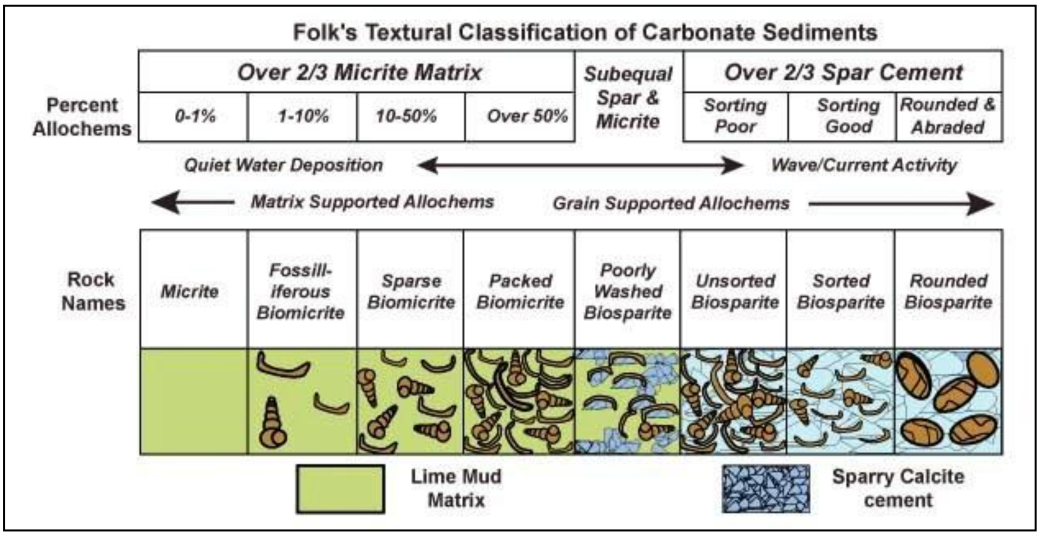

Figure 3.6: A textural spectrum for carbonate deposits defined by Folk (1962).

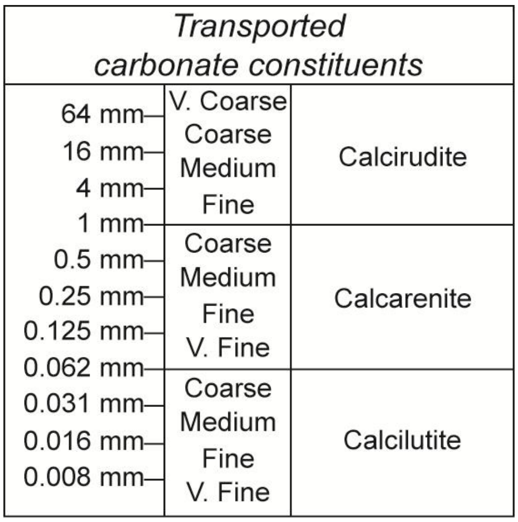

Figure 3.7: A grain-size scale for carbonate rocks defined by Folk (1962). From Scholle & Ulmer-Scholle (2003).

There is also need of an appropriate sandstone classification for the rocks in the study area. The sandstone classification scheme adopted here is from Boggs (2004) (Fig. 3.8). According to Boggs (2004) the sandstone classification is based on the abundances of three mineral components: Q (quartz), F (feldspar) and L (lithic grains, rock fragments). Percentage of argillaceous matrix is represented by a vector extending towards the rear of the ternary diagram. The term arenite is restricted to rocks consisting of 5% or less matrix; sandstones containing more matrix are wackes (Boggs 2004). This scheme is modified from Dott (1964) and Folk *et al.* (1971), and uses appropriate terminologies to describe the ratio of abundance of quartz, feldspar and lithics (Fig. 3.8).

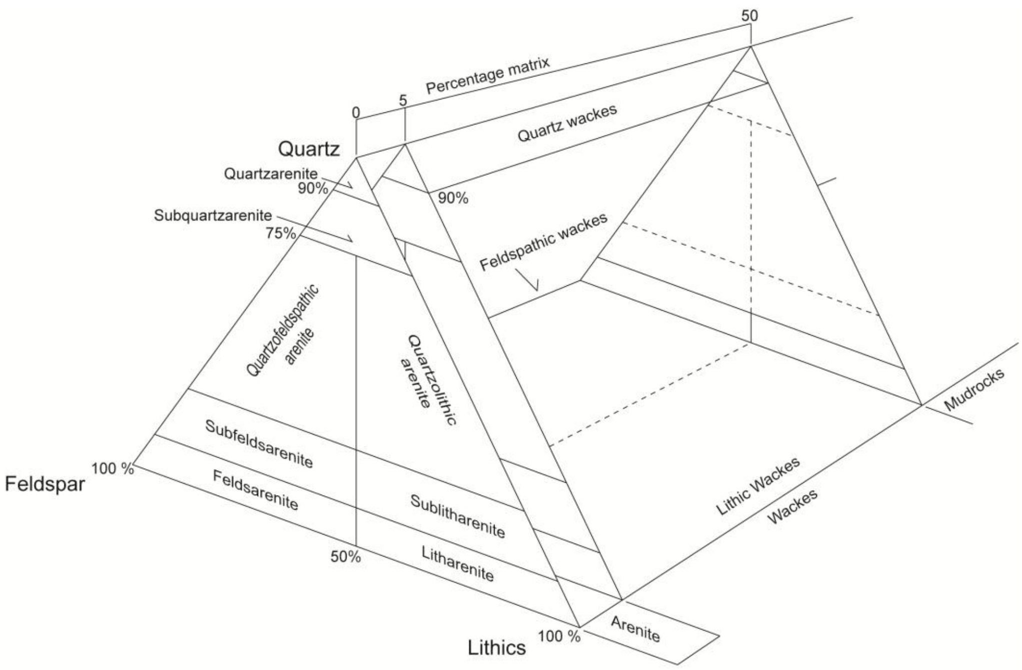

Figure 3.8: Classification scheme for sandstones. Modified from Dott (1964) and Folk *et al.* (1971).

4 Chapter Four

Pliocene stratigraphic nomenclature and lithofacies

4.1 Introduction

The purpose of this chapter is to appropriately define the stratigraphic nomenclature for the Pliocene deposits in the study area, and to establish a lithofacies scheme for their characterisation. This should assist with better understanding the geological evolution of the Pliocene succession in the northern part of the forearc basin seaway.

4.2 Stratigraphic nomenclature

The current lithostratigraphic nomenclature for the Pliocene deposits in the northern Hawke's Bay has been amended in this study to better order and rationalise the Pliocene stratigraphy. Figure 4.1 summarises the lithostratigraphic nomenclature used in this study in comparison to that advanced by Field *et al.* (1997).

Firstly, it is inappropriate to use the name Opoiti for both a member (i.e. Opoiti Limestone Member) and the enclosing formation (i.e. Opoiti Formation) (Hedberg 1976). The proposal here is to elevate the name Opoiti Limestone to formation status, as the oldest of three limestone formations within the Pliocene Mangaheia Group. The name Opoiti Limestone is used despite the highly variable $CaCO_3$ content of the unit, varying from about 30-70%, so that it ranges from sandy limestone to bioclastic sandstone facies. Nevertheless, like the two other younger limestones formations, the Opoiti Limestone is both coarser grained and better cemented than the immediately bounding strata (typically mudstone) and, as a consequence, protrudes prominently in the landscape as a 'cliffline' escarpment typical of the Te Aute limestones in general. So the Opoiti Limestone is a continuously mappable unit at the surface and is also traceable in the subsurface.

The formation names Tahaenui Limestone and Whakapunake Limestone are retained in this study for the younger Pliocene limestones.

There is a need to find a new name for the former Opoiti Formation now that the term ‘Opoiti’ has been restricted here to the lower carbonate bearing unit. The original Opoiti Formation involved principally mudstones (plus muddy sandstones) above the Opoiti Limestone but below the Whakapunake or Tahaenui Limestones. Pliocene mudstones below the Opoiti Limestone were assigned to the Mapiri Formation (late Kapitean-early Opoitian), and those above the Tahaenui Limestone to the Wairoa Formation (Waipipian or younger). However, the three limestones have lensoidal geometries on a range of scales and are typically surrounded by and encased by mudstones, so that it becomes difficult to know which mudstone formation name is appropriate to apply. Moreover, since the mudstones are all lithologically very similar it makes sense to assign them the same name. In this study, the name Wairoa Formation is chosen for the Pliocene age siliciclastic-dominated successions in which the three limestones are encased. If desired, the three limestones can be used to subdivide the Wairoa Formation into (A), (B), (C) and (D) portions, as conceptually portrayed in Fig. 4.2. The potential for subdividing the Wairoa Formation into members of mudstone and sandstone remains, but is not considered in this study. The stratigraphic nomenclature changes made here necessitate a small redefinition of the Mangaheia Group now incorporating only Pliocene strata in the study area, while the Tolaga Group no longer includes any Pliocene deposits (Fig. 4.1).

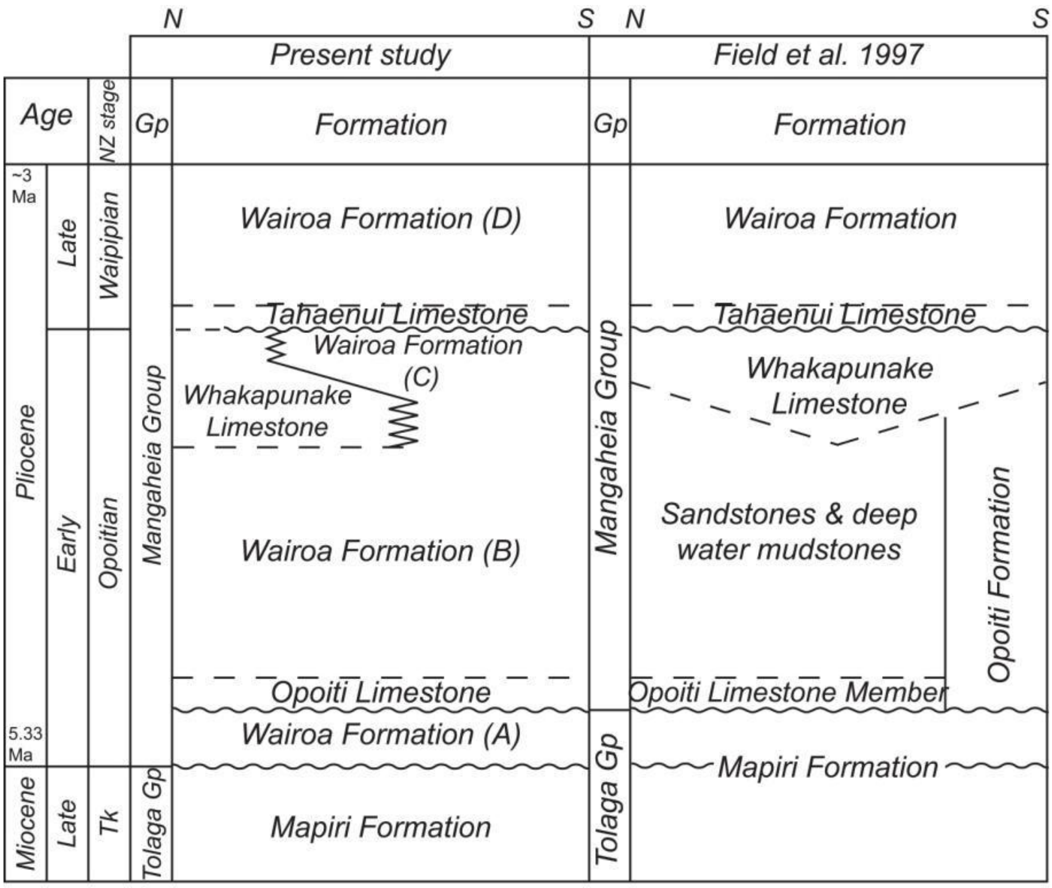

Figure 4.1: Comparison of formational nomenclature formerly applied to the latest Miocene and Pliocene strata of the study area (adapted from Field *et al.* 1997) and that used in the present study.

4.3 Lithofacies

A facies classification for the Pliocene deposits in the northern Hawke's Bay region has been developed in combination with the study by Drinnan (2011). It was our intention to create a simplified facies classification which is able to incorporate all the Pliocene strata in the northern Hawke's Bay. The facies recognised in Drinnan's (2011) area in the wider Mahia area included three facies types which are not present in the present Wairoa study area. The facies classification, developed from field outcrop observations and descriptions of the litho-units, is shown in Table 4.1. The main distinguishing features are the physical characteristics of colour, lithology, texture and sedimentary structures, as well as relative carbonate content. There are twelve additional characteristics included to assist further detailed description of each lithofacies. The fossil content is not considered a major part of the facies descriptions in this case. The various facies have been assigned facies codes for ease of reference on the stratigraphic columns and elsewhere (Table 4.1). It is likely that each lithofacies reflects a particular depositional environment. This study has identified three main lithofacies groups (limestone, sandstone and mudstone) with a total of 9 lithofacies types to encompass the entire Pliocene Mangaheia Group strata in the northern Hawke's Bay region (Table 4.1).

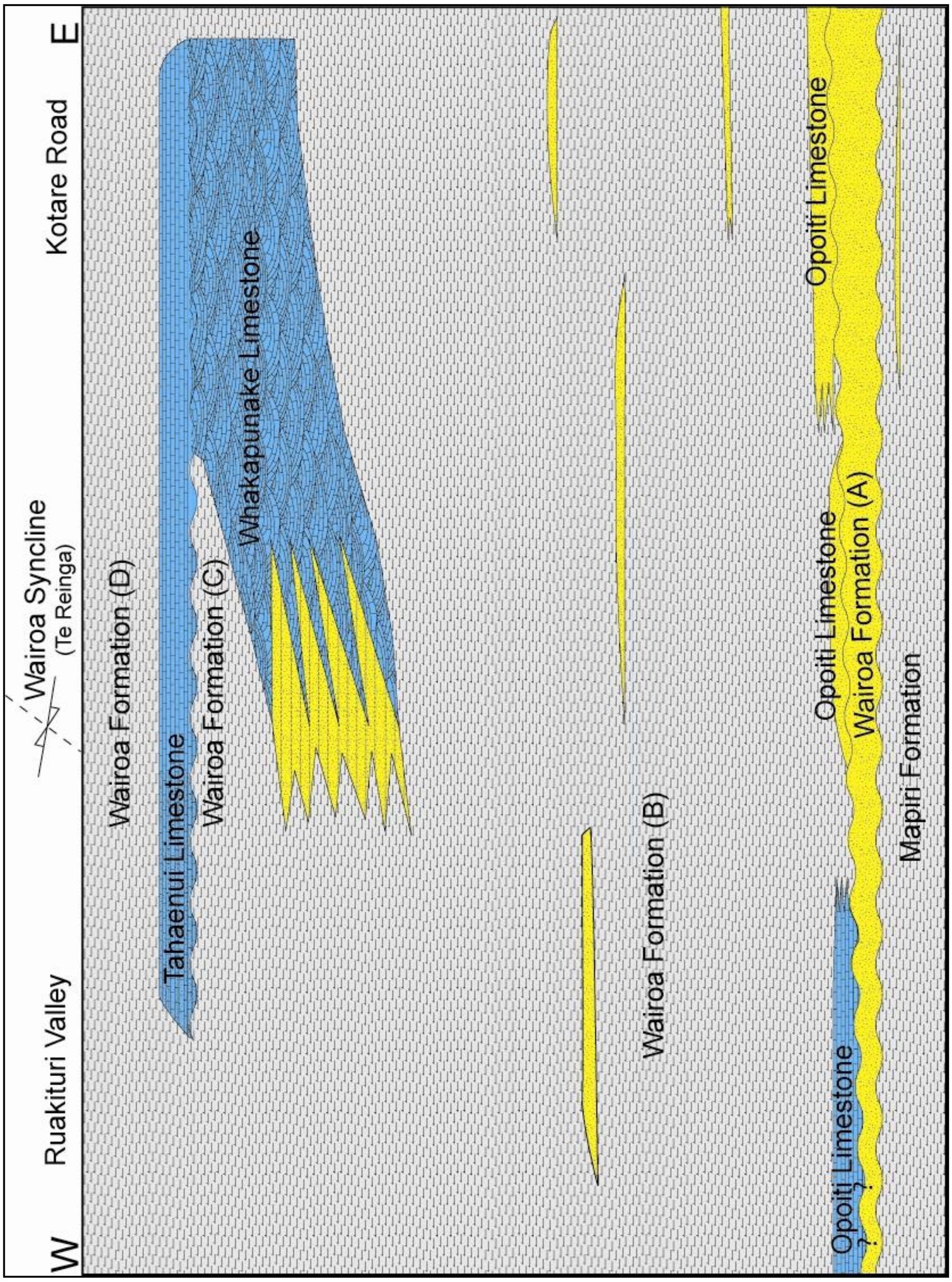

Figure 4.2: Conceptual diagram of the depositional fill from W to E across the Wairoa Syncline.

Table 4.1: Summary of sedimentary lithofacies established for the Pliocene strata in the vicinity of Wairoa, northern Hawke's Bay.

Lithofacies	Description	Other features
Limestone		
L1 Bioclastic limestone	Massive to poorly bedded, variably indurated, barnacle-rich pure limestone	
L2 Coquina	Sandy limestone with indurated coquina shell beds	Hb - Horizontal bedding Xb - Giant cross bedding S - Siliciclastic rich Mc - Mudstone clasts (<5 mm) G - Glauconite rich Gl - Glauconite laminae Bra - Brachiopod rich Biv - Bivalve rich P/O - Pectinid / oyster rich Bio - Bioturbation Bor - Boring Fe - Iron stained
L3 Sandy limestone	Massive to poorly bedded, moderately indurated, mixed siliciclastic-bioclastic limestone	
Sandstone		
S1 Calcareous sandstone	Massive, moderately indurated, calcareous fine sandstone	
S2 Bioclastic sandstone	Thickly bedded, moderately indurated, fossiliferous fine sandstone, with common macrofossils 1 - 2 cm in size	
S3 Volcaniclastic sandstone	Non-calcareous, volcaniclastic fine sandstone	
Mudstone		
M1 Massive mudstone	Massive, weakly to moderately indurated, calcareous mudstone	
M2 Bedded mudstone	Differentially cemented (20 - 30 cm thick), weakly to moderately indurated, highly calcareous mudstone	
M3 Fossiliferous mudstone	Massive, weakly indurated, fossiliferous mudstone	

4.3.1 Limestone lithofacies

Three limestone facies (L1-L3) have been identified within the Pliocene barnacle-dominated limestones (Table 4.1). These are the major facies types in the three carbonate-rich units in the study area – Opoiti Limestone, Whakapunake Limestone and Tahaenui Limestone. The carbonate content of these facies varies from 65 to 85%, thus from sandy/impure limestone to pure limestone. The limestone facies comprise variable amounts of skeletal grain types and siliciclastic materials. The facies commonly contain a conspicuous quantity of barnacle plates and fragments, and locally can also be brachiopod-rich. The degree of cementation across the facies is highly variable, from friable to well lithified. According to Kamp *et al.* (1988), the barnacles represented in Hawke's Bay Te Aute limestone facies more widely are *Notobalanus vestitus* (Darwin), *Austrimegabalanus* (*Notomegabalanus*) *miodecorus* Buckeridge and *A. decorus argyllensis* Buckeridge, *Fosterella tubulatus* (Withers), and *Balanus variegates* Darwin (Buckeridge 1983). The same species probably contribute to the limestone facies in the present day study area as well. The presence of L1 and L2 facies is restricted to the two younger carbonate units, the Whakapunake Limestone and the Tahaenui Limestone, while L3 is almost exclusively the facies building the Opoiti Limestone, with the exception of the basal coquina facies L2. Both Whakapunake Limestone and Tahaenui Limestone share many lithofacies characteristics, and there is no speciation event separated the Opoitian and Waipipian forms of *Phialopecten* (Beu 1995), and so they can be difficult to tell apart in some places.

Bioclastic limestone L1

This facies consists almost entirely of carbonate skeletons and cement, including in exploration cores retrieved from the vicinity of Wairoa. The $CaCO_3$ content often reaches over 70-80%. The facies is generally coarse, shelly and very porous, with usually only of small amounts (<5%) of siliciclastic grains. The carbonate grains are mostly barnacle fragments. The facies commonly includes disarticulated valves and fragments of *Phialopecten marwicki.* Facies L1 is massive to weakly bedded (Fig. 4.3A & B). Where fresh, the facies appears bluish grey in colour and moderately to highly indurated. More commonly outcrops are variably weathered with a pale cream to light brown colour and less indurated (Fig. 4.3C). This facies overlies L2+S1 at the section along the farm track at the end of Kotare Road (Fig. 4.3B). Pectinids date the facies as occurring from late Opoitian to Waipipian age.

Coquina L2

Coquina is a common carbonate lithofacies in the Te Aute type limestones in the wider Hawke’s Bay region of the eastern North Island (Nelson *et al.* 2003). The facies consists of mainly barnacle plates and disarticulated epifaunal bivalve shells of *Phialopecten marwicki* and *Crassostrea ingens* (Fig. 4.3D & E), but also variable amounts of siliciclastic material. A juvenile pectinid of *Phialopecten marwicki* (c. 3-5 cm across; Fig. 4.3F) was found at the limestone scarp along Tiniroto Road, north of Te Reinga. The differentially cemented limestone below the massive to weakly bedded limestone here is likely to be Whakapunake Limestone (Fig. 4.3G). Facies L2 commonly occurs as indurated and thin discrete coquina beds (c. 10-25 cm thick) within the differentially cemented and giant planar cross-bedded outcrops in both the Whakapunake and Tahaenui limestones (Fig. 4.3G). It is commonly interbedded with S1 sandstone facies.

Sandy limestone L3

This lithofacies type almost exclusively belongs within the Opoiti Limestone in the study area. It comprises typically massive to poorly bedded, light to dark brown, moderately indurated, glauconite-rich, mixed siliciclastic-bioclastic limestone (Fig. 4.4A). Disarticulated pectinid shells and fragments of *Towaipecten ongleyi* are common components (Fig. 4.4B). Facies L3 may also include common *Neothyris aff. obtuse* brachiopods and occasional *Tucetona lacticostata* bivalves (Fig. 4.4A). The $CaCO_3$ content ranges from 60-65%. Facies L3 is found only in the ridge exposure on either side of the Ruakituri River, on the western limb of the Wairoa Syncline. At other places the Opoiti Limestone grades into fossiliferous sandstone with abundant pectinids of *Towaipecten ongleyi* and brachiopods.

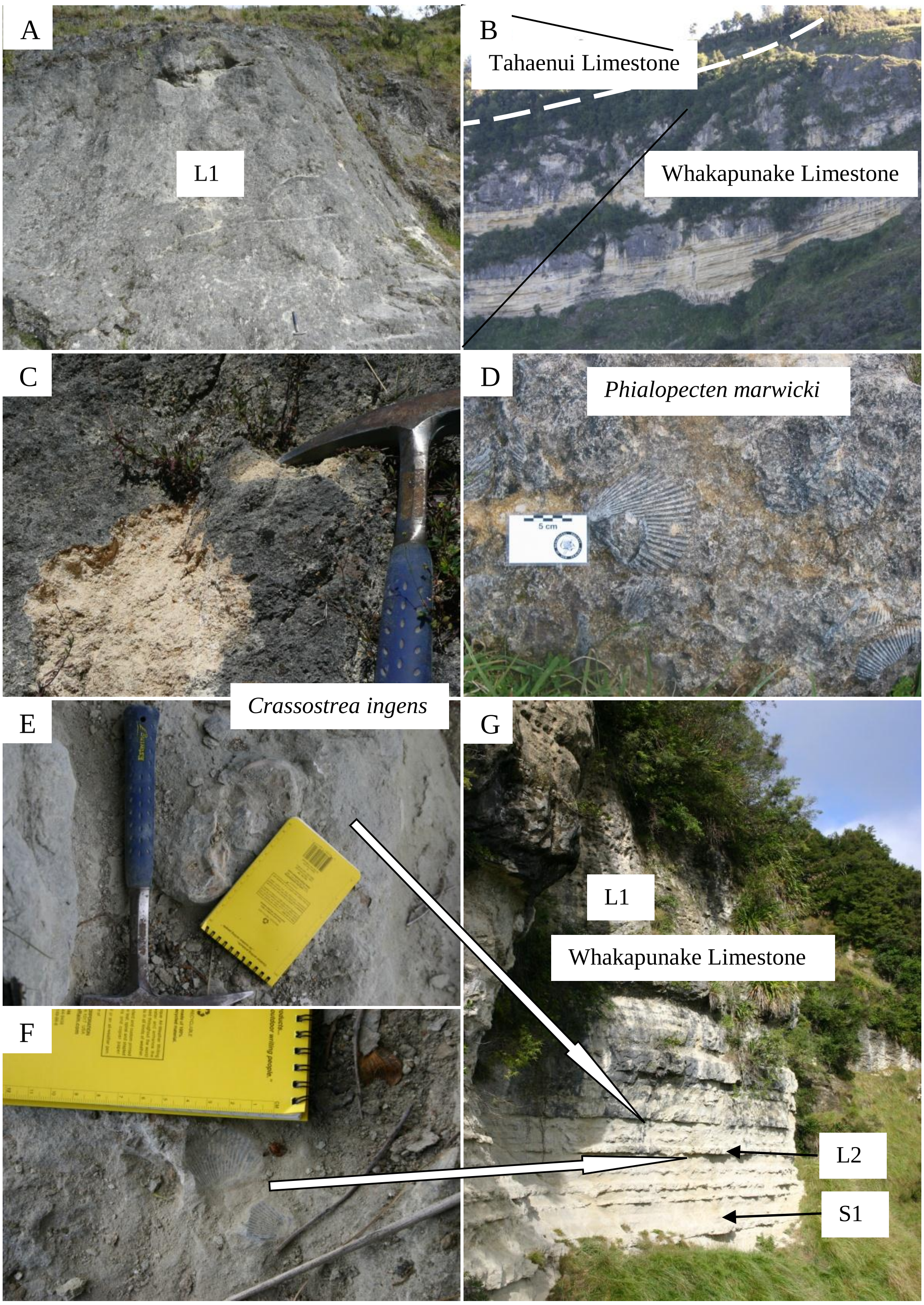

Figure 4.3: A & B) Typical outcrop of massive barnacle and bivalve-rich Tahaenui Limestone (L1) unconformably overlying the differentially cemented coquina beds and calcareous sandstone of Whakapunake Limestone (L2+S1). Photo location: type locality of the Whakapunake Limestone at Haupatanga Gore X19/042468. C) Close up shot of the Tahaenui Limestone, a pale orange colour, slightly weathered, coarse grained barnacle and bivalve-rich limestone (L1) facies, with a dark coloured case-hardened surface. Same location as Fig. 4.3A. D) Figure shows abundant age diagnostic adult pectinids of the Waipipian *Phialopecten marwicki* in Tahaenui Limestone. Location X19/033464. E) The oyster *Crassostrea ingens* within the Tahaenui Limestone (L2), found exposed in the scarps along the Tiniroto Road, north of Te Reinga. Location X18/037550. F) Juvenile *Phialopecten marwicki* occurs at the same locality as in E. Beu (1995) assigned the juvenile pectinids to late Opoitian age, and belongs to the Whakapunake Limestone. At this locality the Tahaenui Limestone may conformably overlie the Whakapunake Limestone. Location X18/037550. G) Differentially cemented limestone, possibly the Whakapunake Limestone, with interbeds L2 and S1, and overlain by Tahaenui Limestone (L1) facies. Location as in Fig. 4.2E.

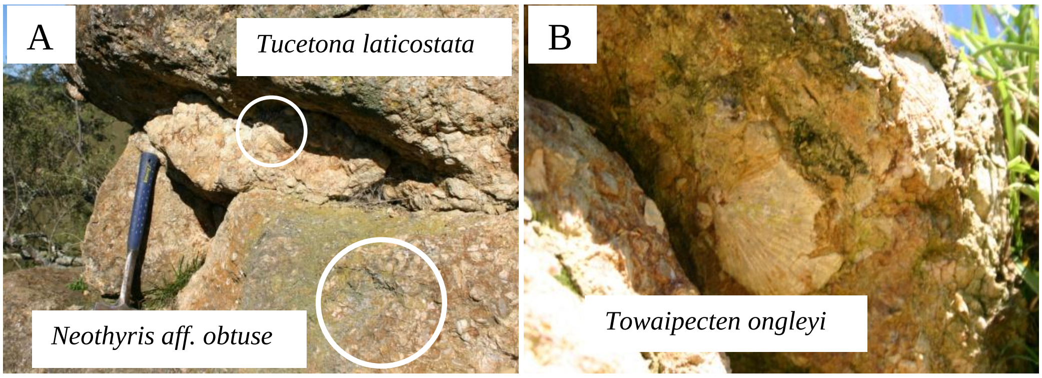

Figure 4.4: A) Typical ridge exposures of Opoiti Limestone in the Ruakituri Valley, on the western limb of the Wairoa Syncline. Figure shows an abundance of the barnacles *Neothyris aff. obtuse* and the bivalves *Tucetona laticostata* in L3. Location X18/958576. B) Typical age diagnostic early Opoitian pectinid of *Towaipecten ongleyi,* about 8-10 cm across, cemented in L3. Location as in Fig.4.4A.

4.3.2 Sandstone lithofacies

Three siliciclastic sandstone lithofacies have been defined for the sedimentary succession in the study area (Table 4.1). They make up a significant proportion of the sedimentary succession in the Wairoa Syncline. The siliciclastic sandstone facies are variable in their thickness, composition and texture. They form massive and thick (4 m) early Opoitian sandstone within Wairoa Formation A and also less indurated, thin (5-10 m) siliciclastic interbeds within the late Opoitian–Waipipian limestone formations. The sandstone facies comprise variable amounts of skeletal and authigenic materials, and have $CaCO_3$ contents ranging from about 30-40%.

Calcareous sandstone S1

Facies S1 is the most widely distributed of the sandstone facies. It often forms an important constituent of the two younger (Whakapunake and Tahaenui) limestone formations. It also occurs as thick and massive early Opoitian sandstones in outcrop. The facies is moderately calcareous (40%), moderately indurated and locally fossiliferous. Facies S1 is variable in texture (from silt to fine sand size) and thickness, ranging from tens of centimetres to a few metres thick. It is often unconformably overlain by any of the three limestone facies, with the contact zone showing evidence of mild to strong bioturbation or burrowing (Fig. 4.5A).

Bioclastic sandstone S2

This lithofacies consists of thick massive to weakly bedded fossiliferous sandstone, often dark brown in colour and moderately to highly indurated. The vaguely bedded sandstone seemingly comprises amalgamated units, each about 0.5-1 m thick, separated presumably by diastems. Facies S2 mostly occurs as the lateral extent of the Opoiti Limestone on the eastern limb of the Wairoa Syncline and in the northernmost outcrops (Fig. 4.5B & C). However, an isolated occurrence was also identified at the section above the Hangaroa River (Fig. 4.5B). The facies often has a glauconite content up to 20%.

Volcaniclastic sandstone S3

The volcaniclastic sandstone facies is a light grey to light brown, structureless, weakly indurated, fine tuffaceous sandstone. It often forms thin and discontinuous beds or lenses (c. 20-30 cm thick) encased within massive mudstone facies (Fig. 4.5D). The origin of these tuff beds is associated with the eruptions generated from Coromandel Volcanic Zone during the Pliocene (5.33-2.59 Ma). All the tuff beds encased within the Mangaheia Group correlate to the particular period of time when Waihi-Kaimai Volcanic Centres' were active. Therefore, these tuff beds are most likely to be the distal fall deposits from eruptions from the Waihi-Kaimai Volcanic Centres (Briggs *et al.* 2005).

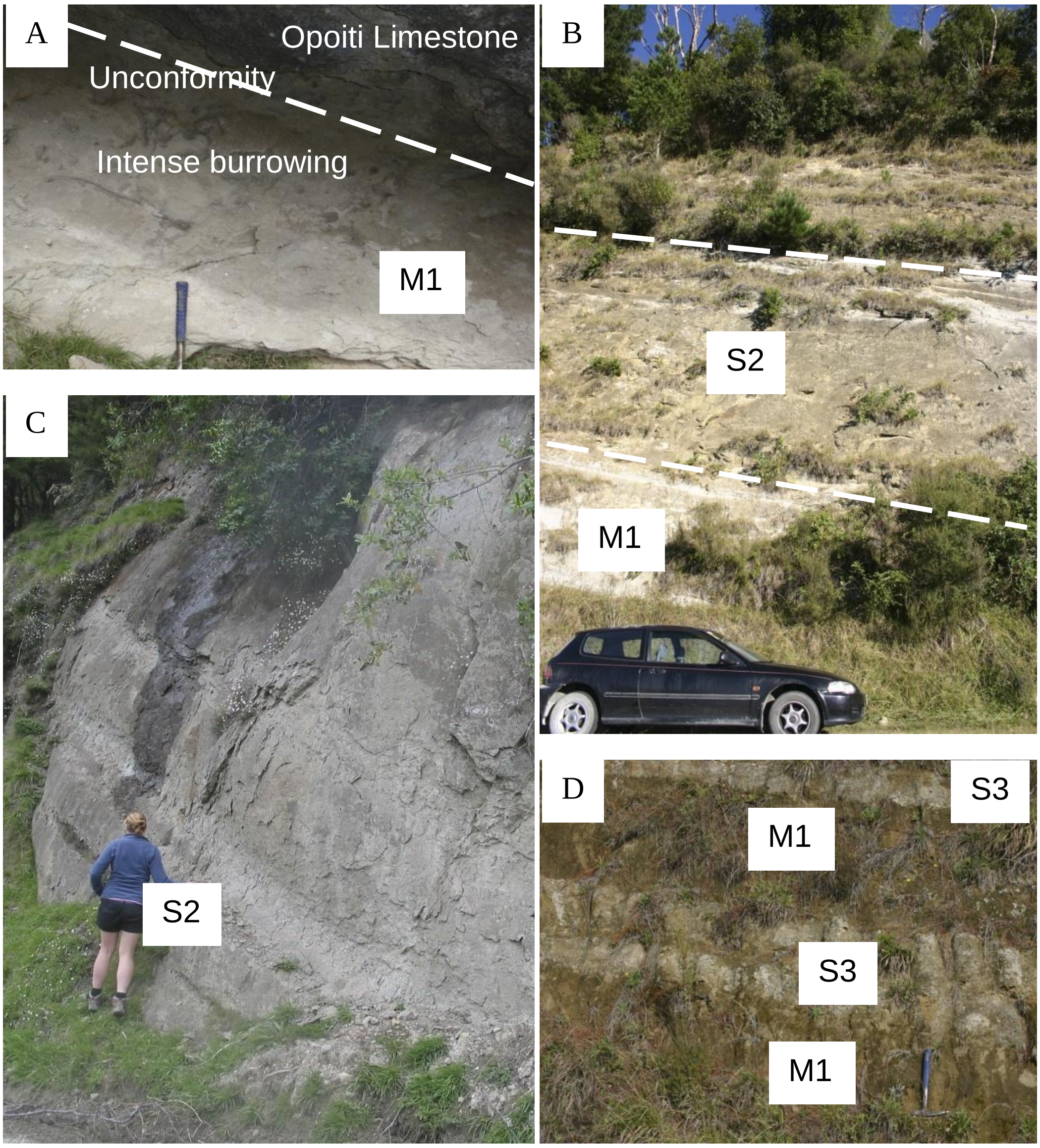

Figure 4.5: A) Massive calcareous sandstone (S1) of early Opoitian Wairoa Formation A is unconformably overlain by the Opoiti Limestone at the limestone type locality. Figure shows moderate to strong burrowing directly below the unconformity. Location X19/062450. B) Massive to weakly bedded, indurated bioclastic sandstone (S2) of Wairoa Formation B gradationally and conformably overlies the calcareous mudstone (M1) in outcrop above the Hangaroa River. Location X18/098658. C) Weakly bedded, moderately indurated bioclastic sandstone (S2) facies of the Opoiti Limestone exposed at the type locality along Mangapoike Road. Location X19/061451. D) Thin beds and lenses of soft volcaniclastic sandstone (S3) of Wairoa Formation B encased within massive calcareous mudstone (M1) along the Parikanapa Road, north of the Whakapunake Trig. Location X18/105594.

4.3.3 Mudstone lithofacies

The mudstone lithofacies is the dominant lithology in the Pliocene Mangaheia Group in the study area, and is often associated with roadside slips in the region. Three mudstone lithofacies types have been identified (Table 4.1). These facies are about 200-300 m thick, and are generally bluish grey in colour, weakly indurated, and slightly fossiliferous in outcrop. They have typically been thoroughly bioturbated. Some show differential cementation. Master bedding surfaces are common feature occurrences within the mudstone facies. The contacts between most of the mudstone facies and their bounding lithofacies are mainly gradational.

Massive mudstone M1

This facies comprises bluish grey, thick (c. 200-300 m), massive and frittery weathering, weakly to moderately indurated calcareous mudstone. Facies M1 is found commonly throughout the siliciclastic-dominated Wairoa Formation, in particular Wairoa Formation A (Fig. 4.6A&B).

Bedded mudstone M2

This facies comprises differentially cemented, thinly bedded (20-30 cm thick), weakly to moderately indurated calcareous mudstone. It is an easily identified lithofacies in the stratigraphy, often forming impressive bluffs (Fig. 4.6C). Facies M2 is mostly noticeable at the Haupatanga Gorge. Here it is disconformably overlain by the L1+L2+S1 facies (Whakapunake Limestone) and dips at 16-18º towards the west (Fig. 4.6C).

Fossiliferous mudstone M3

This facies comprises massive, bluish grey to light grey, weakly indurated, fossiliferous mudstone. The bivalve *Tucetona laticostata* and gastropod *Stiracolpus* sp. dominate the faunal content, with occasional specimens of the pectinid *Phialopecten.* Facies M3 typically represents the gradational zone between a carbonate-rich facies and the mudstone facies (Fig. 4.6D).

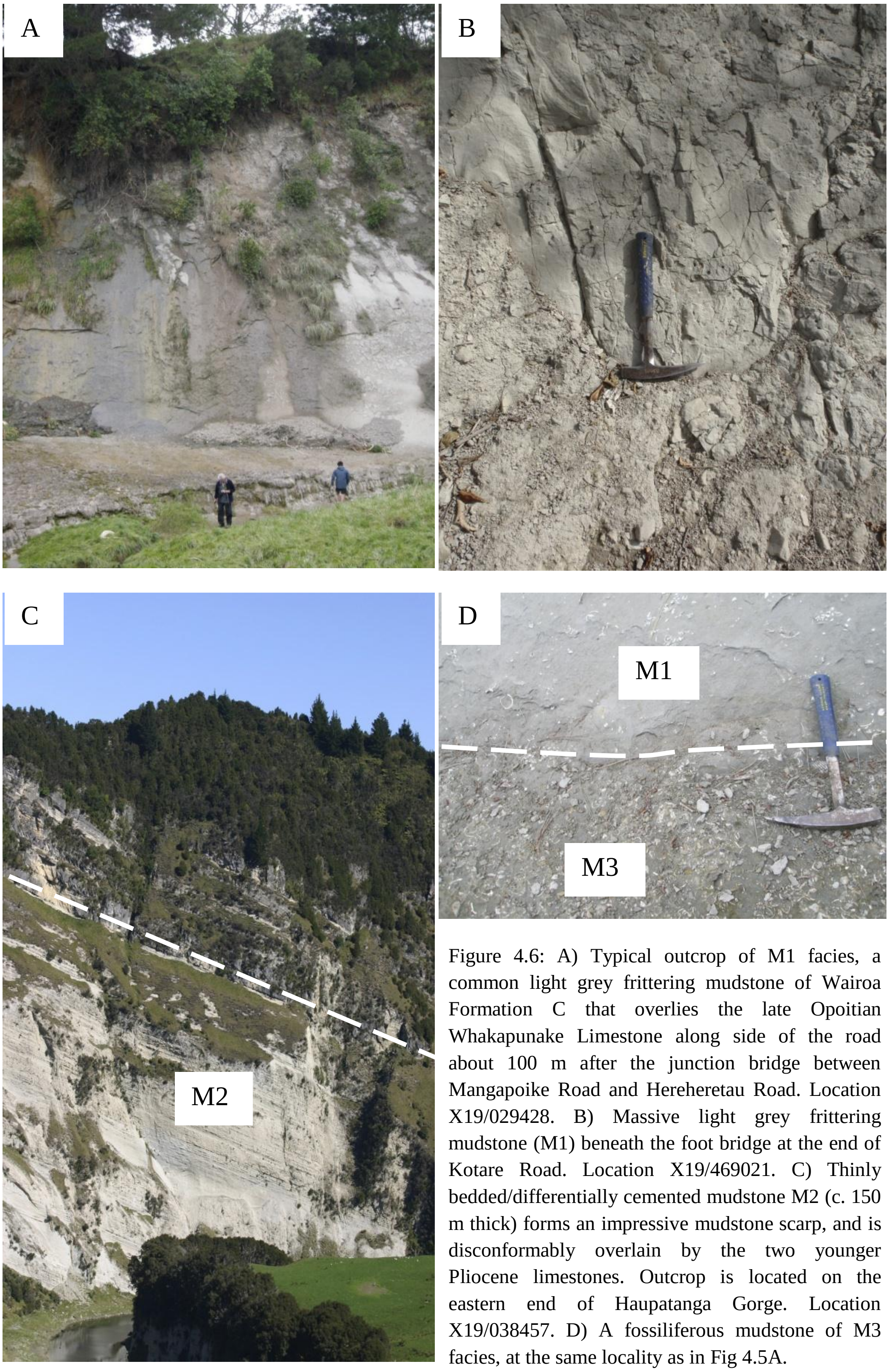

Figure 4.6: A) Typical outcrop of M1 facies, a common light grey frittering mudstone of Wairoa Formation C that overlies the late Opoitian Whakapunake Limestone along side of the road about 100 m after the junction bridge between Mangapoike Road and Hereheretau Road. Location X19/029428. B) Massive light grey frittering mudstone (M1) beneath the foot bridge at the end of Kotare Road. Location X19/469021. C) Thinly bedded/differentially cemented mudstone M2 (c. 150 m thick) forms an impressive mudstone scarp, and is disconformably overlain by the two younger Pliocene limestones. Outcrop is located on the eastern end of Haupatanga Gorge. Location X19/038457. D) A fossiliferous mudstone of M3 facies, at the same locality as in Fig 4.5A.

5 Chapter Five

Opoiti Limestone

5.1 Introduction

This chapter describes for the first time in a moderately comprehensive way the lithostratigraphy, petrology and geochemical characteristics of the Opoiti Limestone (Early Pliocene) deposits in northern Hawke's Bay. The Opoiti Limestone is the oldest of three carbonate-rich units within the Pliocene Mangaheia Group (redefined in this study). Stratigraphic columns were constructed and representative samples of the Opoiti Limestone were collected in the field for laboratory-based petrological work. The stratigraphic columns are presented in Appendix I, which includes definition of all the symbols used on the columns. The laboratory data presented in this chapter for the Opoiti Limestone include standard and cathodoluminescence (CL) petrography, bulk X-ray diffraction, and $CaCO_3$ and grain size analysis results.

5.2 Name and definition

The name Opoiti Limestone is derived from a small settlement about 1 km north of the junction of Tiniroto Road and Kotare Road, west of the Haupatanga Gorge, in northern Wairoa (X19/998481). Beu *et al.* (1980) assigned Opoiti Limestone as a member and the lowest unit of earliest Opoitian age within the Opoiti Formation (redefined as part of the Wairoa Formation in this study), which was later adopted by Field *et al.* (1997). The Opoiti Limestone crops out on both sides of the Wairoa Syncline in the northern Wairoa district. A similar aged limestone, also named Opoiti Limestone, is identified to the east on Mt Moumoukai and along the coastal area on the W and SW side of Mahia Peninsula (Beu 1995; Field *et al.* 1997; Drinnan 2011). The detailed distribution of the limestone is presented later in this chapter.

The Opoiti Limestone contains the age diagnostic pectinid fossil *Towaipecten ongleyi* found in early Opoitian deposits throughout eastern North Island, from Poverty Bay in the north to northern Wairarapa in the south (Beu *et al.* 1980). Other age correlative limestones from outside the present study area are shown in Table 5.1, and include the Ormond Limestone near Gisborne, the Maungaharuru Limestone and Kairakau Limestone within the Titiokura Formation in the central and southern Hawke’s Bay, and the Haurangi Limestone near Martinborough, in southern Wairarapa (Vella & Briggs 1971; Beu *et al.* 1980; Morris 1982; Wells 1989; Bland *et al.* 2004b). In early oil and gas exploration reports the Opoiti Limestone has been called Otamaharua Limestone and Parikanapa Limestone (Beu 1995).

Table 5.1: Early Pliocene age Te Aute limestone units in the eastern North Island, New Zealand (based on Beu 1995; Field *et al.* 1997; Nelson *et al.* 2003). The limestones listed below are part of the widely distributed early Opoitian lateral correlatives that contain the age diagnostic pectinid fossil *Towaipecten ongleyi*.

Age	New Zealand stage and abbreviation	Limestone formation
Early Pliocene	Early Opoitian (Wo)	Ormond, Kairakau, Maungaharuru, Haurangi, Opoiti

The Mangapoike River section has been previously noted in other studies. Edwards (1987) regarded this section as one providing a complete biostratigraphic record of strata from the Late Miocene through most of the Pliocene period, spanning the uppermost part of the Tolaga Group and the Mangaheia Group. The Opoiti Limestone is here treated as the lowest limestone formation within the Pliocene Mangaheia Group, otherwise dominated by shelfal mudstone, sandstone, and thin lensoidal tuff beds. The Pliocene sedimentary record is separated from the underlying Late Miocene (Tongaporutuan–Kapitean) bathyal mudstone and sandstone of the Mapiri Formation by a regional unconformity (Field *et al.* 1997). In the Mangapoike River section the Opoiti Limestone is a 10 m thick, moderately indurated, sandy, shelly, massive to poorly-bedded fossiliferous sandstone with abundant *Towaipecten ongleyi*, which is conformably overlain by 700-800 m of differentially cemented mudstone and sandstone. In this study, Opoiti Limestone is defined as a massive, dark brown to grey, bioclastic sandstone to sandy limestone formation, which unconformably overlies shelfal mudstone and sandstone successions assigned to Wairoa Formation A. The thickness of Wairoa Formation A ranges widely from c. 3 m to nearly 220 m throughout the study area.

5.3 Type locality and reference sections

Beu (1995) formally defined the Opoiti Limestone and established a type locality (X19/061451) as the outcrops on either side of the deeply entrenched Mangapoike River, 2.5 km upstream from the junction with Makaretu Stream (Fig. 5.1). This section represents the easternmost outcrop of the Opoiti Limestone in the present study area. Here the limestone rests unconformably on the Early Kapitean-Late Opoitian sandstone and mudstone formerly assigned to the Mapiri Formation by Beu (1995). The Pliocene portion of the Mapiri Formation is now assigned to the Wairoa Formation A (new name, Fig. 5.2). The upper boundary of the limestone is not exposed at most of the outcrops, but is gradational at the section above the Hangaroa River (Fig. 5.3). The lower part of the limestone is reasonably accessible, and Beu (1995) designated a reference section at the lower falls of the Makaretu Stream alongside Hereheretau Road, 4 km east of the junction with Mangapoike Road (X19/051417), although this site was not visited in the present study.

Figure 5.1: Steeply dipping (c. 30º) Opoiti Limestone type locality, 2.5 km upstream from the junction with Makaretu Stream, in the deeply entrenched Mangapoike Valley. The limestone unconformably overlies the Wairoa Formation A (formerly Mapiri Formation). Location X19/061451.

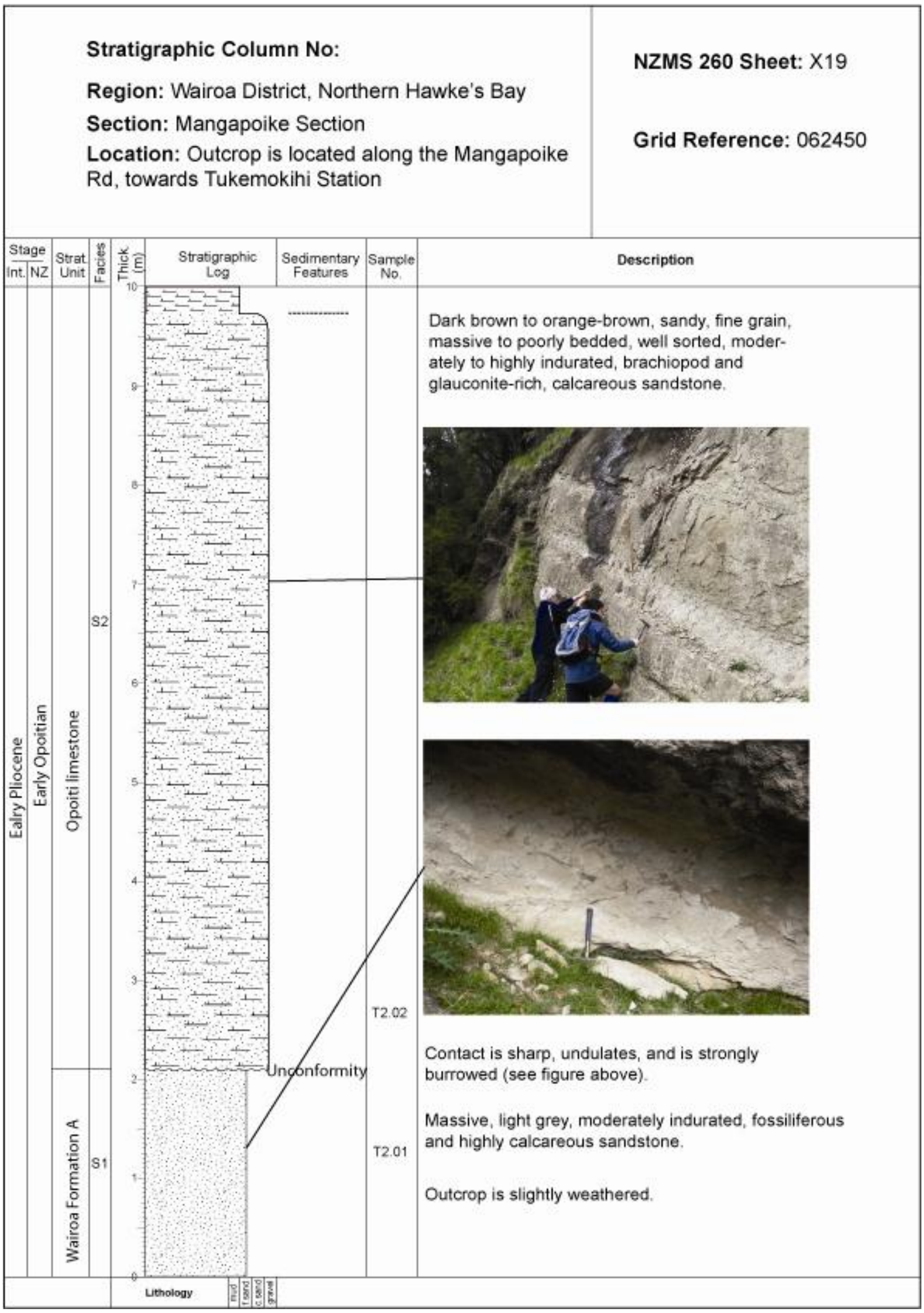

Figure 5.2 Stratigraphic column for the Opoiti Limestone at the type locality along Mangapoike Road (X19/062450).

An excellent, easily accessible additional reference section occurs in the northernmost part of the study area along Tiniroto Road (X18/099658; Fig. 5.3). Hood (1993) briefly described the petrology of the limestone at this locality. Two other good sections are: (1) the ridge exposure on both sides of the Ruakituri River (X18/958577 to 972587); and (2) along Ruakaka Road and upstream of Mangapoipoi Stream (X18/032652 to 035650). A simplified stratigraphic panel diagram for the Opoiti Limestone is presented in Figure 5.4 showing the location of each of the five columns and their dominant facies types. The graphic illustration for each of the stratigraphic columns is presented in Appendix I.

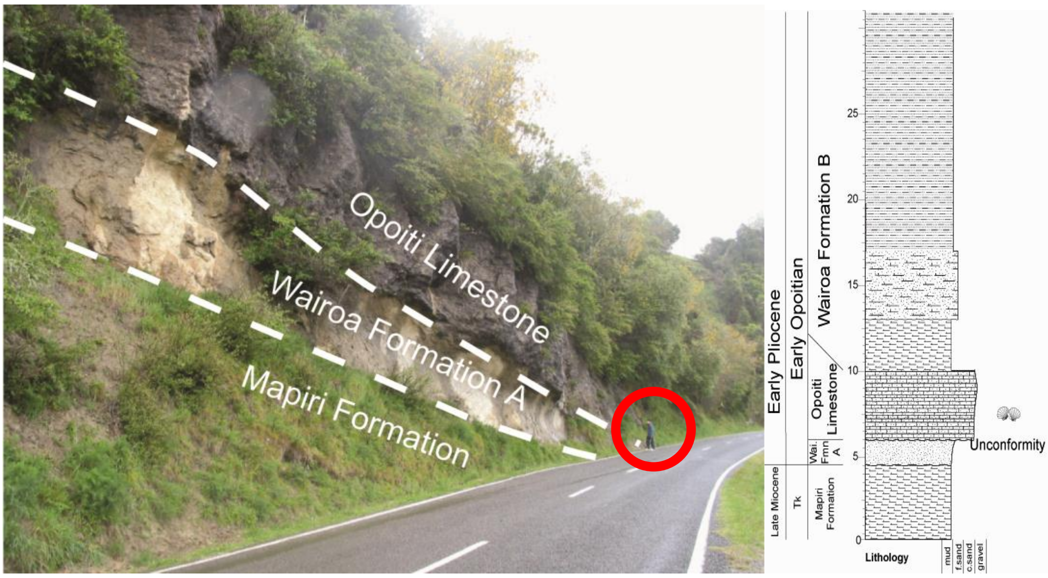

Figure 5.3: Newly designated reference section for the Opoiti Limestone along the Tiniroto Road at X18/099658, above the Hangaroa River (Photograph by C. Nelson).

5.4 Lithology

The Opoiti Limestone is a siliciclastic–rich limestone (L3) to fossiliferous and glauconitic calcareous sandstone (S2) that shows only a relatively small variation in thickness from about 4-12 m over its outcrop extent (Fig. 5.4). Most typically, field exposures of the Opoiti Limestone are more or less massive or structureless, particularly at outcrops above the Hangaroa River and Ruakituri Valley. Sometimes the limestone shows faint bedding as it passes into more siliciclastic-rich or sandstone facies, especially at Ruakaka Road and the type Mangapoike River localities (Fig. 5.4). Opoiti Limestone is typically dark brown to grey in

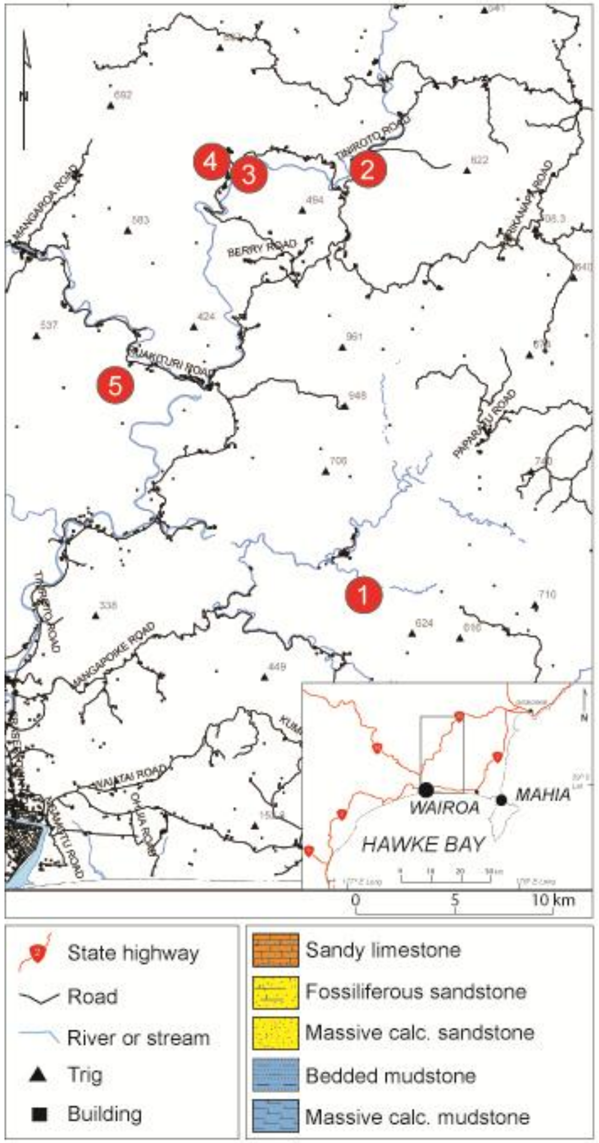

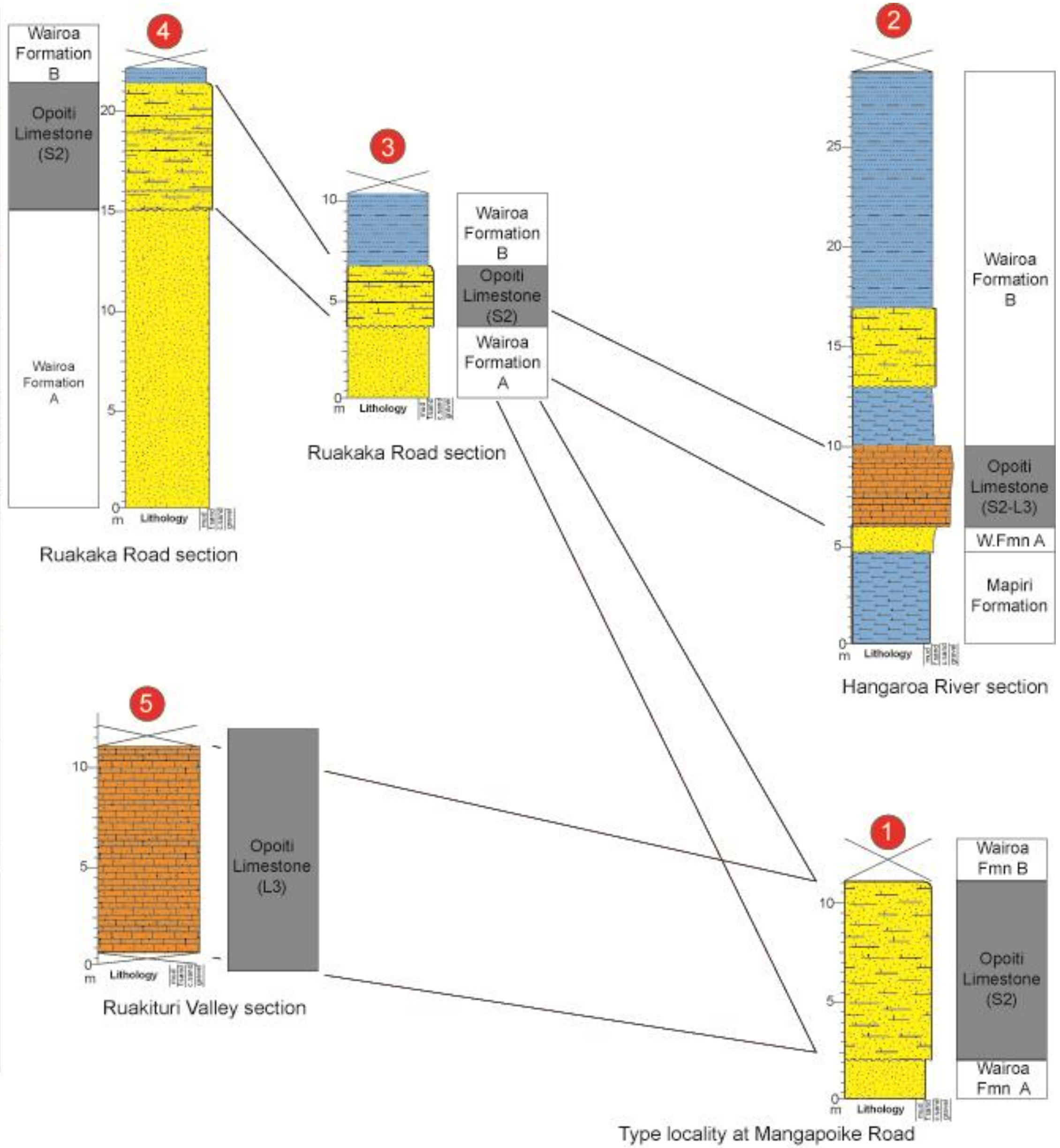

Figure 5.4: Simplified panel diagram for the Early Pliocene Opoiti Limestone north of Wairoa.

colour (Fig. 5.5), and includes common barnacle plates and fragments, and locally disarticulated epifaunal bivalve (8-10 cm) and brachiopod debris. Small (1-2 cm) mudstone clast are common at the base of the limestone, and are conspicuous and larger (8-10 cm) at the Ruakituri Valley locality. The limestone is moderately to highly indurated, with a variable $CaCO_3$ content from about 35-65%. Case hardening is a common feature at most outcrops. The limestone lacks any visible porosity in hand specimen. The Opoiti Limestone can exhibit intense burrowing locally, especially in its basal part. The predominantly massive nature of the Opoiti Limestone likely results from indiscriminant bioturbation.

Mangapoike section (location 1, Figure 5.4)

The Opoiti Limestone is steeply dipping (>20º) towards the SW in the Mangapoike Valley (Fig. 5.5A). At outcrop, this limestone is a dark brown to grey, moderately to highly indurated, glauconitic, macrofossil-bearing sandstone of Facies S2 with abundant *Towaipecten ongleyi*. It is vaguely bedded and contains occasional small mudstone clasts, commonly 1 cm across (Fig. 5.6A).

Hangaroa River section (location 2, Figure 5.4)

The Opoiti Limestone dips 25-30º SW at the locality above Hangaroa River (Fig. 5.5B). The lower 2 m of the formation ranges from a massive, grey, moderately to highly indurated sandstone of Facies S2 to a sandy limestone of Facies L3, and contains common oysters and large pectinid and brachiopod shells visible in both the outcrop and in rock slabs (Fig. 5.6B). The unit grades upwards into a light grey, massive mudstone, and further into an orange brown, moderately weathered, macrofossil-rich, calcareous sandstone.

Ruakaka Road section (locations 3 & 4, Figure 5.4)

Here the Opoiti Limestone dips at c. 10º SE and exhibits variations in lithology (Fig. 5.5C). The basal 1 m is a light grey to light brown, bioclast-rich (mainly brachiopod and bivalve material; Fig. 5.6C), and highly indurated calcareous sandstone. It grades upwards into a barnacle-rich sandstone (Fig. 5.6D).

Ruakituri Valley section (location 5, Figure 5.4)

The Opoiti Limestone is more of a massive sandy limestone (Facies L3) in the Ruakituri Valley (Fig. 5.5D), similar to the limestone above the Hangaroa River. It forms a 3-12 m thick band of light brown to orange, glauconitic coarse sandy limestone of Facies L3 (barnacle and pectinid dominated; Fig. 5.6E) at the top of the ridges on either side of the Ruakituri River. It is thicker on the southern side of the river (c. 10-12 m). The limestone dips 32º SE. This limestone includes small mudstone clasts, c. 1-2 mm in size (Fig. 5.6E).

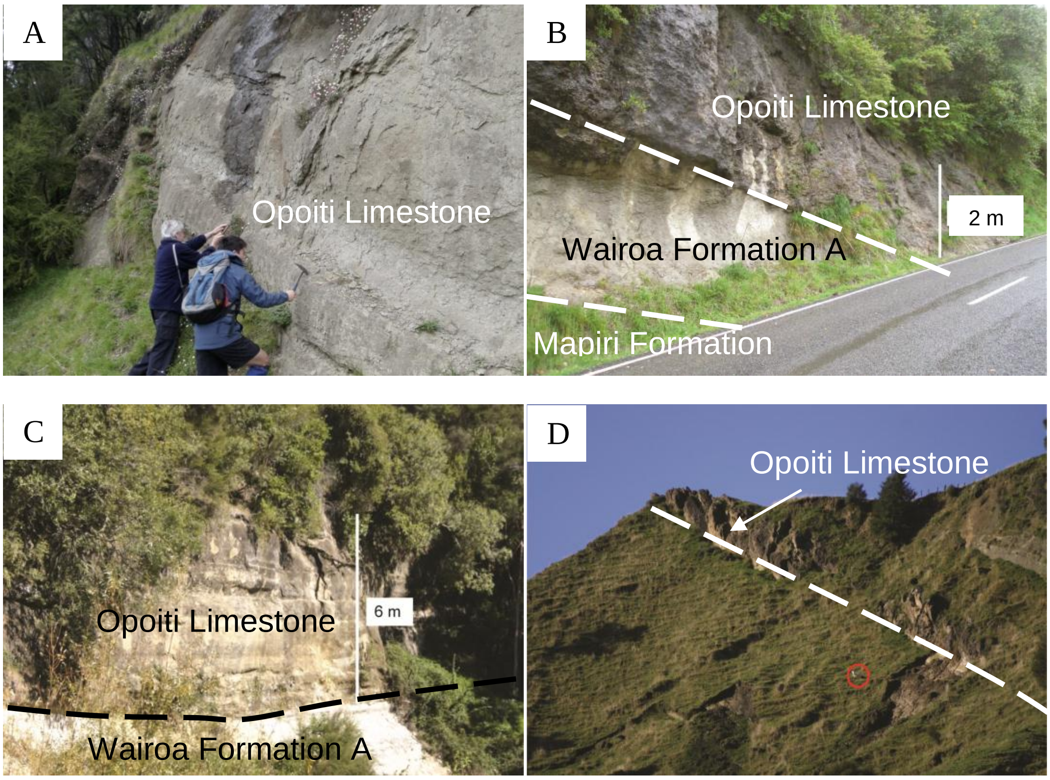

Figure 5.4: A) Type locality of the Opoiti Limestone along Mangapoike Road, showing the vaguely bedded calcareous sandstone facies with a $CaCO_3$ content of about 40%. Location X19/061451. B) The newly designated reference section for the Opoiti Limestone above the Hangaroa River showing a massive or structureless Opoiti Limestone in sharp contact with calcareous sandstone of Wairoa Formation A (c. 2-3 m thick; 35% $CaCO_3$), which in turn rests unconformably on the Tongaporutuan deep-water mudstone of the Mapiri Formation. Location X18/099658. C) Ruakaka Road outcrop shows over 6 m thick of massive, dark brown to grey Opoiti Limestone (40% $CaCO_3$) with faint bedding (separated by diastems). Location X18/033651. D) Dipping Opoiti Limestone comprises 3 m of massive sandy limestone (65% $CaCO_3$) cropping out in the Ruakituri Valley. Location X18/967582. Sheep in foreground is circled.

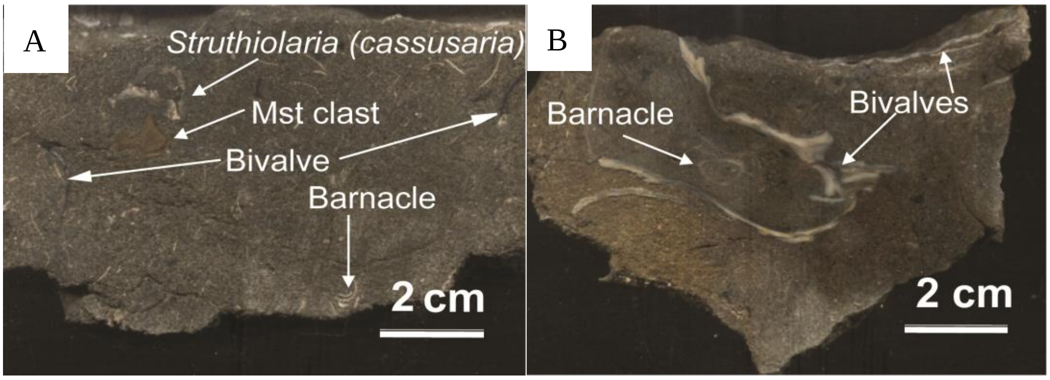

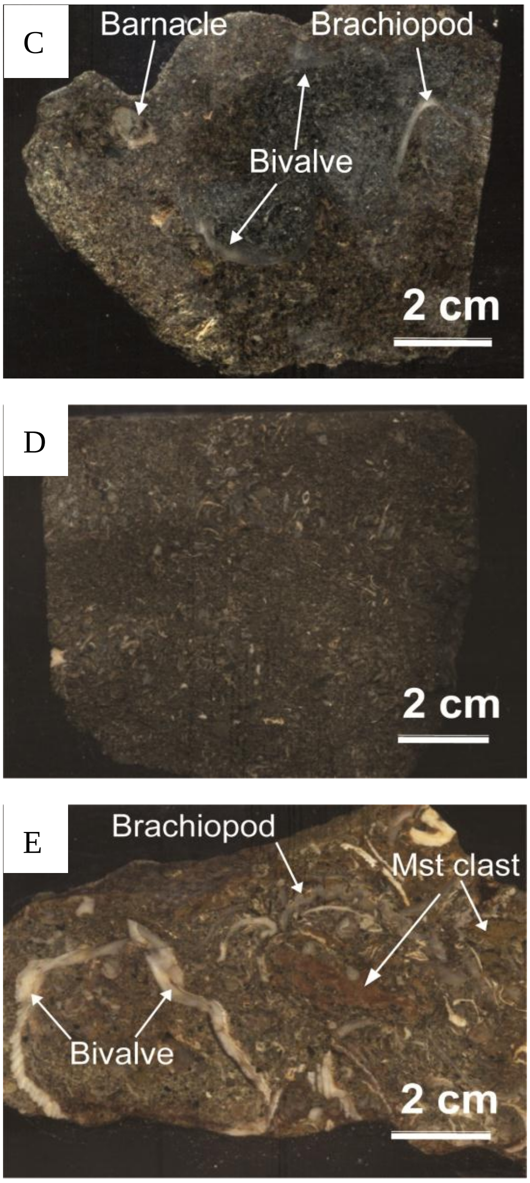

Figure 5.5: Lithological variability of the Opoiti Limestone is evident in slabbed specimens.

A) Fossiliferous sandstone from the type locality contains common bivalves and barnacle fragments, and other common macrofossils from early Opoitian (e.g. *Struthiolaria cassusaria),* and small, irregular shaped mudstone clasts. Sample location X18/099658.

B) Fossiliferous sandstone to sandy limestone from the Hangaroa River locality shows a macrofossil content of whole and disarticulated bivalve shells including the early Opoitian *Towaipecten ongleyi.* Sample location X18/099658.

C & D) Both fossiliferous sandstones collected from Ruakaka Road outcrops on the western limb of the Wairoa Syncline are texturally similar to samples from the type locality, being rich in a range of skeletal fragments. Sample locations X18/033651-036651. C) Includes some intact skeletons of barnacles, bivalves and brachiopods. D) Includes more fragmented carbonate skeletons of bivalves and barnacles set in a sandy matrix.

E) coarse-grained sandy limestone from Ruakituri Valley contains disarticulated bivalve shells of *Towaipecten ongleyi* and brachiopod fragments, and conspicuous, irregularly shaped limonitised mudstone clasts from 1-2 cm across. This facies has a $CaCO_3$ content of 65%, and is the only true limestone in the Opoiti Limestone Formation, occurring on the western limb of the Wairoa Syncline. Sample location X18/958577.

5.5 Lower and upper contacts

The lower contact of the Opoiti Limestone is a sharp disconformity, often heavily burrowed below (Fig. 5.7A, B). This is conspicuous at most outcrops along Tiniroto Road and Ruakaka Road, and in the Mangapoike Valley. At the type locality, the underlying lithology is 220 m of mudstone and sandstone, referred to the Wairoa Formation A. The very top (c. 2 m) of Wairoa Formation A is a calcareous sandstone of facies type S1 exposed at the type locality (Fig. 5.7A). Elsewhere the thickness of Wairoa Formation A varies, and the same facies (S1) of calcareous sandstone is only about 3 m thick at the reference section for the Opoiti Limestone above Hangaroa River. The Wairoa Formation A is a light yellowish grey, massive, moderately indurated, calcareous sandstone or mudstone.

The upper contact appears to be conformable throughout the study area in the form of a gradational contact into thin (c. 4-5 m) mudstone facies of M1 (Fig. 5.7C) which passes up into fossiliferous sandstone facies of S2 in the Wairoa Formation B (Fig. 5.7D). The upper contact has been observed only at the outcrop along Tiniroto Road above the Hangaroa River. There is same 700–800 m of Wairoa Formation B above the Opoiti Limestone. It consists of differentially cemented shallow-marine mudstone and sandstone facies, and common tuff beds (Fig. 5.7E).

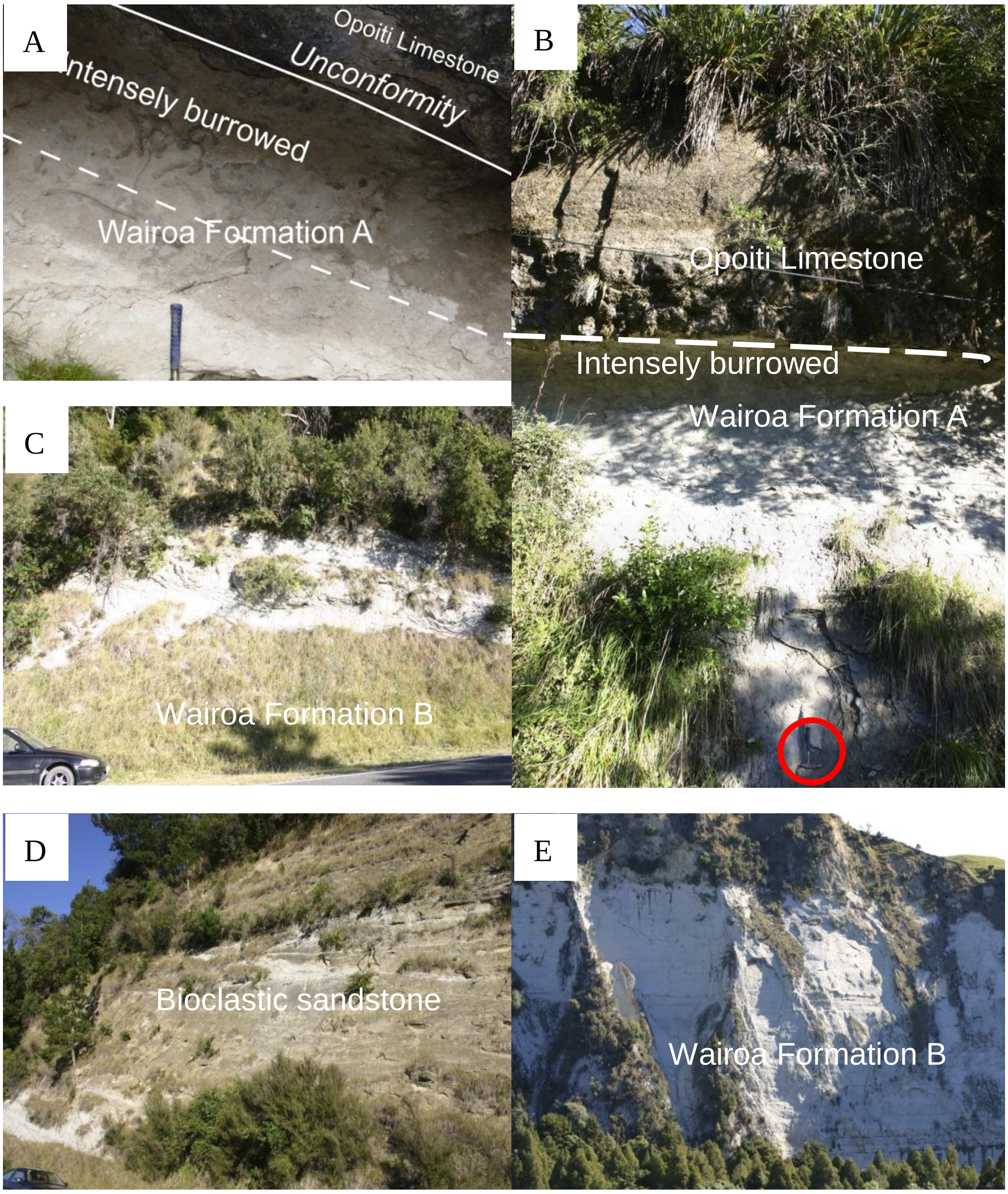

Figure 5.6: A) Facies S2 of Opoiti Limestone and underlying Wairoa Formation A (sandstone facies S1) are separated by a sharp disconformity. The top part of the underlying deposit is heavily bioturbated at the type locality in the Mangapoike Valley and in many other localities. Location X19/061451. B) The Opoiti Limestone (S2) exposed at Ruakaka Road is also separated by a disconformity from underlying massive calcareous sandstone (S1) of Wairoa Formation A, and the contact shows moderate to strong burrowing (hammer as scale circled in red). Location X18/035650. C) Lowermost part of the Wairoa Formation B (M1) conformably overlies (gradational contact) the Opoiti Limestone (S2-L3) at the Hangaroa River section. The deposit comprises massive, light grey, frittery calcareous mudstone (M1). Location X18/099658. D) Bioclastic (bivalve and barnacle fragments) sandstone (S2) overlies massive, light grey mudstone above the Opoiti Limestone at Hangaroa River section. Location X18/099658. E) Differentially cemented shelfal mudstone of M2, and sandstone facies S1 that includes common tuff horizons (S3), overlie bioclastic sandstone (S2) in the Wairoa Formation B at the Hangaroa River section. The thickness of the exposed section is c. 70 m. Location X18/901658.

5.6 Distribution and thickness

Outcrop

The Opoiti Limestone is the most widespread limestone formation in the study area (Fig. 5.8). It varies little in thickness (c. 4-10 m) throughout the study area, cropping out on both sides of the Wairoa Syncline. Dips of about 30º towards the syncline axis are typical. Petroleum drill holes show the absence of the early Opoitian limestone facies near the centre of the syncline, presumably indicating that the limestone has passed laterally into sandstone or mudstone facies typical of the enclosing Wairoa Formation. Thus, despite its extent, the limestone pinches out laterally in different directions, so that in gross form it has a lensoidal geometry.

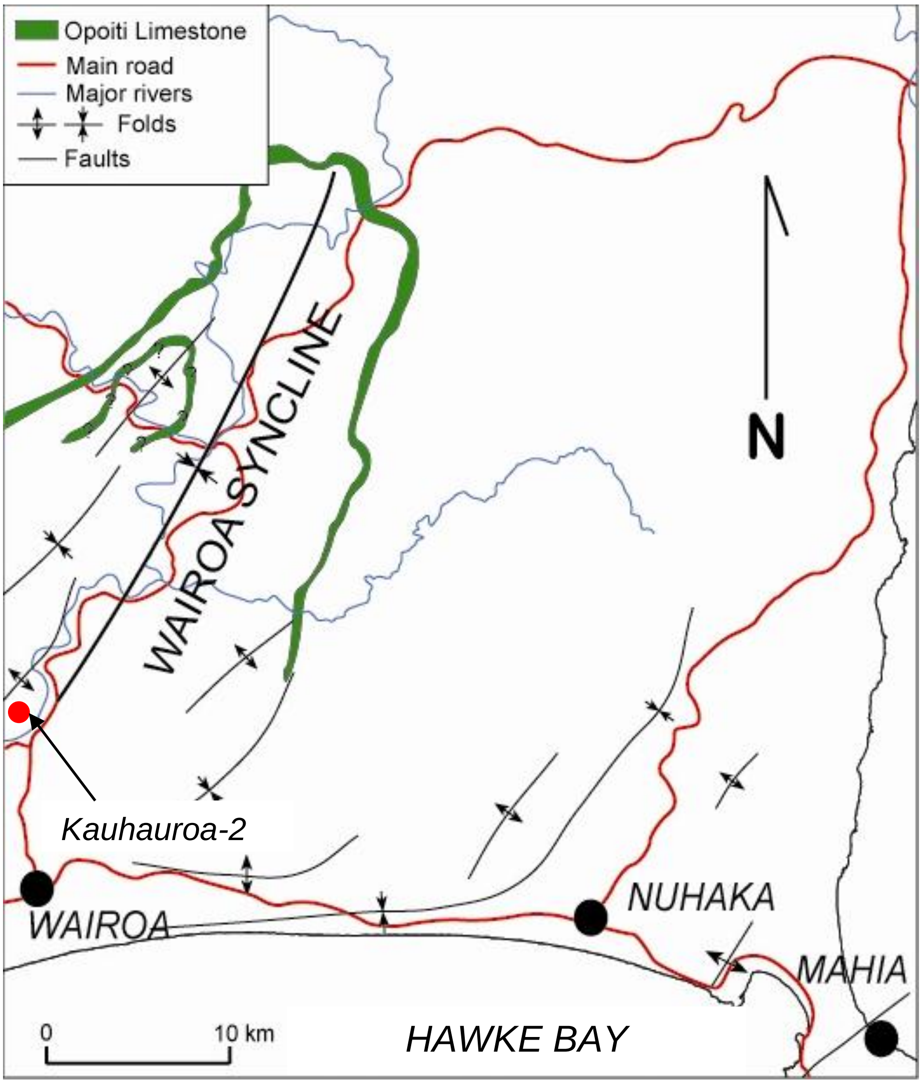

Figure 5.7: Distribution map of the Opoiti Limestone outcrops in the Wairoa Syncline in the study area. The petroleum exploration well Kauhauroa-2, indicated in red some 8 km north of Wairoa township,did intersect Opoiti Limestone. Modified from Moore & Hatton (1985).

Subcrop

The (inferred) Opoiti Limestone is present in only 1 of 11 petroleum wells drilled within the study area. It was intersected in the Kauhauroa-2 (Fig. 5.9) well on the eastern limb of the Kauhauroa Anticline, at a depth of 865.9-876.3 m AHBKB. The Opoiti Limestone here rests on top of a small anticlinal structure that has been reversely faulted. The limestone unconformably overlies the Late Miocene mudstone of Poha Formation (late Tongaporutuan), equivalent to the Mapiri Formation in this study. It is overlain by the Wairoa Formation B, formerly Opoiti Formation. It is the only occurrence of the limestone facies type (L3) of the Opoiti Limestone found within all the petroleum drill holes within the Wairoa Syncline (for stratigraphic nomenclature and relations see section 3.2).

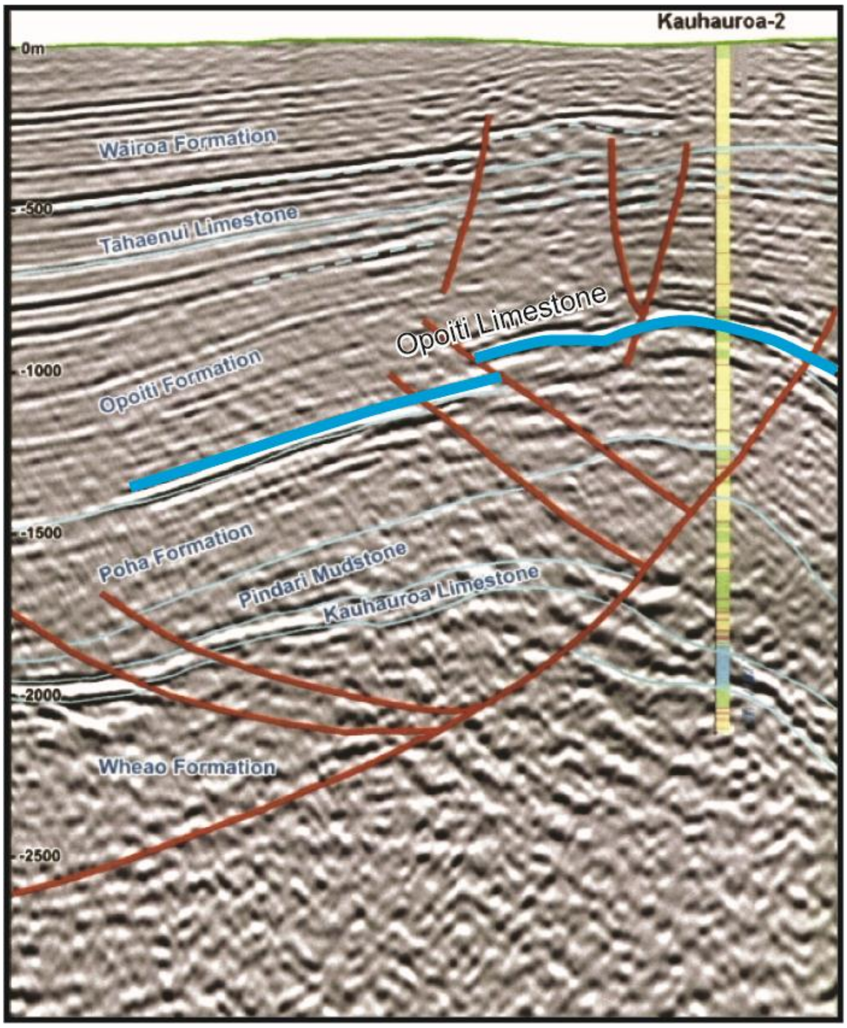

Figure 5.8: Seismic reflection profile shows the inferred presence of Opoiti Limestone which was intersected by Kauhauroa-2 drill hole. Well location X19/918386, between Brownlie's Road and a small tributary of the Wairoa River, 200 m from SH38 intersection (PR2409 1998).

5.7 Paleontology

The Opoiti Limestone is assigned an early Opoitian age based on the presence of the large pectinid *Towaipecten ongleyi* and the key foraminiferal assemblage including *Globorotalia crassaconica* found near the base of the Opoiti Limestone and the enclosing siliciclastic units (Edwards 1987; Beu 1995). The pectinid reaches a moderate size of 6-10 cm (Fig. 5.10A). Beu (1995) notes: "They have numerous low, flat-topped, closely spaced, primary radial ribs with their interstitial secondary and tertiary riblets often reaching almost the same height and width as the primary ribs. Ears, where seen, are moderately unequal and retain a small anterior byssal notch and sinus on large shells. Weak radial folds extend over the umbonal quarter to one third of some specimens, occasionally on all specimens in an otherwise unfolded population." *Towaipecten ongleyi* is widely distributed in the early Opoitian limestones of the Pliocene Te Aute facies throughout eastern North Island.

The dominance of barnacle plates is a most unusual feature of these Pliocene limestones in the eastern North Island. Beu (1995) listed several our species of barnacles commonly represented in the limestones, including *Notobalanus vestitus, Austromegabalanus (Notomegabalanus) miodecorus, Austromegabalanus decorus argyllensis, Fosterella tubulatus and Balanus variegates*. The barnacles lived attached to hard substrates of shells and boulders. The presence of these barnacle taxa indicates that the source of the barnacle plates was subtidal, shedding from the top of carbonate factories (Beu 1995). *Neothyris aff. obtuse* (brachiopods) and bivalve mollusc *Tucetona laticostata* (a facultatively mobile semi-infaunal suspension feeder) are also identified in the L3 facies of the Opoiti Limestone, in the western limb of the Wairoa Syncline. Figure 5.10B shows the two *Tucetona laticostata* (circled in red) and *Neothyris aff. obtuse* scattered in the background.

Figure 5.9: A) The age diagnostic early Opoitian pectinid *Towaipecten ongleyi* at outcrop above Hangaroa River. Location X18/099658. B) *Tucetona laticostata* (circled in red) and abundant *Neothyris aff. obtuse* in the Opoiti Limestone (facies type L3) on the western limb of the Wairoa Syncline. Location X18/958577.

5.8 Lateral age correlatives

Opoitian limestones are the most widespread of all Pliocene limestones, occurring throughout eastern North Island, New Zealand. Lithologically, these limestones are highly variable in the field. In many localities the Opoitian limestones are barnacle-dominated, with scattered layers of molluscs. The lithofacies of the early Opoitian limestones differ from some of the younger Pliocene Te Aute limestones, and they are typically harder and more cemented, siliciclastic-rich (up to >50%) and darker in colour (Beu 1995). Table 5.1 shows the age equivalent early Opoitian carbonate formations of the Te Aute limestone facies. The Whakapunake Limestone, of later Opoitian age, is discussed in Chapter Six.

Ormond Limestone

The Ormond Limestone is a northern age correlative of the Opoiti Limestone that crops out inland from Gisborne in the vicinity of Ormond, such as at Waihirere Reserve (Y17/407805; Fig. 5.11; Harmsen 1985). The Ormond Limestone is a shelly limestone which, along with sandstone and loose sandy conglomerate, was originally assigned by Hector (1877) to the 'Ormond Series' that cropped out in the low hills between Ormond and Gisborne, on the east side of the Waipaoa Valley. Henderson & Ongley (1920) defined the basal limestone cropping out on Rimuhau Hill as part of the 'Ormond Series', and assigned a Lower Pliocene age for the basal limestone. Marwick (1931) listed and described pectinid fossils from the Gisborne district and assigned the 'Ormond Series' to Taranakian (present day Opoitian). Detailed mapping by Kingma (1964) in the Gisborne district included much unpublished data from oil exploration work that concluded that the 'Ormond Series' was of Opoitian age (Bishop 1968). Barber (1989) studied in detail the isolated occurrence of the Ormond Limestone at Rimuhau Hill for the first time as part of an MSc project. She described the Ormond Limestone as a cream-brown, poorly bedded, moderately to highly indurated sandy coquina that petrographically was a calcarenite to calcirudite. The contact between the sandy coquina and the underlying lithology is not seen at Rimuhau Hill, but regionally the Opoitian sandy coquina rests conformably, and locally unconformably, on upper bathyal mudstone of Tongaporutuan age (Barber 1989). Moore *et al.* (1989) have mapped out the distribution of the Ormond Limestone. Beu (1995) confirmed the age of this limestone as early Opoitian, based on the presence of *Towaipecten ongleyi* in most outcrops, and the presence of *Mesopeplum (Borehamia) crawfordi* at Rimuhau Hill. There are no further published studies about the Ormond Limestone in more recent years.

Figure 5.10: Type locality of the Pliocene Ormond Limestone in the Waihirere Reserve, near Ormond, inland from Gisborne. Location X17/407805. Photo: Dr Steve Hood.

Kairakau Limestone

The Kairakau Limestone (Beu *et al.* 1980) carries both *Phialopecten marwicki* and *Towaipecten ongleyi* lineage, cropping out in the northeastern part of the Te Aute Subdivision in southern Hawke's Bay, near the Maraetotara Plateau, and within sea cliffs from south of Kairakau Beach (Fig. 5.12) northwards to Waimarama (Beu *et al.* 1980; Harmsen 1985; Hood 1993; Beu 1995; Caron 2002; Bland *et al.* 2004a). The limestone forming the headland at Cape Turnagain is also referred to Kairakau Limestone, where it features an unusual abundance of pectinds (Beu 1995). The name was first introduced by Beu *et al.* (1980), and formally defined by Harmsen (1985). The type locality of the Kairakau Limestone was designated as the "lower Hogback Limestone" 600 m north of Mt Kahuranaki, on the western edge of the Maraetotara Plateau (V22/423513; Sporli & Pettinga 1980; Harmsen 1985). It consists of greenish grey to yellowish grey, large-scale planar cross-bedded sandy limestone and 2.5 m of cross-bedded calcareous sandstone that is separated from the underlying Mesozoic greywacke basement, Waiauan siltstone, or Tongaporutuan flysch sediments by a regional unconformity. The limestone formation is conformably overlain by the Mokopeka Sandstone. The Kairakau Limestone thickens and thins (c. 3-82 m) laterally, and ranges from a sandy glauconitic limestone to calcareous sandstone, coquina, and rare conglomerate (Beu 1995). Hood (1993) described the limestone proper as a light grey, poorly-bedded to cross-bedded, moderately to highly indurated, barnacle-dominated siliciclastic-rich grainstone.

Figure 5.11: Differentially cemented Pliocene Kairakau Limestone exposed in the Kairakau Beach area, southern Hawke's Bay. Location V22/445319. Photo: Dr. Steve Hood.

Maungaharuru Limestone

The Maungaharuru Limestone (Smith 1877; redefined by Cutten 1994), now part of the Titiokura Formation, crops out in the Maungaharuru Range from Titiokura saddle on the Napier-Taupo Road, northwards almost to Lake Waikaremoana (Bland *et al.* 2007). The name Maungaharuru Limestone is now disused, and the name Titiokura Formation is used to incorporate the lower (Opoitian to Waipipian) limestone package in the Te Waka Range. Smith (1877) was the first to describe the Maungaharuru Limestone. Beu *et al.* (1980) concluded that the limestone unit on the Maungaharuru Range, extending north from Titiokura summit on the Napier-Taihape Road, was the lateral continuation of the Opoiti Limestone in the Wairoa Syncline. The limestone is highly variable in thickness and lithology. It passes into a 100 m thick unit of prominently cross-bedded, alternating calcareous sandstone and sandy limestone beds at the crest of the Maungaharuru Range (Fig. 5.13). Near Pohokura Road, the limestone becomes a hard, dark grey-brown, more siliciclastic-rich, and barnacle plate coquina with *C. (P.) triphooki ongleyi fossils*. Here the limestone thickens dramatically (up to 500 m) compared to the outcrops on the Maungaharuru Range (Beu 1995). De Caen & Darley (1968) documented the limestone unit on the western face of the Maungaharuru Range, just north of Mt Taraponui. There the thickness of the limestone ranges from 40-60 m, and passes into a thick, sandstone (c. 75 m), with a thin mudstone bed and 13 thin limestone beds 1 m thick at Naumai, north of the Pohokura Road. The same limestone (composed chiefly of sandy coquina) crops out on the southern end of the range, 3 km north of Titiokura summit on the Napier-Taupo Road, where the limestone is quarried for agricultural lime and road metal (Beu 1995).

Figure 5.12: Spectacularly differentially cemented siliciclastic and limestone beds of Maungaharuru Limestone in cliff exposures on northern Pohokura Road, central Hawke's Bay. Location V19/391272. Photo: Dr Steve Hood.

Haurangi Limestone

The Haurangi Limestone is also an early Opoitian Te Aute limestone that is exposed in the upper Ruakokopatuna Valley in southern Wairarapa. It is the most widespread limestone formation in the area (Beu 1995). This limestone is a barnacle-dominated coquina unconformably overlying the Makara Greensand, and is in turn overlain by the Bull Creek Limestone (Nukumaruan) in the high hilltop exposure (S28/101796; Fig. 5.14), opposite Haurangi Station homestead on Haurangi Road. Vella & Briggs (1971) identified abundant *Towaipecten ongleyi* of early Opoitian age in the Bull's Creek Limestone at the hilltop. Beu (1995) also assigned the limestone (quarried) in the large Pakohe limeworks on Dyerville Road, west of the Ruakokopatuna Valley, as part of the Haurangi Limestone. At its type locality, the limestone is divided into the upper Dyerville Limestone and lower Haurangi Limestone formations. The two limestones are separated by a stratigraphic break involving 30 cm of greensand. The basal Haurangi Limestone is a 15 m thick, greenish grey, fine- to medium-grained calcarenite with some beds rich in siliciclastic sand. The upper part comprises 30 m of coarse-grained, cross-bedded, barnacle-dominated grainstone containing specimens of *Crassostrea ingens* (Beu 1995).

Figure 5.13: Hill-side view of three discrete limestones at the Haurangi Hairpin. The lower unit is the Miocene Clay Creek Limestone seen in the lower gully to the lower right. The middle unit comprises the upper and lower Haurangi Limestone which is dipping toward middle right. The top limestone in the cliff face is the Pliocene Bulls Creek Limestone. Location S28/101796. Photo: Dr Steve Hood.

5.9 $CaCO_3$ content

Analysis of the $CaCO_3$ content of a lithology is important for assisting with the classification of lithofacies. The term limestone is typically given to a sedimentary rock that has a $CaCO_3$ content of at least 50%. Overall, the Opoiti Limestone has a relatively low $CaCO_3$ content, ranging from calcareous sandstone (30-50%) to limestone (60-70% $CaCO_3$) (Table 5.2). consequently only the limestones from the Ruakituri Valley outcrops are strictly limestone, the others being only calcareous sandstone (Fig. 5.15). Despite this, the Opoiti unit is referred to as the Opoiti Limestone in this study.

Table 5.2: Bulk $CaCO_3$ content of five samples of Opoiti Limestone. Sample localities and raw data are given in Appendix II.

Sample No.	*Facies types*	*% $CaCO_3$*	*% Mud (<63 μm)*	*% Sand (63-2000 μm)*
T2.02	S2	37	30	33
11.02	S2	38	17	45
11.03	S2	43	15	42
H1.02	S2	32	10	58
Ra/op	L3	67	16	17

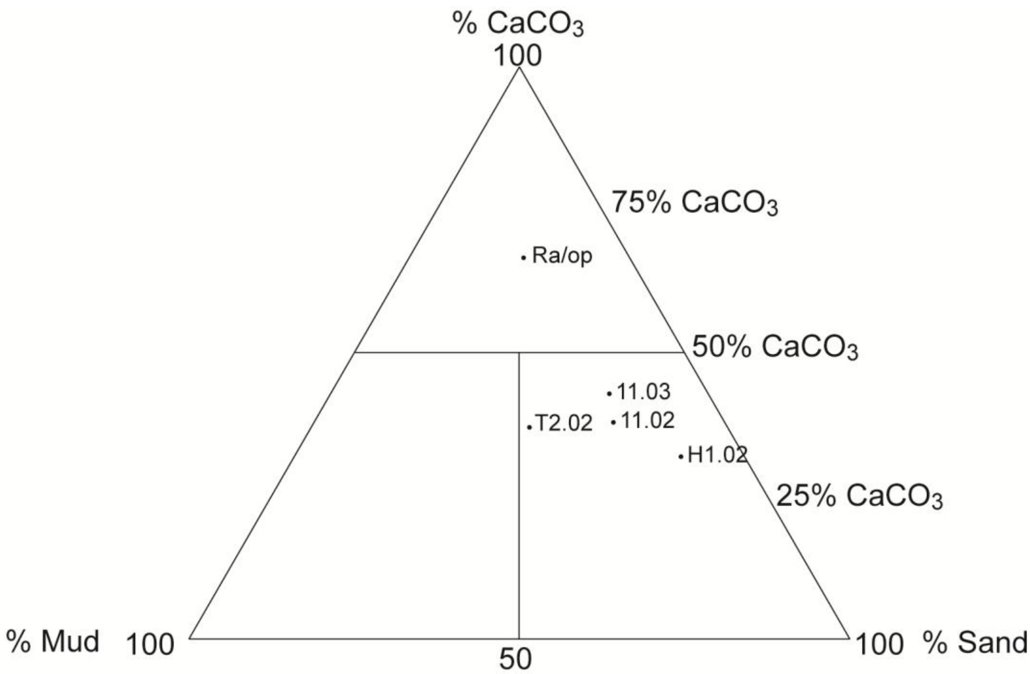

Figure 5.14: Ternary plot of the samples of Opoiti Limestone analysed in Table 5.2.

5.10 Bulk mineralogy

The bulk mineralogical analysis was undertaken of 5 samples using X-ray diffraction (XRD) as described in section 3.3. XRD spectra for the Opoiti Limestone show a range of minerals present in the rocks (Table 5.3). The dominant minerals are low-Mg calcite, quartz and plagioclase feldspar. Low-Mg calcite is common in all the analysed samples, while intermediate-Mg calcite (9 mol%Mg CO_3) is noted in one sample. The common abundance of low-Mg calcite is related to the common occurrence of skeletal grains of barnacles, epifaunal bivalves (pectinids and oysters), and brachiopods, all low-Mg calcite secretors (Kamp *et al.* 1988). Plagioclase feldspar is also present in all samples, but only in rare amounts. Quartz is common to rare in all samples. Dolomite occurs in only one sample, measured at 30.77°2θ, which suggests it contains 46 mol% $MgCO_3$ and is non-stoichiometric dolomite (Goldsmith *et al.* 1961). Rare aragonite is detected in one of the samples. Clay minerals are likely under-represented in samples because of the use of unorientated bulk powder sample mounts. The detection of mica and clay minerals in the samples is related to the presence of biotite, muscovite, and glauconite.

Table 5.3: XRD bulk mineral abundance of representative samples from Opoiti Limestone.

Major minerals	*Dolomite*	*Low-Mg calcite*	*Plagioclase feldspar*	*Aragonite*	*Quartz*	*Clays*	*Mica*
11.02	-	C	S	-	S	R	-
11.03	-	C	S	-	S	R	-
H1.02	-	C	S	-	VC	R	R
Ra/op	-	C	S	R	S	-	-
T2.02	S	C	S	-	C	-	R

Abbreviation	*Description*	*Counts*
-	None	0
R	Rare	1-20
S	Some	21-200
C	Common	201-500
VC	Very common	501-999
A	Abundant	≥1000

5.11 Insoluble grain texture

Grain textural analysis is important for a number of reasons, mostly to provide a lithological name for a given rock, but it can also be useful for aiding interpretation of the environment of deposition. Here, the carbonate rock samples were analysed for the texture of their insoluble grains. The insoluble residues are dominantly of sand size, with subordinate silt particles (Table 5.4). Fig. 5.16 shows that all the insoluble residues from samples of Opoiti Limestone exhibit a silty sand texture. The modal size of the sand materials ranges from 65 to 372 µm, or very fine sand to medium sand.

Table 5.4: Grain texture of the acid insoluble fraction for Opoiti Limestone samples.

Sample No.	*Facies type*	*% Clay (<3.9 µm)*	*% Silt (3.9-63 µm)*	*% Sand (63-2000 µm)*
T2.02	S2	2	46	52
11.02	S2	1	27	72
11.03	S2	1	25	74
H1.02	S2	1	14	85
Ra/op	L3	2	47	51

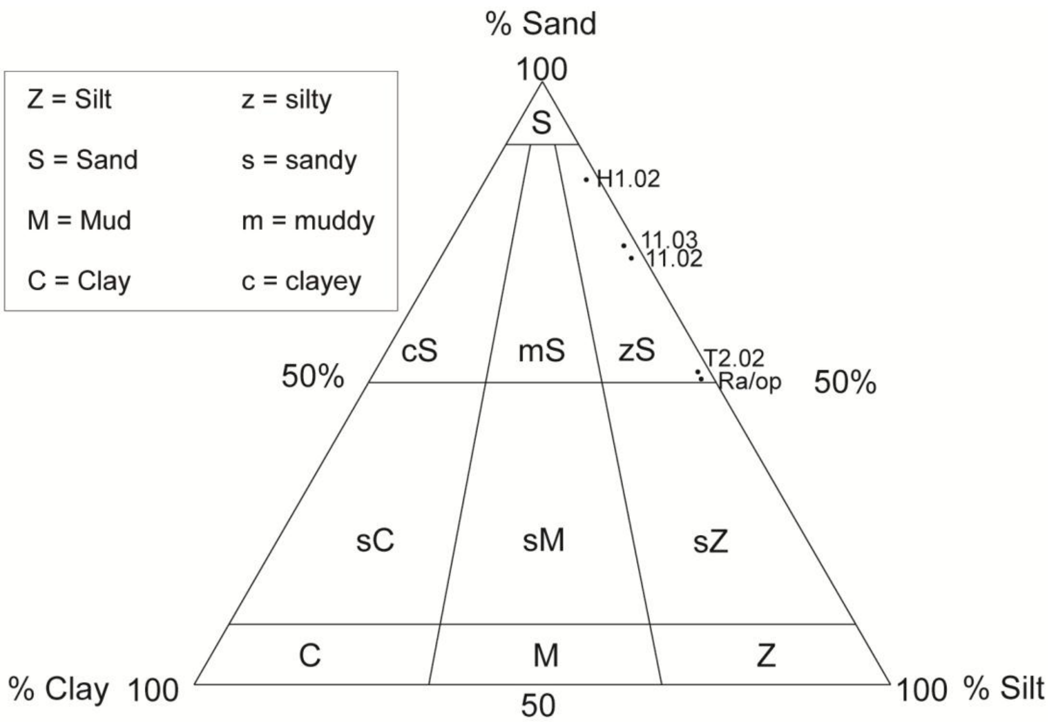

Figure 5.15: Ternary clay (C), silt (Z) and sand (S) plot (%) for the insoluble residue fraction of Opoiti Limestone samples. Textural size classification from Folk (1959).

5.12 Stable isotope analyses

Table 5.5 summarises the stable oxygen and carbon isotope values of representative samples from the Opoiti Limestone, and suggests some possible minimum burial temperatures and burial depths for the deposits in northern Hawke's Bay. The range of $\delta^{13}C$ values (+1.89 to –2.15) is broadly similar to those for the New Zealand modern skeletal carbonates (Nelson & Smith 1996, their Fig. 4A), but the $\delta^{18}O$ values are mainly slightly more negative, falling between 0.26 and –2.50‰ across the fields for New Zealand modern shelf carbonates and their Cenozoic equivalents (Fig. 5.17). Also plotted are Pliocene samples analysed by Drinnan (2011) from the nearby Mahia district. The Wairoa samples from the present study have the most negative $\delta^{18}O$ values, suggestive of at least shallow to moderate burial depths (Nelson & Smith 1996).

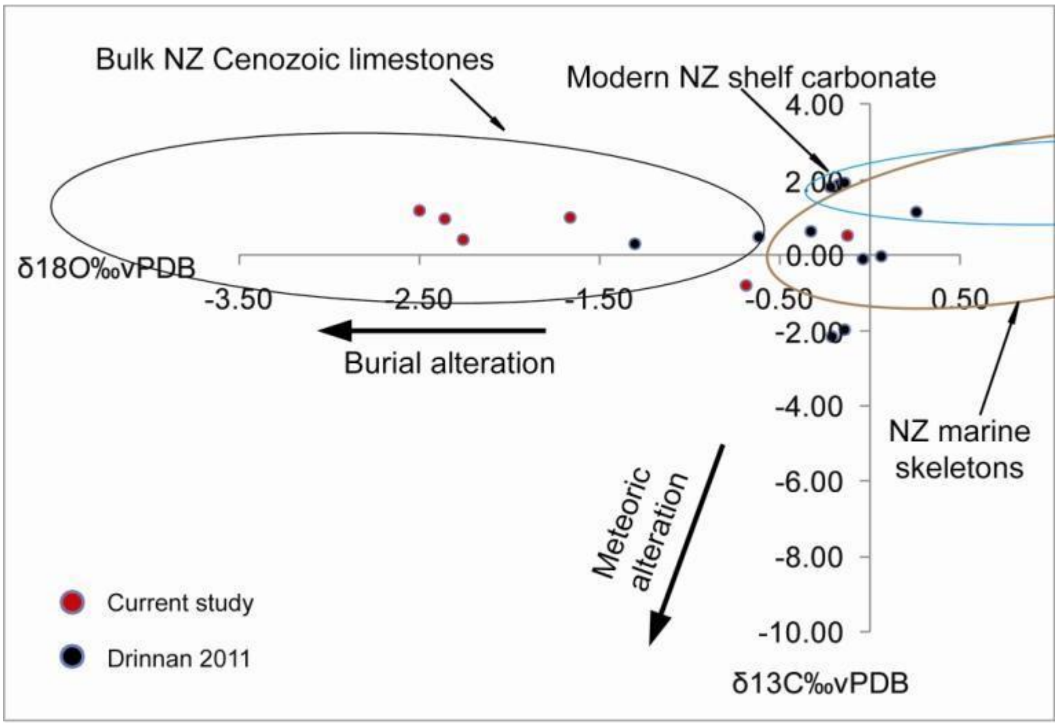

Figure 5.16: Cross-plot of oxygen and carbon isotope values for samples from the Opoiti Limestone in relation to the core fields for New Zealand carbonates from Nelson & Smith (1996).

Calculated minimum burial temperatures for each sample fall between 13°C and 25°C, while minimum burial depths range from less than 40 to over 550 m. Samples from the present study area (Wairoa) generally appear to have undergone deeper burial than those to the east analysed by Drinnan (2011).

Table 5.5: Bulk stable oxygen and carbon isotope data, and possible minimum burial temperatures and burial depths for samples from the deposits for the Opoiti Limestone in northern Hawke's Bay (* data from Drinnan 2011).

Facies types	Opoiti Limestone samples	Bulk calcite ‰		Calcite cement isotope *T*(C°)	Calcite cement paleodepth (m)
		δ^{13}C	δ^{18}O		
S2	11.02	1.18	-2.50	25	552
S2	11.03	0.43	-2.26	24	505
S2	H1.02	0.52	-0.12	15	105
S2	T2.02	-0.82	-0.69	17	208
L3	Ra/op	1.01	-1.66	21	389
S2	H10.03	0.95	-2.36	25	525
L1	120.3*	1.16	0.26	13	38
L2	129.4*	-2.15	-0.21	15	121
L2	129.4*	-1.98	-0.14	15	108
L2	112.1*	0.63	-0.33	15	142
L2	112.1*	0.47	-0.62	16	194
L2	129.1*	0.30	-1.31	20	322
L2	123.2*	1.89	-0.17	15	113
L2	123.2*	1.80	-0.22	15	123
L2	129.6*	-0.11	-0.04	14	90
L2	129.6*	-0.05	0.06	14	73
L3	61.2*	1.91	-0.14	15	109

5.13 Petrography

One of the principal aims of this study was to document the petrographic character of the Pliocene limestones in the northern Hawke’s Bay region. The three Pliocene Te Aute limestones in northern Hawke’s Bay comprise variable amounts of disaggregated barnacle plates, disarticulated and fragmental pectinid materials, brachiopod debris, and other macrofossils and skeletal fragments, along with typically common siliciclastic and some authigenic material. In this chapter, the petrography of the Opoiti Limestone is described, and raw data are included in Appendix V.

The overall bioclast content of the Opoiti Limestone varies from about 30-50%, and the siliciclastic content from 20-50%. The Opoiti Limestone in the study area exhibits facies types L3 and S2, the latter dominating. Figures 5.18A and 5.19A show average whole rock compositions of typical L3 (n=1) and S2 (n=6) facies within the Opoiti Limestone. The L3 facies is bioclast-dominated (47%) and siliciclast-rich (21%). Authigenic minerals are common (16%) and the grains are held together by 15% of mainly microsparite and micrite cements (Fig. 5.18A). The S2 facies is a mix of subequal amounts of siliciclastic (35%) and bioclastic (33%) materials. Authigenic materials (12%) are less common than in facies L3, with 19% of mainly micrite in both intrinsic (pore spaces between grains) and extrinsic (within skeletal grains, bores and skeletal chambers) fills (Fig. 5.19A), but also localised microsparite and equant sparite cement in the moulds of former aragonitic bivalve skeletons. There is no evidence of secondary or mouldic porosity in the thin sections.

Skeletal grains

The skeletal composition diagram for facies L3 (Fig. 5.18B) shows the majority of the skeletal material is brachiopods (67%). However, this sample was taken from a brachiopod-rich bed, so biasing the proportions of the skeletal types in L3. The brachiopod skeletons are mostly very coarse sand size (1-2 mm; Fig. 5.20A) and are clearly visible both in rock slabs (Fig. 5.6) and in outcrop. Other skeletal components include bivalves (11%), barnacles (11%), echinoderms (7%), and both benthic (2%) and planktic foraminifera (2%) (Fig. 5.18B). The skeletal grains have a bimodal size distribution with a primary mode at 1.5 mm (very coarse sand) and a secondary one at 2 mm (very coarse sand). The largest skeletal grain is greater than 5 mm (gravel). The skeletal grains are very poorly sorted but well abraded (Fig. 5.20B).

The skeletal make up of the S2 facies is a subequal mixture of three main skeletal grain types, namely bivalves (27%), barnacles (22) and brachiopods (20%). Other skeletal components include bryozoans (8%), echinoderms (5%), and benthic (10%) and planktic forams (8%) (Fig. 5.19B). These skeletal grains also have a bimodal size distribution, with a primary mode at 1.5 mm (very coarse sand) and a secondary one at 0.5 mm (medium sand to coarse sand). The largest skeletal grain measured in this facies type is also greater than 5 mm (gravel). The skeletal material is poorly sorted but well abraded. No calcareous red algae, gastropods or sponges were identified in either L3 or S2 facies types in thin section.

Non-carbonate materials and infills

The abundance of various siliciclastic components in facies L3 and S2 is plotted together with the authigenic minerals as the non-carbonate material in Figures 5.18C & 5.19C. Siliciclastic materials are ubiquitous and common in the Opoiti Limestone, especially in facies S2.

The L3 facies contains fewer types of non-carbonate materials than S2 that are dominated by quartz (43%) with equal amounts of limonite as mostly intrinsic fills. Other non-carbonate minerals include feldspar (8%) and rock fragments (6%) (Fig. 5.18C). The siliciclastic materials in L3 show a bimodal size distribution, with a primary mode at 0.4 mm (medium sand) and a secondary one at 0.1 mm (very fine sand). The maximum grain size measured is about 0.7 mm (coarse sand). Grains are well sorted, and shape varies from subrounded to rounded.

Facies S2 is also dominated by quartz (41%) and feldspar (24%), with authigenic materials being mostly glauconite infills (25%). Glauconite pellets (8%) and pyrite grains (2%) are less common than in facies L3 (Fig. 5.19C). In facies S2 the size distribution of siliciclastic grains is also bimodal. The primary mode size is 0.12 mm (very fine sand), with a secondary mode at 0.05 mm (silt). The maximum size measured is about 0.3 mm (medium sand). The grains are moderately to well sorted, and their shape ranges from subangular to subrounded. Both facies are rare in phyllosilicate minerals.

Cement/matrix

The typical cement types in facies L3 are primarily microsparite and micrite, occurring most commonly in patches of intrinsic fills. In facies S2 the cements are mostly micrite that accumulated intrinsically, and within skeletal chambers of foraminifera and microborings of other skeletal types. Localised microsparite and subequant sparite replaces former aragonitic bivalve skeletons (Fig. 20C & E). The size of the subequant sparite crystals is approximately 1 mm across. Neomorphism of bivalve skeletons is another very common diagenetic feature within facies S2. The calcite crystals forming these neomorphic fabrics are the result of secondary diagenetic transformation of aragonite skeletons to calcite. The recrystallised calcite crystals preserve some of the original skeletal layers in the aragonitic bivalves as ghost fabrics. There is no clear evidence in the S2 facies of early diagenetic cement fabrics, such as fibrous or syntaxial rim cements around skeletal grains.

Cathodoluminescent petrography (CL)

The skeletal components of the Opoiti Limestone show a range of CL colours from dark purple (former aragonite-infaunal bivalves) to dull orange (calcite based skeletal materials such barnacles and epifaunal bivalves) (Fig. 5.21). The CL signature of brachiopods is also purple coloured, but with fine speckles of dull orange, suggestive of the presence of calcite (Fig. 5.21A & B). The micrite cement and matrix in the background show a moderate to bright orange and yellow luminescence (calcite), while the authigenic grains and infills are non-luminescent as a result of the enrichment of Fe over Mn in these materials. Figures 5.21C & D show that the siliciclastic-rich facies of the Opoiti Limestone from Hangaroa River contains many former aragonitic bivalve skeletons that have been replaced with subequant sparite. The cement colour ranges from reddish purple to dull orange (calcite). Figures 5.21E & F show an echinoderm skeleton whose pore spaces are filled with mainly microsparite and micrite with a dull orange to reddish purple colour. The packed micrite shows a dull orange luminescence. Figures 5.21 G & H show generally calcite skeletons sitting in microsparite which contains speckles of bright orange to yellow luminescence due to non-stoichiometric dolomite. XRD results confirm the presence of the dolomite (Table 5.3).

Petrographic summary of facies type L3

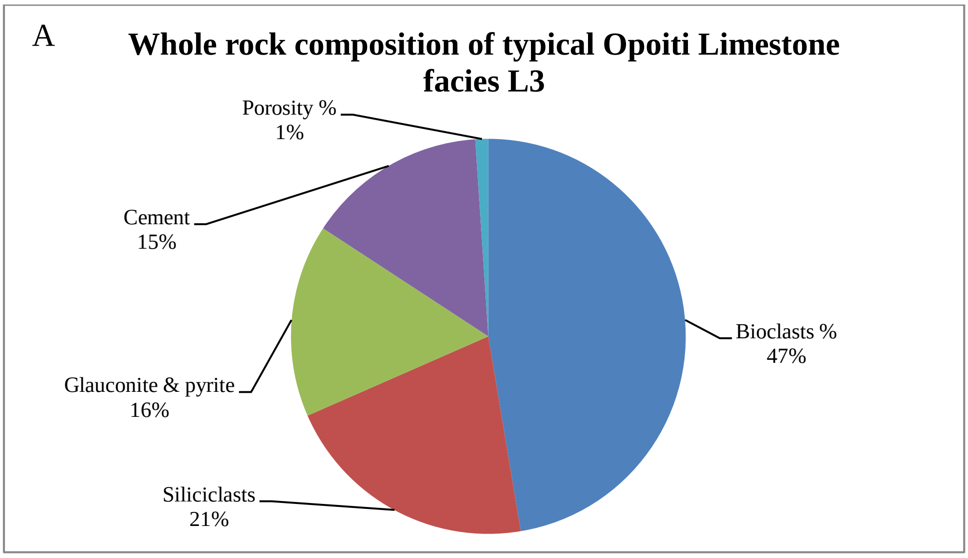

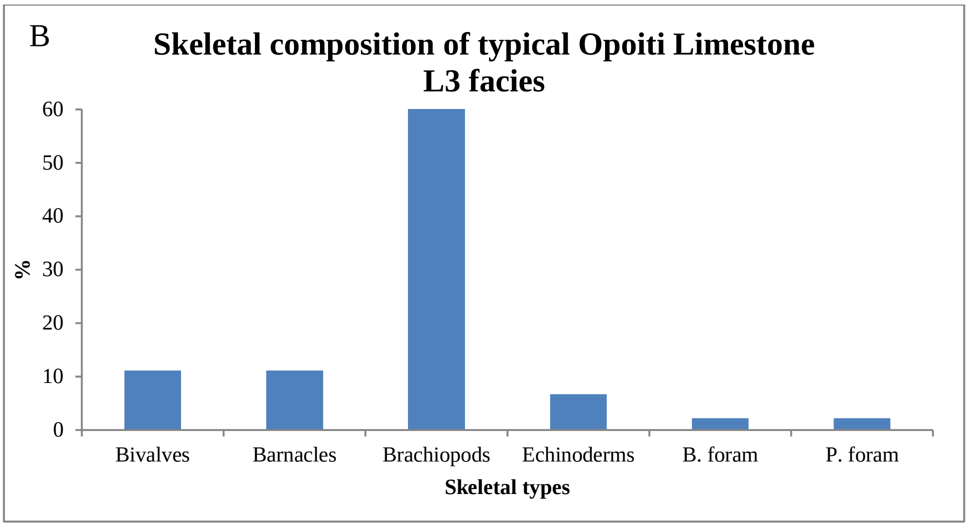

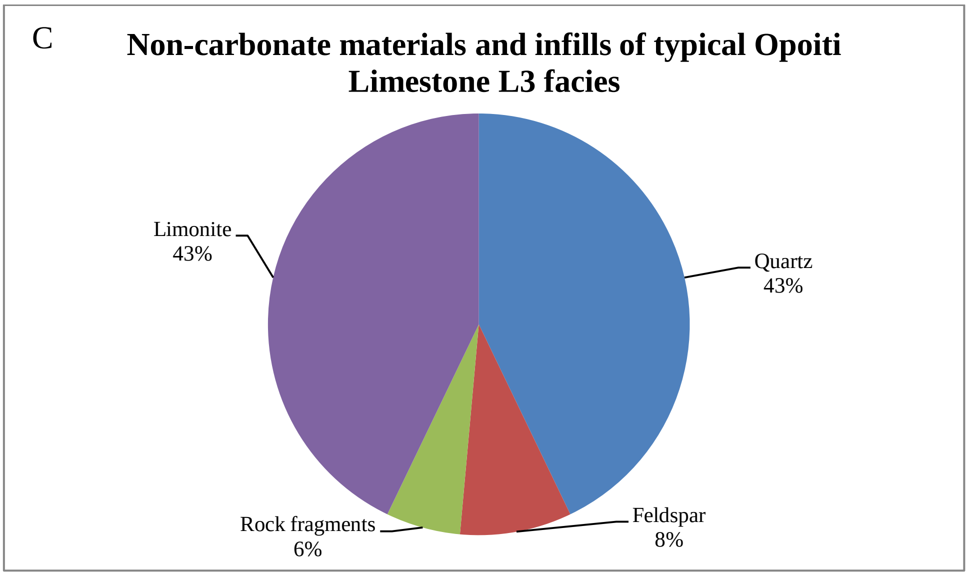

Figure 5.17: Petrographic summary of representative sample of facies L3 in the Opoiti Limestone. (A) whole rock, (B) skeletal types, and (C) non-carbonate materials. B.foram=Benthic foraminifera, P.foram=Planktic foraminifera.

Petrographic summary of facies type S2

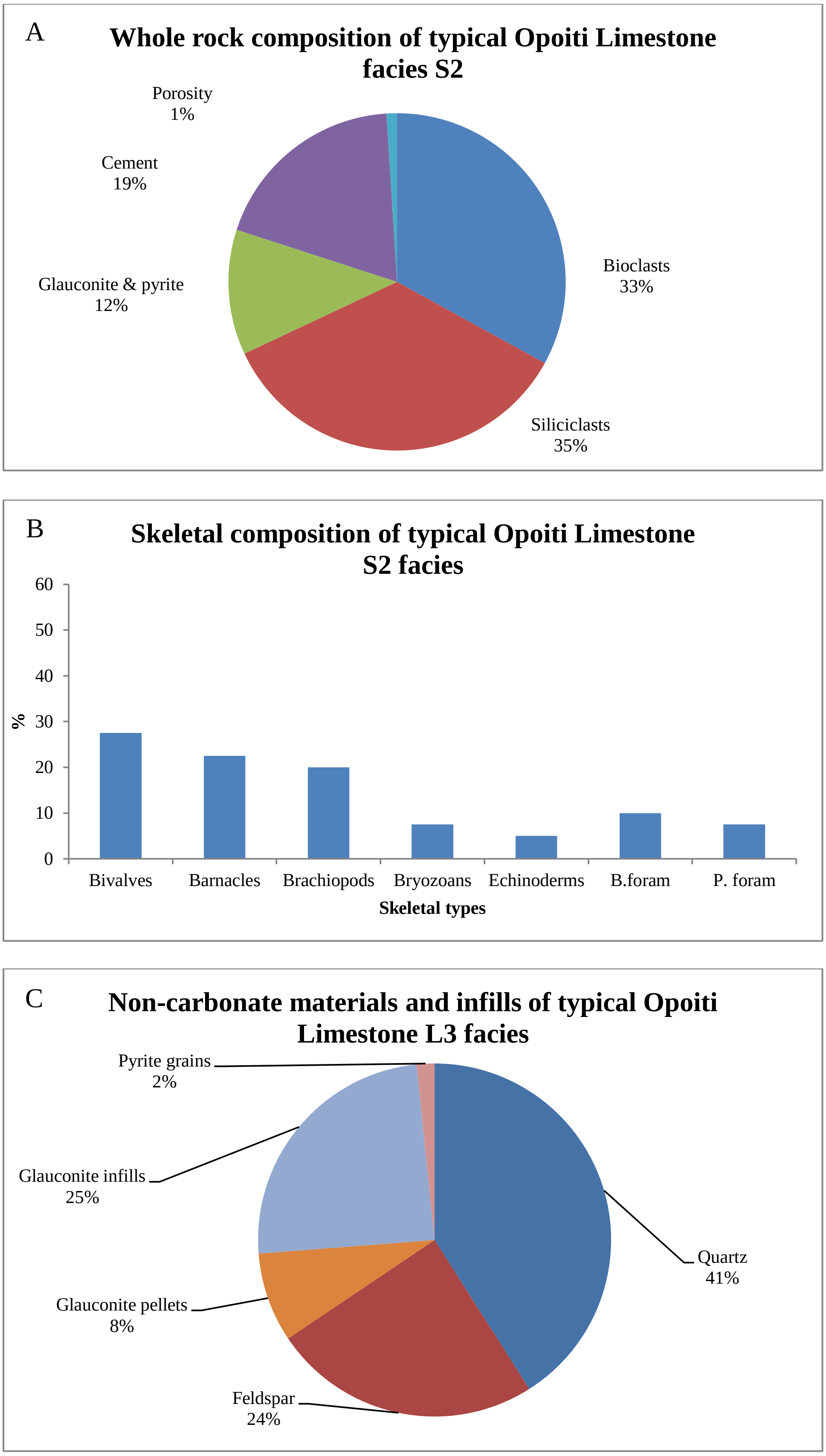

Figure 5.18: Petrographic summary of representative samples from facies S2 in the Opoiti Limestone. (A) whole rock, (B) skeletal types, and (C) non-carbonate materials. B.foram=Benthic foraminifera; P.foram=Planktic foraminifera.

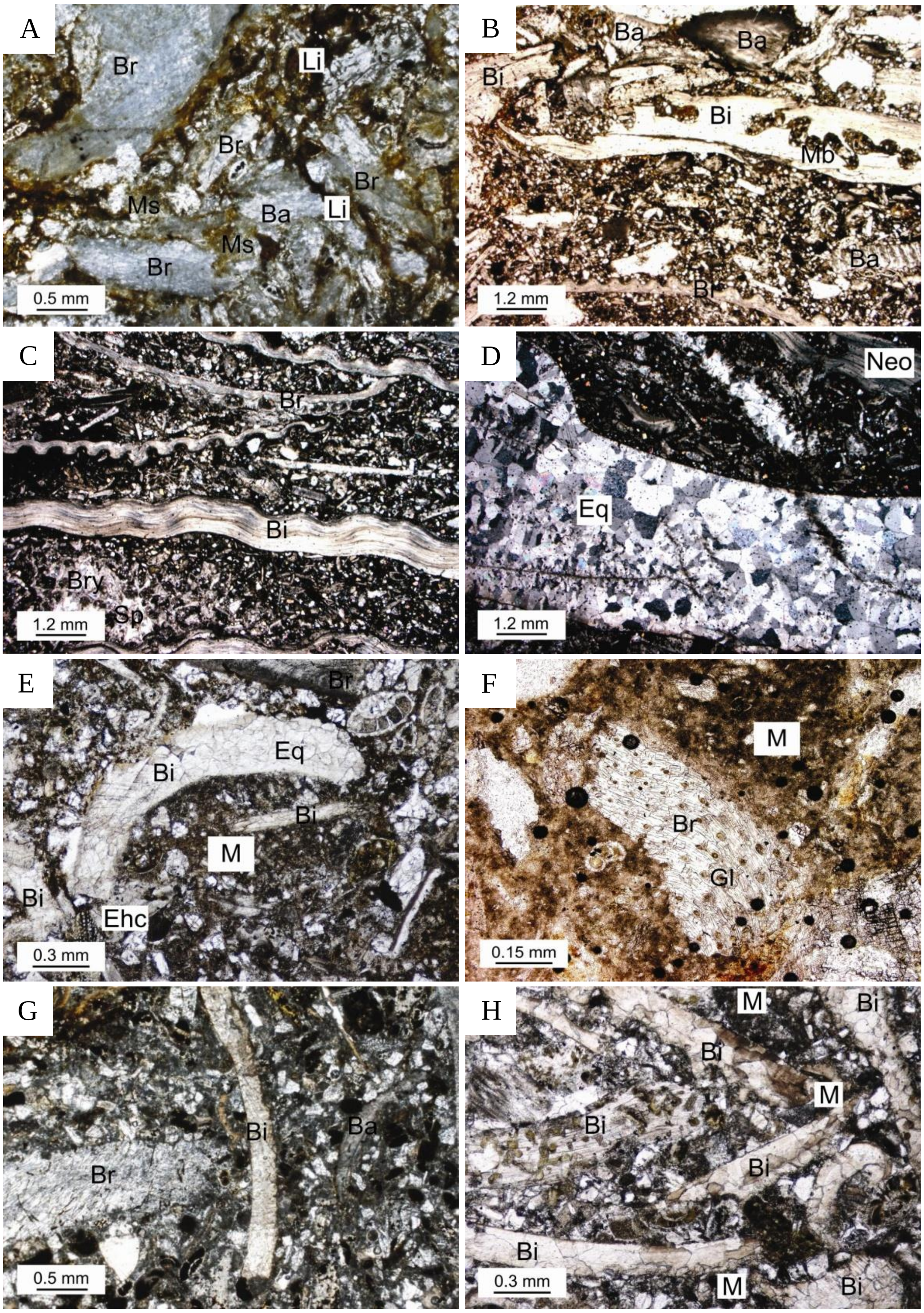

Figure 5.19: Photomicrographs under PPL and XPL. A) Overview image of limonitised biosparrudite (L3) consisting of poorly sorted barnacle (Ba) and brachiopod (Br) skeletons, and intrinsic limonite (Li) and microsparite (Ms), and evidence of weakly developed pressure-dissolution (sample Ra/op). B) Image of packed biomicrudite with poorly sorted barnacle and microbored (Mb) bivalve (Bi) skeletons are that extrinsically filled with bioclastic micrite (sample S15). C) XPL image showing a packed, coarse, poorly sorted bivalve dominated biomicrudite with large (>2 mm) neomorphosed bivalve skeletons packed in a siliciclastic and biomicrite matrix (sample H10.02). D) XPL image of packed, poorly sorted bivalve biomicrudite showing large biomould of former aragonitic bivalve filled with subequant (Eq) sparite in a mixture of fine siliciclastic grains and bioclastic micrite (M) (sample S15). E) Image of biomicrite exhibiting poorly sorted and abraded bivalve and barnacle skeletons, and clear subequant sparite infilled biomoulds (sample H10.02). F) Image of a glauconitic, brachiopod-rich biomicrite showing extrinsically filled glauconite (Gl) packed in micrite (sample 11.03). G) Image of a siliciclastic biomicrudite consisting of poorly sorted and abraded barnacle, bivalve and brachiopod skeletons (sample 11.02). H) Shows subequant sparite infill the aragonitic biomoulds packed in micrite (sample S15).

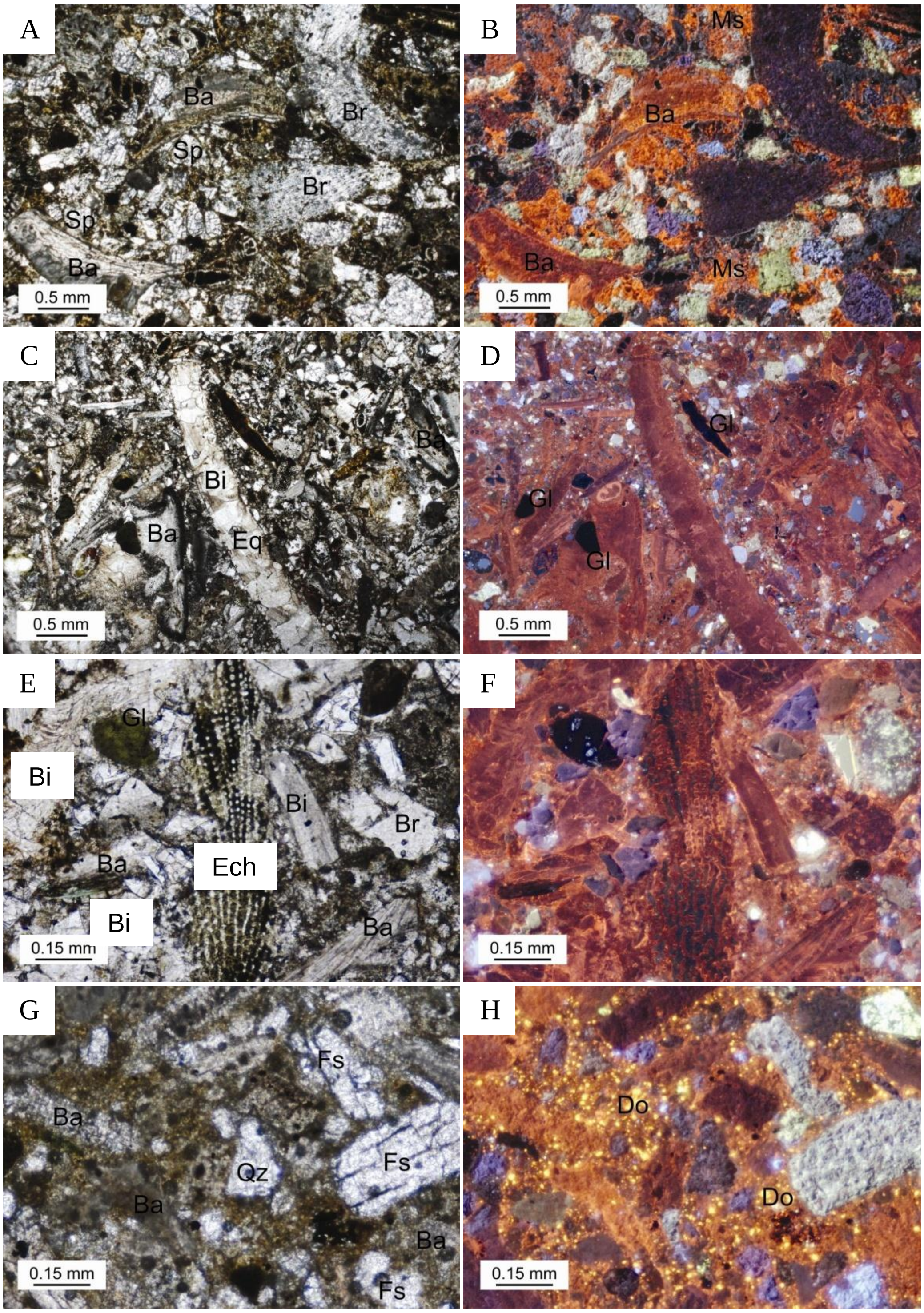

Figure 5.20: Photomicrograph pairs under plane polarised light (PPL) and cathodoluminescence light (CL). A & B) Poorly sorted, abraded brachiopod and barnacle-rich bioclastic sandstone. Barnacle (Ba) (dull orange) and brachiopod (Br) (dark purple) skeletons and subhedral to anhedral shaped siliciclastic grains bounded by microsparite (Ms) and/or micrite (sample 11.03). C & D) Poorly sorted, siliciclastic-rich barnacle (Ba) and bivalve (Bi) biomicrudite with biomoulds of former infaunal bivalve skeletons filled by subequant (Eq) sparite. The siliciclastic grains show a range of shapes and colours from cream to purple. Micrite cement in the background shows moderate orange luminescence. Authigenic grains (glauconite-Gl) are non-luminescent (black) (sample S15). E & F) Poorly sorted siliciclastic biomicrite showing some biomoulds of former aragonitic bivalves (Bi) filled with subequant (Eq) sparite exhibiting reddish to dull orange luminescent, and echinoderm (Ech) and other skeletal fragments cemented by microsparite and/or micrite (sample S15). G & H) Poorly sorted siliciclastic-rich biomicrite contains speckles of bright orange to yellow luminescent non-stochiometric dolomite (Do). Quartz (Qz) and feldspar (Fs) show a range of CL colours from cream to purple (sample T2.02).

Petrographic classification

Petrographically, the Opoiti Limestone samples typically range from being a bioclastic quartzofeldspathic arenite to a limonitised, brachiopod-dominated biosparrudite to poorly sorted, unabraded barnacle and bivalve biosparrudite. Overall the unit is dominated by siliciclastic grains mixed with barnacle and calcitic (epifaunal) bivalve and locally brachiopod debris, well cemented by low-Mg calcite microsparite or micrite, and locally dolomite-bearing, with localised clear subequant calcite sparite infilling former infaunal aragonitic bivalve skeletons.

6 Chapter Six

Whakapunake Limestone

6.1 Introduction

This chapter describes the lithostratigraphy, petrology and geochemical characteristics of the Whakapunake Limestone (late Opoitian, Early Pliocene), mostly a mixed sandstone and limestone unit in northern Hawke's Bay. Stratigraphic columns have been constructed (Appendix I) and representative samples of the formation were collected in the field for laboratory-based petrological work, including standard and cathodoluminescence (CL) petrography, bulk X-ray diffraction, and $CaCO_3$ content and grain size analysis.

6.2 Name and definition

The name Whakapunake Limestone derives from the Whakapunake Trig (961 m; X18/092561, Fig. 6.1), 7 km ENE of Te Reinga. The limestone was first mentioned by Smith (1877) who was also the first to map the limestone in the area, as far south as Te Hiwera, and at Mt Moumoukai inland from Morere (Beu 1995). Beu *et al.* (1980) informally gave the name to the thick limestone on the Whakapunake dipslope, near Te Reinga and around the Haupatanga Gorge on the eastern limb of the Wairoa Syncline in the present study area. Beu (1995) also assigned the name Whakapunake Limestone to an age correlative unit to the east, in the West Mahia Syncline (Drinnan 2011).

The Whakapunake Limestone is the youngest Opoitian carbonate-rich deposit. It disconformably overlies undifferentiated late Opoitian mudstone and sandstone of Wairoa Formation B, and either passes gradationally up into mudstone of Wairoa Formation C or is unconformably overlain by the Waipipian Tahaenui Limestone in the present study area. The Whakapunake Limestone is absent on the western limb of the Wairoa Syncline. The Whakapunake Limestone comprises alternating sandstone and shelly limestone beds, and is a typically barnacle and bivalve-dominated formation containing late Opoitian *Phialopecten marwicki* pectinids (Beu 1995). The apparent dip of the limestone is about 20º W. Beu (1995) suggested that the total thickness of the limestone was 460 m, but Nelson *et al.* (2003) thought this value was possibly an aggregate thickness across a series of clinoforms, and suggested the thickness was nearer 150 m.

There are two age correlative limestone formations in the Pliocene Te Aute facies from outside the present study area (Table 6.1), namely the Dyerville Limestone above the early Opoitian Haurangi Limestone near Martinborough in southern Wairarapa, and the Waiouru Limestone near west and south of the Napier-Taihape Road in central Hawke's Bay.

Table 6.1: Early Pliocene (late Opoitian) age Te Aute limestone units in the eastern North Island, New Zealand (based on Beu 1995; Field *et al.* 1997; Nelson *et al.* 2003) that contain small/juvenile specimens (< 10 cm size) of the age diagnostic pectinid fossil *Phialopecten marwicki.*

Age	New Zealand stage and abbreviation	Limestone formations
Early Pliocene	Late Opoitian (Wo)	Dyerville, Waiouru, Whakapunake

6.3 Type locality and reference section

Beu (1995) designated the type locality for the Whakapunake Limestone as the section exposed on the farm track over the limestone massif on the northern side of the Haupatanga Gorge (X19/041468) at the end of Kotare Road (Fig. 6.1). Here the limestone disconformably overlies late Opoitian differentially cemented shelfal mudstone and sandstone formerly assigned to the Opoiti Formation, but now to Wairoa Formation B (Fig. 6.2). The Whakapunake Limestone is separated from the overlain Waipipian Tahaenui Limestone by a regional angular unconformity. Beu (1995) also designated a reference section within the Haupatanga Gorge where the limestone dipslope is cut through by the Mangapoike River to expose nearly 100 m thick of differentially cemented, crossbedded barnacle and pectinid-dominated limestone. This reference section contains the most complete record of the Whakapunake Limestone but it is largely inaccessible, except from location A for a short distance by dinghy boat at the western end of the gorge (Fig. 6.1).

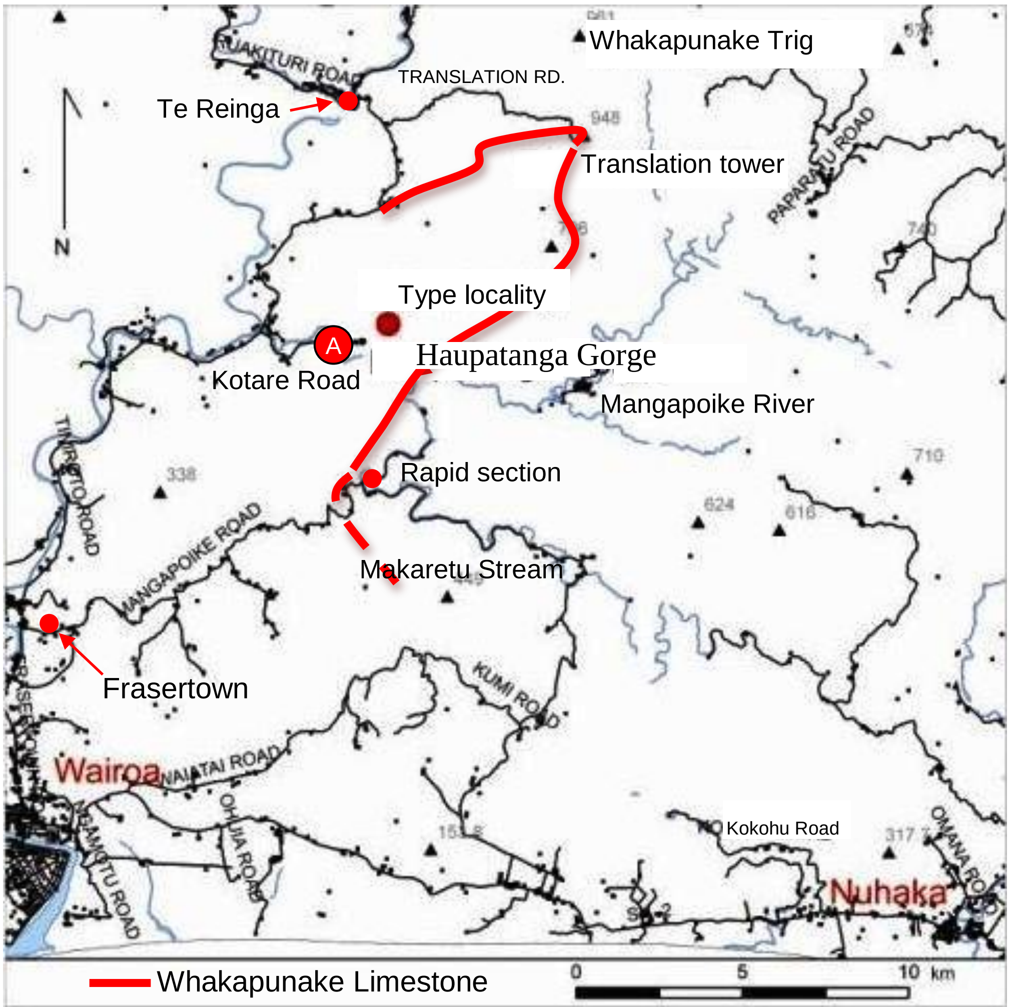

Figure 6.1: Location of the type locality (X19/041468) for the Whakapunake Limestone showing in red dot.

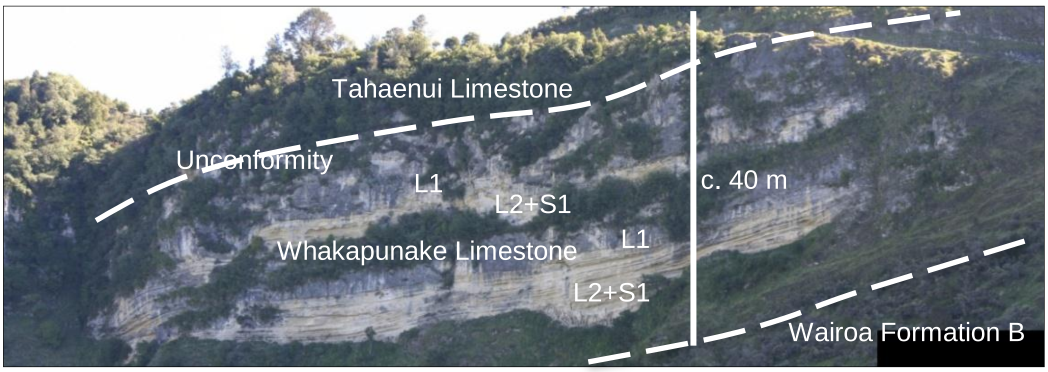

Figure 6.2: Impressive limestone scarp involving the Whakapunake Limestone at its type locality on the farm track at the end of Kotare Road. Location X19/041468.

6.4 Lithology

The total observed thickness of the Whakapunake Limestone varies from c. 30 to nearly 100 m in the study area. It generally dips 16-19° SW on the eastern limb of the Wairoa Syncline. The unit is mainly much thicker than the other limestone units (Opoiti and Tahaenui Limestones) in the study area, despite loss of some original thickness beneath the regional angular unconformity at its top. The unit exhibits differential cementation or comprises alternating beds of well cemented thin limestone (c. 20-30 cm) (L2) with less cemented calcareous sandstone (30-50 cm) (S1), collectively conveniently called a limestone. The well cemented limestone beds often include large (>15 cm) *Crassostrea ingens* oyster shells and coarse barnacle and bivalve skeletal fragments. The less cemented grey to pale yellow, calcareous sandstone beds contain small (<9 cm), disarticulated *Phialopecten marwicki* bivalve shells and other common macrofossils. There is no species separation in pectinid biostratigraphy (*Phialopecten marwicki*) between the late Opoitian and Waipipian rocks in the present study area, although the former typically has smaller (≤10 cm) specimens (Beu 1995). The Whakapunake Limestone also occurs as a pale yellow to cream, massive to poorly bedded, barnacle and bivalve-dominated limestone (L1) (Fig. 6.4A) within the differentially cemented portion. The $CaCO_3$ content varies between 14 and 85% for all three facies.

Rapid section (Fig. 6.1)

The Rapid section is located on the west side of Mangapoike Road, 300 m north of the junction of the Mangapoike Road and Hereheretau Road (Fig. 6.3A; X19/029429). This outcrop represents the southern extremity of the Whakapunake Limestone. Only the top 5-10 m of the formation is exposed here. The limestone is a massive to poorly bedded (Fig. 6.3B), pale yellow, well indurated, barnacle and pectinid-dominated limestone (L1) (Fig. 6.4B). It dips c. 16° SW, and is conformably overlain by 10-15 m of massive, light grey, soft, calcareous mudstone (M1) of the late Opoitian Wairoa Formation C.

Whakapunake dipslope

The Whakapunake Limestone forms an impressive scarp along base of the Whakapunake dipslope on Pohaturoa Station on the eastern side of Tiniroto Road (S.H. 36), north of Te Reinga (Fig. 6.3C). The limestone is thick (40 m), more prominent, and massive to poorly bedded in the north (Fig. 6.3D), and southwards becomes interbedded sandstone and limestone (Fig. 6.3E) and eventually mainly a sandstone (Fig. 6.3F) just north of Te Reinga. The Whakapunake Limestone forms a N-S trending ridgeline for c. 15 km from the Whakapunake trig south to the Haupatanga Gorge (X18/098561-038457, Fig. 6.1) on the eastern side the dipslope. The Whakapunake Limestone south of the Translation Road is on Mahurangi Station. The thickness of the limestone varies from 30-60 m; the thickest c. 60 m occurrence is at the Whakapunake Trig and marks the northern extremity of the Whakapunake Limestone. Overall, the limestone comprises interbeds of fine-grained calcareous sandstone (S1) (Fig. 6.4C & D) and sandy limestone (L2) (Fig. 6.4E & F), sometimes especially pronounced by weathering differences.

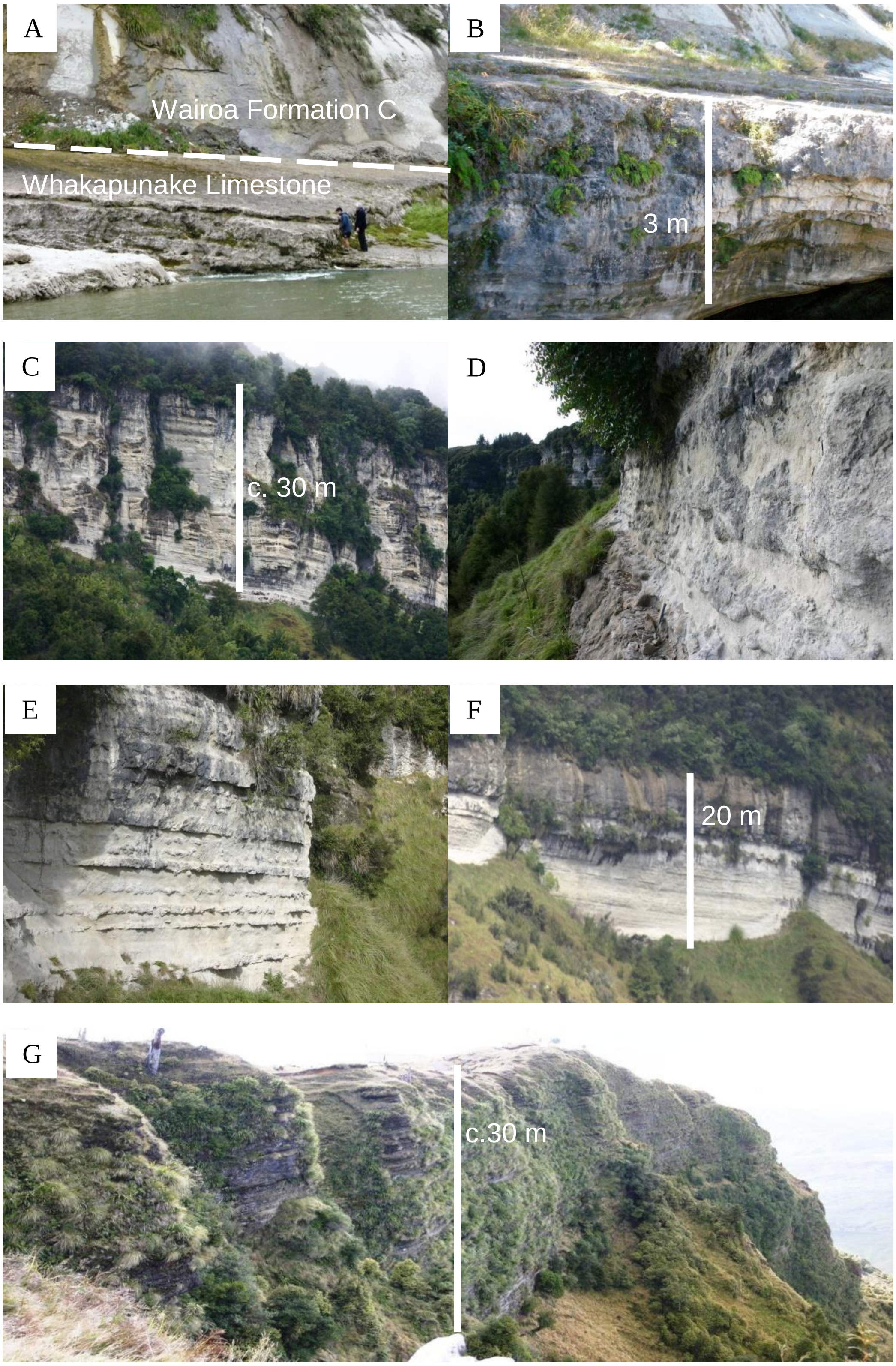

Figure 6.3: A) Whakapunake Limestone outcrop at the Rapid section showing the poorly bedded limestone (L1) overlain by Wairoa Formation C (M1). Location X19/029429. B) Close-up view of the pale yellow-cream, weakly bedded limestone (L1). C) The limestone scarp along the eastern side of Tiniroto Road, north of Te Reinga. Location X18/037550. D) The base of the limestone scarp on Tiniroto Road looking northwards. The limestone here becomes poorly bedded and flaggy (L1). E) Same locality as previous image, looking towards south. The limestone becomes more differentially cemented involving facies L2 and S1. F) Further south, the basal differentially cemented portion becomes calcareous sandstone, immediately north of Te Reinga. G) Whakapunake Limestone near the translation tower is strongly differentially cemented. Location X18/090528.

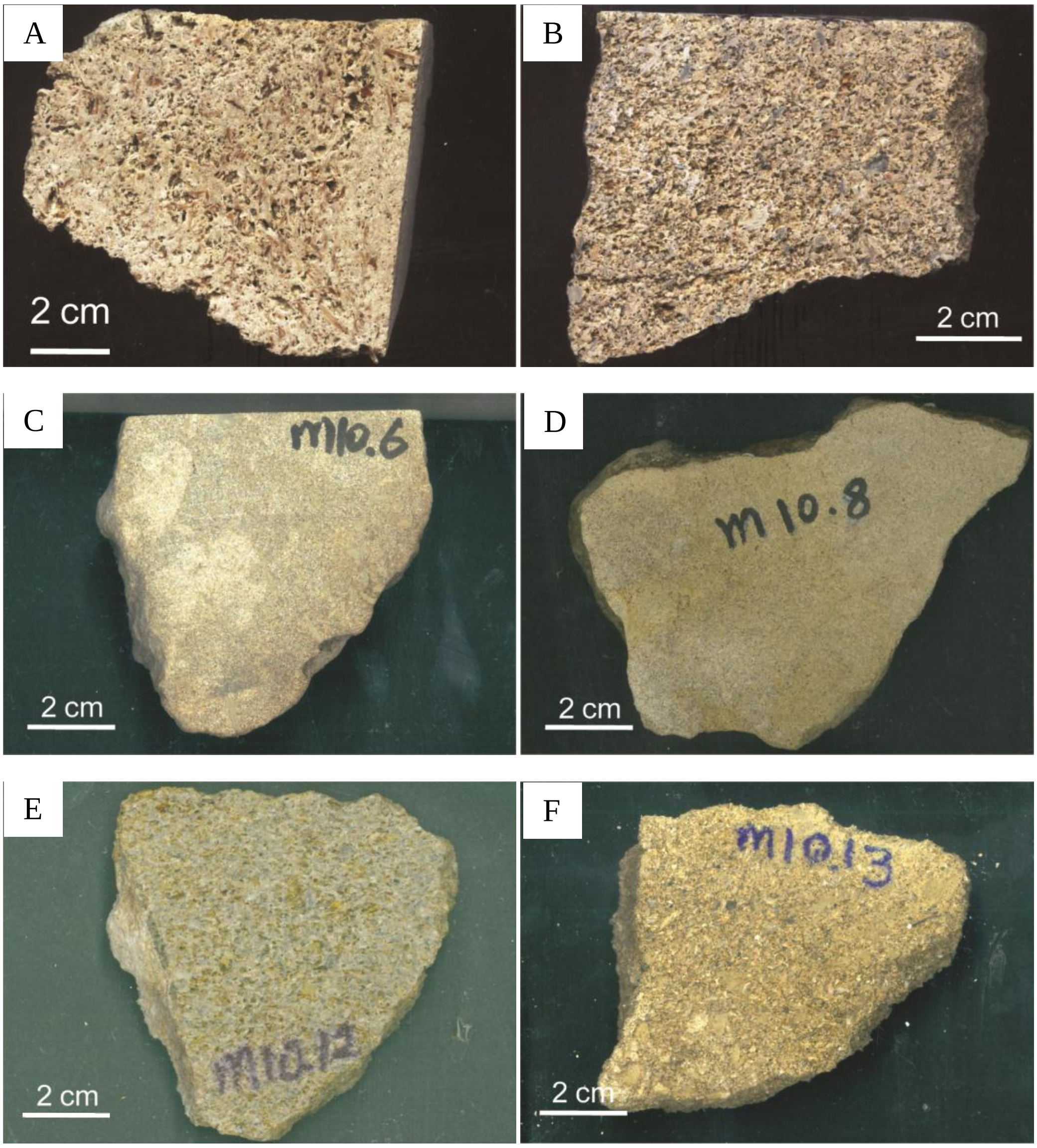

Figure 6.4: Cut rock slabs show the typical fabric of the three facies in the Whakapunake Limestone in the study area. Facies L1 – barnacle and pectinid-dominated limestone, A) Along the Kotare farm track (sample Ko1.02), and B) At the Rapid section (R1.02). Facies S1 – massive calcareous sandstone interbeds, C & D) below the Kotare farm track. Facies L2 – well-cemented, shell limestone, E & F) below the Kotare farm track.

6.5 Lower and upper contacts

The Whakapunake Limestone disconformably overlies the late Opoitian mudstone and sandstone of the Wairoa Formation B (M1, M2, S2 and S3). At the type locality it disconformably overlies the Opoitian differentially cemented, light grey, calcareous mudstone (M2) of Wairoa Formation B. The Whakapunake Limestone is unconformably overlain by the Tahaenui Limestone, which locally reduces its true stratigraphic thickness. This unconformity separates the Opoitian (Early Pliocene) from Waipipian (Late Pliocene) rocks (Fig. 6.5A).

The lower contact is a disconformity over the present study area. At Haupatanga Gorge the Whakapunake Limestone disconformably overlies late Opoitian differentially cemented mudstone (M2). There is no change of dip angle below and above the contact (Fig. 6.5A). The contact itself is sharp and easily recognisable in outcrops, especially from afar (Fig. 6.5B).

The upper contact varies from place to place and identifying an unconformity can be difficult. Early workers at the type locality mistook the Whakapunake Limestone as having a Waipipian age, partly because the unconformity is less pronounced where the Waipipian Tahaenui Limestone sits directly on the Whakapunake Limestone. Also, the lack of speciation for the pectinids makes the differentiation harder. Edwards & Hornibrook (1980) identified the same unconformity between the upper Tahaenui Limestone (Waipipian) and underlying Wairoa Formation B, 1 km south of Haupatanga Gorge, above the Makaretu Stream (X19/040443) (Beu 1995). Here the Whakapunake Limestone is cut out by this unconformity.

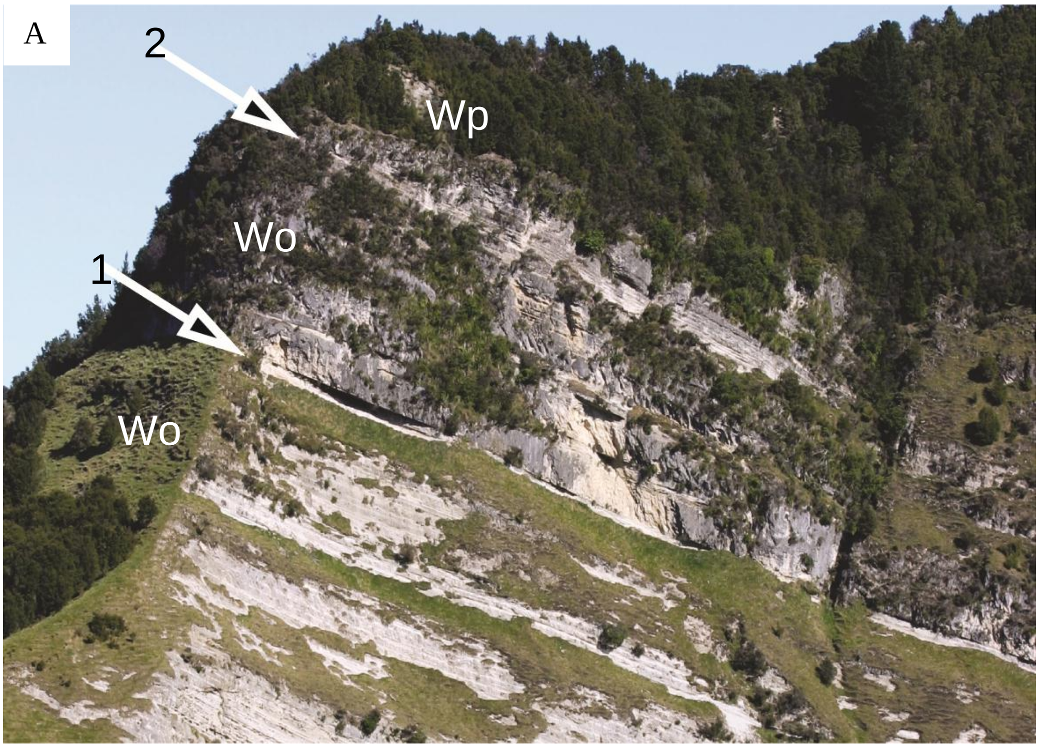

Figure 6.5: A) The disconformable contact 1 between Whakapunake Limestone and the differentially cemented mudstone below, and the low-angle unconformity 2 marking here the Opoitian-Waipipian stage boundary that separates the Whakapunake and the Tahaenui Limestones along the scarp of the Haupatanga Gorge. B) Lower contact of the Whakapunake Limestone below the Kotare farm track X19/040466.

6.6 Distribution and thickness

Outcrops

The Whakapunake Limestone only crops out on the eastern limb of the Wairoa Syncline in the present study area (Fig. 6.1). The limestone forms the lower portion of the bluffs on both sides of the Whakapunake dipslope. On the western side, the limestone crops out along the eastern side of Tiniroto Road from north of Te Reinga to Whakapunake Trig. On the eastern side of the dipslope it forms a limestone ridge running continuously from Whakapunake Trig southwards to Haupatanga Gorge. The Whakapunake Limestone has very limited accessible outcrop. The most complete section occurs through the narrow and deeply incised Haupatanga Gorge, but is largely inaccessible. The Whakapunake Limestone varies in thickness from c. 5-60 m, thickening to the north (30-60 m) and thinning (5-20 m) at the surface in the southern part of the study area.

Subcrops

The Whakapunake Limestone is inferred to be present in the subsurface north of Frasertown, being intersected by two petroleum wells drilled within the Wairoa Syncline in the present study area, namely Kauhauroa-4 and -5 (PR 2256 1999; PR2431 1999). The minimum thickness of the limestone intersected in these drill holes is 10 m. The limestone from Kauhauroa-5 was described as a dark grey calcarenite, being moderately well indurated and comprising medium to very coarse sand-size carbonate grains, with well sorted, fine sand-size subangular quartz (PR2431 1999).

6.7 Paleontology

The Whakapunake Limestone hosts common *Phialopecten marwicki* (Fig. 6.6A), barnacles including *Notobalanus vestitus, Austromegabalanus (Notomegabalanus) miodecorus, Austromegabalanus decorus argyllensis, Fosterella tubulatus and Balanus variegates,* and the oyster *Crassostrea ingens* (Fig. 6.6B) (Beu 1995).

The late Opoitian pectinids from many localities around North Island are similar to early Waipipian specimens in valve convexity (including discrepancy between the two valves), in disc and auricle shape, and in the primary costae bearing three radial riblets, particularly on the left valve. Therefore, both Opoitian and Waipipian specimens are regarded as a single species of *Phialopecten marwicki*. Also through these stages the only obvious change is a long-continued, gradual increase in both mean and maximum shell size (< 10 cm) with small *Phialopecten marwicki* being restricted to late Opoitian strata (Beu 1995).

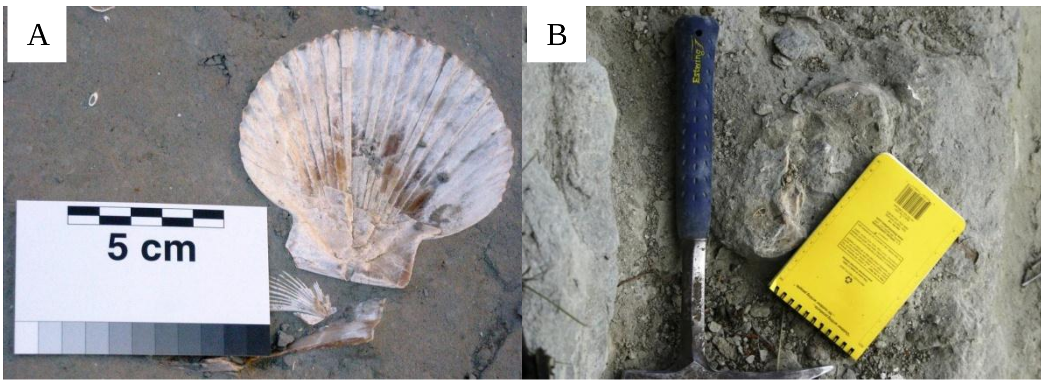

Figure 6.6: A) Late Opoitian *Phialopecten marwicki* specimens in Wairoa Formation C, directly above the Whakapunake Limestone at the Rapid section (X19/029429). B) *Crassostrea ingens* oysters in the less cemented sandstone facies (S1) of the Whakapunake Limestone (X18/037550).

6.8 Lateral age correlatives

Dyerville Limestone

The Dyerville Limestone was proposed by Beu (1995) for the limestone overlying the Haurangi Limestone near Pakohe Quarry, in Dyerville, SE of Martinborough. Beu (1995) also assigned the name to the 'upper Haurangi Limestone' exposed at Haurangi hairpin bend, in the nearby upper Ruakokopatuna Valley (Fig. 6.7). Beu (1995) designated the type locality as the 20 m thick limestone bluffs cropping out NE of the Pakohe Quarry (S27/102853 to 106854). At this locality, the limestone strikes NE-SW and dips 25° NW. It is a weakly bedded to differentially cemented, coarse, softly to moderately indurated, barnacle-dominated grainstone, typical of the Te Aute type facies. The limestone is paraconformably overlain by Mangapanian Bull Creek Limestone at Haurangi hairpin bend. Beu (1995) identified the moderately common presence of disarticulated *Phialopecten marwicki* (≤ 9.5 cm) within the Dyerville Limestone in the Pakohe Quarry area, which gives the late Opoitian age.

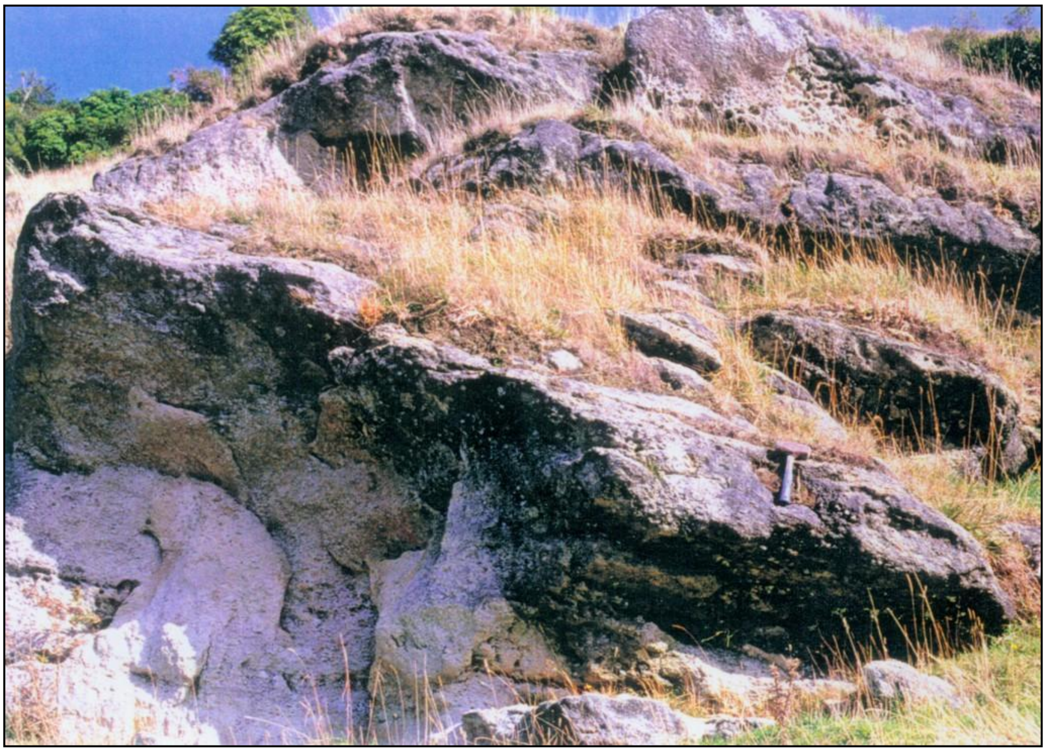

Figure 6.7: Poorly bedded, softly to moderately indurated, late Opoitian (Early Pliocene) Dyerville Limestone, Haurangi hairpin, Wairarapa (S28/100979). Photo: Dr Steve Hood.

Waiouru Limestone

The Waiouru Limestone (late Opoitian) is a sandy limestone exposed in isolated outcrops widely distributed in the Waiouru area, on the western side of Napier-Taihape Road, and on the Mangaohane Plateau in the western Ruahines to the south of the Napier-Taihape Road (Beu 1995). Beu (1995) described the limestone as a sandy, grey, impure limestone involving alternating sandstone and limestone interbeds. Samples collected by R. D. Black contained small *Phialopecten marwicki* specimens (<110 mm), indicative of a late Opoitian age (Beu 1995).

6.9 $CaCO_3$ content

The $CaCO_3$ content of the Whakapunake Limestone typically varies from c. 45-85% (Table 6.2). Facies L1 is the purest limestone, with a $CaCO_3$ content from 70-85%, and represents the relatively massive portion of the limestone. Facies L2 is an impure limestone with a $CaCO_3$ content of c. 55%, and forms the well cemented limestone interbeds in the differentially cemented portions of the formation. Facies S1 is the least well cemented and comprises sandstone beds with a highly variable $CaCO_3$ contents from c. 15-50% (Fig. 6.8). The siliciclastic sand and mud content for the Whakapunake Limestone is shown in Table 6.2, with sand contents from c. 10-65%, and mud contents from c. 5-25%. The raw carbonate and size data are given in Appendix II.

Table 6.2: Bulk $CaCO_3$ and insoluble sand and mud content of eight samples of Whakapunake Limestone. Facies types defined in Table 4.1.

Sample No.	*Facies type*	*% $CaCO_3$*	*% Mud (<63 μm)*	*% Sand (63-2000 μm)*
M10.6	L2	54	10	36
M10.8	L2	55	15	30
M10.10	S1	50	17	33
Ko1.02	L1	84	4	12
R1.02	L1	69	24	7
P1.02	S1	44	25	31
P1.05	L2	53	24	23
trig 1.03	S1	14	23	63

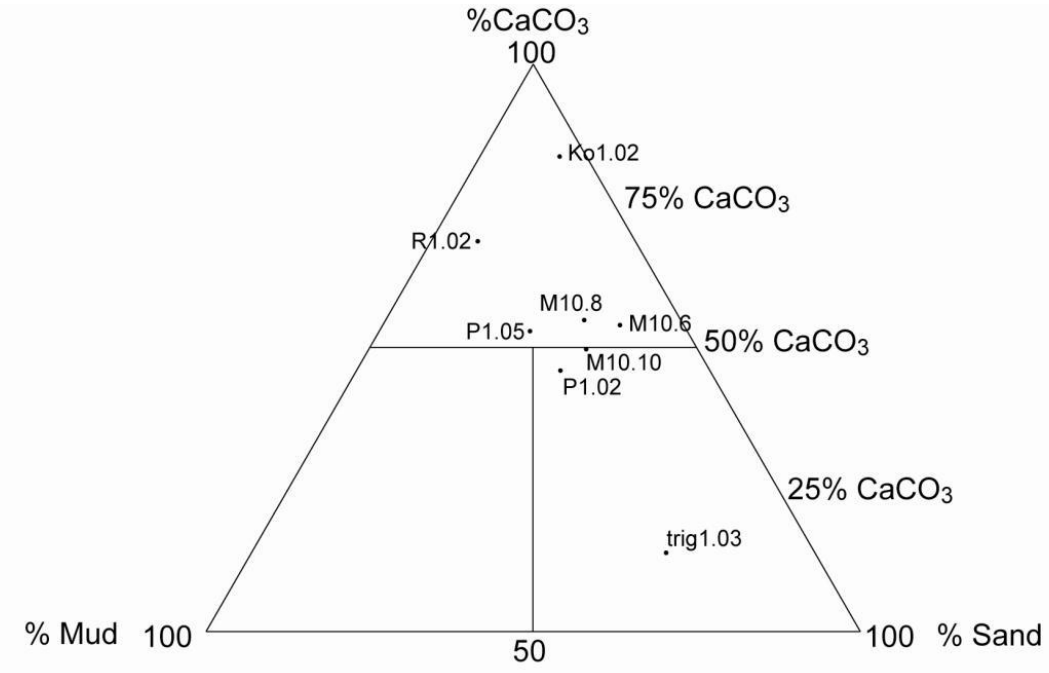

Figure 6.8: Ternary carbonate-sand-mud plot of samples from the Whakapunake Limestone.

6.10 Bulk mineralogy

Bulk mineralogical analysis was undertaken on three carbonate-rich samples from facies L1 and L2 and two samples from facies S1 of the Whakapunake Limestone using X-ray diffraction (XRD), as described in section 3.3. The dominant minerals present are low-Mg calcite, quartz and plagioclase feldspar (Table 6.3). Low-Mg calcite (c. 4 mol% $MgCO_3$) is expectedly common to very common in most of the samples, while two of the samples also show the presence of non-stoichiometric dolomite having c. 45 mol% $MgCO_3$ (Table 6.3). The common abundance of low-Mg calcite is related to the dominant constituents of skeletal grains of low-Mg calcite secretors, along with cement materials. Plagioclase feldspar and quartz are of secondary importance.

Table 6.3: XRD bulk mineral abundance in representative samples from Whakapunake Limestone.

Major minerals	*Dolomite*	*Low-Mg Calcite*	*Plagioclase feldspar*	*Quartz*	*Clays*	*Mica*
Ko1.02	-	VC	S	S	-	-
R1.02	S	C	S	S	-	-
P1.02	-	C	S	VC	R	
P1.05	S	VC	S	C	-	-
trig1.03	-	S	C	VC	R	-

Abbreviation	*Description*	*Counts*
-	None	0
R	Rare	1-20
S	Some	21-200
C	Common	201-500
VC	Very common	501-999
A	Abundant	≥1000

6.11 Insoluble grain texture

The texture of insoluble grains in Whakapunake Limestone is shown in Table 6.4. Sand forms 25-80% of the insoluble fraction, silt 20-70%, and clay <10%. Fig. 6.9 shows that most of the insoluble grains in the Whakapunake Limestone exhibit a silty sand texture, and two a sandy silt texture. The modal size of grains ranges from 74 to 190 µm, or very fine sand to fine sand.

Table 6.4: Bulk insoluble grain texture for eight samples of Whakapunake Limestone.

Sample No.	*Facies type*	*% Clay (<3.9 µm)*	*% Silt (3.9-63 µm)*	*% Sand (63-2000 µm)*
M10.6	L2	2	20	78
M10.8	L2	3	31	66
M10.10	S1	3	27	67
Ko1.02	L1	1	25	73
R1.02	L1	6	71	23
P1.02	S1	1	44	55
P1.05	L2	3	48	49
Trig1.03	S1	1	26	73

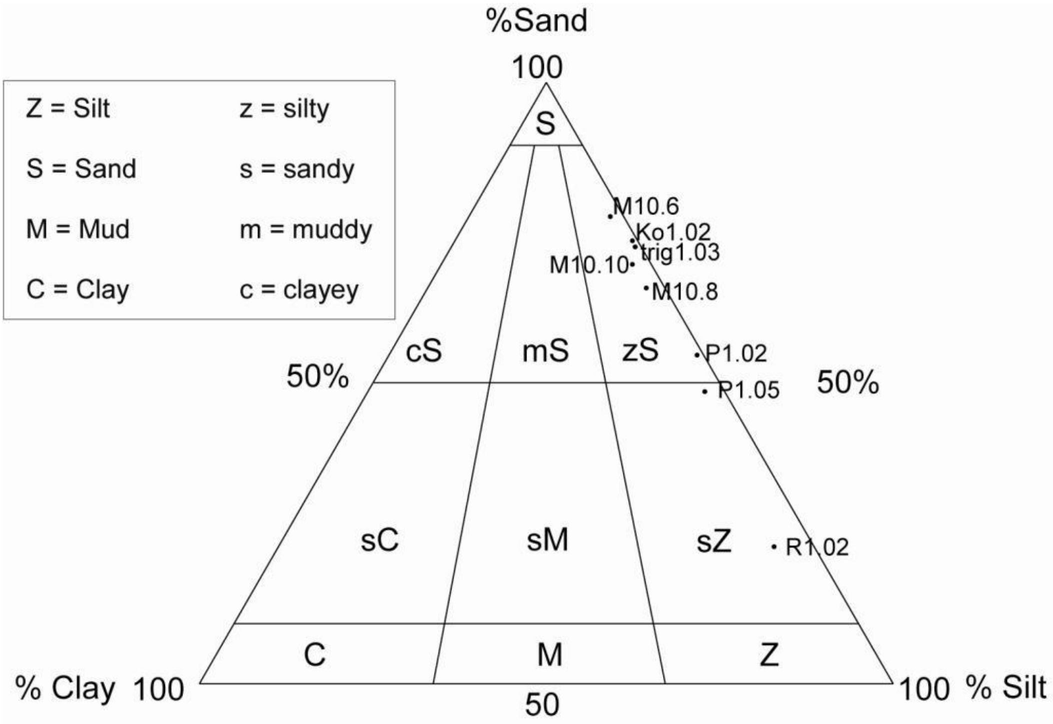

Figure 6.9: Ternary clay (C), silt (Z) and sand (S) plot (%) for the insoluble residue fraction from Whakapunake Limestone samples. Textural size classification from Folk (1959).

6.12 Stable isotope analysis

Table 6.5 summarises the stable oxygen and carbon isotope values of 7 representative samples from the Whakapunake Limestone, and suggests some possible minimum burial temperatures and burial depths for the deposits in northern Hawke's Bay (see section 3.5 for calculation method). Also plotted are samples analysed by Drinnan (2011) for Whakapunake Limestone correlative deposits from nearby Mahia district. The range of $\delta^{13}C$ values (-8.62 to +1.74‰) predominantly fall within or near the field for modern New Zealand skeletal carbonates, while the $\delta^{18}O$ values mainly fall between -1.53 and -0.59‰ near the fields for New Zealand modern carbonates and marine skeletons (Fig. 6.10). The majority of samples from the present study area show slightly negative $\delta^{18}O$ values, suggestive of at least shallow burial depth. Two samples from the type locality show a strong meteoric influence with moderately negative $\delta^{13}C$ values (Fig. 6.10) (Nelson & Smith 1996).

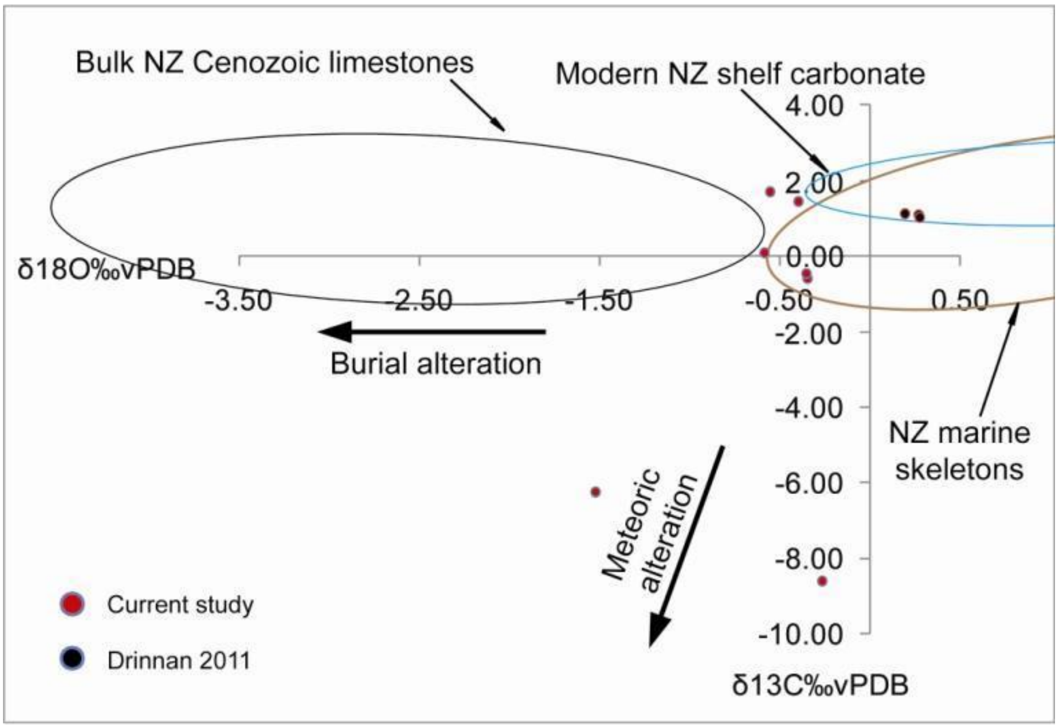

Figure 6.10: Cross-plot of oxygen and carbon isotope values for samples from the Whakapunake Limestone in relation to the core fields for NZ cool-water carbonates from Nelson & Smith (1996).

Calculated absolute minimum burial temperatures for samples fall between 16°C and 24°C, while the minimum burial depths range from 150 to over 300 m. Samples from the present Wairoa study area appear to have undergone mainly deeper burial than those to the east analysed by Drinnan (2011).

Table 6. 5: Bulk stable oxygen and carbon isotope data, and possible minimum burial temperatures and burial depths for samples from Whakapunake Limestone, northern Hawke's Bay (* data from Drinnan 2011).

Facies type	Whakapunake Limestone	Bulk calcite ‰		Calcite cement isotope *T*(°C)	Calcite cement paleodepth (m)
		$\delta^{13}C$	$\delta^{18}O$		
L2	M10.06	0.09	-0.59	19	303
L2	M10.08	-8.62	-0.27	18	244
S1	M10.10	-6.24	-1.53	24	483
L2	M10.12	-0.57	-0.35	18	260
S1	M10.15	-0.44	-0.36	18	261
L2	M.Flow	1.45	-0.40	18	268
L1	R1.02	1.74	-0.56	19	298
L3	106.2*	1.13	0.19	16	161
L3	108.2*	1.10	0.27	16	147
L3	108.2*	1.04	0.27	16	146

6.13 Petrography

The Whakapunake Limestone is the 'mid-aged' Pliocene carbonate-rich formation in the present study. The limestone comprises three field facies, including massive barnacle and pectinid-dominated limestone (L1), well cemented limestone (L2) and highly calcareous sandstone (S1). The petrography of each facies is presented in this section. The two limestone facies are typically dominated by skeletal fragments of barnacles and pectinids cemented by low-Mg calcite sparite, with localised dolomite rhombohedral crystals. The less well cemented calcareous sandstone facies interbeds are typically macrofossil-rich. The raw petrographic data for the Whakapunake Limestone are included in Appendix V.

The overall bioclast content for the Whakapunake Limestone varies from 30-60%, and the siliciclastic material content from 5-30%. The Whakapunake Limestone in the study area exhibits facies type L1, L2 and S1 (Table 4.1), the last two dominating. Figures 6.11A and 12A show average whole rock compositions of typical L1 (n=2) and L2 (n=5) facies within the Whakapunake Limestone. The typical L1 is a porous (13%) and sparry (20%), bioclast (55%)-dominated facies. Neither siliciclastic (7%) nor authigenic (5%) materials are common in this facies. The grains are held together by mostly microsparite and/or sparite cement. The whole rock composition of facies L2 is quite similar to L1, but with fewer bioclasts (40%) and a slight increase in cement materials (30%) and siliciclastic (15%) and authigenic (10%) grains. Figure 6.13A shows the whole rock composition of the soft sandstone interbeds of facies S1 (n=1). It is dominated by siliciclastic (28%) and authigenic (20%) materials, with only 30% bioclasts and 20% microsparite cement.

Skeletal grains

Figure 6.11B shows the proportions of major skeletal grains in facies L1 within the Whakapunake Limestone. The skeletal types are dominated by a subequal mix of bivalve (41%) and barnacle (41%) fragments, followed by fewer bryozoans (6%), echinoderms (6%) and some benthic (3%) and planktic (3%) foraminifera (Fig. 6.11B). The skeletal grains show a bimodal size distribution involving a primary mode at 1 mm (coarse sand) and a secondary mode at 2.4 mm (granule). The skeletal grains are poorly sorted but well abraded.

The skeletal composition of the L2 facies is a subequal mixture of three main skeletal grain types, namely bivalves (26%) and benthic (29%) and planktic (22%) foraminifera. Other skeletal components include barnacles (12%), brachiopods (2%), bryozoans (5%) and echinoderms (4%) (Fig. 6.12B). These carbonate grains have a unimodal size distribution, with a mode size at approximately 0.25 mm (medium sand). The skeletal grains are moderately to well sorted, and well abraded.

Barnacle fragments (35%) are the major skeletal component in facies S1, and then bivalves (13%), brachiopods (13%), and benthic (8%) and planktic (5%) foraminifera. The carbonate grains show a bimodal size distribution, with a primary mode at 0.2 mm (fine sand) and a secondary one at 0.1 (very fine sand). They are moderately sorted and well abraded.

Non-carbonate grains and infills

The average abundances of the non-carbonate components in the Whakapunake Limestone are plotted in Figures 6.11C, 6.12C and 6.13C. Facies L1 is dominated by subequal amounts of quartz (28%), feldspar (28%) and glauconite pellets (22%), with lesser amounts of glauconite infills (13%) and pyrite grains (9%). The siliciclastic grains show a bimodal size distribution, with a primary mode at 0.3 mm (medium sand) and a secondary mode at 0.2 mm (fine sand). These grains range from poorly to well sorted, and shapes vary from subangular to rounded.

Facies L2 is dominated by feldspar (36%) and subequal amounts of quartz (29%) and glauconite pellets (20%), with lesser amounts of glauconite infills (8%) and pyrite grains (7%). The siliciclastic grains show a bimodal size distribution, involving a primary mode at 0.2 mm (fine sand) and a secondary mode at 0.1 mm (very fine sand). These grains range from moderately to well sorted with subangular to subrounded shapes.

Facies S1 involves subequal quantities of quartz (29%), glauconite pellets (23%), less feldspar (19%) and glauconite infills (19%), and occasional pyrite grains (4%), mica (2%), rock fragments (2%) and pyrite infills (2%). The siliciclastic grains show a bimodal size distribution, with a primary mode at 0.2 mm (fine sand) and a secondary mode at 0.1 mm (very fine sand). These grains are well sorted with shapes ranging from subangular to subrounded.

Cement/matrix

The typical cement types in the limestone facies L1 and L2 are primarily microsparite and clear subequant sparite (Fig. 6.14A, B & C). The subequant sparite is second generation cement, and tends to have a granular fabric that formed atop thin (0.06-0.1 mm) isopachous cement fringes around typically barnacle and bivalve skeletons. It also infills biomoulds of former aragonitic skeletons, and leaves no retention of the former skeletal microarchitecture (Fig. 6.14C & D). In facies S1, the cements are mostly micrite, with some microsparite that precipitated intrinsically (Fig. 6.14E). Some pressure dissolution and micro-fractures occur between the grains in the well packed, unsorted barnacle-bivalve biosparites (Fig. 6.14F).

Cathodoluminescent petrography

The skeletal components of the Whakapunake Limestone show a range of CL colours from dark purple (formerly aragonitic bivalves) to dull orange (calcitic skeletal materials such as barnacles and epifaunal bivalves), with authigenic materials being non-luminescent (Fig. 6.15A & B). The cement materials show up clearly under CL, and colours range from purple/dull orange (isopachous fringe cement) to orange (subequant sparite) (Fig. 6.15C & D) to bright yellow (dolomite, which often contains zoned well-defined rhombohedral cores and/or zones) (Fig. 6.15E & F). The zoning represents growth stages of the dolomite, presumably a result of compositional changes of the dolomitising solutions (Katz 1971).

Petrographic summary of L1

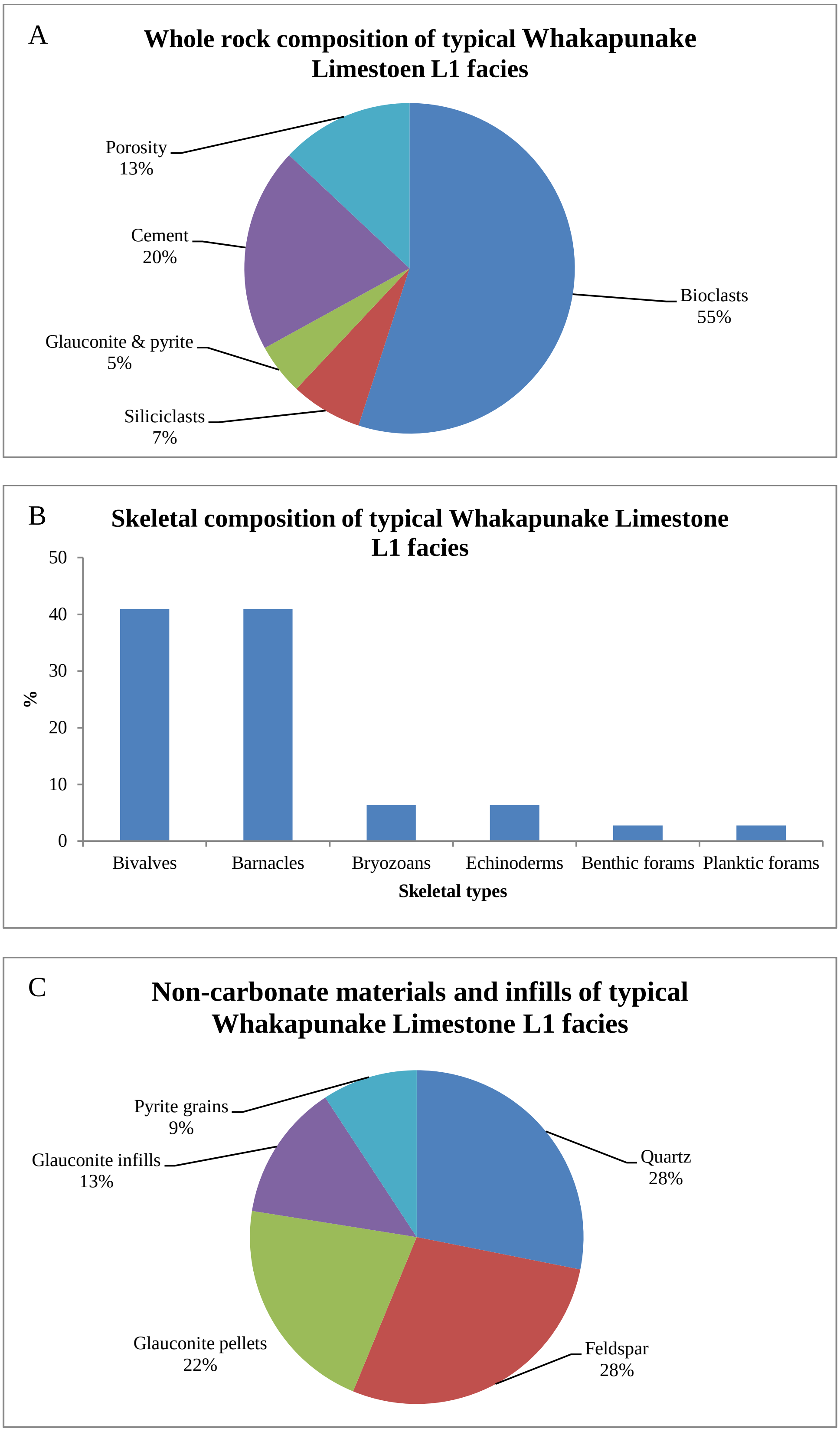

Figure 6.11: Petrographic summary based on representative samples (n=2) of Whakapunake Limestone (facies L1): (A) whole rock, (B) skeletal types, and (C) non-carbonate materials.

Petrographic summary of L2

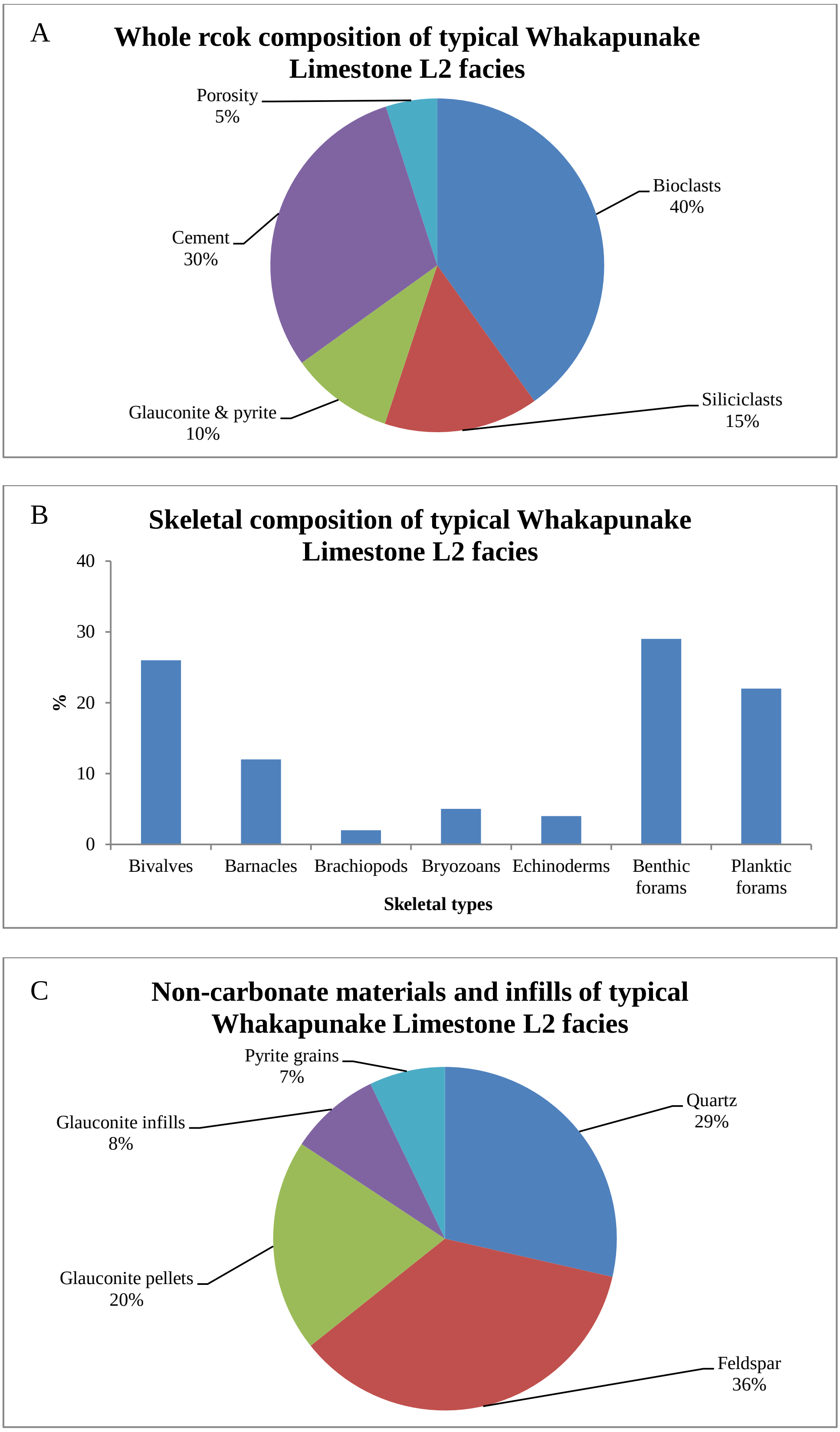

Figure 6.12: Petrographic summary based on representative sample (n=5) of Whakapunake Limestone (facies L2): (A) whole rock, (B) skeletal types, and (C) non-carbonate materials.

Petrographic summary of S1

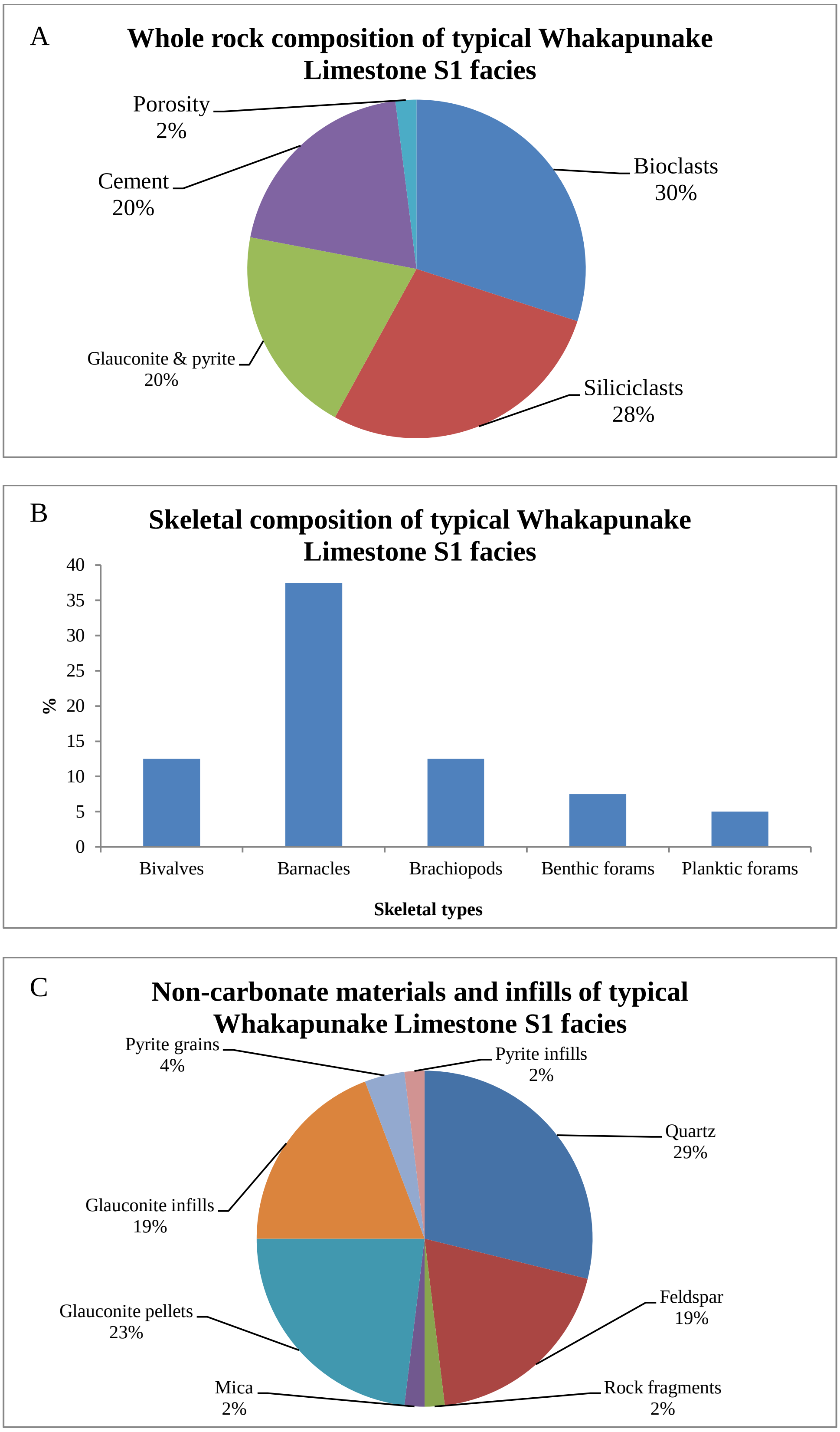

Figure 6.13: Petrographic summary based on representative sample (n=1) of Whakapunake Limestone (facies S1): (A) whole rock, (B) skeletal types, and (C) non-carbonate materials.

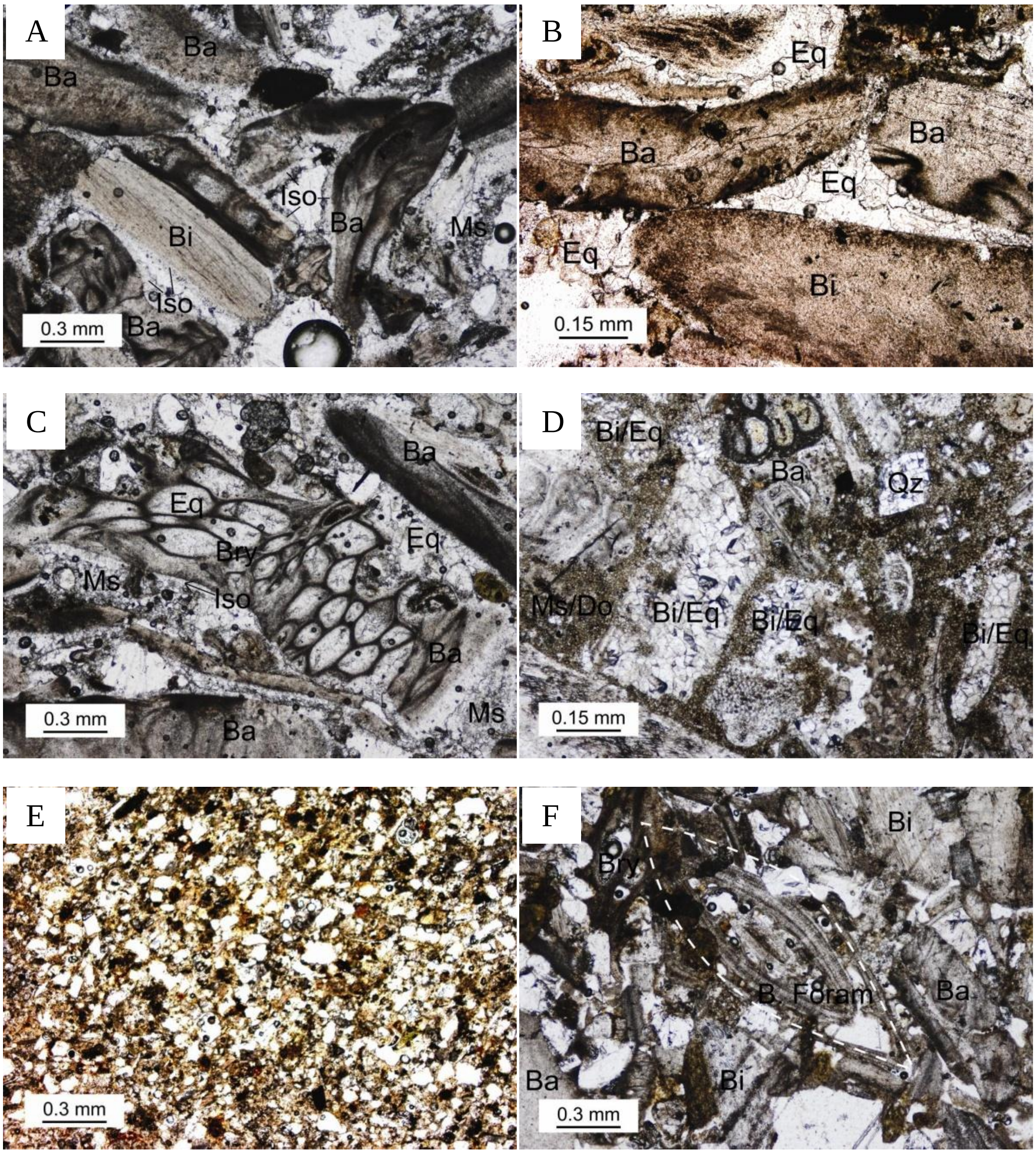

Figure 6.14: Photomicrographs of Whakapunake Limestone samples. A) Moderately sorted and well abraded barnacle (Ba) and bivalve (Bi) dominated biosparite. Clear isopachous fringe (Iso) cements (c. 0.1 mm thick) form around skeletal grains with microsparite partially infilling occluded pores (sample M10.12). B) An unsorted, well abraded bivalve-barnacle biosparrudite with clear and blocky subequant (Eq) sparite infilling the occluded pore spaces (sample M10.05). C) Poorly sorted and well abraded biosparrudite with skeletal grains coated by isopachous fringe cement (Iso), and microsparite and subequant spar cement (Eq) forming in skeletal chambers of the bryozoan (Bry) and barnacle (Ba) (sample M10.12). D) Packed dolomite-bearing biomicrite consisting of bivalve (Bi) and barnacle (Ba) skeletons with localised subequant (Eq) sparite infilling biomoulds of former aragonitic bivalve (Bi) skeletons (sample R1.02). E) Glauconitic, mature quartzofeldspathic arenite of facies S1 showing moderately to well sorted siliciclastic grains cemented by microsparite and/or micrite (sample M10.14). F) Tightly packed biomicrite showing subhedral to anhedral shape siliciclasts pressure dissolved into a football shape benthic foraminifera. Other skeletal grains are also either pressure dissolved or fractured.

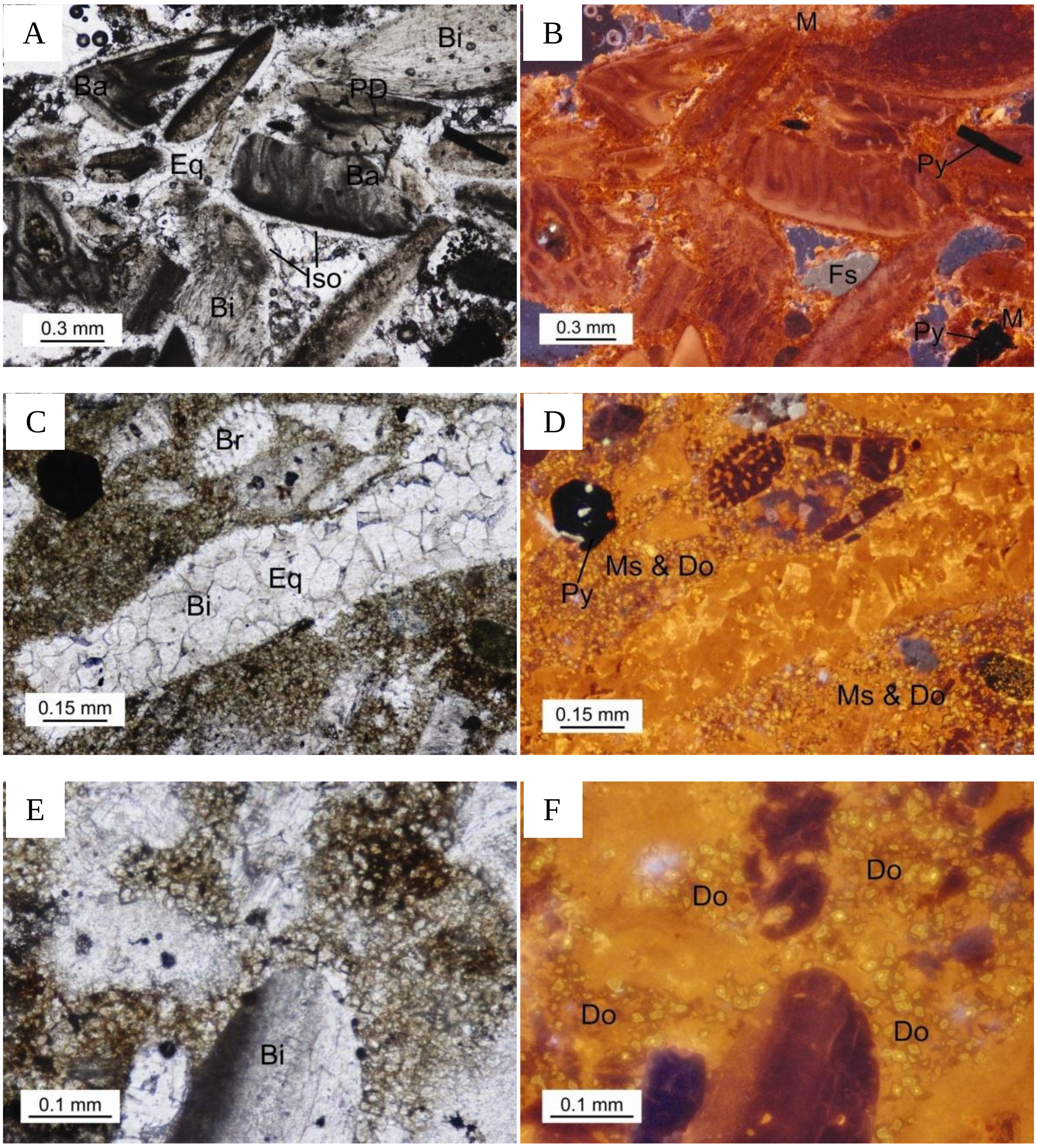

Figure 6.15: Photomicrograph pairs under PPL (left) and CL (right). A & B) Image of a moderately sorted and well abraded bivalve and barnacle biosparite. Skeletal grains are coated with thin fringe cement, exhibiting reddish to a dull orange luminescence, and well distinguished from occluded pores. The fringe cements (c. 0.06 mm thick) show reddish luminescent at the edge of the skeletal grains and brighten to orange porewards (sample M10.12). C & D) Packed biomicrite showing biomould of a former aragonitic bivalve infilled with clear subequigranular sparite and with no retention of the skeletal microarchitecture. The skeletal and other grain types exhibit a purple to reddish luminescent and are cemented with dolomite-bearing micrite (sample R1.02). E & F) Close-up view of the dolomite-bearing micrite matrix showing the well-defined rhombohedral core and/or zones of dolomite crystals (sample R1.02).

Petrographic classification

Petrographically, the Whakapunake Limestone samples range from packed, dolomite-bearing biomicrite to well rounded, bivalve-barnacle fine biosparrudite. Overall the limestone is skeletal grain-dominated and locally dolomite-bearing, with quartzofeldspathic arenite interbeds, cemented by low-Mg calcite (micro)sparite and/or micrite, and common subequant sparite infilling the pores and biomoulds of former infaunal aragonitic bivalve skeletons.

7 Chapter Seven

Tahaenui Limestone

7.1 Introduction

This chapter describes the lithostratigraphy, petrology and geochemical characteristics of the Tahaenui Limestone (late Pliocene; Waipipian) deposits in northern Hawke's Bay. Tahaenui Limestone is the youngest of three carbonate-rich units within the Pliocene Mangaheia Group in the present day study area. Stratigraphic columns were constructed (Appendix I) and representative samples of the limestone were collected in the field and from exploration cores drilled north of Wairoa for laboratory-based petrological work, including standard and cathodoluminescence (CL) petrography, bulk X-ray diffraction, and $CaCO_3$ and grain size analysis.

7.2 Name and definition

The name Tahaenui Limestone is derived from the Tahaenui River 4 km west of Nuhaka village (Fig. 7.1). It crops out extensively in the northern Hawke's Bay region and is the uppermost carbonate-rich unit in the Pliocene strata of the study area. Lateral age equivalents of the Tahaenui Limestone occur to the east in the area studied by Drinnan (2011), including on Mahia Peninsula. Beu *et al.* (1980) broadly mapped the limestone and assigned a Waipipian age. The Tahaenui Limestone forms locally impressive bluffs and ridge tops and, along with the Whakapunake Limestone, is prominent in the landscape in the inland northern Hawke's Bay. The name Tahaenui Limestone was used informally by Moore & Hatton (1985) and Edwards (1988). The name was formalised and defined by Beu (1995) for the upper limestone formation formerly confused as the Whakapunake Limestone in the Haupatanga Gorge and above the Makaretu Stream in the present study area. Beu (1995) also assigned the name to its lateral age equivalent in the Nuhaka Syncline (WNW of Nuhaka), on the summit of Mt Moumoukai (NW of Morere), and at Long Point in the West Mahia Syncline (Drinnan 2011).

The Tahaenui Limestone is separated from the underlying late Opoitian shallow-marine mudstone and sandstone (Wairoa Formation B and C) or the mixed siliciclastic-carbonate deposits of Whakapunake Limestone by a regionally widespread unconformity at the base of the Waipipian Stage (Field *et al.* 1997). The limestone both conformably and gradationally passes up into undifferentiated siliciclastic sandstone, and slightly fossiliferous and tuffaceous mudstone of the Wairoa Formation D (new name; formerly known as the Wairoa Formation). In the study area, Tahaenui Limestone crops out on both limbs of the Wairoa Syncline, and dips towards the syncline axis. The detailed distribution of the Tahaenui Limestone is presented later in this chapter.

The Tahaenui Limestone is a cream to pale yellow, typical barnacle-dominated formation containing the age diagnostic pectinid fossil *Phialopecten marwicki* of Waipipian age (Beu 1995). Other age correlative limestones from outside the present study area are shown in Table 7.1. These include the Awapapa Limestone forming Te Mata Peak and nearby limestone ridges in southern Hawke's Bay, the Titiokura Limestone (presently part of the Titiokura Formation) north and south of the Napier-Taupo Road at Titiokura Summit in central Hawke' Bay, and the Rongomai Limestone in Wairarapa. Generally, a Waipipian period of limestone deposition is recognised throughout eastern North Island.

Table 7.1: Late Pliocene age Te Aute limestone formations in the eastern North Island, New Zealand (based on Beu 1995; Field *et al.* 1997; Nelson *et al.* 2003). The limestones listed below are part of the widely distributed Waipipian lateral correlatives that contain the age diagnostic pectinid fossil *Phialopecten marwicki*.

Age	New Zealand stage and abbreviation	Limestone formation
Late Pliocene	Waipipian (Wp)	Awapapa, Titiokura, Rongomai, Tahaenui

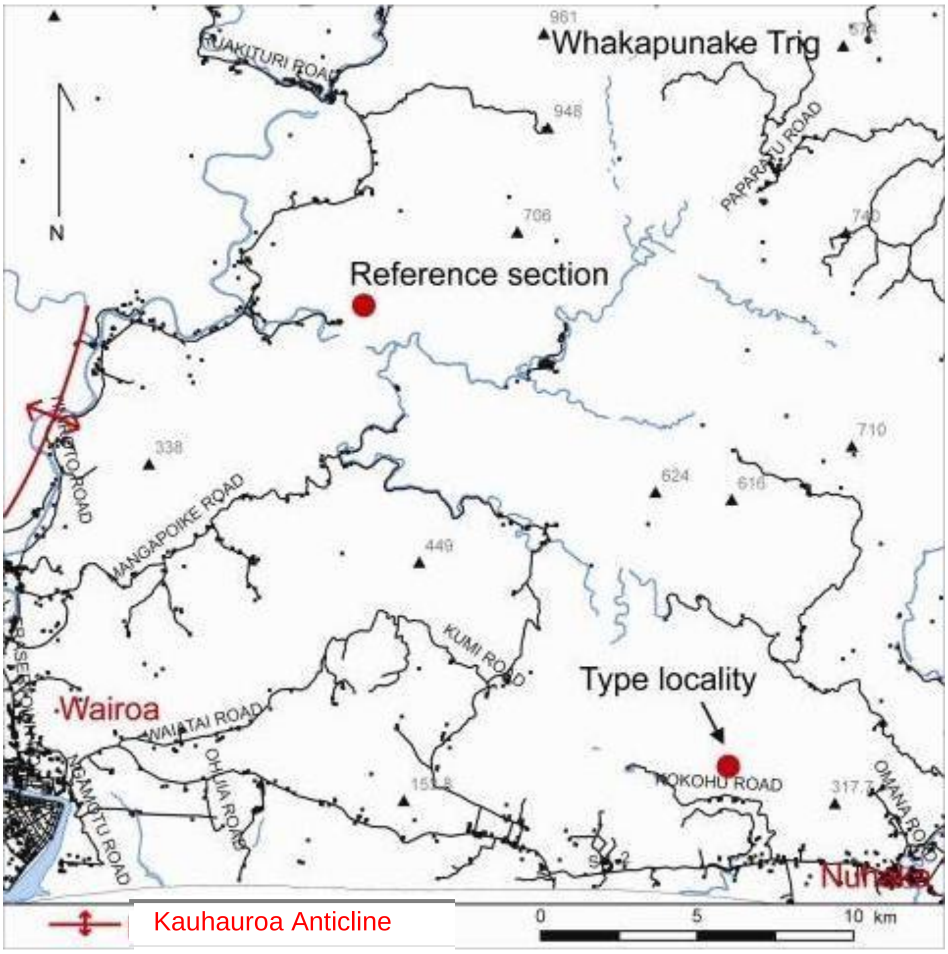

Figure 7.1: Location of the type locality (X19/136315) and the reference section (X19/041467) for the Tahaenui Limestone.

Figure 7.2: Steeply dipping (up to 52°) Tahaenui Limestone type locality, in quarry along Kokohu Road, in the tightly folded Nuhaka Syncline, WNW of Nuhaka. The limestone is overlain conformably by Late Pliocene mudstone of Wairoa Formation D. Location X19/136315.

7.3 Type locality and reference section

Beu (1995) designated the type locality of the Tahaenui Limestone as the disused quarry beside Kokohu Road, in the tightly folded Nuhaka Syncline, WNW of Nuhaka (X19/136315; Fig. 7.2). The limestone quarry is presently being operated by QRS Wairoa. At the type locality, Beu (1995) described the limestone as up to 80 m of pale yellow-grey calcarenite, with abundant large *Phialopecten marwicki* and *Mesopeplum (Borehamia) crawfordi*. The differentially cemented limestone is steeply dipping (up to 52°) towards the SE within the Nuhaka Syncline (Mazengarb & Speden 2000). The type locality has been visited but is not in the present study area. It has been described in detail by Drinnan (2011).

The present study area contains a reference section for the Tahaenui Limestone. Beu (1995) designated this reference section at the summit of the Kotare farm (unsealed) track just north of the Haupatanga Gorge on the eastern limb of the Wairoa Syncline (X19/041467; Fig. 7.1), where the massive barnacle and pectinid-rich limestone is easily accessible (Fig. 7.3). At the reference section the Tahaenui Limestone is resting on an erosional contact upon Whakapunake Limestone (Fig. 7.4). This does not distinguish the two limestones. This section is also a stratigraphic reference section for the Pliocene strata in all the petroleum exploration drill holes in the vicinity of Wairoa Syncline. At Haupatanga Gorge, the Tahaenui Limestone dips westwards at 9°, which is about 16° less than the dip of Whakapunake Limestone. Thus, the missing Opoitian time interval represented by the unconformity is significantly greater at the up-dip end than the down-dip end, which can be observed along the farm track at the end of Kotare Road (Beu 1995). Other good sections of Tahaenui Limestone are: (1) the thin lens-like exposure on Kauhauroa Station, 4 km NE of Frasertown (X19/959421); (2) an enclosed section behind Te Reinga Marae (X18/026539); (3) the Ruakituri Valley cliff section behind the Ruakituri Station farm house (X18/996545) on the western limb of the Wairoa Syncline; (4) a Hereheretau Road section at the end of the farm track on Anewa Station, 1.5 km off the Hereheretau Road. A nearby section above the Makaretu Stream also contains the Tahaenui Limestone; and (5) Whakapunake translation tower, at the end of Translation Road (X19/092531), 7 km east of Te Reinga (Fig. 7.5). The spectacular scarp of Tahaenui Limestone in the Haupatanga Gorge itself was not accessed in this study.

In the subsurface the Tahaenui Limestone has been intersected by petroleum drill cores retrieved by Westech Energy NZ on the Kauhauroa Station in the Kauhauroa Anticline, north of Frasertown (Fig. 7.1). Furthermore, Francis (1993) has briefly logged the limestone drill cores held by QRS Wairoa, in relation to the quality of the limestone for agricultural and industrial usage.

Figure 7.3: Reference section for the Tahaenui Limestone near Haupatanga Gorge along a farm track at the end of Kotare Road, on the eastern limb of the Wairoa Syncline. Location X19/041467.

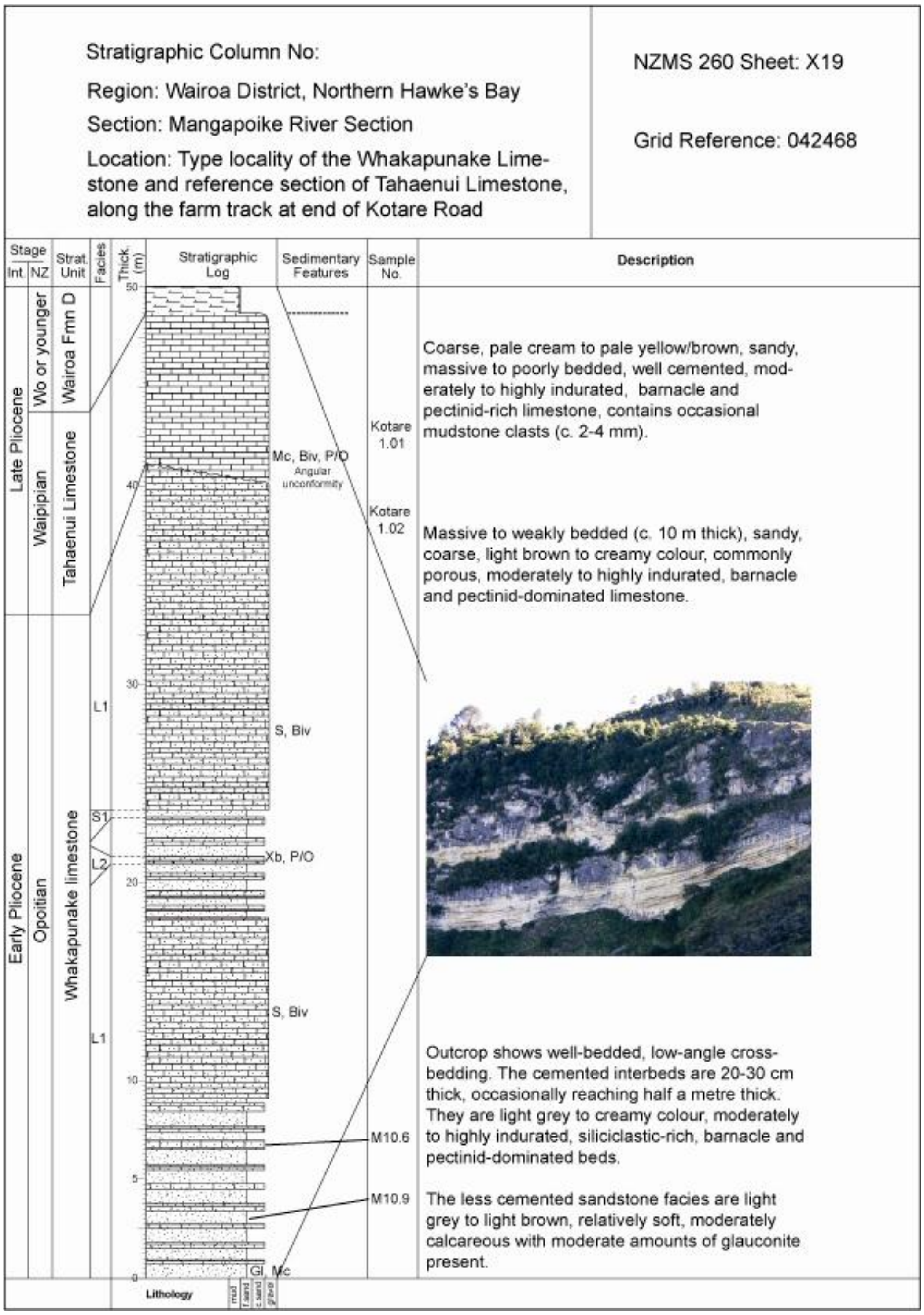

Figure 7.4: Stratigraphic column for the Tahaenui (and Whakapunake) Limestone at the reference section along the farm track at the end of Kotare Road. Location X19/041467. Facies and sedimentary features are defined in section 4.3.

7.4 Lithology

The lithological characteristics of Tahaenui Limestone are broadly similar to those of the underlying late Opoitian barnacle-dominated Whakapunake Limestone. The Tahaenui Limestone is typically pale yellow to cream in colour, barnacle-dominated and pectinid-rich, and locally glauconite-bearing. The thickness of the limestone varies from c. 10 m to over 30 m, and is typically (facies L1) massive to poorly bedded (Fig. 7.5) and well indurated, with a variable $CaCO_3$ content from 60 to about 80%. In places, it passes into a differentially cemented or slightly flaggy limestone formation, especially at the outcrops in the vicinity of Te Reinga and Ruakituri Station. Around Haupatanga Gorge (Fig. 7.5, locality 6), the limestone is c.10 m thick and is a massive to poorly bedded, yellowish grey, siliciclastic-rich limestone with common barnacle plates (Fig. 7.7E & F), strongly cemented in some parts, with abundant large *Phialopecten marwicki* pectinids and rare *Mesopeplum crawfordi* pectinids. It passes down-dip towards the downstream mouth of the gorge (X19/026465) into a strongly cemented yellow-grey limestone with abundant barnacle plates and *Phialopecten marwicki*, both of which tend to support a pink stain, while the outcrop is often covered by a dark, soft precipitate of secondary calcite. The limestone is locally large scale cross-bedded, much like the Whakapunake Limestone, and is difficult to distinguish the two limestones in outcrop. Beu (1995) defined the maximum pectinid shell-size reached to differentiate the two limestones in outcrops. The Tahaenui Limestone contains *Phialopecten marwicki* of 12 cm or larger in size, while no pectinids over 10 cm size were found in the Whakapunake Limestone. The Tahaenui Limestone generally dips towards west at c. 8-10°, whereas the Whakapunake Limestone dips steeper at c. 16-19° SW.

Kauhauroa Station (locality 1-Fig. 7.5)

The isolated exposure of Tahaenui Limestone in the vicinity of the Kauhauroa Station (Fig. 7.6A) is situated on a small anticlinal structure (X19/959421) on the eastern limb of the Kauhauroa Anticline (Fig. 7.1). The limestone crops out at the top of the hill, running in a N-S direction for nearly 1 km. This limestone has been assigned a Waipipian age by Mazengarb & Speden 2000, although a small size (5 cm) *Phialopecten marwicki* was identified within a fallen block in the present study, possibly indicating the presence of Whakapunake Limestone at this locality (Fig. 7.6B). Most of the pectinid shells are present as a thin band about 5 m above ground level; and noticeable amounts of brachiopod skeletons also occur (Fig. 7.6B). At the locality, the limestone is about 8-10 m thick, massive to weakly bedded, pale cream in colour, moderately to highly indurated, and barnacle-dominated and pectinid-rich (facies type L1) (Fig. 7.7A).

Te Reinga Marae (locality 2-Fig. 7.5)

A secluded valley section of the Tahaenui Limestone crops out behind the Te Reinga Marae, next to SH 36, near the corner of Tiniroto Road and Ruakituri Road (X18/026539). This outcrop is located roughly in the middle of the Wairoa Syncline, and is the lateral continuation of those seen along Tiniroto Road. The limestone is assigned a Waipipian age at this locality. It forms vertical cliffs of 20-30 m height on either side of the valley (Fig. 7.6C & D). Rock samples were taken near the bottom of the cliff. Here the Tahaenui Limestone is a massive to poorly bedded to flaggy (facies type L1xb), pale cream (bluish grey when fresh, Fig. 7.6E), highly indurated limestone. The lower contact of the limestone is not exposed. There are no macrofossils visible within rock slabs (Fig. 7.7). Figure 7.6D shows the Tahaenui Limestone on the western side of the valley is a flaggy limestone over 30 m thick (L1) that dips into the junction between the Hangaroa River and the Ruakituri River. The lateral extent of the limestone on this side of the valley is likely passes into calcareous sandstone in the deeply incised Te Reinga Fall (Fig. 7.1). Figure 7.6C shows outcrop on the eastern side of the valley that comprises a massive to poorly bedded limestone about 20 m thick.

Ruakituri Road (locality 3-Fig.7.5)

The Tahaenui Limestone is exposed on the steep hill behind the Ruakituri Station farm house in the Ruakituri Valley (X18/996545; Fig. 7.6F). The limestone here is a light grey, moderately to highly indurated, barnacle and bivalve dominated, glauconitic limestone (Fig. 7.7C). It exhibits a slightly flaggy and cross-bedded nature, with the thickness of individual beds from 20 to 25 cm. The outcrop runs for 150-200 m along the steep hill side. The maximum thickness exposed at this locality is about 10-12 m, which is probably a conservative value. Neither the lower nor upper contact of the Tahaenui Limestone is exposed here. The underlying massive calcareous mudstone is assigned to Wairoa Formation B.

Anewa Station & Makaretu Stream (locality 4-Fig.7.5)

The Tahaenui Limestone on Anewa Station (X19/035410) unconformably overlies 1 m of silty sandstone that contains, mostly angular to slightly rounded rip-up mudstone clasts derived from the underlying mudstone unit (Wairoa Formation B/C). The limestone itself is a 1-4 m thick, slightly sandy barnacle-pectinid-bryozoan limestone (facies type L1). Its lower part comprises shell hash which grades upward into a coarse bivalve-dominated, barnacle and bryozoan-rich unit. The uppermost part of the limestone is a 20 cm thick brachiopod bed that is conformably overlain by sandstone and mudstone. The limestone dips WNW and thickens towards the centre of the Wairoa Syncline (Fig. 7.6G). The Tahaenui Limestone is similar at the Makaretu Stream section (X19/035422) where it unconformably overlies mudstone (Wairoa Formation B) and conformably passes upward into a massive light grey, fossiliferous mudstone (facies type M3) (Wairoa Formation D).

Whakapunake translation tower (locality 5)

The Tahaenui Limestone crops out nearby the Whakapunake translation tower, at the top of the dipslope (X19/092531; Fig. 7.6H). Here the limestone is only a thin (40-50 cm) patchy unit but contains large *Phialopecten marwicki* indicative of a Waipipian age. The limestone sits directly on differentially cemented Whakapunake Limestone (Fig. 7.6H). The thin Waipipian unit is a massive, cream to pale yellow, well indurated, bivalve-dominated limestone (Fig. 7.7D). The limestone increases in thickness to the west from the dipslope, and the variable thicknesses may be related to erosion of the dipslope itself.

Marumaru drill cores (Fig. 7.1)

Three limestone cores were drilled east of Marumaru (X19/981448) in early 2005, and designated as Tahaenui Limestone (Francis 2005). The cores are 100% recovered, and drilled in a N-S trending direction, at c. 100 m apart. The limestone was intersected about 5 m below the land surface, and all three cores extend to a depth of c. 43.5 m. The lower bound of this limestone was not reached. Thus, the thickness of the Tahaenui Limestone is at least 37.5 m in the subcrop at this locality. It is typically a pale yellow to cream, variably indurated, barnacle-dominated and pectinid-rich limestone (Fig. 7.7G). The colour of the cores changes from a pale yellow to light grey at a depth of 29 m (Fig. 7.7H).

Kauhauroa Station drill cores (Fig. 7.1)

The Tahaenui Limestone was intersected in the Kauhauroa-2, 4 and 5 petroleum exploration wells, and shows slight variations in both lithology and thickness between these wells. The limestone varies from 5-15 m thick and from a skeletal limestone dominated by bivalve and barnacle fragments to a light brownish grey, poorly to well bedded and well cemented/indurated calcareous siltstone (PR2409 1998; PR2256 1999; PR2431 1999).

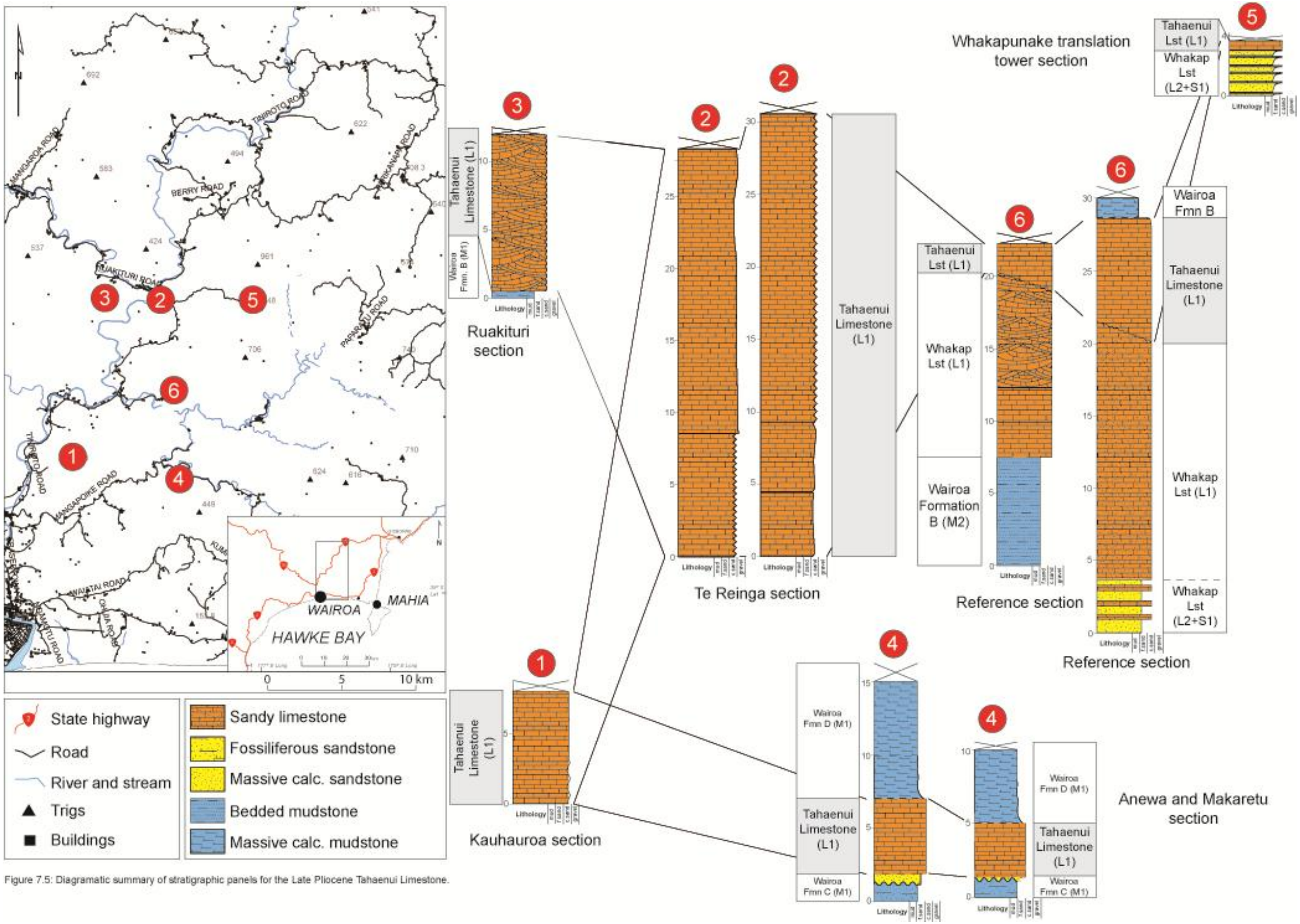

Figure 7.5: Diagramatic summary of stratigraphic panels for the Late Pliocene Tahaenui Limestone.

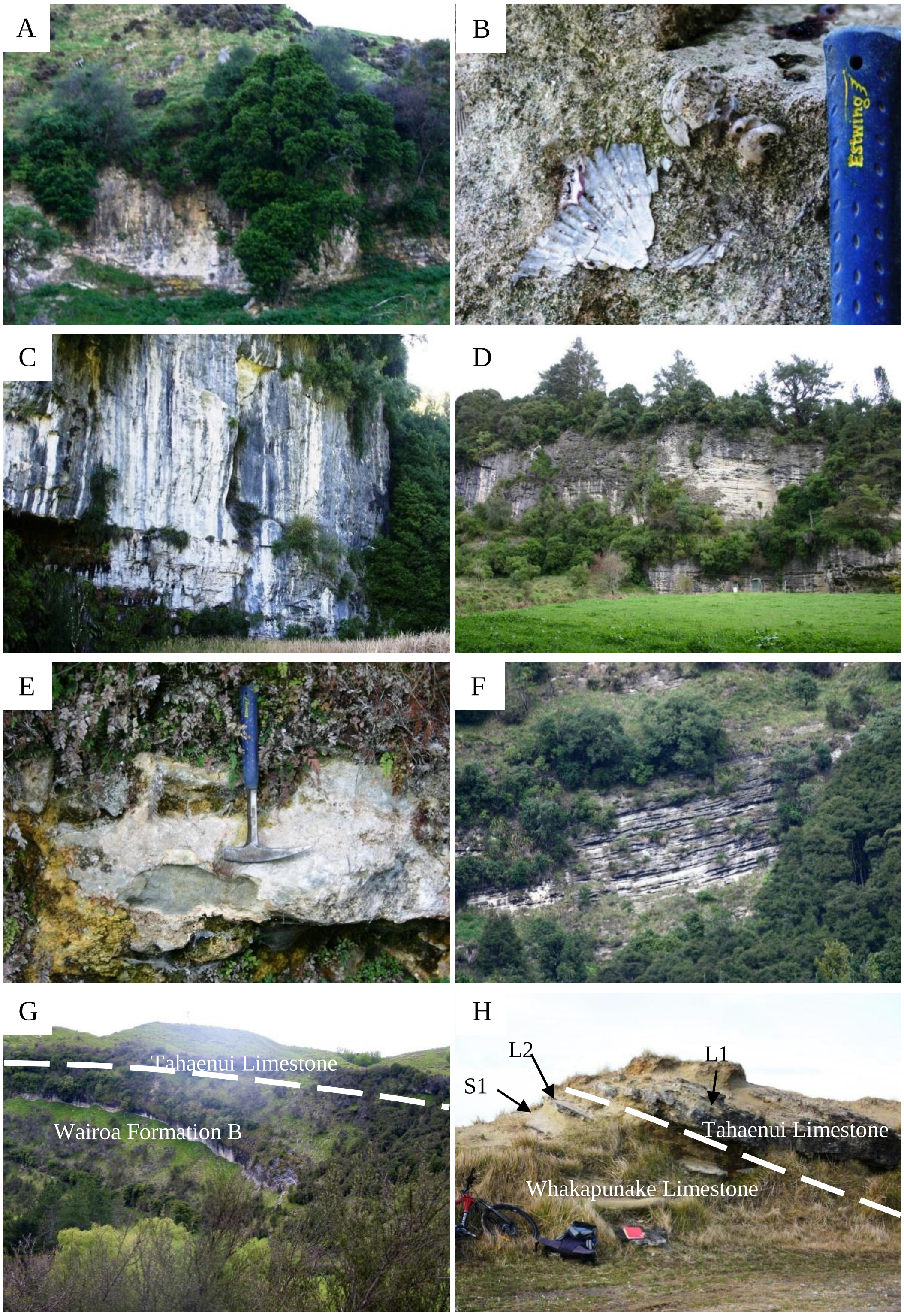

Figure 7.5: A) Tahaenui Limestone outcrop on Kauhauroa Station showing 8-10 m of weakly bedded limestone (facies L1). Location X19/959421. B) *Phialopecten marwicki* (<10 cm) within the Tahaenui Limestone on Kauhauroa Station, including also brachiopod skeletons (to the right of the pectinid). C & D) 20-30 m thick, massive to poorly bedded, and flaggy Tahaenui Limestone outcrops behind Te Reinga Marae. Location X18/026539. E) Close-up view of fresh, light grey, fine-grained limestone (facies L1) at Te Reinga. F) The 10-12 m thick, flaggy, and possibly cross-bedded Tahaenui Limestone (L1) outcrop behind the Ruakituri Station farm house, in the Ruakituri Valley. Location X18/996545. G) Thin Tahaenui Limestone overlies late Opoitian mudstone above the Makaretu Stream. Location X19/035422. H) At the top of the Whakapunake dipslope thin (40-50 cm) Tahaenui Limestone (L1) directly overlies differentially cemented Whakapunake Limestone. Location X19/092531.

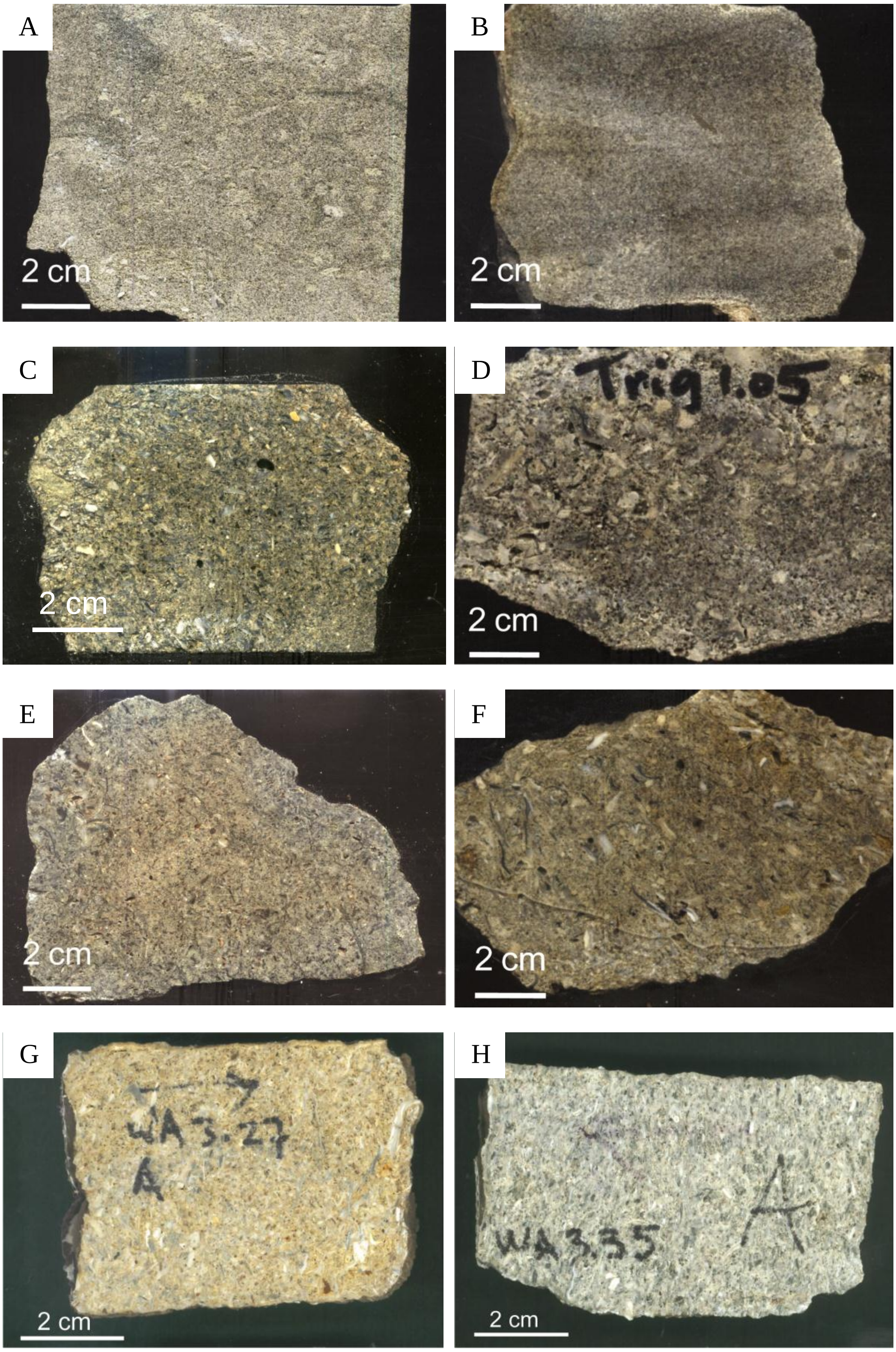

Figure 7.6: Cut rock slabs show barnacle and bivalve-dominated Tahaenui Limestone (L1) from different localities, and variations in texture from coarse-grained to fine-grained within L1 facies in the present study area. A) Kauhauroa Station (sample Ka1.01), B) Te Reinga Marae (sample Ma10.1), C) Ruakituri Station (sample Ra/ta), D) Whakapunake translation tower (sample trig1.05), E & F) Kotare farm track. G & H) Drill core from near Marumaru at a subsurface depth of 13 m (sample Wa3.27) and 43 m (sample Wa3.35), respectively.

7.5 Lower and upper contacts

The Tahaenui Limestone overlies a regional unconformity upon the late Opoitian strata (Field *et al.* 1997). In turn, the limestone then conformably passes into sandy mudstone of Wairoa Formation D in the study area (Fig. 7.5). The lower contact of the Tahaenui Limestone varies from place to place in the time it represents (Beu 1995). At the northern end of the Whakapunake dipslope, the Tahaenui Limestone unconformably overlies the late Opoitian Whakapunake Limestone, but the unconformity is much less pronounced. Southwards from the reference section of the Tahaenui Limestone, the unconformity becomes more conspicuous, angular and of increasingly greater time magnitude (Fig 7.8B). The underlying Whakapunake Limestone can be cut out by this unconformity, with Tahaenui Limestone resting directly on top of late Opoitian mudstone of Wairoa Formation B on the scarp south of Haupatanga Gorge (Beu 1995).

At the reference section at the summit of the Kotare farm track (Fig. 7.2) the lower contact of the Tahaenui Limestone is rather difficult to pick-up in outcrop (Fig. 7.8A). The same unconformity can be found on the scarp immediately south of the reference section (Fig. 7.8B), where the Waipipian limestone rests unconformably on 700-800 m thick late Opoitian, massive and differentially cemented mudstone and sandstone. The same strata are disconformably overlain by the thick Whakapunake Limestone on the northern side of the Mangapoike River. The lower contact of the Tahaenui Limestone here is a sharp, low angle unconformity that represents the boundary between the Early and Late Pliocene (Opoitian and Waipipian or younger). According to Edwards (1988), it represents c. 300,000 years of early Waipipian time. The angular unconformity itself dips at 11° NW. However, it is difficult to pick out this contact at localities where the Tahaenui Limestone rests directly on the late Opoitian Whakapunake Limestone. At the Whakapunake Trig the position of the unconformity is less obvious. Beu (1995) suggested that at this locality the unconformity between the Tahaenui Limestone and the Whakapunake Limestone becomes a paraconformity.

The upper contact appears to be conformable throughout the study area as a gradational one into massive mudstone facies (M1) of Wairoa Formation D. This upper contact of the Tahaenui Limestone is best exposed along the farm track at end of the Kotare Road.

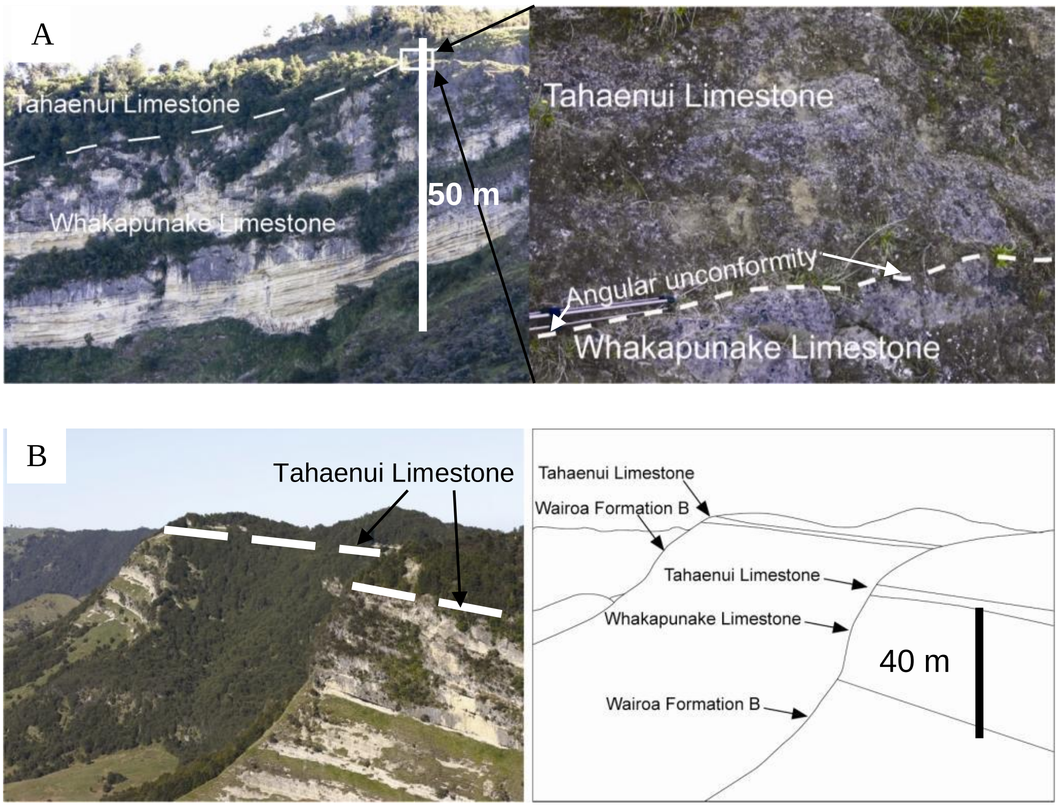

Figure 7.7: A) Tahaenui Limestone rests unconformably on the Whakapunake Limestone along Kotare farm track. Location X19/041467. B) Looking towards the south from the summit of Kotare farm track, the angular unconformity represents increasingly more missing time in that direction.

7.6 Distribution and thickness

Outcrops

The Tahaenui Limestone is presently known from outcrops associated with the flanks of the Wairoa, Nuhaka and West Mahia synclines (Beu 1995; Mazengarb & Speden 2000; Drinnan 2011). The limestone is the topmost Pliocene carbonate-rich formation within the Mangaheia Group succession in the Wairoa Syncline. It forms a large part of the top surface of the Whakapunake dipslope, from as far north as the Whakapunake Trig south to the outcrops above the Makaretu Stream (Fig. 7.1). It is exposed nicely along the farm track cut in the late 1980s through the back of the Kotare Station at the end of Kotare Road. Tahaenui Limestone is identifiable from its Waipipian pectinid fossils near the northern end of the Whakapunake Plateau (around the Whakapunake repeater tower), and is likely to be the northern extremity of this limestone. The Tahaenui Limestone varies little in thickness (c. 5-30) across the study area, unlike its Waipipian equivalents (c. 10-60 m) in the Nuhaka Syncline and along the west coast of Mahia Peninsula. At Haupatanga Gorge the limestone is estimated to be c. 5-10 m thick, with a consistent dip towards the west. To the south of Haupatanga Gorge the limestone forms ridge tops until it descends and crosses Makaretu Stream (X19/036422).

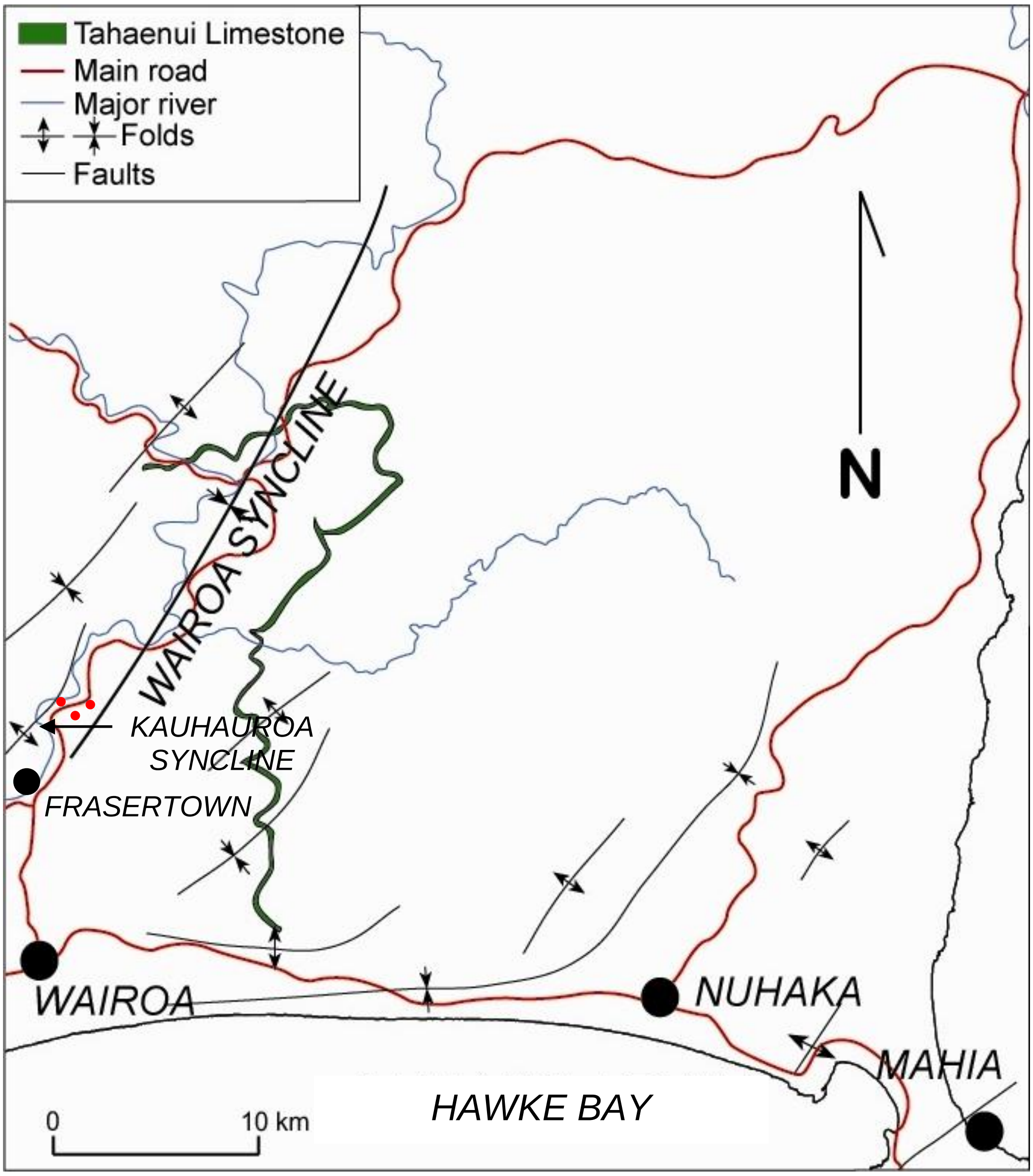

Figure 7.8: Distribution map of the Tahaenui Limestone outcrops on the flanks of the Wairoa Syncline. The petroleum exploration wells are indicated in red, on the outskirts of Frasertown.

Subcrops

The (inferred) Tahaenui Limestone is also present in the subsurface north of Frasertown, being intersected in 3 of 11 petroleum wells drilled within the Wairoa Syncline in the study area, namely Kauhauroa-2, 4 and 5 (PR2409 1998; PR2256 1999; PR2431 1999). The inferred Tahaenui Limestone shows as a strong reflector in seismic reflection profiles being present on either side of the drilled anticlinal structure (Fig. 7.10). The Tahaenui Limestone rests unconformably on Late Opoitian strata in all 3 wells. Well logs show the thickness of Tahaenui Limestone varies from 5-15 m in the vicinity of the Kauhauroa Syncline.

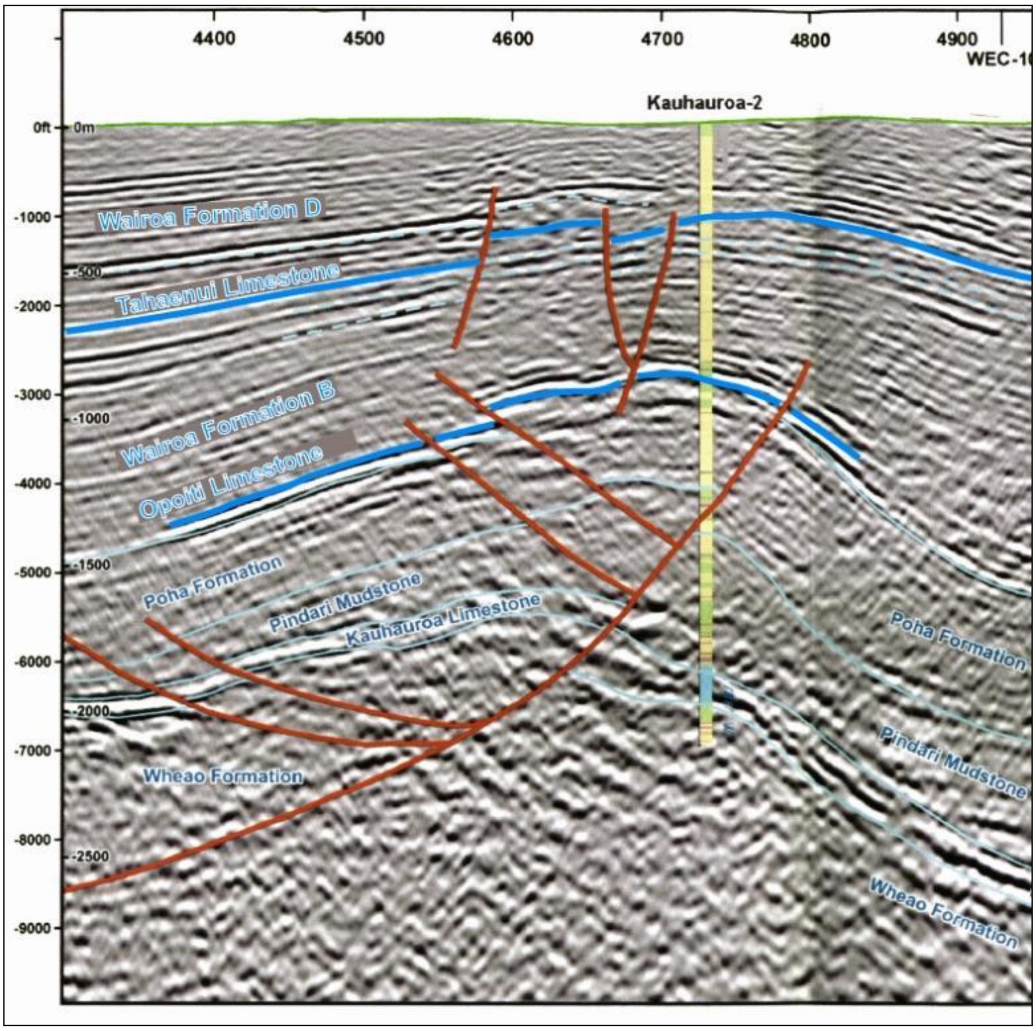

Figure 7.9: Seismic reflection profile showing the inferred presence of Tahaenui Limestone which was intersected by Kauhauroa-2 drill hole. Well location X19/918386, between Brownlie's Road and a small tributary of the Wairoa River, 200 m from SH38 intersection (PR2409, 1998).

7.7 Paleontology

Beu (1995) used mainly pectinid biostratigraphy to resolve the long standing problem of identifying the different Pliocene limestones throughout eastern North Island. From the same study, he discovered there was a lack of speciation between the late Opoitian and Waipipian pectinids, and that limestones from both time periods could contain the same *Phialopecten marwicki*. However, the size of the specimens was apparently diagnostic, and the Tahaenui Limestone was assigned a Waipipian age based on the presence of more mature, large (12-15 cm) *Phialopecten marwicki* specimens (Fig. 7.11). The pectinid *Mesopeplum (Borehamia) crawfordi* was also identified at almost all Tahaenui Limestone localities (Beu 1995), but is rare in other stages in the Pliocene.

The species of barnacles present as a major constituent of the Tahaenui Limestone are probably those typical of the Te Aute limestones in general, including *Notobalanus vestitus, Austromegabalanus (Notomegabalanus) miodecorus, Austromegabalanus decorus argyllensis, Fosterella tubulatus and Balanus variegates* (Beu 1995). The brachiopod *Neothyris aff. obtuse* is also present locally in some outcrops.

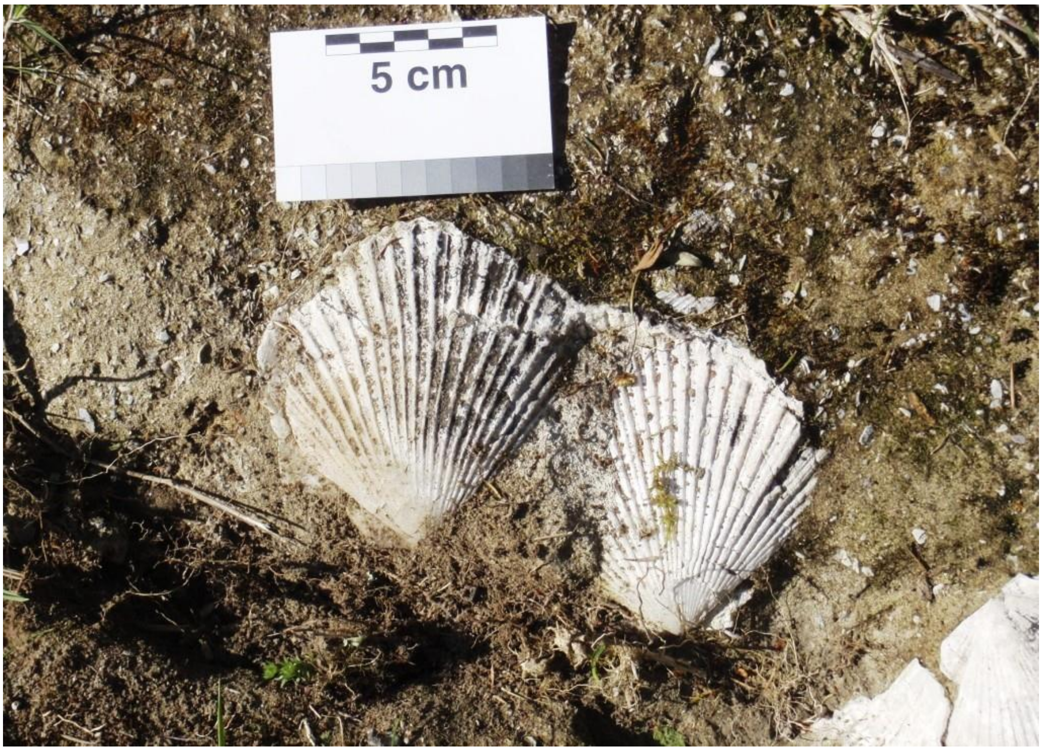

Figure 7.10: *Phialopecten marwicki* specimens in Tahaenui Limestone along the farm track at the end of Kotare Road (X19/026465).

7.8 Lateral age correlatives

Waipipian limestones are the classical Te Aute lithofacies, being characteristically soft, cream to pale yellow, coarse, barnacle and pectinid-dominated limestones (Beu 1995; Nelson *et al.* 2003). In northern Hawke's Bay, the Waipipian Tahaenui Limestone is relative thin but widespread compared to other age correlative formations. For example, the Titiokura Limestone (now known as the limestone bearing deposit within the Titiokura Formation; Bland *et al.* 2007) only covers a relatively small inland area in central Hawke's Bay, on the western side of the ancient forearc seaway. In contrast, the Tahaenui Limestone in northern Hawke's Bay extends from the top of the Whakapunake dipslope south and east to Tahaenui River (west of Nuhaka) and down onto the western side of Mahia Peninsula (Beu 1995). Below are mentioned three of the Waipipian age equivalent Te Aute limestone deposits located elsewhere in the East Coast Basin. They are broadly similar to each other, but record subtle differences in their depositional conditions.

Awapapa Limestone

The Awapapa Limestone was introduced informally by Spörli & Pettinga (1980) for the upper interbedded coquina limestone and cross-bedded sandstone on the ridge along the western part of the Maraetotara Plateau, north of Mt Kahuranaki (Harmsen 1985). The name is derived from a farm in the vicinity (V22/445517) of northeastern Te Aute Subdivision. Harmsen (1985) formalised the name Awapapa Limestone for the Waipipian Te Mata Limestone mapped by Beu *et al.* (1980). In the same study, the name was elevated to formation status, which defines the uppermost limestone exposures in the face below the northeastern ridge of Te Mata Peak (V22/450596), and designated this outcrop as the type section of the Awapapa Limestone (Fig. 7.12). She also included the Whetukura Limestone (Beu *et al.* 1980, informal) in the Dannevirke Subdivision as part of the formation. The reference section for this latter limestone was designated in the Dannevirke Subdivision where the Waipipian limestone rests on the Mangatoro Formation (Opoitian; U23/919062), 1 km west of the junction with Te Uri Road and 6 km south of Whetukura (Beu 1995). In general, the Awapapa Limestone rests unconformably on Mesozoic basement rocks, Tongaporutuan strata, or conformably on Mokopeka Sandstone. The limestone is highly variable in thickness, reaching a maximum of 120 m. Lithologically the limestone varies from a barnacle-dominated, interbedded limestone to cross-bedded sandstone with minor conglomerate and occasional shell beds. Awapapa Limestone displays a variety of sedimentary structures, ranging from well developed tabular cross-bedded or trough cross-bedded units. It contains macrofossils of *Phialopecten, Crassostrea, and Mesopeplum crawfordi*, which rarely occur in rocks older than Waipipian (Beu *et al.* 1980).

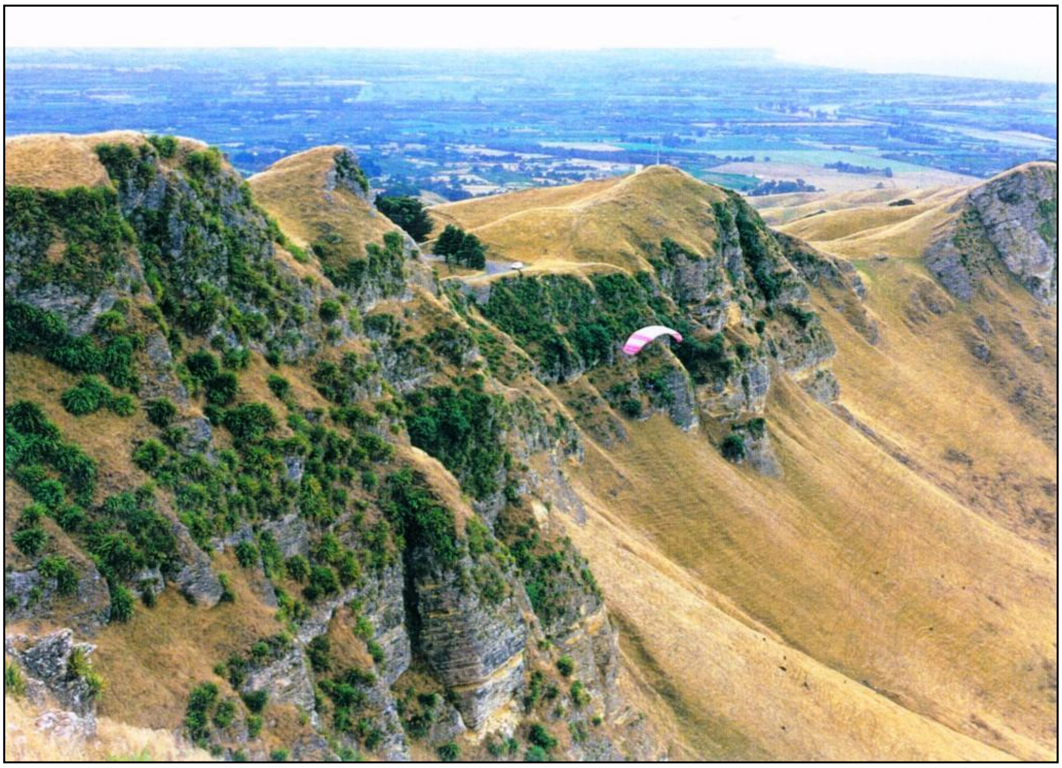

Figure 7.11: View from Te Mata Peak showing an escarpment of westward-dipping Awapapa Limestone, characterised by weakly to moderately cemented, well bedded, and often cross-bedded limestones (V22/450596). Photo: Dr Steve Hood.

Titiokura Limestone

Titiokura Limestone was informally defined by Beu *et al.* (1980), and was formalised as a formation by Beu (1995). He defined the formation as the Waipipian limestone in the Te Waka Range and near Te Pohue, south of the Napier-Taupo Road at the Titiokura Summit, underlying the Te Waka Limestone.

He also designated the type locality of the Titiokura Limestone as the bluff on the crest of the Te Waka Range, c. 500 m south of the Napier-Taupo Road (V20/278148). The unit has recently been studied by Bland *et al.* (2004), who subsequently redefined the Waipipian age limestone as part of the Titiokura Formation (Opoitian-Waipipian) which underlies the uppermost Waipipian to Mangapanian age Te Waka Formation in the Te Waka Range in central Hawke's Bay. Beu *et al.* (1980) sampled the Titiokura Limestone at Pohokura Road (Fig. 7.13) (V19/405218), and described the limestone as a pale grey to yellow-grey and pale brown, bedded, weakly to moderately indurated sandy and muddy fine-grained grainstone, with common small molluscan, barnacle and bryozoan fragments. At this locality, the limestone dips to the east at 20° and is a massive to poorly bedded to occasional cross-bedded, coarse-grained limestone including differentially cemented thick sandy seams (Hood 1996).

Figure 7.12: The Pliocene Titiokura Limestone, a massive to poorly bedded coarse-grained limestone with differentially cemented sandy seams, off Pohokura Road, central Hawke's Bay (V19/405218). Photo: Dr Steve Hood.

Rongomai Limestone

The name Rongomai Limestone is derived from the small settlement of Rongomai (T25/403636), 9 km northeast of Eketahuna. The name was formally used by Beu (1995). The limestone is a persistent and easily recognised unit in the Eketahuna district. The limestone was mapped throughout the area by Neef (1974), and is exposed continuously along the scarp face of the Puketoi Range for at least 30 km northeastward. Beu (1995) designated the type section as the cuttings on Makuri-Owahanga Road (T25/670689), 2.5 km southeast of Makuri. At the type locality, the formation is c. 53 m thick, and is a highly indurated, sandy barnacle and bivalve-dominated grainstone with common moderately large *Phialopecten marwicki* (120-150 mm) which confirms a Waipipian age. It covers the crest of the Puketoi Range. The thickness of the limestone changes dramatically from the type locality to less than 1 m east of Waipori Stream (T25/605622).

7.9 $CaCO_3$ content

The $CaCO_3$ content of the Tahaenui Limestone varies from 60-80% (Table 7.2), so it is a true limestone. Samples from the northern part of the Wairoa Syncline and on the western limb (sample Ra/ta and trig1.01) have the lowest $CaCO_3$ contents (c. 60%). Elsewhere, the Tahaenui Limestone has a typical $CaCO_3$ content of c. 75%. It is also variable in its siliciclastic sand and mud content, with sand values from c. 15-35% and mud from c. 5-25% (Fig. 7.14). The raw carbonate and size data are given in Appendix II.

Table 7.2: Bulk $CaCO_3$ and insoluble sand and mud content of five samples of Tahaenui Limestone. Facies types defined in Table 4.1.

Sample No.	*Facies types*	*% $CaCO_3$*	*% Mud (<63 µm)*	*% Sand (63-2000 µm)*
Ka1.02	L1	78	6	16
Ma1.01	L1	73	11	16
Ra/ta	L1	62	16	23
Ko1.01	L1	68	12	20
trig1.01	L1	60	6	34

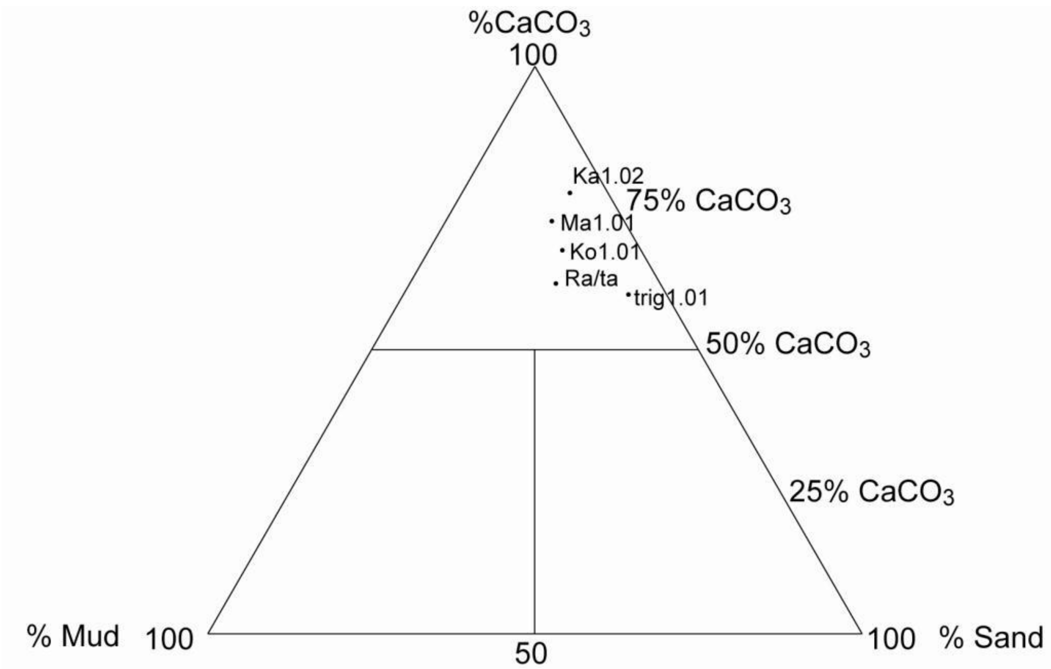

Figure 7.13: Ternary $CaCO_3$-sand-mud plot for samples from Tahaenui Limestone.

7.10 Bulk mineralogy

Bulk mineralogical analysis was undertaken on 7 samples of Tahaenui Limestone using X-ray diffraction (XRD), as described in section 3.3. XRD spectra for the Tahaenui Limestone show the dominant minerals present are low-Mg calcite, quartz and plagioclase feldspar (Table 7.3). Low-Mg calcite (c. 4 mol% $MgCO_3$) is expectedly common to abundant in all the analysed samples, while mica is noted in one sample (Table 7.3). The common abundance of low-Mg calcite is related to the dominant constituents of skeletal grains of barnacles, epifaunal bivalves and brachiopods, all low-Mg calcite secretors, along with cement materials. Plagioclase feldspar and quartz are few common in all outcrop samples. No plagioclase or quartz was detected in the limestone cores from Marumaru. Clay minerals are likely present in the samples but missing on the XRD spectra because of the use of unorientated bulk powder sample mounts.

Table 7.3: XRD bulk mineral counts (peak height) for seven Tahaenui Limestone samples.

Major minerals	*Dolomite*	*Low-Mg Calcite*	*Plagioclase feldspar*	*Aragonite*	*Quartz*	*Clays*	*Mica*
Ka1.01	-	VC	S	-	S	-	-
Ma1.01	-	A	C	-	S	-	-
Ra/ta	-	VC	C	-	S	-	S
Ko1.01	-	C	S	-	S	-	-
trig1.01	-	C	S	-	S	-	-
Wa1.01	-	C	-	-	-	-	-
Wa1.02	-	C	-	-	-	-	-

Abbreviation	*Description*	*Counts*
-	None	0
R	Rare	1-20
S	Some	21-200
C	Common	201-500
VC	Very common	501-999
A	Abundant	≥1000

7.11 Insoluble grain texture

The texture of insoluble grains in the Tahaenui Limestone is shown in Table 7.4. Sand forms 20-85% of the insoluble fraction, silt 15-70%, and clay <10%. Figure 7.15 shows that all insoluble samples from the Tahaenui Limestone but one exhibit a silty sand texture. The modal size of grains ranges from 18 to 204 µm, or medium silt to fine sand.

Table 7.4: Bulk insoluble grain texture for five samples of Tahaenui Limestone.

Sample No.	*Facies type*	*% Clay (<3.9 µm)*	*% Silt (3.9-63 µm)*	*% Sand (63-2000 µm)*
Ka 1.02	L1	9	71	20
Ma 1.01	L1	1	24	75
Ra/ta	L1	2	40	58
Ko 1.01	L1	2	36	62
trig 1.01	L1	1	14	85

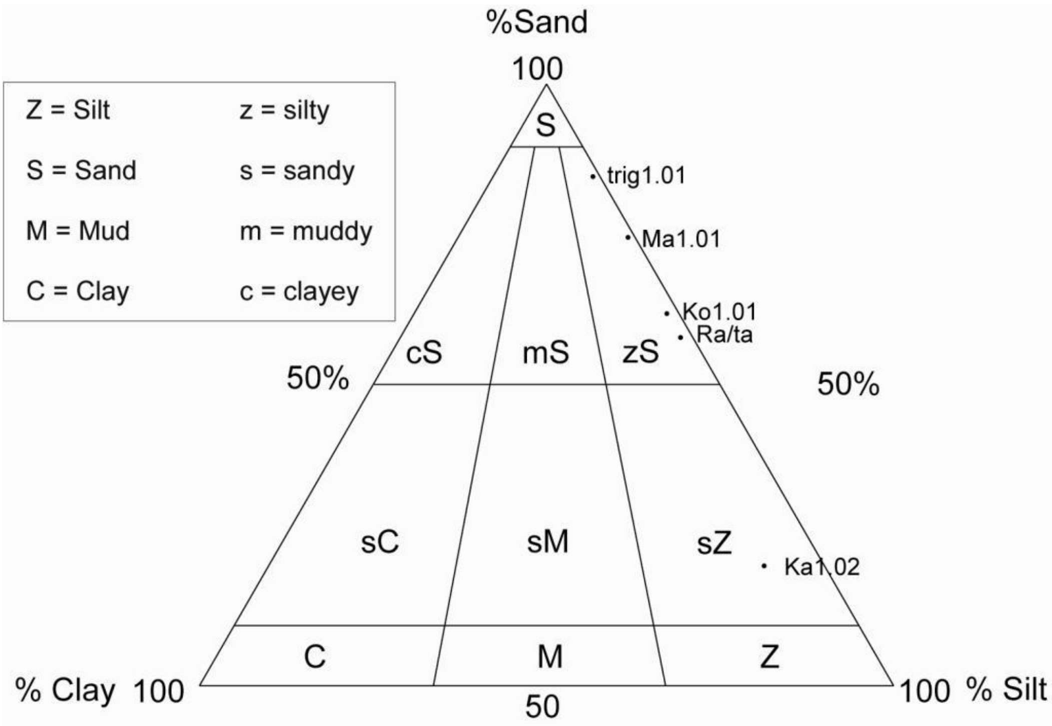

Figure 7.14: Ternary clay (C), silt (Z) and sand (S) plot (%) for the insoluble residue fraction from Tahaenui Limestone samples. Textural size classification from Folk (1959).

7.12 Stable isotope analyses

Table 7.5 summarises the stable oxygen and carbon isotope values of 5 representative samples from the Tahaenui Limestone, and suggests some possible minimum burial temperatures and burial depths for the deposits in northern Hawke's Bay (see section 3.5 for calculation method). Also plotted are Tahaenui Limestone samples analysed by Drinnan (2011) from the nearby Mahia district. The range of $\delta^{13}C$ values (-0.25 to +1.56‰) is broadly similar to those for the modern New Zealand skeletal carbonates, while the $\delta^{18}O$ values are mainly slightly more negative, falling between c. 0.37 and -3 .13‰ across the fields for New Zealand modern and Cenozoic carbonates (Fig. 7.16). The Wairoa samples from the present study have the most negative $\delta^{18}O$ values, suggestive of at least shallow to moderate burial depth (Tucker & Marshall 2004).

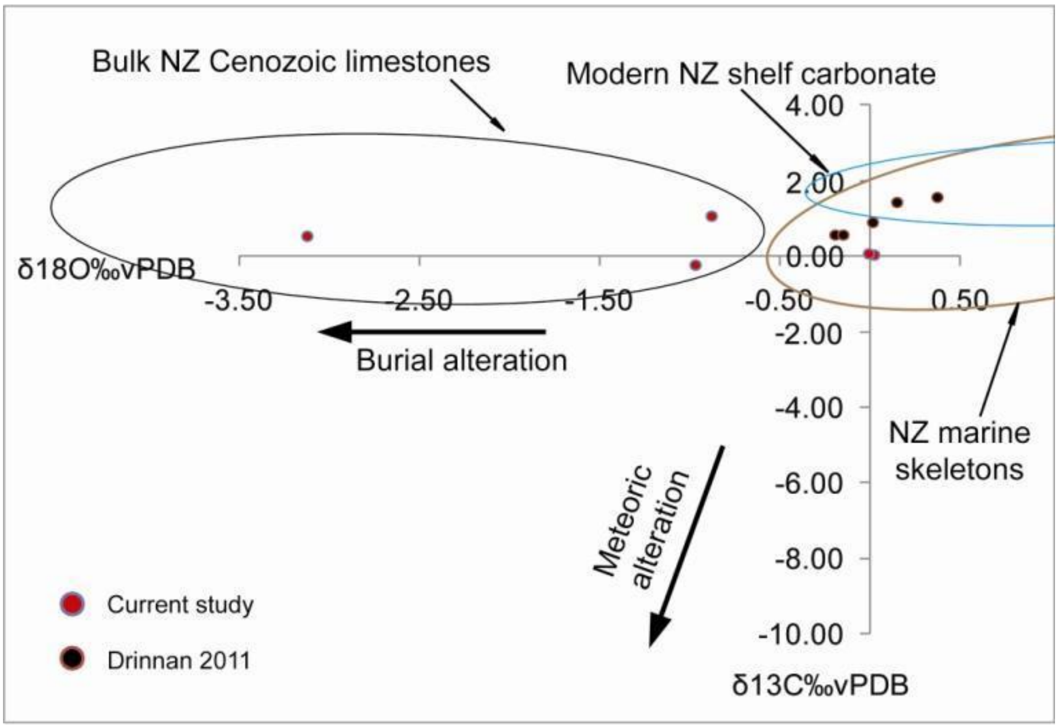

Figure 7.15: Oxygen and carbon isotope cross-plot for Tahaenui Limestone samples in relation to the core fields for typical New Zealand cool-water carbonates (Nelson &Smith 1996).

Calculated absolute minimum burial temperatures for samples fall between 14°C and 30°C, while the minimum burial depths range from 70 to over 700 m. Samples from the present Wairoa study area appear to have undergone mainly deeper burial than those to the east analysed by Drinnan (2011).

Table 7.5: Bulk stable oxygen and carbon isotope data, and possible minimum burial temperatures and burial depths, for samples from Tahaenui Limestone, northern Hawke's Bay (* data from Drinnan 2011).

Facies type	Tahaenui Limestone	Bulk calcite ‰		Calcite cement isotope *T*(C°)	Calcite cement paleodepth (m)
		$\delta^{13}C$	$\delta^{18}O$		
L1	Ma1.01	-0.25	-0.97	20	313
L1	Ka1.02	0.02	0.02	15	132
L1	Ko1.01	0.05	-0.01	15	137
L1	trig1.01	0.54	-3.13	30	737
L1	Ra/ta	1.04	-0.88	19	296
L1	3*	1.56	0.37	14	70
L1	3*	1.43	0.15	15	108
L1	107*	0.57	-0.19	16	170
L1	107*	0.56	-0.15	16	163
L1	128.1*	0.90	0.01	15	133

7.13 Petrography

Tahaenui Limestone is the youngest carbonate-rich unit in the northern Hawke’s Bay region. On average, the limestone is the least siliciclast-bearing deposit in the study area. It is typically a barnacle and epifaunal bivalve dominated limestone, well cemented by low-Mg calcite sparite along with small amounts of micrite material. The raw petrographic data for the Tahaenui Limestone are included in Appendix V.

The overall average whole rock composition diagram for the Tahaenui Limestone emphasizes its greater purity compared to two older (Opoitian) formations (Fig. 7.17A). It comprises only facies type L1, which is a bioclast-dominated limestone. The limestone contains up to 80% of mainly low-Mg calcite (skeletal grains and cements). The overall bioclast content of the Tahaenui Limestone varies from about 40-65%, the cement content from 20-40%, and the siliciclast content from 1-20%.

Figure 7.17A shows the average whole rock compositional breakdown for the typical L1 facies (n=21) comprising the Tahaenui Limestone: 50% bioclasts (barnacles and bivalves), 5% siliciclasts, 7% authigenic materials, and c. 30% of both intrinsic and extrinsic microsparite. Also recorded is 10% porosity represented by open, interparticle pore space and locally secondary mouldic porosity (Fig. 7.17A, 18A, 19A & B).

Skeletal grains

The average content of the different skeletal types in the total skeletal composition of the Tahaenui Limestone is shown in Figure 7.17B. Subequal amounts of barnacles (37%) and bivalves (31%) dominate. These two skeletal types are often clearly visible in both outcrop and within rock slabs (Fig. 7.7). Other skeletal components include both benthic (8%) and planktic (10%) foraminifera, bryozoans (7%), echinoderms (6%) and brachiopods (2%). The skeletal grains have a bimodal size distribution with an average primary mode at 1.1 mm (very coarse sand) and a secondary one at 1.4 mm (very coarse sand). The skeletal materials varies from poorly to well sorted, and moderately to well abraded, with microboring locally observed in thin sections (Fig. 7.18B). The skeletal grains can support isopachous fringe cements (Fig. 7.18C), show neomorphic fabrics (Fig. 7.18D), and pressure-dissolution features are relatively common (Fig. 7.18E).

Non-carbonate grains and infills

The average abundance of the various siliciclastic components is plotted together with the authigenic minerals as the non-carbonate material in Figure 7.17C. Siliciclastic materials are not common components in the Tahaenui Limestone. They mainly comprise glauconite pellets (37%), feldspar (23%) and quartz (16%), with lesser amounts of glauconite infills (15%) and pyrite grains (7%). The grain size of the siliciclastic materials often shows a bimodal size distribution, with a primary mode 0.24 mm (fine sand) and a secondary one at 0.33 mm (medium sand). The maximum size measured is about 2 mm. The siliciclastic grains are mainly reasonably well to moderately sorted, with shapes ranging from subangular to subrounded.

Authigenic minerals account for over half of the non-carbonate composition. They comprise mainly glauconite pellets (35%) and glauconite infills (12%) (Fig. 7.17C), and are ubiquitous but scattered. Pyrite grains and infills are rare.

Cement/matrix

The dominant material between the skeletal and non-carbonate grains is mainly spar cement (Fig. 7.18F), and it also occupies many extrinsic spaces. Microsparite and subequant sparite occur extrinsically (Fig. 7.18G), and also as isopachous fringe cement around the skeletal grains. Those fringe cements around skeletal grains often form ‘dog tooth’ like or scalenohedral shapes (Fig. 7.18H). The isopachous fringe cements about certain skeletons are an early diagenetic cement (Fig. 7.18B & E). They tend to be host-specific, favouring barnacle and bivalve fragments, and preserve the intrinsic pore spaces. The subequant cements are typically non-marine cement, possibly derived from dissolution of formerly aragonitic skeletons, and infilled the existing porosities between the skeletal grains during shallow burial (c. 100 m below seafloor). Neomorphism of bivalve skeletons is a common alteration feature of certain bivalve skeletons in the Tahaenui Limestone (Fig. 7.18D). The neomorphic fabrics suggest the former presence of infaunal bivalves and other aragonitic skeletons as part of the skeletal make-up.

Cathodoluminescent petrography

The skeletal components of the Tahaenui Limestone show a range of CL colours from dark purple (former aragonite-infaunal bivalves) to dull orange (calcitic barnacles and epifaunal bivalves), with each individual grain clearly shown (Fig. 7.19A & B). The isopachous/fringe cements show up clearly under CL, and colours range from purple (immediately surrounding skeletal grains) to dull orange (further outwrds from the surface of the skeletal grains), and with a thin bright yellow edging on the subequant sparite (Fig.7.19C & D). This change in cement colour suggests a change in the chemical composition of percolating fluids, perhaps associated with increasing burial depth. The extent of pressure-dissolution between grains suggests relatively shallow burial depths, and much of the compaction of the skeletal sediments occurred before the growth of the cements (Fig. 7.19E & F).

Petrographic summary of facies type L3

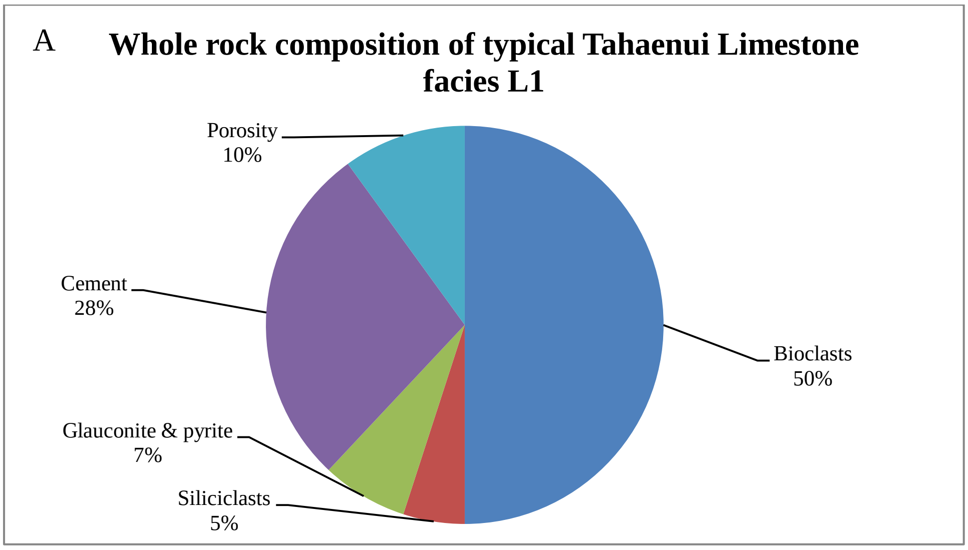

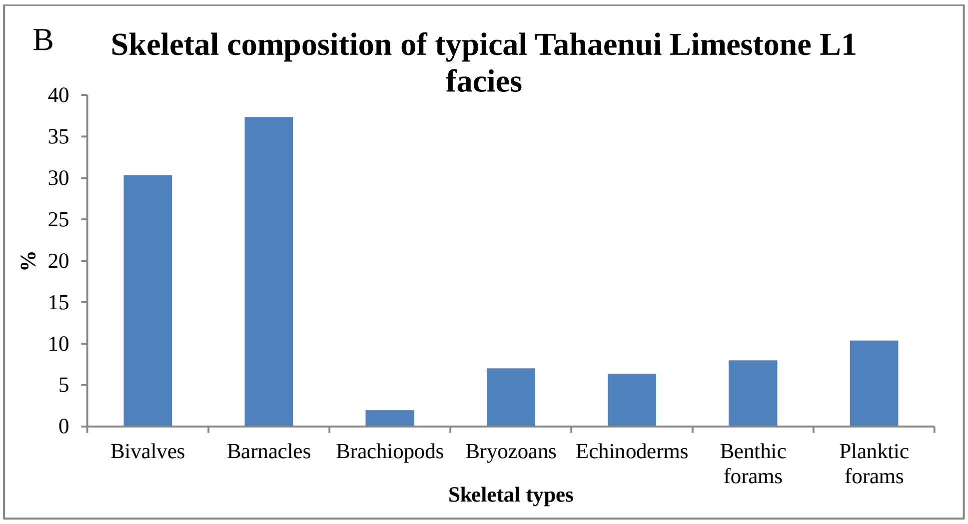

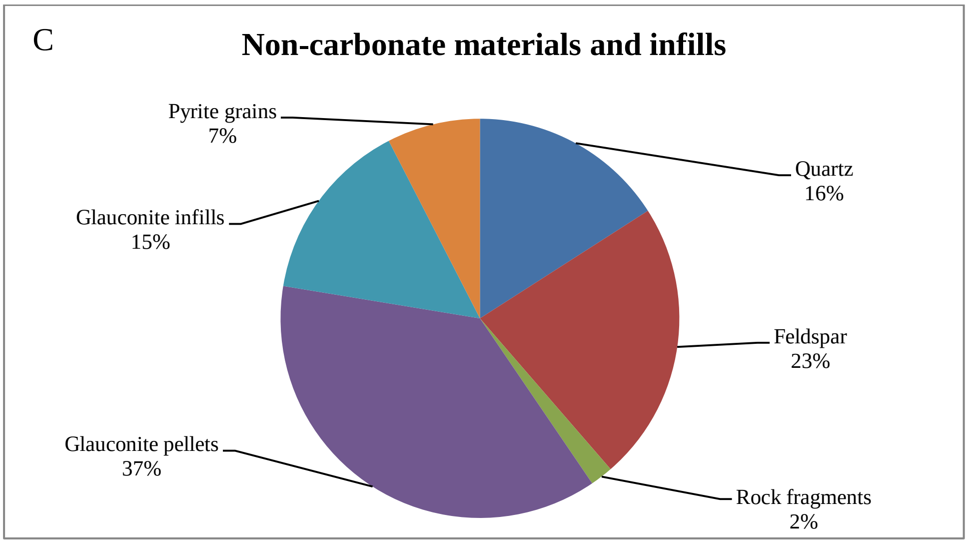

Figure 7.16: Petrographic summary based on representative samples (n=21) of Tahaenui Limestone (facies L1): (A) whole rock, (B) skeletal types, and (C) non-carbonate materials.

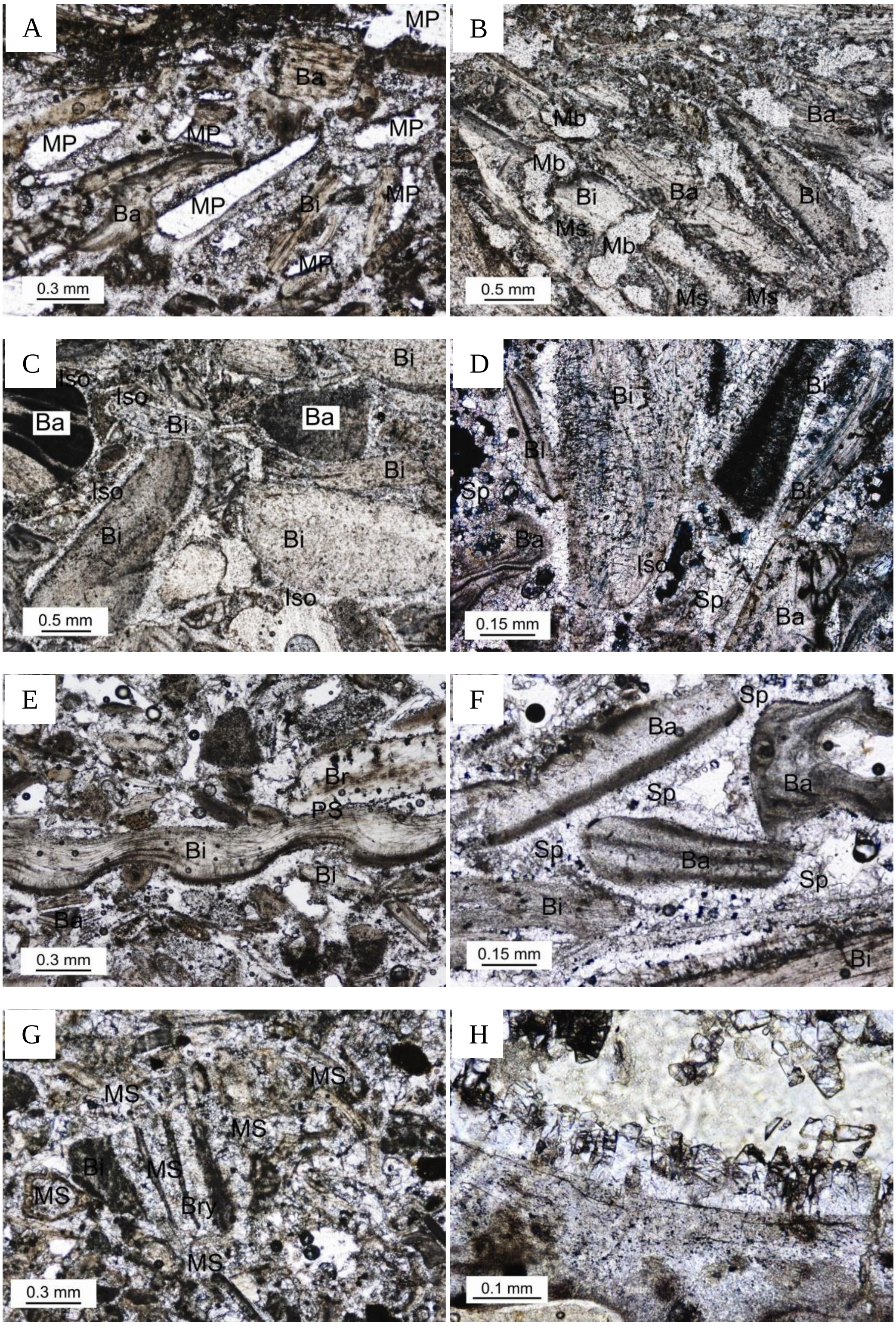

Figure 7.17: Photomicrographs of Tahaenui Limestone samples. A) PPL image of a coarse bivalve-barnacle biosparite showing secondary mouldic porosities (MP) from former aragonitic bivalve skeletons (sample Wa1.08). B) Image of a porous, poorly sorted biosparrudite consisting of microbored skeletons of bivalve (Bi) and barnacle (Ba) skeletons (sample Wa1.03). C) Well abraded and poorly sorted bivalve (Bi) and barnacle (Br) biosparrudite. Skeletons coated with thin fringe cement (Sample Wa1.02). D) XPL image shows a common feature of neomorphosed bivalve skeletons in a biosparite (sample Wa3.02). E) Poorly sorted, abraded skeletal grains showing pressure dissolution (PD) (sample Wa1.05). F) Well abraded skeletal grains coated with fringe (Fr) cement and partial pore occlusion by microsparite (sample Wa2.01). G) Poorly sorted biosparite showing microsparite infill of all pores (sample Ma1.01). H) Close-up view of bivalve grain coated with isopachous fringe cement consisting of scalenohedral sparite (sample Wa2.01).

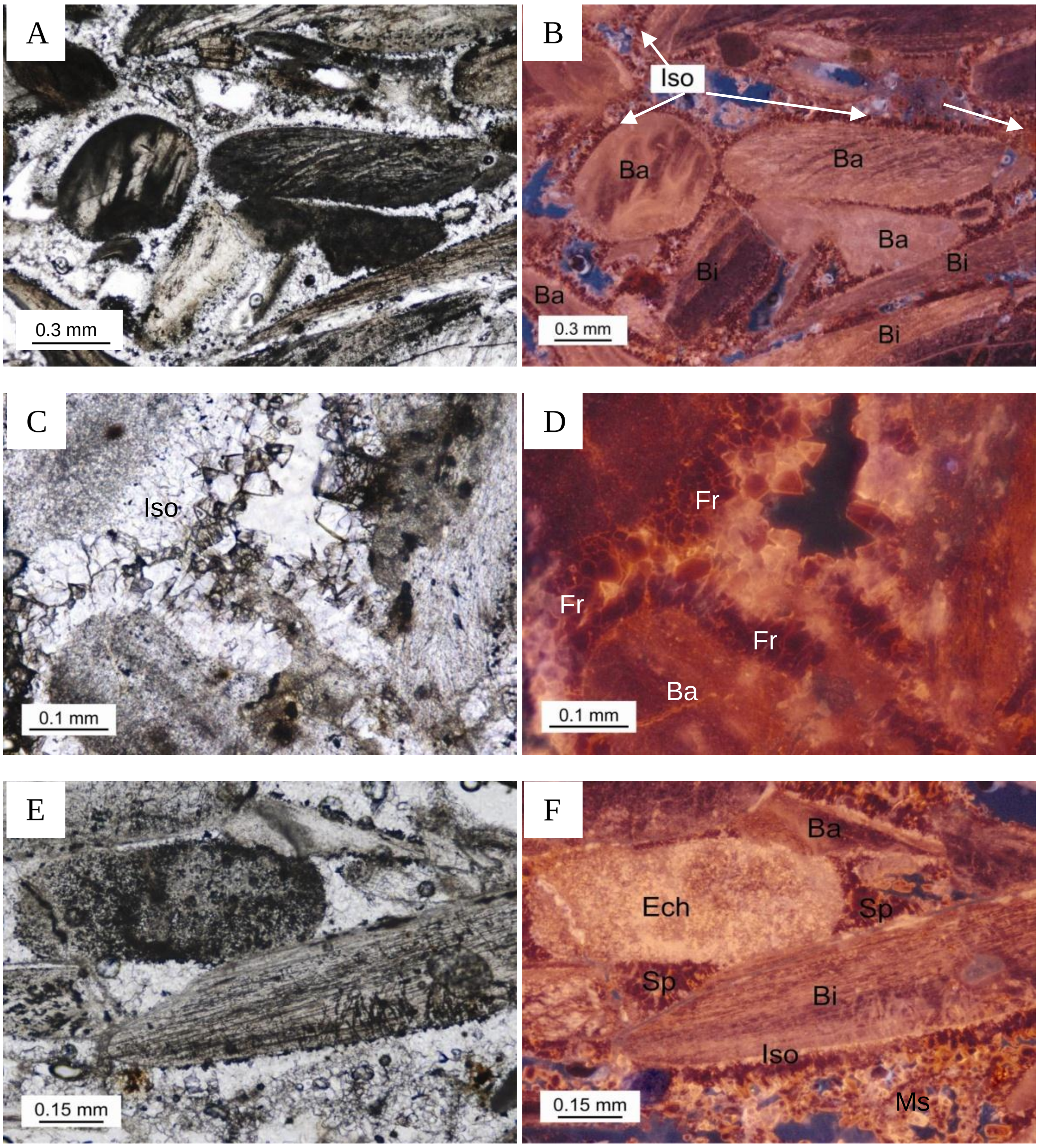

Figure 7.18: Photomicrograph pairs under PPL (left) and CL (right). A & B) Overview image of biosparite consisting of well abraded bivalve (Bi) and barnacle (Ba) skeletons, exhibiting a dull orange luminescence, coated with a thin (c. 0.06 mm) and clear isopachous (Iso) dull reddish orange luminescent fringe cement (sample Wa2.03). C & D) Close-up view of abraded barnacle (Ba) fragments coated with an uneven bladed fringe (Fr) cement of initially dull purple luminescence that becomes moderately bright orange porewards. Later and partial pore occlusion is by clear microsparite (Ms) with moderately bright orange CL (sample Wa2.01). G & H) Close-up of abraded barnacle (Ba) and bivalve (bi) and echinoderm (Ech) grains showing rare, weakly developed pressure dissolved contacts which appear to predate cement generations established in A to D above (sample Wa1.05).

Petrographic classification

Petrographically, the Tahaenui Limestone samples typically range from moderately to well sorted, well abraded, porous bivalve and barnacle biosparite to porous bivalve and barnacle fine biosparrudite. Overall the unit is dominated by well rounded barnacle and calcitic (epifaunal) bivalve skeletons, well cemented by low-Mg calcite microsparite and granular subequant sparite.

8 Chapter Eight

Wairoa Formation

8.1 Introduction

The thick siliciclastic-dominated lithologies containing the three limestones in the Pliocene Mangaheia Group in northern Hawke's Bay have in the past been assigned various names, depending on their stratigraphic position and geographic location in the region. The siliciclastic-dominated units above the Tolaga Group and underlying the Opoiti Limestone were labeled Mapiri Formation by Beu (1995) and Field *et al.* (1997). The deposits between the Opoiti Limestone and Whakapunake Limestone were named Opoiti Formation in early petroleum exploration reports, and this term was used by Beu (1995) and Field *et al.* (1997), despite duplication of the name Opoiti. The siliciclastic deposits above the Tahaenui Limestone were called Wairoa Formation. However, all these siliciclastic units fundamentally comprise very similar lithofacies. Consequently, in this study the stratigraphic naming of these siliciclastic facies has been refined (section 4.2) and the name Wairoa Formation chosen to encompass all of the Pliocene undifferentiated sandstone and mudstone deposits. This chapter briefly presents some laboratory-based analytical data for some major lithofacies in the Wairoa Formation, including $CaCO_3$ content, bulk mineralogy and insoluble grain textures.

8.2 Name and definition

Outside of the three limestone formations, all of the Pliocene sandstone and mudstone units in the Wairoa Syncline are assigned to Wairoa Formation. Their relationship to the three limestone formations can be useful for subdividing the Wairoa Formation into A, B, C and D portions, from oldest to youngest (Fig. 4.1 and 4.2). The Wairoa Formation A (M1, S1 and S3) was formerly part of the Mapiri Formation in the Tolaga Group (Field *et al.* 1997). It comprises mainly massive sandstone and mudstone facies that unconformably overlie Late Miocene (Kapitean) mudstone of Mapiri Formation (the name Mapiri Formation is retained but now covers only the Late Miocene/Kapitean deposits). At the Mangapoike River section along the Mangapoike Road (Fig. 8.1A) an angular unconformity of 3° occurs which involves some 0.5-1 my of missing section based on foraminiferal evidence (Edwards 1987). Zircon from a thin tephra bed in the upper part of the Mapiri Formation (Kapitean) directly below the unconformity has been fission track dated at of 5.8±0.55 my (Hornibrook 1984). The thickness of Wairoa Formation A varies from c. 2 (mainly northern part of Wairoa Syncline) (Fig. 8.1B) to 220 m (near the Mangapoike Valley, Fig. 1.2). In turn the Wairoa Formation A is unconformably overlain by the thin, sandy Opoiti Limestone (Early Pliocene). The unconformity has a broadly undulating surface and is intensely burrowed (Fig. 5.7A).

The Opoiti Limestone passes gradationally into Wairoa Formation B (M1, M2, S2 and S3), which is disconformably overlain by the late Opoitian Whakapunake Limestone (Fig. 8.1C). This mudstone-dominated, often differentially cemented, and locally glauconitic and bioclast-rich sandstone unit was formerly named the Opoiti Formation or the Mangapoike Formation (Fig. 8.1E) (Bremner *et al.* 1934; Francis 1993). Thin tuff or volcaniclastic sandstone and mudstone beds (c. 20-30 cm thick) occur in many outcrops of this unit (Fig. 8.1F). The estimated maximum thickness of the Wairoa Formation is c. 700-800 m (Field *et al.* 1997).

The Wairoa Formation C (late Opoitian) stratigraphically sits between the Whakapunake and Tahaenui Limestones, and passes laterally into sandstone and mudstone of Wairoa Formation B. However, a regional unconformity marking the start of the Waipipian Stage cuts out most of the Wairoa Formation C in the present study area. The Tahaenui Limestone often sits directly upon Whakapunake Limestone, so that exposures of Wairoa Formation C (M1) are limited.

The Waipipian Tahaenui Limestone conformably passes upwards into the locally tuffaceous, mudstone-dominated Wairoa Formation D (M1) (Waipipian). The variation of lithofacies within these siliciclastic successions gives the potential for further subdivision the Wairoa Formation into mudstone and sandstone members within the Wairoa Syncline.

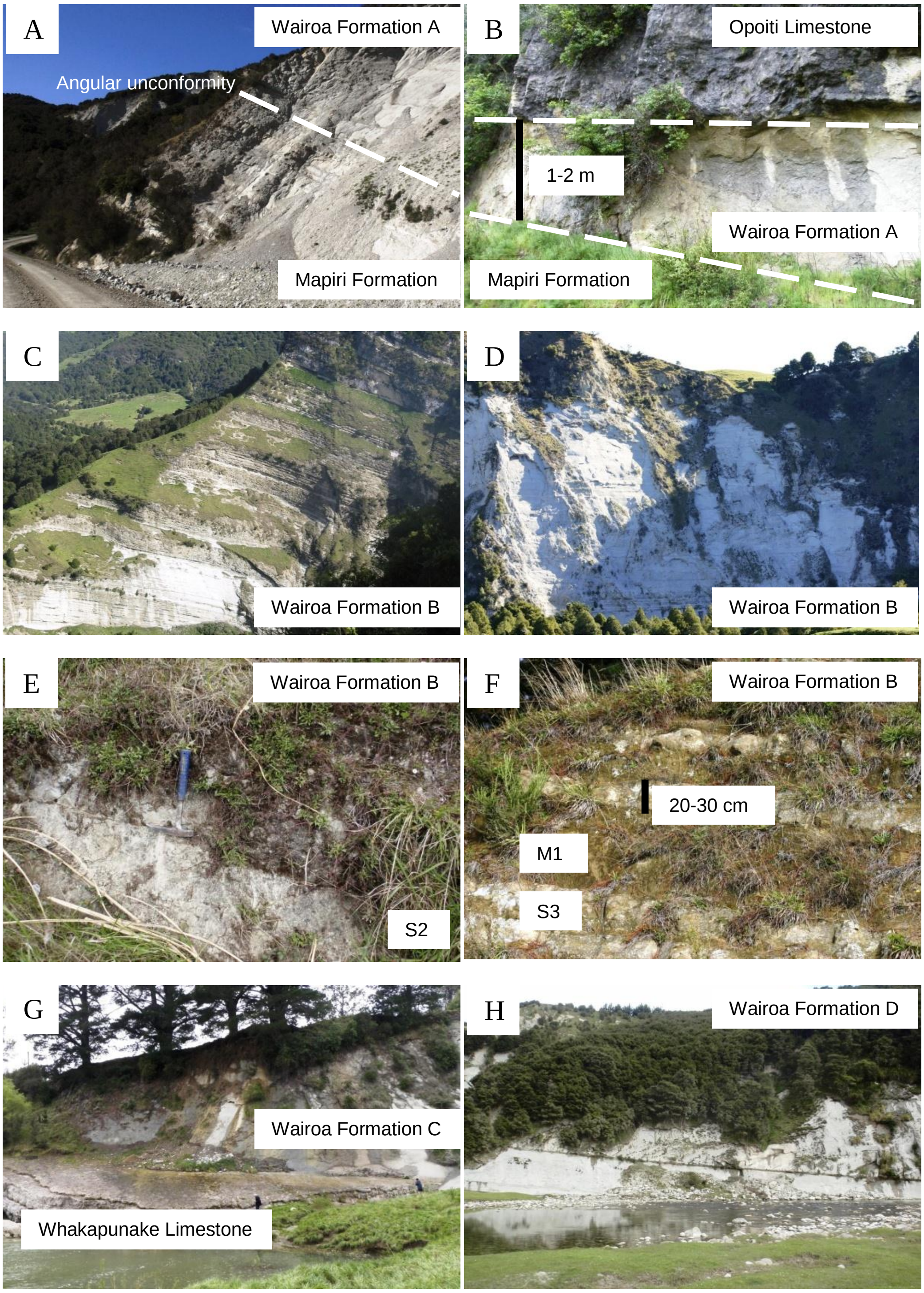

Figure 8.1: A) Mudstone facies (M1) of Wairoa Formation A unconformably overlies the Late Miocene thinly bedded mudstone and tuff beds of Mapiri Formation above the Mangapoike Road. Location X19/072450. B) Outcrop above the Hangaroa River showing the sandstone facies of Wairoa Formation A overlying the Mapiri Formation which in turn is unconformably overlain by the Opoiti Limestone. The Pliocene/Miocene separation is not presevered. Location X18/099658. C) Differentially cemented mudstone bluff in Wairoa Formation B at Haupatanga Gorge. Location X19/038458. D) Differentially cemented mudstone facies above the Hangaroa River. Location X19/091658. E) Glauconitic and bioclastic sandstone (S2) of Wairoa Formation B. Location X19/057454. F) Thin volcaniclastic sandstone (c. 20-30 cm) and mudstone beds which correlate to the period of Waihi-Kaimai Volcanic Centres' eruptions (Briggs *et al.* 2005). Location X18/103594. G) The massive mudstone facies (M1) of Wairoa Formation C overlies the Whakapunake Limestone below the Mangapoike Road. Location X19/028428. H) Wairoa Formation D above the Mangapoike River at the end of Kotare Road. Location X19/020465.

8.3 $CaCO_3$ content

The $CaCO_3$ content of eight samples representative of the major lithofacies within the Wairoa Formation varies from 5-45% (Table 8.1). Siliciclastic sand and mud contents are also variable, from 15-70% and c. 15-80%, respectively (Fig. 8.2).

Table 8.1: Bulk $CaCO_3$ and insoluble sand and mud content of eight representative samples of Wairoa Formation. Facies types defined in Table 4.1.

Sample No.	*Facies type*	*% $CaCO_3$*	*% Mud (<63 µm)*	*% Sand (63-2000 µm)*
P1.01	M1	12	48	40
R1.01	M1	3	81	16
Ta/m	M1	43	44	13
Pa1.05	M1	5	56	39
11.01	S1	3	26	70
T2.01	S1	27	31	42
H1.01	S1	7	42	51
T1.02	S2	25	14	61

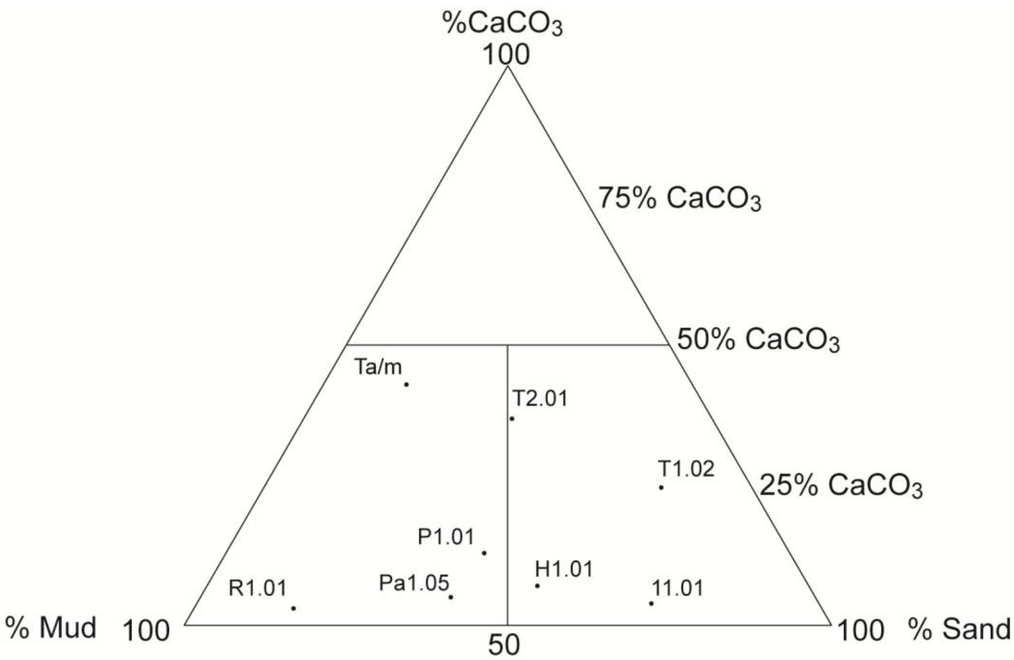

Figure 8.2: Ternary $CaCO_3$-sand-mud plot for samples from Wairoa Formation.

8.4 Bulk mineralogy

X-ray diffraction (XRD) analysis of 17 samples from the Wairoa Formation show the main minerals present are quartz, plagioclase feldspar and low-Mg calcite (c. 4 mol% $MgCO_3$) (Table 8.2). Quartz and plagioclase feldspar are expectedly common in all samples. The presence of low-Mg calcite is related to the carbonate constituents comprising occasional skeletal fragments of barnacles, epifaunal bivalves and brachiopods, all low-Mg calcite secretors, and micrite matrix. Phyllosilicate minerals, including glauconite, constitute the clay material.

Table 8.2: XRD bulk mineral analysis of 17 samples from the Wairoa Formation. (P=present).

Wairoa Formation	Sample No.	*Dolomite*	*Low-Mg calcite*	*Plagioclase feldspar*	*Quartz*	*Clays*
A	H1.01	-	P	P	P	P
A	T2.01	-	P	P	P	P
B	P1.01	-	P	P	P	P
B	H1.04	P	P	P	P	P
B	H1.05	-	P	P	P	-
B	H1.06	-	P	P	P	P
B	H1.07	-	P	P	P	P
B	H1.08	P	P	P	P	P
B	T1.01	-	P	P	P	P
B	T1.02	-	P	P	P	P
B	Pa1.05	-	P	P	P	P
B	Ta/m	P	-	P	P	P
B	11.01	-	P	P	P	P
B	O1.01	-	P	P	P	P
B	Pa1.01	-	P	P	P	-
B	Pa1.04	-	-	P	P	P
C	R1.01	-	P	P	P	P

8.5 Insoluble grain texture

The texture of insoluble grains in the Wairoa Formation is shown in Table 8.3. Sand forms 20-80% of the insoluble fraction, silt 15-80%, and clay <5%. Figure 8.3 shows that all the samples are dominated by sand and silt sizes, varying between silty sand and sandy silt in texture.

Table 8.3: Bulk insoluble grain textures for 27 samples of Wairoa Formation.

Sample No.	*Facies type*	*% Clay (<3.9 µm)*	*%Silt (3.9-63 µm)*	*% Sand (63-2000 µm)*
P 1.01	M1	2	52	46
R 1.01	M1	3	81	16
Ta/m	M1	3	74	23
Pa 1.05	M1	2	57	41
G1.03	M1	3	52	45
G1.04	M1	5	64	31
G1.10	M1	5	65	30
G1.12	M1	3	49	48
G1.13	M1	5	75	20
G1.14	M1	5	53	42
G1.15	M1	3	55	42
G1.16	M1	6	66	28
G1.18	M1	3	52	45
G1.19	M1	5	60	35
11.01	S1	1	27	72
T 2.01	S1	2	41	57
H 1.01	S1	1	44	55
G1.01	S1	3	42	55
G1.02	S1	5	41	54
G1.05	S1	4	40	56
G1.06	S1	1	14	85
G1.07	S1	2	21	77
G1.08	S1	4	46	50
G1.09	S1	4	33	63
G1.11	S1	3	43	54
G1.17	S1	5	45	50
T 1.02	S2	1	17	81

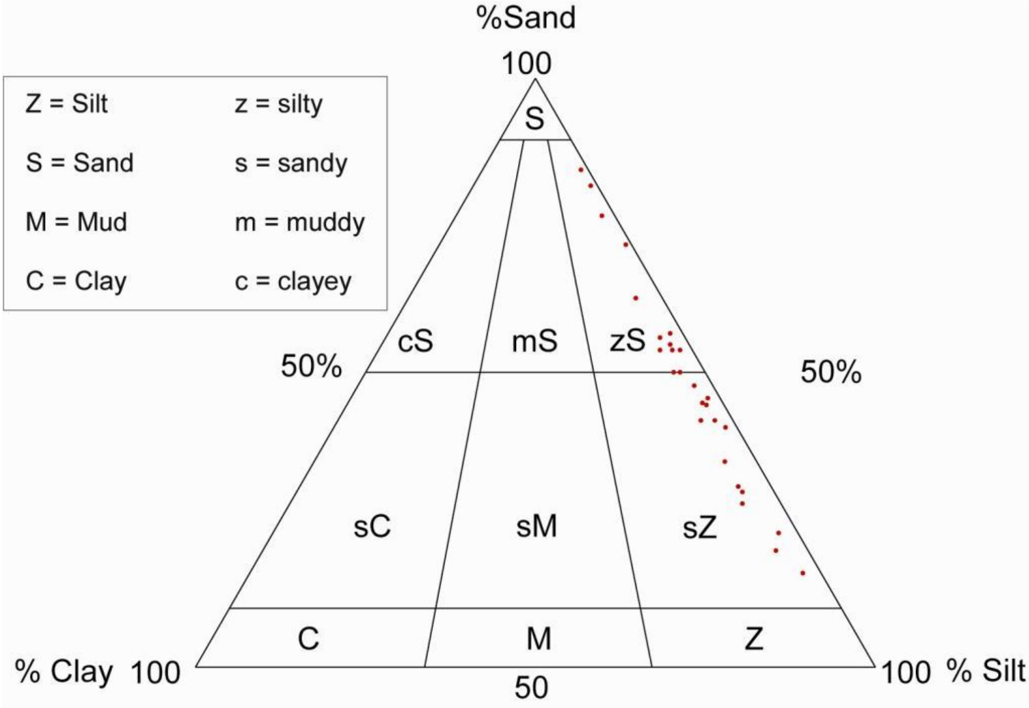

Figure 8.3: Ternary clay (C), silt (Z) and sand (S) plot (%) for the insoluble residue fraction from Wairoa Formation samples. Textural size classification from Boggs (2004).

9 Chapter Nine

Discussion

9.1 Pliocene stratigraphic nomenclature

The stratigraphic nomenclature applied to the Pliocene deposits in northern Hawke's Bay has been reviewed in this study to better order and rationalise the Pliocene stratigraphy. The names Opoiti, Whakapunake and Tahaenui Limestones used by earlier workers have been retained for the three Te Aute type limestone lithofacies occurring in the Wairoa Syncline. The thick (up to 2000 m) Pliocene mudstones and fine-grained sandstones of broadly similar lithofacies to one another in which the limestones sit have been grouped together into a single formation, named the Wairoa Formation (Fig. 4.1). Collectively, these Pliocene formations belong in the Mangaheia Group.

The classic Te Aute limestone lithofacies is by far the dominant limestone type in eastern North Island (Fig. 1.6) (Beu 1995). The Te Aute limestones have a long and complex history of stratigraphic nomenclature. The name Te Aute was formally given to the Pliocene limestone units, and describes the broadly similar, coarse skeletal calcarenites and calcirudites with variable amounts of siliciclastic material in the East Coast forearc basin. The earlier work tended to simply lump the separate limestone occurrences into a single formation (Te Aute Formation) without considering their age, geographic location or detailed lithology (Nelson *et al.* 2003). Beu (1995) attempted to formalise the stratigraphic nomenclature for the formations by assigning them to particular Pliocene stages based on their pectinid biostratigraphy. In conjuction with their geographic location he subdivided the limestones into 6 groups, 45 formations, and 12 members. Figure 1.4 shows the complex stratigraphic distribution of some of the main Te Aute limestone occurrences in onshore eastern North Island. The current study deals only with the three skeletal-rich limestones found in the Wairoa district in northern Hawke's Bay – the Opoiti Limestone, Whakapunake Limestone and Tahaenui Limestone – all of formationsal rankings. Like most of the Te Aute limestones in the forearc basin, they are unconformity bound, either by an angular unconformity or a disconformity, which suggests variable degrees of tilting, uplift and erosion have been ongoing in the area during Pliocene sedimentation.

Stratigraphic naming of the Pliocene siliciclastic-dominated deposits in the study area is difficult because they comprise broadly similar lithofacies of mudstone and fine-grained sandstone. Formerly these units bore separate names according to their age: Mapiri Formation (Kapitean-early Opoitian), Opoiti Formation (Opoitian) or Wairoa Formation (Waipipian or younger). However, it is generally inmpossible to distinguish between these units on the basis of field lithology and so in this study they are lumped together into a single formation, the Wairoa Formation. In places the Wairoa Formation can be subdivided into four informal units based on their stratigraphic position in relation to the three limestones (Fig. 4.1), namely Wairoa Formation A, B, C or D.

9.2 Pliocene lithofacies

The facies classification in this study (Table 4.1) has been developed in combination with the study by Drinnan (2011), and is a simplified version for all the Pliocene strata in the northern Hawke's Bay region. The term lithofacies is used in this study in a purely descriptive sense, and is based on the outcrop characteristics and relative carbonate contents of the different rock types. Each individual lithofacies forms under certain conditions of sedimentation and therefore reflects a particular depositional environment. This study has identified three main lithofacies groups, with a total of 9 lithofacies types being identified in the Wairoa study area, including additional characteristics to assist further detailed description.

There are three limestone lithofacies types (L1-L3) identified for the Pliocene carbonate-rich deposits in this study (Table 4.1). These limestone facies comprise variable amounts of siliciclastic material, from a bioclastic limestone to sandy limestone with carbonate contents varying from 65-85%. L1 and L2 facies are restricted to the two younger limestone units, the Whakapunake Limestone and the Tahaenui Limestone, while L3 is almost exclusively the facies building the Opoiti Limestone, with the exception of its basal coquina facies L2. Both Whakapunake Limestone and Tahaenui Limestone share many lithofacies characteristics, suggesting similarity in their depositional processes.

There are two main lithofacies associations encompassing the rest of the siliciclastic-dominated portion of the Pliocene sequence. Three sandstone (S1-S3) and three mudstone (M1-M3) lithofacies occur in this study. The siliciclastic sandstone facies are found mainly within Early Pliocene deposits. They are variable in thickness, composition and texture, and often form massive sandstone within Wairoa Formation A but also less indurated, thin (5-10 cm) siliciclastic interbeds within the late Opoitian–Waipipian limestone formations over most of the study area. The sandstone facies comprise variable amounts of skeletal and authigenic materials, and have $CaCO_3$ contents ranging from about 30-40%. The mudstone lithofacies are the thickest (total c. 1000 m), dominant lithology in the Pliocene Mangaheia Group in the study area (Fig. 4.1). They are genuinely massive, weakly indurated and thoroughly bioturbated, and some show differential cementation.

9.3 Pliocene paleogeography

Four paleogeography maps illustrate the changes in land masses, sea water and sedimentary facies during the Pliocene (Bland *et al*. 2008). The Opoiti Limestone was deposited in the present day Wairoa Syncline and western Mahia Peninsula during the early Opoitian (5.25 Ma) (Fig. 9.1A), and overlies Late Miocene (Tongaporutuan) deep-water mudstone and sandstone (Beu 1995; Mazengarb & Speden 2000; Bland *et al.* 2008). Substantial subsidence occurred in the Wairoa area where shelfal mudstone of Wairoa Formation B was deposited over the Opoiti Limestone during a period of high sea-level, extensive shoaling and erosion of shelf platforms and shallow parts of the forearc basin seaway (Fig. 9.1A) (Bland *et al.* 2008). Whakapunake Limestone was deposited atop or about sea-floor highs (active growth folds) in the Wairoa and Mahia areas in the late Opoitian (c. 4 Ma) (Beu 1995). The source of siliciclastic sediments in the Whakapunake Limestone was likely from erosion of islets formed from older Neogene sediments to the east of Wairoa Syncline (Fig. 9.1B).

In the Late Pliocene, the eastern margin of the forearc basin seaway progressively emerged as a consequence of subduction accretion along the Hikurangi Margin (Bland *et al.* 2008), which produced a regional unconformity in the northern Hawke's Bay region that separates the Opoitian and Waipipian stages. Continued growth of fold structures in the Wairoa area provided sources of siliciclastic sediments for Wairoa Formation B (Fig. 9.2A), followed by deposition of the Tahaenui Limestone atop sea-floor highs (Fig. 9.2B), which graded on the limbs of the Wairoa Syncline down to outer shelf to upper bathyal depth as the Wairoa Formation. Later, the Wairoa Formation accumulated over much of the Wairoa-Mahia area as the sea-level continued to rise during upper Waipipian (Bland *et al.* 2008).

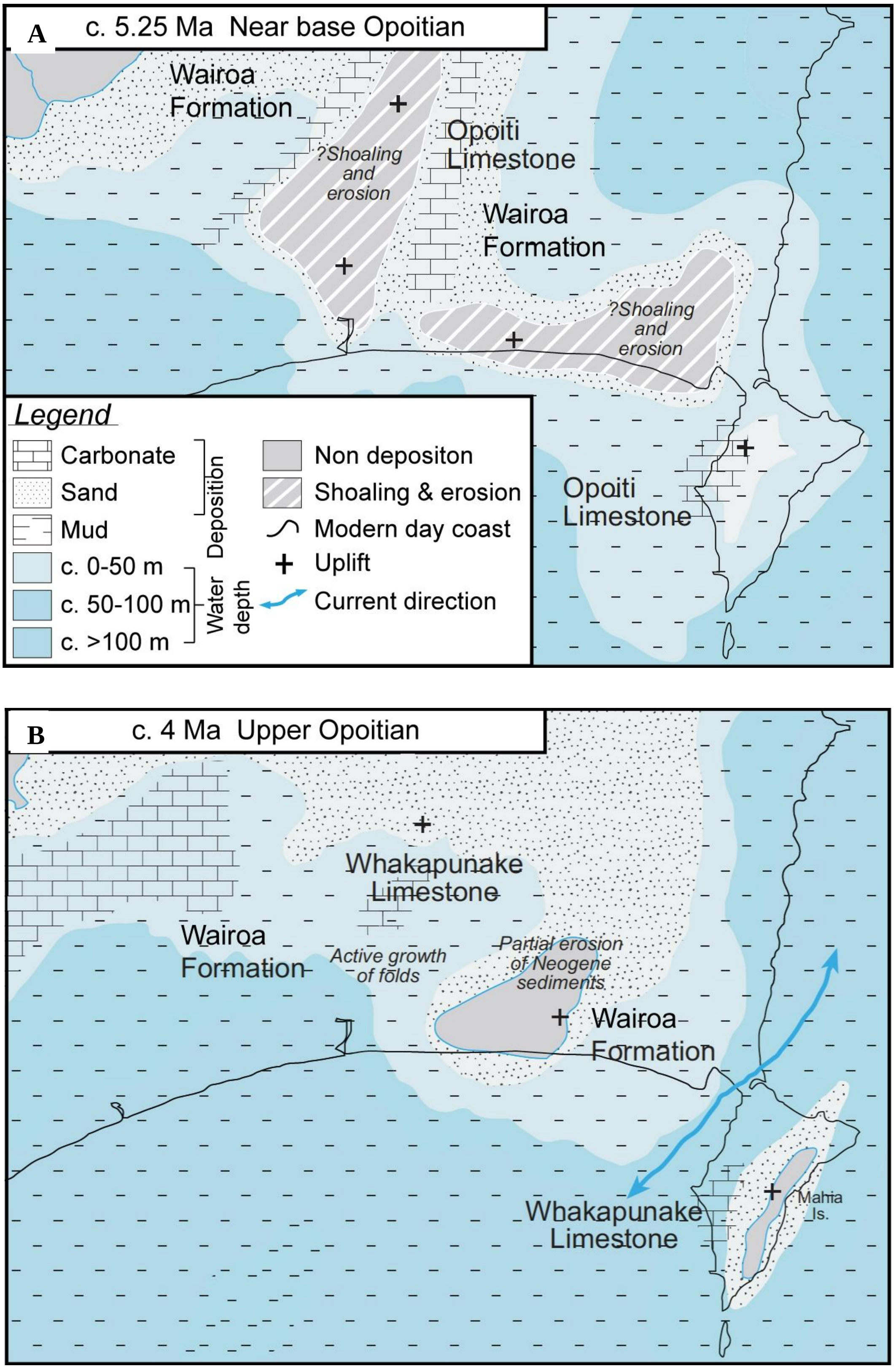

Figure 9.1: Paleogeographic maps during Opoitian (Early Pliocene) time. A) Deposition of the Opoiti Limestone at near base of the Opoitian (5.25 Ma). B) Whakapunake Limestone was deposited during the upper Opoitian (4.0 Ma). Adapted from Bland *et al.* (2008). Legend in A applies in B.

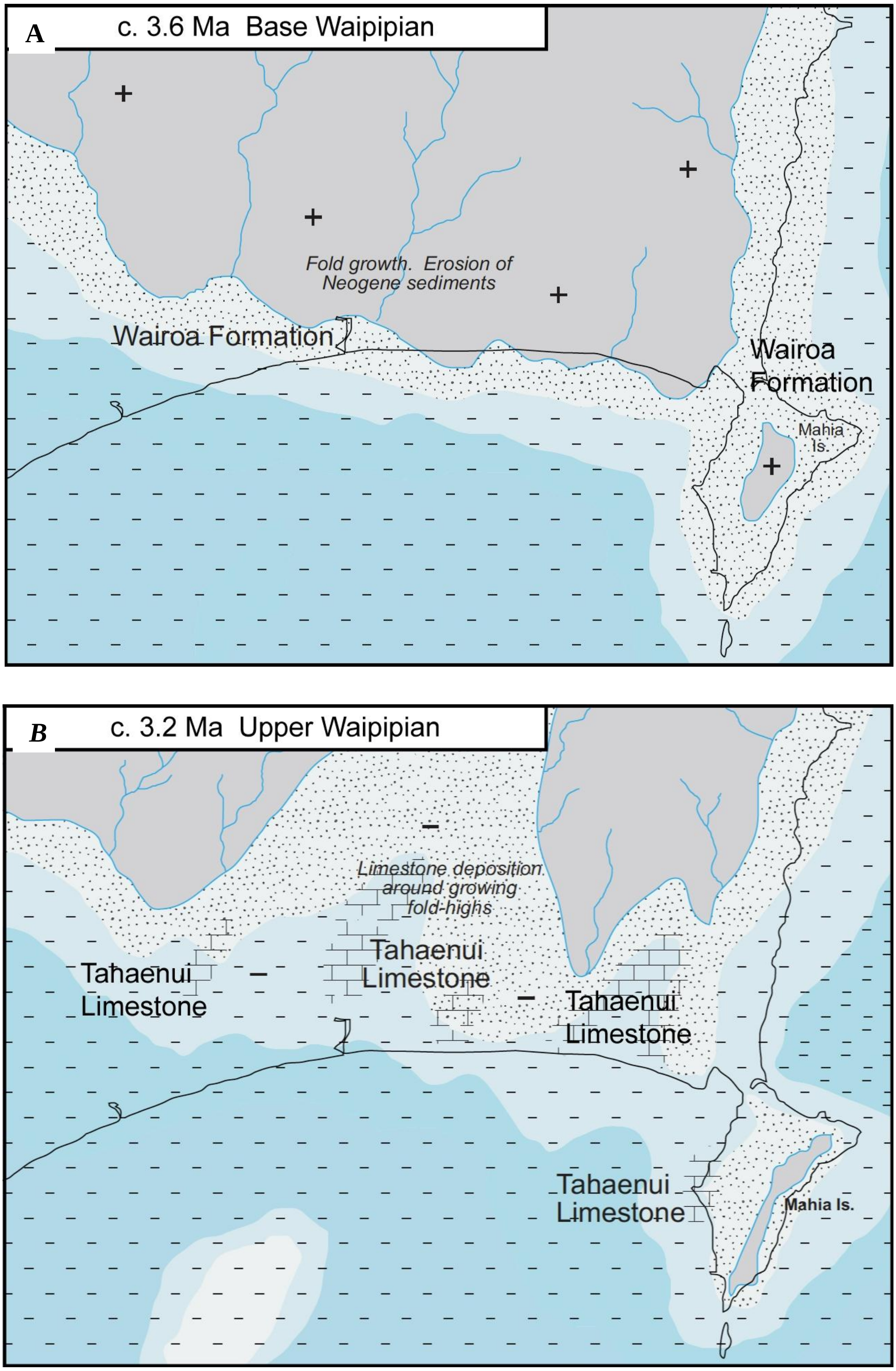

Figure 9.2: Paleogeographic maps during Waipipian (Late Pliocene) time. A) Uplift and erosion of Neogene sediments at base of the Waipipian (3.6 Ma). B) Deposition of the Tahaenui Limestone within the Wairoa Syncline during the upper Waipipian (3.2 Ma). Adapted from Bland *et al.* (2008). Key to symbols in Fig. 9.1A.

9.4 Depositional paleoenvironments

The Pliocene limestones throughout East Coast Basin in eastern North Island accumulated on the margin of a narrow forearc basin seaway within the Hikurangi subduction complex (Nelson *et al.* 2003). The complex stratigraphic architecture of these limestone deposits nearest the upthrusting imbricate ridges on the eastern margin of the seaway were mainly a result of the active convergent setting in response to subduction from the east together with Pliocene glacioeustatic sea-level fluctuations.

Three basic features indicate that the paleo-depositional setting for the three Pliocene limestones was a moderate to high energy, current-swept, shallow-marine setting (Kamp *et al.* 1988). Firstly, the major influence of the paleo-depositional setting was the development of the forearc basin seaway (Ruataniwha Strait) from the Late Miocene through to Pliocene (Fig. 1.6) (Beu 1995). Imbricate ridges of small upthrust anticlines and bordering synclines, and the inversion of slope basins, all resulted from uplift on the eastern margin of the Wairoa Syncline, which promoted deposition of carbonate sediments (Caron *et al.* 2004a). Secondly, these limestones preserve horizontal and especially cross-bedded sedimentary structures on a wide range of scales from ripple to giant sets in the Opoiti and Whakapunake Limestones, indicative of strong currents and flow directions. Thirdly, the skeletal composition of the Tahaenui and Whakapunake Limestones, in particular their consistently coarse-grained barnacle and bivalve-dominated nature, is suggestive of very similar depositional conditions that were repeated in time and space in the study area.

Shallowing of the forearc basin seaway was prominent in the early Opoitian (Caron *et al.* 2004a), especially in the present study area (Fig. 9.1A). The inverted slope basins and their narrow bounding structural highs formed broad, elevated platforms for carbonate deposition along mainly the eastern margin of the Wairoa Syncline (Kamp *et al.* 1988). The time of carbonate accumulation atop the antiforms was usually short lived as a result of progressive thrusting and uplifting in different parts of the margin. The availability of accommodation space forced continuous shifting of local depocentres, which significantly restricted the deposition of voluminous and continuous sheets of limestone.

Cross-bedded sedimentary structures within the Whakapunake and Tahaenui Limestones suggest the strong influence of strong tidal flows that produced high-energy hydraulic conditions which suspended and by-passed fine-grained siliciclastic sediments from “highs” and assisted nutrient renewal in the seaway, factors promoting the production of the unique barnacle and bivalve-dominated cool-water carbonates (Caron *et al.* 2004a). The abundance of barnacle and epifaunal bivalve material in all three limestones is supportive of moderate to high energy and shallow (<30 m) or inner shelf water depth settings, which may explain the paucity of bryozoans and certain other typical cool-water skeletal components such as echinoderms and calcareous red algae (Kamp & Nelson 1988).

9.5 Sedimentation controls

Three major factors control the sedimentation and facies distribution within a depositional environment, namely tectonism, variations in sea-level and source of the sediments (Bland 2001). These three factors all contribute to the characteristics of a sedimentary sequence, but each factor has a different level of involvement during the period of deposition.

The Te Aute limestones are somewhat unique as they record temperate-latitude carbonate sedimentation in an active subduction margin setting during a time of frequent glacioeustatic sea-level fluctuations (Caron *et al.* 2004). The development of their depositional sites was mainly in response to the evolution of the Hikurangi Margin plate boundary as a consequence of subduction from the east of the oceanic Pacific Plate beneath continental crust of the Australian Plate since the earliest Miocene (c. 23 Ma). This forced the uplift, subsidence and shortening of continental crust and formed the trench, accretionary slope and forearc basin setting along the eastern North Island, and especially so during the Pliocene (Kamp 1986; Kamp *et al.* 1988; Lewis & Pettinga 1993; Nelson *et al.* 2003). As a result, the formation of numerous NE-SW striking sub-basins created suitable basin-flanking environments for the development of carbonate factories atop the basin-bounding antiforms. In turn, the redeposition or ‘shedding’ of the carbonate sediments occurred into the associated synforms due to either further tectonic inversion and shallowing or as a result of transport by the strong tidal currents (Figure 9.3). The NE-SW orientation of these sub-basins also dictated the geometry and continuity of the carbonate deposits. These anticlinal structures consist of uplifted and faulted Miocene and/or older rocks and sediments, and are potential suppliers of (some) siliciclastic components in the limestones.

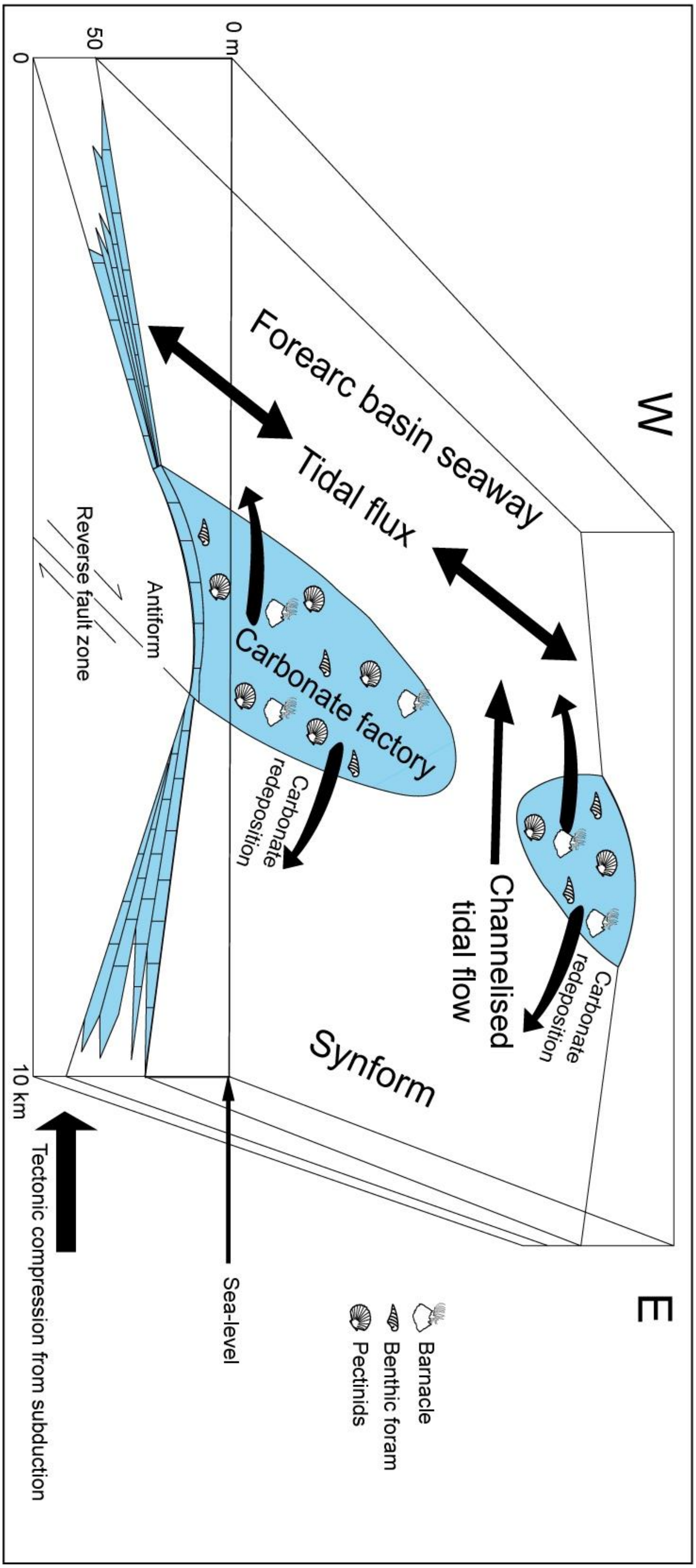

Figure 9.3: Schematic depositional model for the Pliocene limestones. Modified from Nelson *et al.* (2003).

9.5.1 Tectonics

Kamp & Nelson (1987) concluded that tectonism was the dominant controlling element on the formation of limestones in eastern North Island throughout most of the Neogene. Limestone deposition during this time was a result of tectonically induced shoaling and its effect on directing terrigenous sediment pathways. The major tectonic influences on the development of the Neogene succession in the forearc basin have been in response to progressive uplift of the basement rocks along the North Island axial ranges and differential subsidence and uplift of subparallel strips east from here accompanied by progressive shortening of the subduction complex by thrust-related faulting and folding since the earliest Pliocene (Nelson *et al.* 2003). The distribution of the Pliocene limestones follows this distinctive pattern of sub-parallel faulting and folding produced by shortening in the forearc basin and sub-basins immediately to the south of the forearc basin (Kamp *et al*. 1988).

Localised uplift caused by reverse fault thrusting forced a lowering in relative sea-level (to <30 m), creating ecologically favourable conditions for carbonate screting animals to form carbonate sediments atop the antiforms and for their downslope shedding. Accommodation space was created by deepening in the associated synforms. The outcrop patterns in the Nuhaka and Mahia area of Drinnan (2011) reflect this classic depositional setting and are similarly reproduced in the vicinity of Wairoa in the present study area (Fig. 9.4). Here, the forearc basin is (now) represented by the Wairoa Syncline. All three limestones crop out on the eastern limb of the syncline, and two immediately west of the syncline axis (Fig. 9.4).

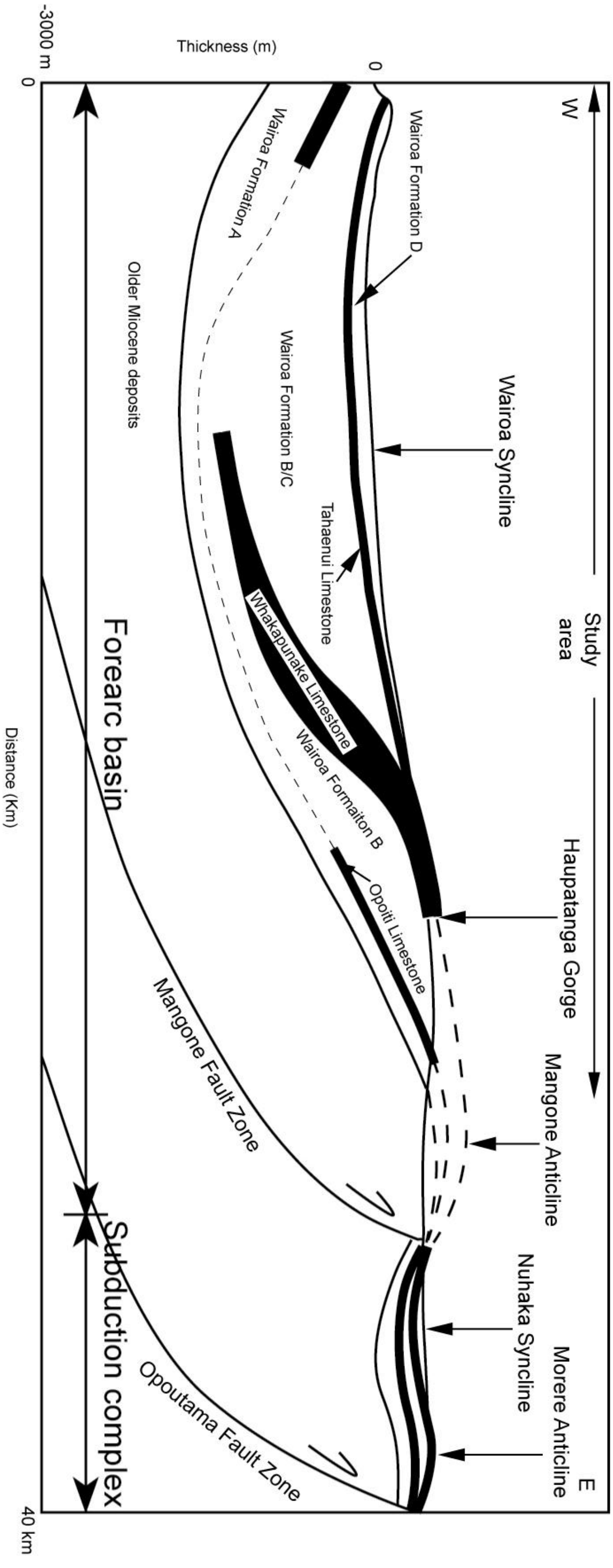

Figure 9.4: Schematic W-E cross section through the Wairoa Syncline.

9.5.2 Sea-level

In many cases, sea-level variations have been associated with the vertical facies distribution of the Pliocene strata in the forearc basin, eastern North Island (Bland 2001). Studies on the western margin of the forearc basin, mainly in central and southern Hawke's Bay, have revealed numerous cyclothems within the Pliocene successions inferred to have developed in response to high-frequency (obliquity-controlled) glacioeustatic oscillations in sea-level (Haywick 2000; Bland 2001; Caron *et al*. 2004). Fluctuations in sea-level have also indirectly controlled the supply of siliciclastic sediments, with reduced rateds leading to the deposition of limestones in the Ruataniwha Strait during late Neogene.

The Pliocene limestones in the present study area are separated from the enclosing thick siliciclastic sediments by unconformities, suggestive of broad-scale tectonic influences. The major facies changes, such as from mudstone to limestone facies, were likely associated with relative movements between sea-level changes (forced change due to tectonism) and tectonic uplift and subsidence, and that glacioeustatically controlled sea-level fluctuations played a subordinate role in this case. However, the geometry and thickness of the Pliocene limestones in northern Hawke's Bay suggest that the periods of limestone deposition probably occurred when the rate of uplift and subsidence matched the eustatic sea-level luctuations (Fig. 9.5). Water depths remained relatively uniform at carbonate production sites for a long period of time. During the Early Pliocene (5-4 Ma), the overall global climatic conditions were cool, but warmer than in the Late Miocene and Late Pliocene–Pleistocene. The retreat of ice sheets on Antarctic during Late Pliocene–Pleistocene may have contributed to the period of long and steady sea-level rise.

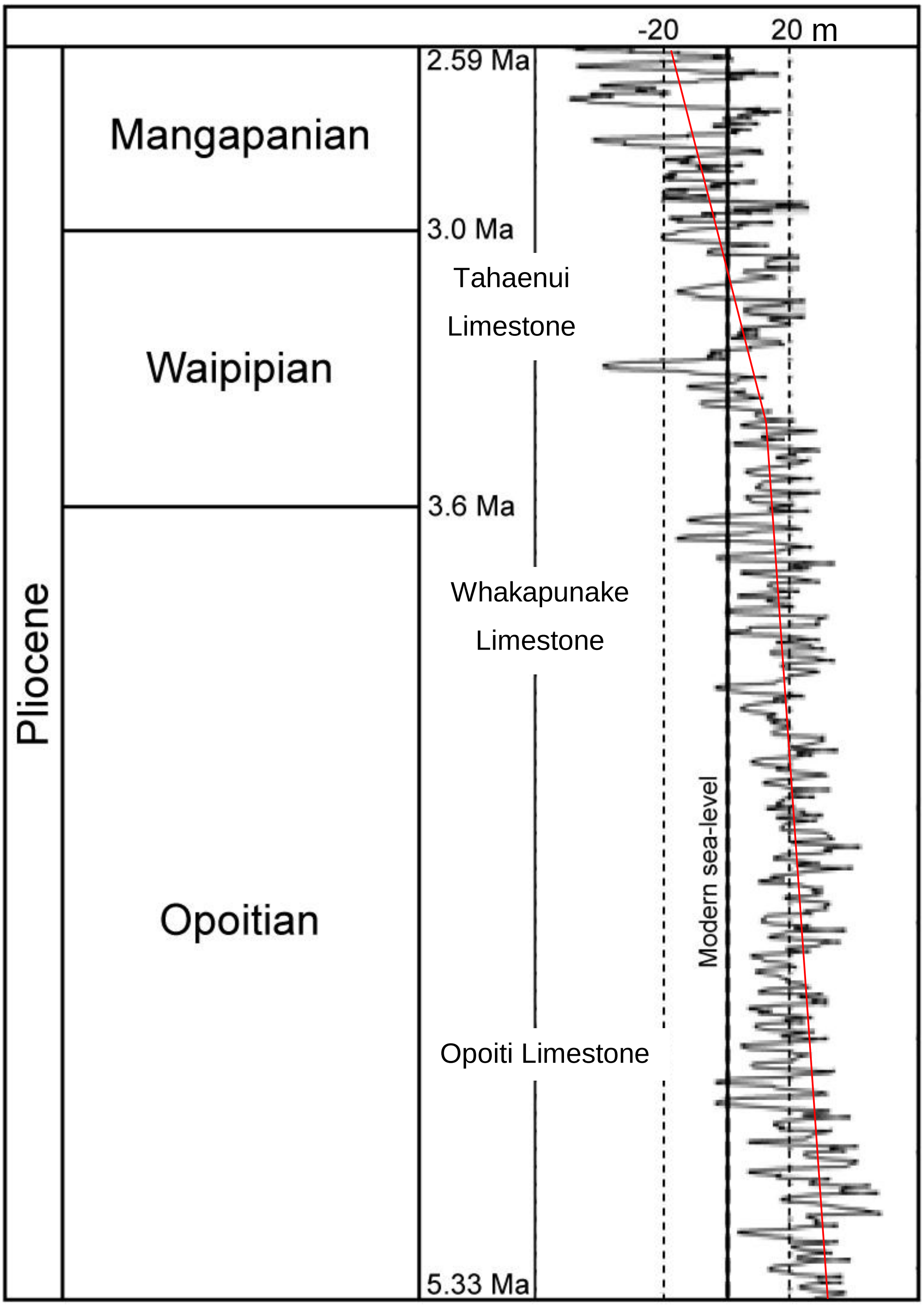

Figure 9.5: Relative sea-level record for Pliocene. Red line indicates the general trend of sea-level movement. Adapted from Raymo *et al.* (2011).

9.5.3 Sediment supply

The Pliocene siliciclastic deposits in the study area are dominated by shallow-marine sandstone and mudstone (Field *et al.* 1997) assigned here to the Wairoa Formation. These sediments were likely sourced from both the basement of the uplifted axial ranges to the west and north of the forearc basin and uplifted and reworked Miocene sediments flanking these ranges or exposed in upthrust structural highs (antiforms). The sporadic Pliocene age volcaniclastic deposits in the study area were sourced from the Coromandel Volcanic Zone (5.33-2.59 Ma) (Briggs *et al.* 2005). The fine tuffaceous sand and silt lenses within the Wairoa Formation sediments possibly correspond to explosive events from Waihi Volcanic Centre (Briggs *et al.* 2005).

The Opoiti Limestone (Early Pliocene) in the study area is a mostly siliciclastic-rich unit compared to the two younger limestones, suggesting a shallower and certainly higher influx of terrigenous sediment during deposition. The distribution and geometry of this limestone are strongly suggestive of a ‘shoreface connected’ setting, more or less landlocked in the north and with a wider opening to deeper water in the south (Fig. 9.1A). The fine texture of the siliciclastic components suggests reworking of the sediments. These siliciclastic materials were sourced from shoaling and erosion of older Miocene sediments off the rising antiforms in the forearc basin (Fig. 9.1A).

The sediment influx into northern Ruataniwha Strait was high throughout the Pliocene, particularly during the Opoitian. Active subsidence from early Opoitian allowed large quantities of siliciclastic sediment to accumulate in the Wairoa Syncline in the northern segment of the forearc basin. Regional uplift followed by steady subsidence on the eastern margin of the forearc basin towards the end of the Opoitian created an ideal depositional setting for the thick Whakapunake Limestone (Fig. 9.1B), and provided time and accommodation space for carbonate accumulation.

9.6 Sequence stratigraphy

Sequence stratigraphy is a branch of stratigraphy that subdivides sedimentary basin fills into generic packages bounded by chronostratigraphically related discontinuities and their correlative unconformities in response to sea-level changes (Emery & Myers 1996; Carter & Naish 1998). Sequence stratigraphic concepts focus on surfaces or system tracts to construct depositional models. These models are based on the cyclic rise and fall of sea-level, and relative positions of the shoreline advancing towards or retreating from the landmass (Fig. 9.6). Sea-level fluctuations can be caused by glacioeustasy and/or tectonic movements of the Earth's crust. The fluctuation of sea-level and tectonic subsidence and uplift control the availability of accommodation space, and act as a regulator on sedimentation to produce different system tracts. This section applies sequence stratigraphic concepts to the formation of the three Pliocene limestones in the study area.

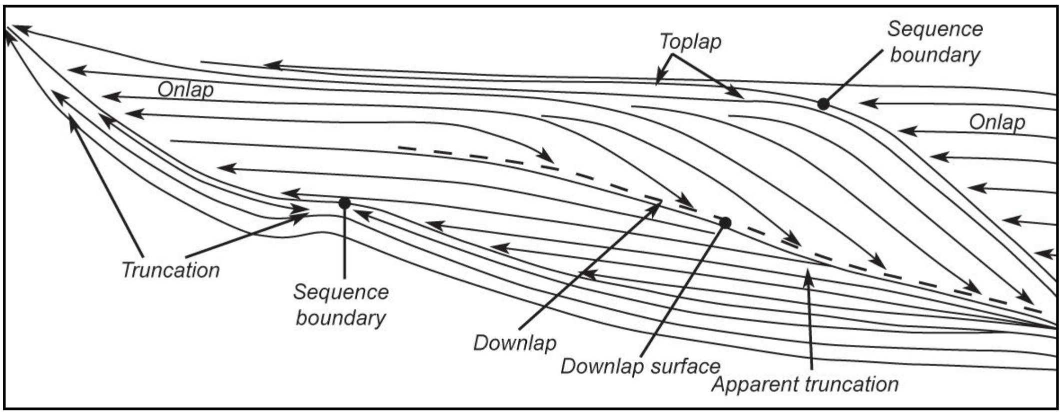

Figure 9.6: Conceptual stratigraphic architecture produced by hypothetical relative fluctuations in sea-level (Naish & Kamp 1997).

Globally, the sea-level controlled depositional nature of Plio-Pleistocene sedimentary successions results from a systematic oscillation of sea-level generated by the Earth's orbital beats (Fig. 9.5) (Naish & Kamp 1997). However, sedimentary fills within the late Neogene forearc basin seaway in the East Coast Basin have been most strongly influenced by tectonic movements along this active subduction margin, with global eustasy likely playing a lesser role.

In an active margin setting, basins undergo complex spatial and temporal variations in subsidence, uplift, sediment dispersal, and source-area erosion. During this time, sediment input and accommodation space are controlled by movements of basin-bounding faults and variations in the rates and geometries of crustal tilting produced by faulting and folding. These variations can produce strikingly different stratigraphic signatures over short distances (Dorsey & Umhoefer 2000). The stratigraphic evolution of East Coast Basin has been influenced by the onset of the present phase of subduction in the Late Oligocene to Early Miocene. This resulted in emplacement of the East Coast Allochthon, uplift and erosion of the axial ranges, and deposition of thick siliciclastic successions (Nelson *et al.* 2003). Rapid subsidence during the Late Miocene further produced thick deep-water siliciclastic sedimentary successions. Compression and deformation of the continental shelf produced a series of subparallel antiforms and wedge-shaped synforms which acted as sediment traps. The synforms filled with sediments and became sub-basins during the Late Miocene to Early Pliocene (Field *et al.* 1997). A large part of the forearc basin was submerged during the Pliocene, and was later uplifted to generally mid- to inner-shelf depth within the forearc basin in the Late Pliocene. Undoubtedly, tectonism has played an important role in the evolution of the forearc basin, and the inferred tectonically influenced sedimentation with different orders of cyclothems is likely presevered in the stratigraphic record during the Pliocene (Bland 2001).

In the past, many sequence stratigraphic studies of the Pliocene deposits in the forearc basin have focused in the vicinity of Hawke's Bay towards the western side of the former forearc seaway (e.g. Haywick 2000; Bland 2001, 2006; Caron 2002; Baggs 2004; Dyer 2005). The cyclothemic nature of several Pliocene units has been reported by previous workers to be the result of 41 k.y. cycle orbital variations (Haywick & Henderson 1991; Haywick *et al.* 1992; Beu 1995; Haywick 2000; Caron 2002; Bland 2006).

Drinnan (2011) was the first to attempt to reconstruct sequence stratigraphic records for the Pliocene deposits in the Nuhaka and Mahia areas, on the eastern side of the former forearc seaway. She suggested that glacioeustatic sea-level changes were a primary influence on the deposition of the Pliocene succession in that region. Although sea-level change is a crucial element and indeed a principal cause of stratigraphic sequences, the rapid changes of facies in outcrop could suggest otherwise. A tectonic influence is the prefered explanation for the changes in facies above and below the limestone-bounding unconformities in the present study area. The successions towards the western side of the forearc seaway, where undoubtedly the deposits are less tectonically influenced, show a more cyclic nature. The sedimentary successions in the central and eastern part of the forearc basin are locally fault bounded. The availability of accommodation space was controlled by the formation of antiforms and synforms due to reverse-thrust faulting that created rather localised transgressive and regressive system tracts.

Figure 9.5 shows possible sea-level movements for the period of deposition involving the three Pliocene limestones and their associated siliciclastic-dominated deposits of the Wairoa Formation in northern Hawke's Bay. The long-term overall sea-level is somewhat steady but with small fluctuations throughout the Pliocene (Fig. 9.5). These small fluctuations could explain the common occurrence of differentially cemented units within some of the mudstones and limestones. The differentially cemented mudstones and limestones could reflect 41 k.y. cycle orbital variations.

Transgressive surfaces of erosion (TSEs)

Transgressive surfaces of erosion develop when sea-level rises and correspond to the process of landwards erosion of the shoreface profile. This process involves an intense reworking and winnowing of pre-existing deposits by the action of wave and storm currents in the uppermost part (c. top 30 m) of the water column (Nummedal & Swift 1987; Caron *et al.* 2004b). TSEs are often interpreted to form immediately after maximum regression of the shoreline, at the start of a transgressive sequence (Bhattarcharya 1993; Embry 1995). TSEs are sharp surfaces (erosional with a relief up to 50 cm) and underlie deepening-upwards TST deposits. A good example is seen in the present study area in the road side outcrop above Hangaroa River in the northern extremity of the present study area (Fig. 9.7A). Beneath the ravinement surface, older deposits of the Wairoa Formation A have been top-truncated during transgression with appearance of intensely burrowed sediment overlain by coarse bioclastic shoreface sediments of the Opoiti Limestone (TST) (Fig. 5.2). The limestone in turn is then overlain by early Opoitian transgressive mudstone and sandstone of Wairoa Formation B (possibly up to HST in the late Opoitian) (Fig. 9.7A).

Forced regressive system tract (FRST)

A forced regressive system tract is usually a sharp response of sedimentation to sea-level fall. This type of regression occurs during a period of base level fall following a high stand of sea-level (Catuneanu 2002). During this time the shoreline is forced to retreat by the falling base sea-level irrespective of the sediment supply. In the case of a tectonically active setting the FRST will likely be induced by inversion (uplift) of the sea floor. In this study, sudden uplift along the forearc basin margin could produce a FRST as a response to reverse-thrust faulting. Such a forced regression is suggested to be represented by the differentially cemented Whakapunake Limestone (Fig. 9.7B). A combination of the sudden shallowing of the sea floor and strong tidal flows within the forearc basin produced a regressive surface of marine erosion as the sharp boundary between the Whakapunake Limestone and the underlying shallow-marine mudstone. The small mudstone clasts contained near below the regressive surface of marine erosion in the underlying mudstone demonstrate that a certain level of scouring was taking place prior to deposition of the carbonate sediments. Due to the tidal current-dominated nature of the depositional setting, the wave scouring depth probably extended beyond the shoreface into shelfal depths.

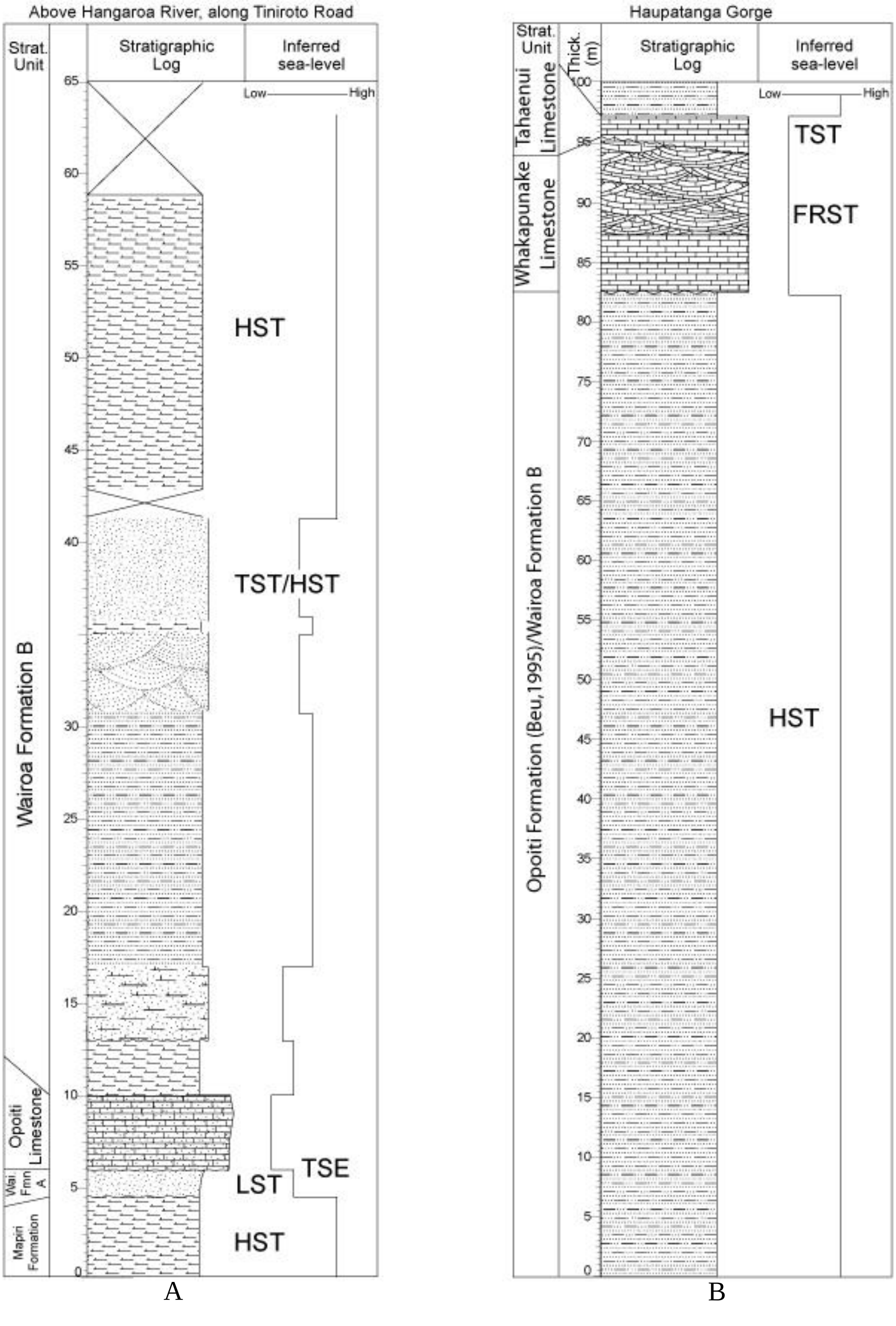

Figure 9.7: Stratigraphic columns with interpreted sequence stratigraphic system tracts from two localities in the study area. A) Outcrop above the Hangaroa River, along Tiniroto Road, and B) exposure in the Haupatanga Gorge. The relative changes in sea-level are inferred from lithologies.

9.7 Sedimentation rates

The Pliocene stratigraphy in the study area is dominated by terrigenous sedimentation throughout the period (Wairoa Formation) with interspersed intervals of carbonate accumulation in early and late Opoitian and Waipipian times. A maximum thickness of c. 1500 m of Pliocene deposits has been identified in this study.

The period of highest siliciclastic sediment flux (max. 700-800 m) occurred during the Early Pliocene (early Opoitian, Wairoa Formation B), up until deposition of the Whakapunake Limestone in the late Opoitian (c. 1 myr). The calculated "rock" sedimentation rate is c. 0.7-0.8 m/ka, reasonably close to the 1 m/ka proposed by Kamp & Nelson (1987). The value could also be considered as an average rate of subsidence during that period given there is little change in facies type through Wairoa Formation B. The siliciclastic sedimentation rates were lowest during the accumulation of the three limestones.

In the absence of fauna capable of constructing wave-resistant structures, carbonate sediments in cool-water environments tend to be shed off the production site by high-energy waves and tidal currents, and form prograding dunes on the antiform flanks, which enable further accumulation of new carbonate sediments without the influence of tectonism. The typically low accumulation rate of cool-water carbonate (<0.1 m/ka) means the formation of carbonates can be quite sensitive to sea-level change (Caron *et al*. 2004a). During sea-level rise, carbonate accumulation will eventually cease as the result of the increase in water depth and influx of large amounts of siliciclastic materials.

Cool-water shelf carbonates typically accumulate at much slower rates than their tropical counterparts, ranging from 0.01-0.5 m/ka (Nelson *et al.* 1988b; Haywick *et al.* 1992; James 1997; Caron *et al.* 2004a). Nelson *et al.* (2003) established accumulation rates for some of the Te Aute limestones in the East Coast Basin, with values rangingvaries from 0.02-1 m/ka (Fig. 9.8).

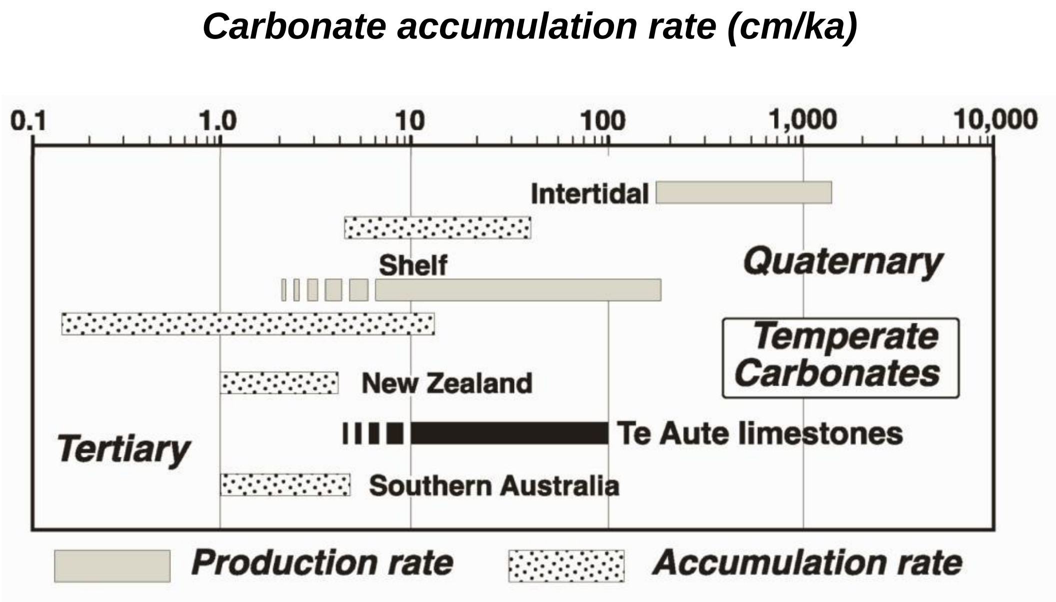

Figure 9.8: Estimates of production and accumulation rates for cool-water carbonates of different ages from various shelf depositional settings, including typical non-tropical occurrences from the mid Tertiary in New Zealand and southern Australia, in comparison to rates estimated for the Pliocene Te Aute limestones from Nelson *et al.* (2003), on the basis of their thickness and age.

9.8 Petrographic considerations

The general petrographic data for the Pliocene limestones in northern Hawke's Bay are summarised schematically in Figure 9.9. All three limestone facies (L1, L2 and L3) are typically coarse-grained calcarenites or calcirudites that classify petrographically using the Folk (1959) scheme as moderately to well sorted biosparites and biosparrudites, with less common biomicrites. The general petrographic characteristics are rather similar to their age equivalent limestones in central and southern Hawke's Bay, as summarised by Nelson *et al.* (2003).

The three limestones are also similar in their skeletal composition being dominated by bivalve material and barnacle plates, with locally important bryozoan and brachiopod fragments, and some echinoderm and benthic foraminiferal grains. A barnacle-rich skeletal makeup is uncommon amongst cool-water limestones in general, which are most typically dominated by the remains of bryozoans, echinoderms, molluscs, and foraminifera (Hayton *et al*. 1995; Nelson *et al.* 2003). Kamp *et al.* (1988) inferred that the abundant barnacle populations in the limestones likely resulted from very high nutrient levels associated with strong tidal flows between and over the antiform ridges in the ancient forearc seaway, with a hard substrate being provided by the large pectinids and oysters acting as the principal attachment sites.

9.8.1 Mineralogy

Typical cool-water carbonates are commonly calcitic deposits, with skeletons composed primarily of low-Mg calcite (<4 mol% $MgCO_3$) and intermediate-Mg calcite (4-12 mol% $MgCO_3$), and occasionally high-Mg calcite (Caron & Nelson 2009). Bulk XRD results (Appendix III) indicate that the primary mineralogy of the three Te Aute limestones near Wairoa is (now) exclusively low-Mg calcite, reflecting especially the preponderance of barnacle and epifaunal bivalve remains in the deposits. Any original aragonitic skeletons, such as infaunal bivalve remains, are either replaced by calcite or preserved as calcite-filled moulds. Nevertheless, trace amounts of aragonite were detected in at least one sample from each of the studied limestones, which supports the former presence of aragonitic shells in these limestones. Many photomicrographs reveal that the former aragonitic bivalve skeletons display a spectrum of alteration textures such as retention of ghost fabrics within former aragonitic shells to subequant sparite infilled biomoulds, and *in situ* detrital bioclastic micrite produced by the collapse of dissolved skeletons (Caron & Nelson 2009). Trace amounts of dolomite have been detected in two samples from both the Whakapunake and Opoiti limestones, an otherwise rare phenomenon in New Zealand Neogene rocks. Petrographic and XRD data reveal that the near stoichiometric (c. 45 mol% $MgCO_3$) dolomite occurs as scattered rhombs, 5-10 μm in size (Fig. 6.15).

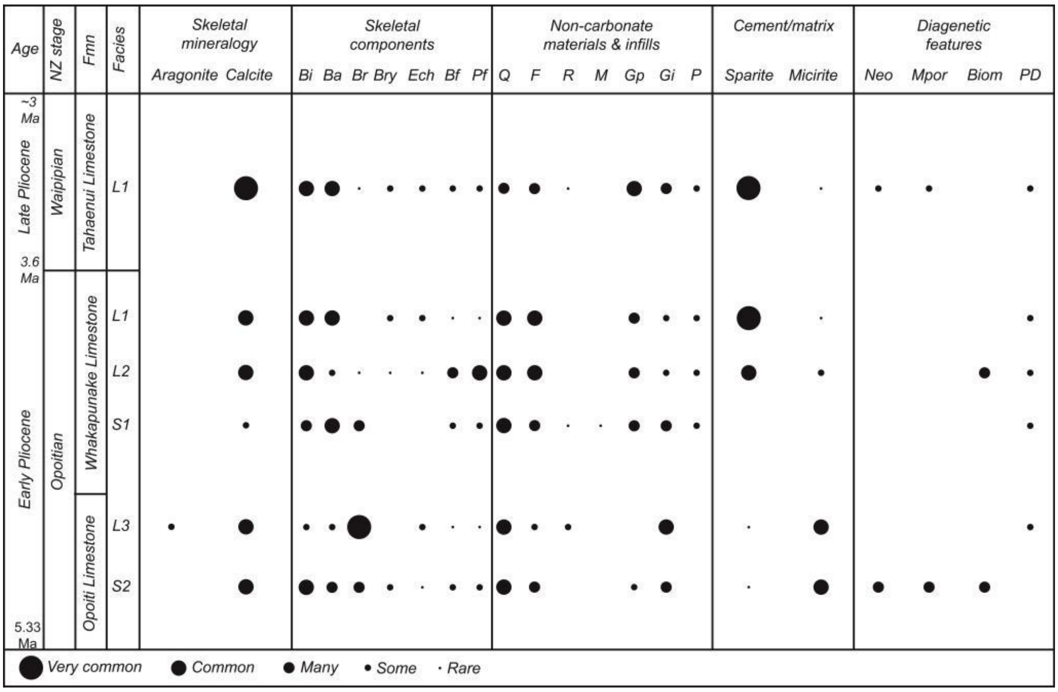

Figure 9.9: Petrographic summary sheet showing the relative importance of various petrographic properties for the three limestones and their facies. The raw petrographic data are available in Appendix V. Abbreviations: Bi=bivalve, Ba=barnacle, Br=brachiopod, Bry=bryozoan, Ech=echinoderm, Bf=benthic foram, Pf=planktic foram, Q=quartz, F=feldspar, R=rock fragment, M= other minerals, Gp=glauconite pellets, Gi=glauconite infill, P=pyrite, Neo=neomorphism, Mpor=mouldic porosity, Biom=biomould, PD=pressure-solution.

9.9 Diagenetic considerations

Despite their young age and generally similar depositional setting and lithofacies types, the degree of lithification of the three Pliocene limestones is highly variable, both areally and temporally. Strong differential cementation is a conspicuous feature of bedding in outcrops in the study area. Compared to older limestones in New Zealand, the Pliocene limestones are typically porous and variably cemented, which suggests only shallow to moderate burial depths. Petrographic study of the cements can provide some insights about the inferred diagenetic environments (Caron 2002).

9.9.1 Compaction

Compaction is often a mechanical process in younger deposits which have undergone less burial. In the case of the three Pliocene limestones, the carbonate sediments were buried under shallow to moderate depths (c. 200-550 m). An increasing pressure from overburden materials causes the skeletal grains to become lightly fractured. If the skeletal grains are not already cemented, grain fracture takes place and porosity is lowered by a closer packing (Tucker & Wright 1990). Then, the skeletal grains began to dissolve at points of contact to produce seams and concavo-convex contacts depending on the hardness of individual grains. Figure 9.10A and B show slightly fractured skeletons, mainly bivalve skeletal grains. There is also evidence of the skeletal grains being slightly pressure dissolved during burial (Fig. 9.10A & B). There is no cement formed within fractures, indicating they post-date the formation of cement materials, which occurred in the later stages of burial. However, there is no evidence for any chemical compaction having taken place in these young limestones.

9.9.2 Cementation

Cementation is a major diagenetic process and takes place when pore-fluids are supersaturated with respect to the cement phase and there are no kinetic factors inhibiting the precipitation. Carbonate cementation requires an enormous input of $CaCO_3$ and an efficient fluid flow mechanism for complete lithification. The source of $CaCO_3$ varies according to different diagenetic environments (Tucker &

Wright 1990). During and following the early stages of deposition, the carbonate sediments were in marine and shallow-burial condition. Small amounts of non-ferroan, fibrous to scalenohedral, and isopachous spar fringe cements were host-specifically precipitated about skeletal grains, which assisted with preservation of open interparticle textures. These spar cement types occur commonly within both Whakapunake and Tahaenui Limestones (Fig. 9.10C), and are possibly sourced from dissolution of aragonite skeletons into the pore fluids. In other cases, detrital, bioclastic micrites are identified, mainly in Opoiti Limestone (Fig. 9.10D). These micrites possibly filtered into pore spaces from the seafloor in a relatively low energy environment during the initial stages of deposition (Nelson *et al.* 2003).

9.9.3 Neomorphism

The term neomorphism was first introduced by Folk (1965), and refers to the processes of chemical replacement of the original minerals with a change in mineralogy (Tucker & Wright 1990). In the case of limestones, neomorphism commonly takes place in the presence of water through dissolution of aragonite, followed by reprecipitation as calcite. Most of the neomorphism in all three Pliocene limestones is of the aggrading type, which leads to a general increase in crystal size. The subequant sparite infilled biomoulds shown in some of the thin sections are clear evidence this process took place (Fig. 9.10E), and also suggests the presence of aragonite in the diagenetic environment.

9.9.4 Dissolution

The process of dissolution in carbonate rocks takes place on a small or large scale when pore-fluids are undersaturated with respect to the carbonate mineralogy (Tucker & Wright 1990). This process does not necessarily result in the reprecipitation or recrystallisation of calcite crystals. Individual skeletal grains may be completely dissolved out, especially of aragonitic mineralogy (e.g. infaunal bivalve skeletons), which is less stable than calcite. Unfilled mouldic porosities often form as a result of the aragonitic skeletal dissolution (9.10F). The presence of these moulds of former aragonitc skeletons indicate that the diagenetic pore fluids that flowed through the limestones were undesaturated with

$CaCO_3$. However, the solubility of calcite increases with increasing Mg^{2+} content; calcite with 12.5 mol% $MgCO_3$ has a similar solubility as aragonite (Walter 1985).

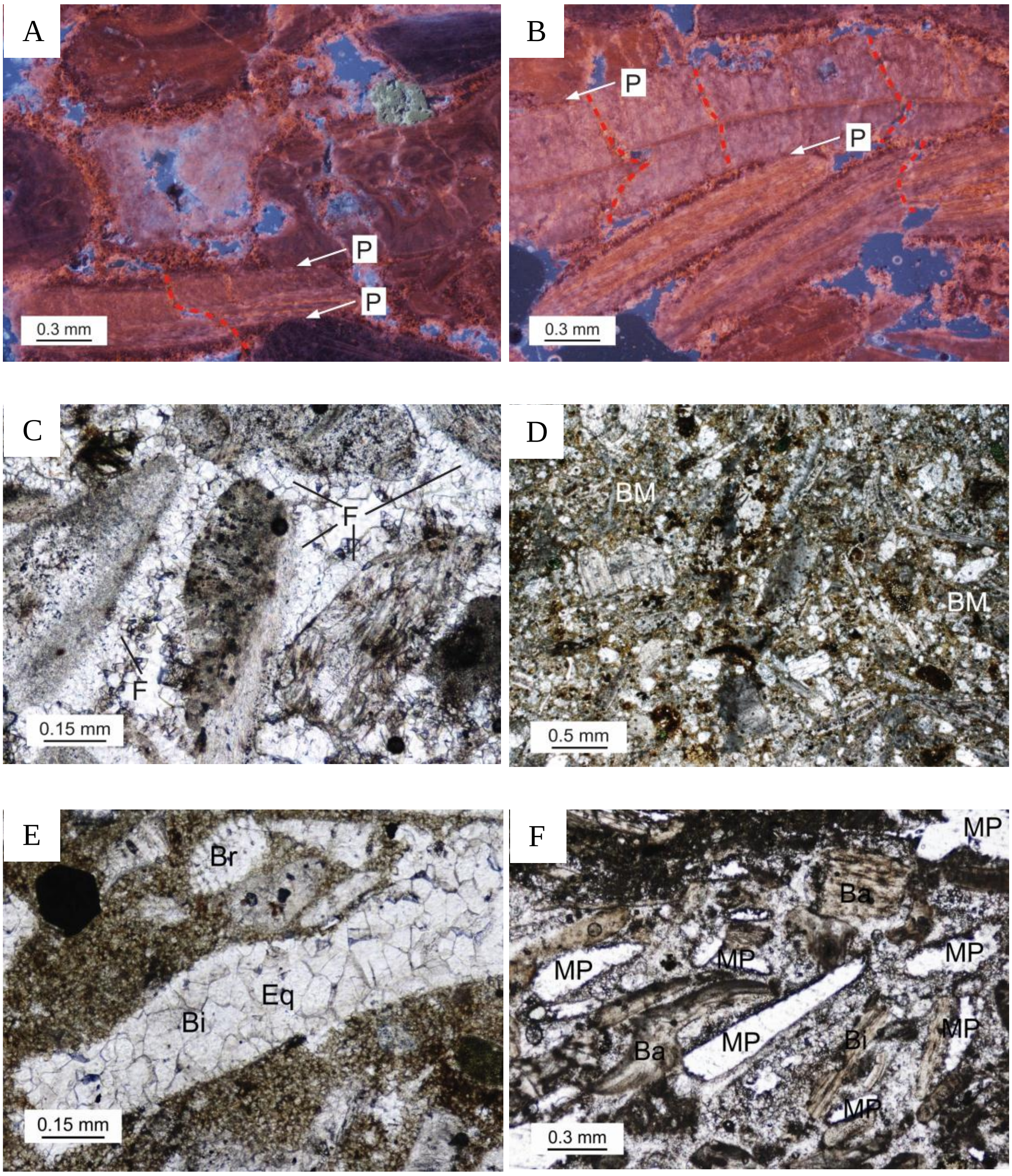

Figure 9.10: Photomicrographs under CL: A) & B) Coarse bivalve and barnacle-dominated biosparites showing signs of slight fractures (indicated by red dash) and pressure-solution (P) produced by physical compaction during burial. Photomicrographs under PPL: C) Biosparite showing typical scalenohedral and isopachous fringes (F) of early spar cements formed around bivalve skeletons during shallow-burial, which preserved interparticle pore space (c. 10%) in both Whakapunake and Tahaenui Limestones. D) Biomicrite showing detrital, bioclastic micrite (BM) cements, mainly formed in Opoiti Limestone. E) Biomicrite from Whakapunake Limestone showing presence of subequant sparite (Eq) infilled biomoulds, indicatingthe former presence of aragonite in the diagenetic environments. F) Biosparite showing unfilled mouldic porosities (MP) as a result of aragonitic skeletal dissolution.

9.9.5 Stable isotopes

Figure 9.11 shows a cross-plot of oxygen ($\delta^{18}O$) and carbon ($\delta^{13}C$) isotope values for the three Pliocene limestones in northern Hawke's Bay in relation to the core fields for New Zealand cool-water carbonates from Nelson & Smith (1996). The bulk $\delta^{18}O$ and $\delta^{13}C$ values for the Te Aute limestones from northern Hawke's Bay range widely from small positive to moderately negative values. The overall average results are near -0.2‰ for both stable isotopes (see Appendix IV). Published $\delta^{18}O$ and $\delta^{13}C$ isotope data from other studies of New Zealand Cenozoic carbonates (Nelson & Smith 1996) show that the influence of meteoric diagenesis can significantly lower $\delta^{13}C$ values, with a less well defined decrease in $\delta^{18}O$ values. In contrast, burial diagenesis produces large negative $\delta^{18}O$ values but relatively smaller changes to $\delta^{13}C$ values. The spread of data in Fig. 9.11 emphasises the wide range of diagenetic settings that have influenced the different limestones, including marine, shallow-burial, and meteoric realms.

Calculated absolute minimum burial temperatures for all three limestones in the study area ranges from 15-30°C, while the associated minimum burial depths range from 150 to over 700 m. The limestones have generally undergone slightly deeper burial than those to the east at Mahia analysed by Drinnan (2011). However, the bulk isotope values of typical skeletal dominated limestones are influenced by the isotope signatures of both the enclosed skeletons and cements. The strong meteoric influence of two of the Whakapunake Limestone samples is likely a result of cementation by coarse subequant sparite cement within the limestone.

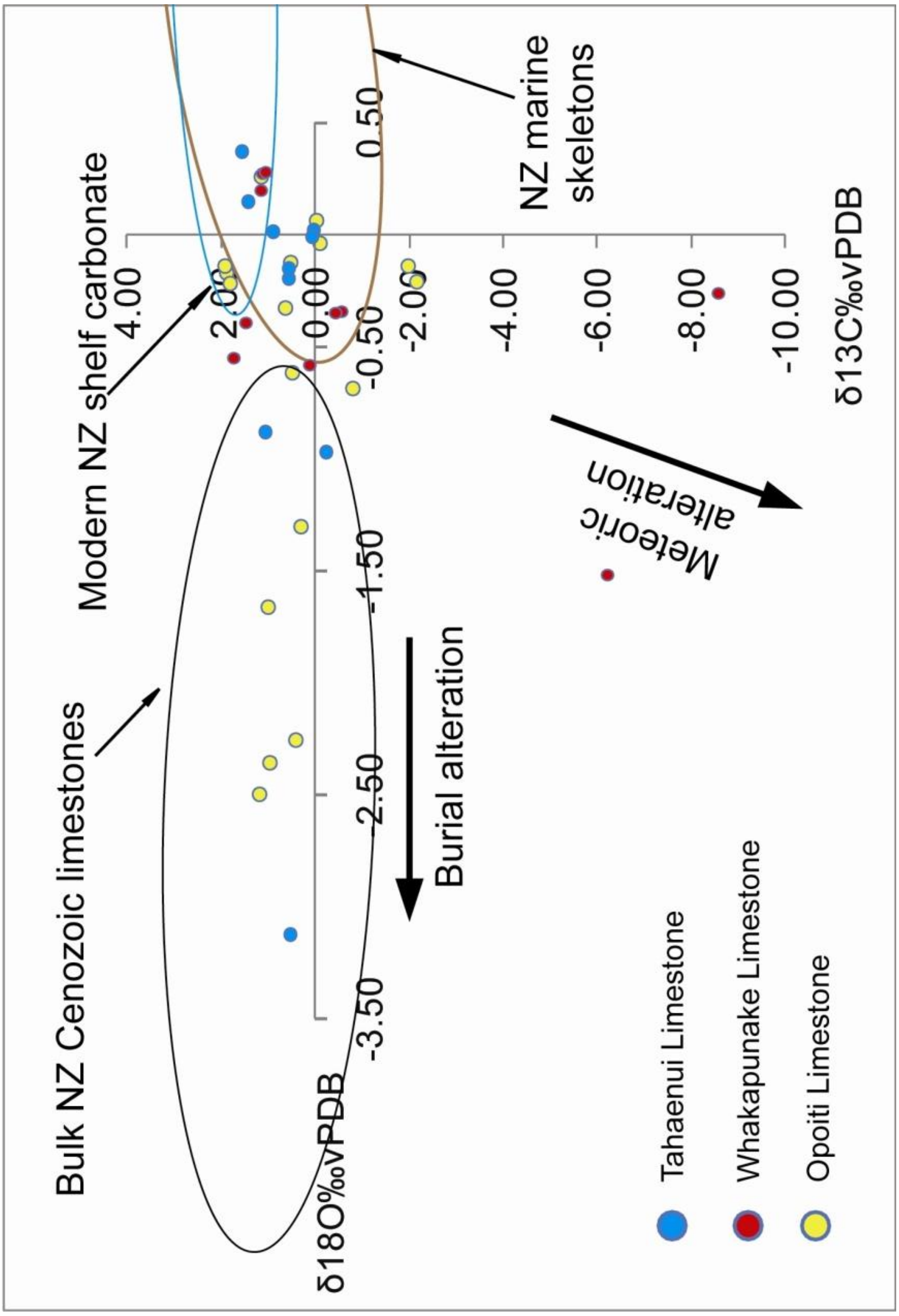

Figure 9.11: Summary cross-plot of oxygen and carbon isotope values for samples from all three Te Aute limestones, including Drinnan's (2011) data, in relation to the fields for New Zealand cool-water carbonates from Nelson & Smith (1996). Data in see Appendix IV.

9.10 Economic considerations

The Te Aute limestones have long been identified as potential hydrocarbon reservoir rocks in the East Coast Basin, especially considering the predominance of mudstones in the stratigraphy (Beu 1995). The limestones are also an important hard rock resource in the region, for aggregate, agricultural and industrial purposes.

9.10.1 Hydrocarbon potential

The three limestones were deposited in response to differential uplift along the eastern margin of an ancient forearc seaway, in shallow and tidal flow-dominated environments. The outcrops and subsurface seismic reflection profiles of the Neogene succession suggest that their depositional environments were associated with reverse fault thrusted antiforms and synforms (Harmsen 1985). Over 300 oil and gas seeps are known, and more than 40 wells have been drilled since the 1870s in the onshore East Coast region. These demonstrate that hydrocarbon sources and generation are widespread and that migration has been occurring and continue. These hydrocarbons may finally reside within some the Neogene limestones through the faults and folds that bound the forearc basin margin (Beu 1995; Crown Minerals 2003).

Source rocks and generation

The onshore oil and gas seeps indicate source rocks must exist and have entered the oil window. Funnell *et al.* (1999) evaluated the hydrocarbon generating potentials of both the onshore and offshore part of the Hawke's Bay area. The basin-wide Late Cretaceous to Paleogene marine shales of Waipawa and Whangai formations have both been identified as the primary hydrocarbon source rocks in the East Coast Basin, onshore and offshore (Field *et al.* 1997). The Waipawa Formation was determined to generate 104 bbl/acre-ft and the Whangai Formation was forecasted to generate 16 bbl/acre-ft using a best-fit linear geothermal gradient of 24°C/km and a surface temperature of 14°C (Frederick *et al*. 2000). While, the Whangai Formation (up to 500 m) is much thicker than Waipawa

Formation (20-30 m), and mostly organic-poor, only the upper calcareous member exhibits the potential of being a hydrocarbon source rock. Thus the upper member of the Whangai Formation and the Waipawa Formation (black shales) are the most likely source rocks within East Coast Basin (Field *et al.* 1997). However, neither of these two source rocks was identified within the exploration drill holes in the vicinity of the present study area, but the Waipawa Formation is recorded on the eastern side of Mahia Peninsula (Drinnan 2011).

Reservoir rocks

A drilling campaign by Westech in the 1990s discovered a sub-commercial high-pressure gas field at Kauhauroa-1 (Fig. 9.12). The well was the first in a seven well programme drilled to test a series of structural traps with potential Miocene and Pliocene reservoirs in the Wairoa district (PR 2346 1998). It was drilled through the top of the Kauhauroa Anticline, and detected significant gas shows within Miocene sandstones (Makareao and Rere sandstones) and fractured bioclastic limestone (Kauhauroa Limestone). Previous workers speculated on the reservoir potential of the Pliocene limestones in the Wairoa Syncline, with permeabilities ranging into darcies (Francis 1993; Beu 1995). In several drill holes (Awatere-1 and Kauhauroa holes), the Tahaenui Limestone is thickly developed across structural highs with apparent amplitutde pinchout down-dip. However, drilling showed the limestone is strongly cemented with no visible porosity indicating that the diagenetic environment was moderate (600-700 m) (Frederick *et al.* 2000). Limestone outcrops on the margin of the syncline may not have been buried to such depth, or may have been modified by meteoric diagenesis (Frederick *et al.* 2000).

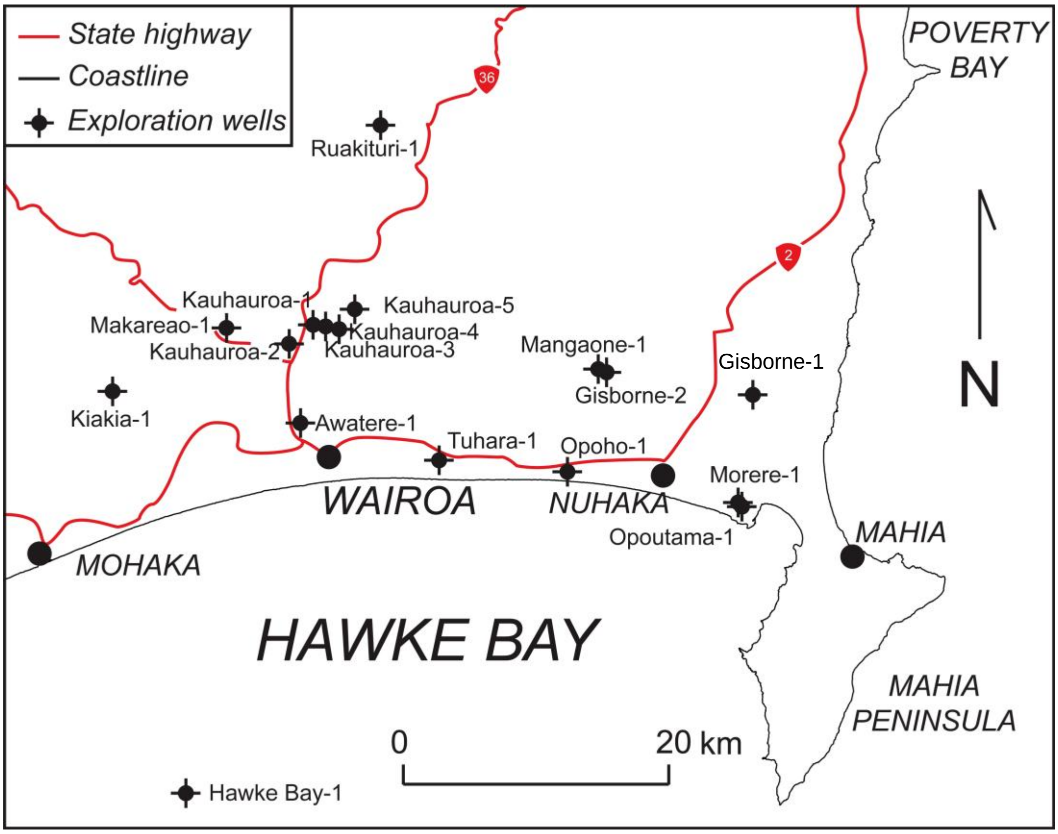

Figure 9.12: Petroleum exploration wells drilled both onshore and offshore in the northern Hawke Bay area.

9.10.2 Other economic possibilities

The most common use of the Te Aute limestones locally is as agricultural lime and roading aggregate, including especially in the northern Hawke's Bay region. A lack of hard rock resources in the wider East Coast region makes the limestones a prime target for commercial extraction (Moore & Hatton 1985; Mazengarb & Speden 2000). To the east of the present study area, the Tahaenui and Clonkeen quarries in the Nuhaka Syncline (Fig. 10.3A, B, C & D in Drinnan 2011) are currently operating in the Tahaenui Limestone to support the local needs for roading aggregate.

10 Chapter Ten

Summary and conclusions

10.1 Lithostratigraphy

The newly defined Pliocene Mangaheia Group (Opoitian-Waipipian) cropping out in northern Hawke's Bay is c. 2.5 km thick. It is the youngest fill of the forearc basin in this region. This succession comprises mainly siliciclastic sandstone and mudstone lithologies, but includes three distinctive barnacle and bivalve-dominated limestone deposits, namely the Opoiti (early Opoitian), Whakapunake (late Opoitian) and Tahaenui (Waipipian) Limestones. The limestones are prominent in outcrop and are treated as formations in this study. The Opoiti and Tahaenui Limestones crop out on both limbs of the Wairoa Syncline, while the Whakapunake Limestone is exposed only on the eastern limb of the Syncline. They are highly variable in both thickness (c. 5-50 m) and $CaCO_3$ content (c. 15-85%). Naming of the siliciclastic-dominated deposits in the Mangaheia Group has been inconsistent in the past, including assignment to the Mapiri Formation, Opoiti Formation, Mangapoike Formation and/or Wairoa Formation, despite their overall lithologically similarity. In this study, the name Wairoa Formation is used for all of the Pliocene siliciclastic-dominated deposits of the Mangaheia Group in northern Hawke's Bay.

The Wairoa Formation is subdivided into four informal units (Wairoa Formation A, B, C and D) according to their relative positions above or below the three limestones. Wairoa Formation A is a 2-220 m thick, earliest Opoitian unit that overlies a regional unconformity between the Miocene and Pliocene strata, and is unconformably overlain by Opoiti Limestone. The Opoiti Limestone is the olderst carbonate-rich unit in the study area. It crops out on both limbs of the Wairoa Syncline and dips towards the syncline axis at c. 30°. Despite its limestone name, it has a $CaCO_3$ content ranging from 30-70% and varies from a fossiliferous sandstone to a brachiopod (*Neothyris*)-rich sandy limestone that contains the Opoitian age diagnostic pectinid *Towaipecten ongleyi*. Outcrop thicknesses vary from about 5-12 m across the study area. The Opoiti Limestone passes gradationally above into Wairoa Formation B (Opoitian) that is 700-800 m thick and comprises massive to differentially cemented mudstone facies with local tuffaceous material and horizons. The thick (up to 150 m) late Opoitian Whakapunake Limestone unconformably overlies Wairoa Formation B. It contains the Opoitian age diagnostic pectinids *Phialopecten marwicki* (up to 10 cm across) and *Mesopeplum crawfordi*. The distribution of Whakapunake Limestone is restricted to the eastern limb of the Wairoa Syncline. It forms impressive limestone bluffs around the Whakapunake Plateau, and dips at c. 20° W. In outcrop, this limestone shows strong differential cementation. It comprises interbeds of indurated, relatively pure limestone ($CaCO_3$ 70-85%) and massive calcareous sandstone ($CaCO_3$ 15-50%), evident from their slightly protruding and recessive nature respectively. The Whakapunake Limestone conformably passes up into massive calcareous mudstone of Wairoa Formation C (latest Opoitian). Wairoa Formation C has very limited exposure in the study area, being restricted to the Rapid's section c. 4 km south of Haupatanga Gorge. Tahaenui Limestone (Waipipian) overlies a sharp unconformity that marks the boundary between the Opoitian (Early Pliocene) and Waipipian (Late Pliocene) stages. This unconformity removed c. 300,000 yrs of rock record at the end of the Opoitian (Edwards 1987) so that preservation of Wairoa Formation C in limited in outcrop. Tahaenui Limestone is the youngest Pliocene carbonate unit in the study area. It is a barnacle-dominated and pectinid-rich (*Phialopecten marwicki*) limestone, locally glauconite-bearing. The thickness of the Tahaenui limestone varies from c. 10 m to over 30 m, and is typically massive to poorly bedded and sometimes flaggy. Its $CaCO_3$ content ranges from 60-80%. The limestone forms a large part of the top surface of the Whakapunake dipslope, from as far north as the Whakapunake Trig south to the outcrops above the Makaretu Stream on the eastern limb of the Wairoa Syncline. The same limestone is exposed along the hills on the southern side of the Ruakituri River on the western limb of the Syncline.

10.2 Lithofacies

A simplified facies classification for the Pliocene deposits in the northern Hawke's Bay region has been developed in combination with the study by

Drinnan (2011). Three distinct lithofacies groups (limestone, sandstone and mudstone) have been identified and described in the course of this study. The three groups invovle 9 different lithofacies types as shown in Table 4.1, each having distinctive field characteristics that likely reflect their particular depositional environment. The three limestone facies (L1, L2 and L3) occur in the carbonate formations and were deposited in a tidal current-swept shelfal-depth setting. The sandstone (S1, S2 and S3) and mudstone facies (M1, M2 and M3) encompass all the siliciclastic-dominated deposits of shallow to deepest shelf origin.

Opoiti Limestone is dominated by bioclastic sandstone lithofacies S2 and local sandy limestone facies L3. The differentially cemented nature of the Whakapunake Limestone involves alternations of massive barnacle and pectinid-dominated limestone (L1), well cemented limestone (L2) and highly calcareous sandstone (S1). Tahaenui Limestone hosts exclusively bioclast-dominated limestone facies (L1) throughout the study area.

10.3 Petrography

The Opoiti Limestone (lithofacies S2 and L3) ranges from being a bioclastic quartzofeldspathic arenite to a limonitised, brachiopod-dominated biosparrudite to poorly sorted, unabraded barnacle and bivalve biosparrudite. It is overall siliciclastic sand-dominated, with a skeletal component of barnacles, calcitic (epifaunal) bivalves and, locally, brachiopods. The limestone is well cemented by low-Mg calcite microsparite or micrite (c. 15%), is locally dolomite-bearing, and can include clear subequant calcite sparite infills of former infaunal aragonitic bivalve skeletons. The overall bioclast content of the Opoiti Limestone varies from about 30-50%, and the siliciclastic content from 20-50%. The S2 facies comprises a subequal mix of siliciclastic (35%) and skeletal (33%) materials. The L3 facies is bioclast-dominated (47%) and siliciclast-rich (21%). Authigenic minerals are common (16%) in S2 facies, slightly less so (12%) in facies L3. The CL signature of the skeletal components ranges from dark purple (former aragonite-infaunal bivalves) to dull orange (calcitic skeletal materials such as barnacles and epifaunal bivalves)

Whakapunake Limestone ranges from packed, dolomite-bearing biomicrite to well rounded, bivalve-barnacle fine biosparrudite. The limestone is skeletal grain-dominated and locally dolomite-bearing, with quartzofeldspathic arenite interbeds, cemented by low-Mg calcite (micro)sparite and/or micrite. Subequant sparite infills and biomoulds of former infaunal aragonitic bivalve skeletons are common. The skeletal content of the limestone varies from 30-60%, and the siliciclastic material ranges from 5-30%. The Whakapunake Limestone in the study area exhibits facies types L1, L2 and S1. L1 is a porous (13%) and sparry (20%), bioclast (55%)-dominated facies. Siliciclastic (7%) and authigenic (5%) materials are less common. The cement is mostly microsparite and/or sparite. Facies L2 contains fewer bioclasts (40%) than L1, but a slight increase in the amount of cement materials (30%) and siliciclastic (15%) and authigenic (10%) grains. Facies S1 is dominated by siliciclastic (28%) and authigenic (20%) materials, with only 30% bioclasts and 20% cement. The CL signature of skeletal components ranges from dark purple (formerly aragonitic bivalves) to dull orange (calcitic skeletal materials such as barnacles and epifaunal bivalves), with authigenic materials being non-luminescent. Cement types show colours ranging from purple/dull orange (isopachous fringe cement) to orange (subequant sparite) to bright yellow (dolomite, which often includes zoned well-defined rhombohedral cores). Zonation within the dolomite rhombs reflects growth stages due to chemical changes in the diagenetic fluids.

Petrographically, the Tahaenui Limestone ranges from moderately to well sorted, well abraded, porous bivalve and barnacle biosparite to fine biosparrudite. It is made up of mainly rounded barnacle and calcitic (epifaunal) bivalve skeletal grains that are well cemented by low-Mg calcite microsparite and granular subequant sparite. Tahaenui Limestone has higher $CaCO_3$ contents (up to 80%) compared to the two older (Opoitian) limestone formations. It comprises only facies type L1, which is a bioclast-dominated limestone. The overall skeletal content of the Tahaenui Limestone ranges from about 40-65%, with c. 30% of mainly clean spar cement and variable amounts of siliciclastic material (1-20%). It also has c. 10% porosity represented by open interparticle pore space and locally secondary moulds. The CL colour of the skeletal components ranges from dark purple (former aragonite-infaunal bivalves) to dull orange (calcitic barnacles and epifaunal bivalves). The isopachous/fringe cements show colours ranging from purple (immediately surrounding skeletal grains) to dull orange (further outwards from the margin of the skeletal grains), and with a thin bright yellow edging on the subequant sparite.

10.4 Depositional environments

The three Pliocene limestones in the northern Hawke's Bay region, part of the widespread Pliocene Te Aute limestone facies throughout the East Coast Basin of North Island, formed in a tectonically active subduction margin setting (Nelson *et al.* 2003). The complex stratigraphic architecture of these limestone deposits is a result of the active tectonism that produced many NE-SW trending upthrust imbricate ridges along the eastern margin of the Pliocene forearc basin seaway (Ruataniwha Strait).

The depositional environments for the three Pliocene limestones in northern Hwake's Bay was broadly similar, involving moderate to high energy, current-swept, shallow-marine settings (Kamp *et al.* 1988). The development of the forearc basin seaway during the Late Miocene and Pliocene produced imbricate ridges of small upthrust anticlines and bordering synclines, and resulted in inversion of slope basins and uplift on the eastern margin of the seaway that promoted deposition of carbonate sediments (Caron *et al.* 2004a). Various scales of horizontal and cross-bedded sedimentary structures in these limestone are indicative of strong tidal current flows and directions. The coarse-grained barnacle and bivalve-dominated nature of the Whakapunake and Tahaenui Limestones in particular suggests that similar depositional conditions were repeated in time and space in the study area.

Carbonate factories formed atop the narrow fault-bounded structural highs on the eastern margin of the Wairoa Syncline (Kamp *et al.* 1988). The time of carbonate accumulation atop the antiforms was usually short lived as a result of progressive thrusting and uplifting along different parts of the margin. This caused carbonate sediments to be shed from the tops of antiforms, and redeposited nearby on the flanks of adjacent subbasins. The rather complex distribution and geometry of these limestones in outcrop are a consequence of this kind of volatile depositonal setting.

Cross-bedded sedimentary structures within the Whakapunake and Tahaenui Limestones suggest the strong influence of high-energy hydraulic conditions which suspended and by-passed fine-grained siliciclastic sediments from “highs” and assisted nutrient renewal in the seaway. These factors promoted the production of the barnacle and bivalve-dominated cool-water carbonates (Caron *et al.* 2004a).

The rhythmic carbonate-siliciclastic nature of the Whakapunake Limestone possibly reflects cyclic storm emplacements or the repetitive rise and fall of sea-level (Drinnan 2011). The flaggy nature of the Tahaenui Limestone is possibly due to similar depositonal conditions.

The variabilities of cementation and porosity are high in the three Pliocene limestones compared to some older limestones in New Zealand, which suggests only shallow to moderate burial depths. $\delta^{18}O$ values can be used to infer that these burial depths were in the order of perhaps 200-700 m. Processes of fracturing and pressure dissolving of bivalve skeletons post-date the formation of cement materials, which suggests these features occurred in the later stages of burial. The sparite cement occurs commonly within both Whakapunake and Tahaenui Limestones, and have been sourced from dissolution of aragonite skeletons into the pore fluids. Detrital or bioclastic micrites are present mainly in Opoiti Limestone. These micrites are likely derived from slow seafloor deposition in a relatively low energy environment (Nelson *et al.* 2003). The occurrence of subequant sparite infilled biomoulds suggests the presence of aragonite in the diagenetic environment. The presence of these moulds of former aragonitc skeletons indicates that the diagenetic pore fluids that flowed through the limestones were undersaturated with respect to aragonitic carbonate.

10.5 Economic potential

The Pliocene limestones are important reservoir targets in the East Coast Basin. The three barnacle-rich limestones within the siliciclastic-rich Mangaheia Group display high amplitude reflections in many seismic profiles from the study area (Harmsen 1989). The depositional environment of the three Pliocene limestones was associated with reverse fault thrusted antiforms and synforms (Harmsen 1985). Many petroleum exploration wells have been drilled in the study area, and demonstrate that hydrocarbon sources and generation are widespread and that migration has been occurring and continues. The forearc basin margin limestones afford potential reservoirs due to their high porosities, and have hydrocarbon prospectivity in the immediate area of Hawke's Bay (Beu 1995; Crown Minerals 2003). The limestones are also viable hard rock resources in the northern Hawke's Bay region. The primary use of Tahaenui Limestone in the northern Hawke's Bay region is for aggregate.

References

Alexandersson, E. T. 1978, 'Destructive diagenesis of carbonate sediments in the eastern Skagerrak, North Sea ', Geology, vol. 6, pp. 324-327.

Alexandersson, E. T. 1979, 'Marine maceration of skeletal carbonates in the Skagerrak, North Sea', *Sedimentology*, vol. 26, pp. 845-852.

Baggs, R. A. 2004, Sedimentary geology of the cyclothemic Petane Group deposits, Matapori - Omaha region, central Hawke's Bay, Thesis, University of Waikato.

Ballance, P. F. 1993, 'The New Zealand Neogene Forearc Basins', in P. F. Ballance (ed.), *Sedimentary Basins of the World*, Elsevier, Amsterdam.

Barker, D. H. N., Sutherland, R., Henrys, S. & Bannister, S. 2009, 'Geometry of the Hikurangi subduction thrust and upper plate, North Island, New Zealand', *Geochem. Geophys. Geosyst.*, vol. 10.

Barnes, P. M. & Audru, J. C. 1999, 'Quaternary faulting in the offshore Flaxbourne and southern Wairarapa basins, southern Cook Strait, New Zealand', *New Zealand Journal of Geology & Geophysics*, vol. 42, pp. 349–367.

Barnes, P. M. & Mercier de Lépinay, B. 1997, 'Rates and mechanics of rapid frontal accretion along the very obliquely convergent southern Hikurangi margin, New Zealand', *Journal of Geophysical Research*, vol. 102, pp. 24931–24952.

Barnes, P. M. & Nicol, A. 2004, 'Formation of an active thrust triangle zone associated with structural inversion in a subduction setting, eastern New Zealand', *Tectonics*, vol. 23, pp. 1-25.

Barnes, P. M., Mercier de Lépinay, B., Collot, J. Y., Delteil, L. & Audru, J. C. 1998, 'Strain partitioning in the transition area between oblique subduction and continental collision, Hikurangi margin, New Zealand', *Tectonics*, vol. 17, pp. 534–557.

Beanland, S. 1995, The North Island Dextral Fault Belt, Hikurangi Subduction Margin, New Zealand, Unpublished PhD thesis, Victoria University of Wellington, Wellington, New Zealand.

Beu, A. G. 1995, *Pliocene limestones and their scallops: lithostratigraphy, pectinid biostratigraphy and paleogeography of eastern north island late Neogene limestone, Institute of Geological and Nuclear Sciences Monograph 10: 1-243.*

Beu, A. G., Grant-Taylor, T. L. & Hornibrook, N. d. B. 1980, *The Te Aute limestone facies: Poverty Bay to Northern Wairarapa. 1:250 000.*, New Zealand Department of Scientific and Industrial Research, Wellington.

Bhattarcharya, J. P. 1993, *The expression and interpretation of marine flooding surface and erosional surfaces in core; examples from the upper Cretaceous Dunvegan Formation, Alberta Foreland basin, Canada*, Balckwell.

Bland, K. J. 2001, Analysis of the Pliocene forearc basin succession Esk River catchment, Hawke's Bay, Unpublished Thesis, University of Waikato.

Bland, K. J., Kamp, P. J. J. & Nelson, C. S. 2004b, 'Stratigraphy and development of the Late Miocene-Early Pleistocene Hawke's Bay forearc basin', *New Zealand Petroleum Conference*, Auckland, pp. 13.

Bland, K. J., Kamp, P. J. J. & Nelson, C. S. 2007, *Systematic lithostratigraphy of the Neogene succession exposed in central parts of Hawke's Bay Basin, eastern North Island, New Zealand, PR3724*, Unpublished Petroleum Report 3724.

Bland, K. J., Kamp, P. J. J., Pallentin, A., Graafhuis, R., Nelson, C. S. & Caron, V. 2004a, 'The early Pliocene Titiokura Formation: stratigraphy of a thick, mixed carbonate-siliciclastic shelf succession in Hawke's Bay Basin, New Zealand', *New Zealand Journal of Geology & Geophysics*, vol. 47, pp. 675-695.

Bland, K. J., Kamp. P. J. J., Nelson, C. S. 2008, 'Late Miocene - Early Pleistocene paleogeography of the onshore central Hawke's Bay sector of the forearc basin, eastern North Island, New Zealand, and some implications for hydrocarbon prospectivity', *New Zealand Petroleum Conference,* Auckland, pp 1-21.

Boggs, S. 2004, *Principals of sedimentology and stratigraphy*, Pearson Prentice Hall, New Jersey.

Boyle, S. F. 1987, Stratigraphy and sedimentology of Scinde Island Formation, Napier: mixed terrigenous-carbonate shelf facies in a late Pliocene forearc basin, Unpublished Thesis, University of Waikato.

Briggs, R. M., Houghton, B. F., McWilliams, M. & Wilson, C. J. N. 2005, '40Ar/39Ar ages of silicic volcanic rocks in the Tauranga-Kaimai area, New Zealand: Dating the transition between volcanism in the Coromandel Arc and Taupo Volcanic Zone', *New Zealand Journal of Geology & Geophysics*, vol. 48, no. 3, pp. 459-469.

Buckeridge, J. S. 1983, 'Fossil barnacles (Cirripedia: Thoracica) of New Zealand and Australia', *New Zealand Geological Survey, Paleontological Bulletin*, vol. 50, pp. 151.

Campbell, K. A., Francis, D. A., Collins, M., Gregory, M. R., Nelson, C. S., Greinert, J. & Aharon, P. 2008, 'Hydrocarbon seep-carbonates of a Miocene forearc (East Coast Basin), North Island, New Zealand', *Sedimentary Geology*, vol. 204, no. 3-4, pp. 83-105.

Caron, V. 2002, Petrogenesis of Pliocene limestones in southern Hawke's Bay, New Zealand: a contribution to unravelling the sequence stratigraphy and diagenetic pathways of cool-water shelf carbonte faceis, Unpublished Thesis, University of Waikato.

Caron, V. & Nelson, C. S. 2009, 'Diversity of neomorphic fabrics in New Zealand Plio-Pleistocene cool-water limestones: insights into aragonite alteration pathways and controls', *Journal of Sedimentary Research*, vol. 79, pp. 226-246.

Caron, V., Nelson, C. S. & Kamp, P. J. J. 2004, 'Contrasting carbonate depositional systems for Pliocene cool-water limestones cropping out in central Hawke's Bay, New zealand', *New Zealand Journal of Geology & Geophysics*, vol. 47, pp. 697-717.

Cater, R. M. & Naish, T. R. 1998, 'A review of Wanganui Basin, New Zealand: global reference section for shallow marine, Plio–Pleistocene (2.5–0 Ma) cyclostratigraphy', *Sedimentary Geology*, vol. 122, pp. 37–52.

Chave, K. E. 1967, 'Recent carbonate sediments: an unconventional view', *Geological Education*, vol. 15, pp. 200-204.

Cole, J. W. & Lewis, K. B. 1981, 'Evolution of the Taupo-Hikurangi subduction system', *Tectonophysics*, vol. 72, pp. 1-21.

Collot, J.-Y., Lewis, K. B., Lamarche, G. & Lallemand, S. E. 2001, 'The giant Ruatoria debris avalanche on the northern Hikurangi margin, New Zealand; results of oblique seamount subduction', *J. Geophys. Res*, vol. 106, pp. 19271–19297.

Collot, J. Y., Delteil, L., Lewis, K. B., Davy, B. W., Lamarche, G., Audru, J. C., Barnes, P. M., Chanier, F., Chaumillon, E., Lallemand, S. E., Mercier de Lépinay, B., Orpin, A. R., Pelletier, B., Sosson, M., Toussaint, B. & Uruski, C. I. 1996, 'From oblique subduction to intra-continental transpression: structures of the southern Kermadec–Hikurangi margin from multibeam bathymetry, side-scan sonar and seismic reflection', *Mar. Geophys. Res.*, vol. 18, pp. 357–381.

Cooke, P. J., Nelson, C. S. & Crundwell, M. P. 2008, 'Miocene isotope zones, paleotemperatures, and carbon maxima events at intermediate water-depth, site 593, Southwest Pacific', *new Zealand Journal of Geology & Geophysics*, vol. 51, pp. 1-22.

Crampton, A. T., Gregg, R. C. & Kilops, V. 1993, in (ed.), *An introduction to the petroleum geology of New Zealand*, Minstry of Commerce, Wellington.

Crown Minerals 2003, *Explore New Zealand Petroleum*, ministry of Econimic Development, Wellington.

Davey, F. J., Hampton, M., Childs, J., Fisher, M. A., Lewis, K. B. & Pettinga, J. R. 1986, 'Structure of a growing accretionary prism, Hikurangi margin, New Zealand', *Geology*, vol. 14, pp. 663–666.

Dorsey, R. J. & Umhoefer, P. J. 2000, 'Tectonic and eustatic controls on sequence stratigraphy of the Pliocene Loreto basin, Baja California Sur, Mexico', *Geological Society of America Bulletin*, vol. 112, pp. 177-199.

Drinnan, M. M. 2011, Stratigraphy and sedimentology of Pliocene limestones in northern Hawke's Bay: the Opoiti, Whakapunake and Tahaenui Limestones, Unpublished Thesis, University of Waikato.

Dyer, S. D. J. 2005, Sedimentary geology of the cyclothemic depostis in the Mason Ridge - Maraekakaho region, central Hawke's Bay, Thesis, University of Waikato.

Edwards, A. R. 1987, *An integrated biostratigraphy, magnetostratigraphy and oxygen isotope stratigraphy for the late Neogene of New Zealand*, DSIR, Lower Hutt.

Embry, A. F. 1995, *Sequence boiundaries and sequence hierarchies: problems and proposals*, Stavanger, Elsevier, Amsterdam.

Emery, D. & Myers, K. J. (ed) 1996, *Sequence Stratigraphy*, Blackwell Science, London.

Field, B. D., Uruski, C. I. & Others, A. 1997, in (ed.), *Cretaceous - Cenozoic Geology and Petroleum Systems of the East Coast Region, New Zealand*, Institute of Geological & Nuclear Sciences Limited, Lower Hutt, pp. 301.

Folk, R. L. 1959, Practical petrographic classification of limestones, *American Association of Petroleum Geologists Bulletin*, vol. 43, pp. 1-38.

Francis, D. A. 1993, *Report on the geology of the Mangaone-Opoutama area Northern Hawke's Bay adjacent to offshore PPL38321*, Ministry of Economic Development New Zealand Unpublished Petroleum Report 1927.

Frederick, J. B., Smith, P. G., Leask, W. L., Spancers, D. & Williams, T. J. 2000, 'East Coast offshore exploration', New Zealand Petroleum Conference Proceedings, pp. 19-22.

Gamble, J. A. & Wright, I. C. (ed) 1995, *The Southern Havre Trough: geological structure and magma petrogenesis of an active backarc rift complex. Backarc Basins*, Plenum Press, New York.

Goldsmith, J. R., Graf, D. L. & Heard, H. C. 1961, 'Lattice constants of the calcium-magnesium carbonates', *American Mineralogist*, vol. 46, pp. 453-457.

Harmsen, F. J. 1984, Stratigraphy, depositional history, and diagenesis of the Te Aute Group, a Pliocene temperate carbonate-bearing sequence in southern Hawke's Bay, New Zealand, Unpublished Thesis, Victoria University.

Harmsen, F. J. 1985, 'Lithostratigraphy of Pliocene strata, Central and Southern Hawke's Bay, New Zealand', *New Zealand Journal of Geology & Geophysics*, no. 28, pp. 413-433.

Harmsen, F. J. 1989, Te Aute Group Limestones: a potential reservoir rock in the East Coast Basin, *In*: 1989 New Zealand Oil Exploration Conference Proceedings. Wellington, Petroleum and Geothermal Unit, Ministry of Commerce. pp. 181–190

Haw, D. 1958, *Compilation report on the Kauhauroa Structure*, Ministry of Economic Development New Zealand Unpublished Petroleum Report 309.

Hayton, S., Nelson, C. S. & Hood, S. D. 1995, 'A skeletal assemblage classification system for non-tropical carbonate deposits based on New Zealand Cenozoic limestones', *Sedimentary Geology*, vol. 100, no. 1-4, pp. 123-141.

Haywick, D. W. 1992, 'Sedimentology of 40 OOO year Milankovitch-controlled cyclothems from central Hawke’s Bay, New Zealand', *Sedimentology*, no. 39, pp. 675-696.

Haywick, D. W. (ed) 2000, *Recognition and distinction of normal and forced regression in cyclothemic strata: a Plio-Pleistocene case study from eastern North Island, New Zealand., Geological Society of London Special Publication*, vol. 172, pp. 193–215.

Healy, J. (ed) 1992, *Central Volcanic Region*, Longman Paul.

Hector, J. 1887, Progress report, Geological Survey of New Zealand, *Reports of geological explorations during 1874-76*, vol. 9.

Hedberg, H. D. (ed) 1976, *A guide to stratigraphic classification, terminology and procedure*, John Wiley and Sons, New York.

Henrys, S., Reyners, M., Pecher, I., Bannister, S., Nishimura, Y. & Maslen, G. 2006, 'Kinking of the subducting slab by escalator normal faulting beneath the North Island of New Zealand', *Geology*, vol. 34, pp. 777–780.

Holt, W. E. & Haines, A. J. 1995, 'The kinematics of northern South Island, New Zealand, determined from geological strain rates', *Journal of Geophysical Research*, vol. 100, pp. 17991–18010.

Hood, S. D. 1993, Skeletal and diagenetic petrofacies of temperate-latitude Limestones, North Island, New Zealand, Unpublished Thesis, University of Waikato.

Hornibrook, N. d. 1984, '*Globorotalia* (planktic foraminifera) at the Miocene/Pliocene boundary in New Zealand.', *Palaeogeogr., Palaeoclimatol., Palaeoecol.*, vol. 46, pp. 107-117.

James, N. P. 1997: *The cool-water carbonate depositional realm*. In: James, N. P., Clarke, J. A. D. (ed) *Cool-water carbonates*, *SEPM Special Publication* 56: 1–20.

Kamp, P. J. J. 1986, 'The mid-Cenozoic Challenger Rift System of western New Zealand and its implications for the age of Alpine fault inception', *Geological Society of America Bulletin*, vol. 97, pp. 255–281.

Kamp, P. J. J. 1988, 'Tectonic geomorphology of the hikurangi Margin: surface manifestations of different models of subduction', *Zeitschrift fur Geomorphologie N.F. Suppl. -Bd*, vol. 69, pp. 55-67.

Kamp, P. J. J. 1992, 'Tectonic Architecture of New Zealand', in J. M. Soons & M. J. Selby (ed.), *Landforms of New Zealand*, Longman Paul Limited, Auckland, pp. 1-30.

Kamp, P. J. J., Harmsen, F. J., Nelson, C. S. & Boyle, S. F. 1988, 'Barnacle-dominated limestone with giant cross-beds in a non-tropical, tide-swept, Pliocene forearc seaway, Hawke's Bay, New Zealand', *Sedimentary Geology*, vol. 60, no. 1-4, pp. 173-195.

Kamp, P. J. J. & Nelson, C. S. 1987, 'Tectonic and sea-level controls on nontropical Neogene limestones in New Zealand', *Geology*, vol. 15, pp. 610-613.

Kamp, P. J. J. & Nelson, C. S. 1988, 'Nature and occurrence of modern and Neogene active margin limestones in New Zealand.', *New Zealand Journal of Geology and Geophysics*, vol. 31, pp. 1-20.

Kamp, P. J. J., Xu, G. 2002, 'Neogene thermal history of Opoutama-1, Hawke's Bay Basin: Implications for hydrocarbon prospectivity', *New Zealand Petroleum Conference*, Auckland.

Kann, J. F. 1960, *Report on the seismic survey of the Wairoa area.*, Ministry of Economic Development New Zealand Unpublished Petroleum Report 403.

Kelsey, H. M., Cashman, S. M., Beanland, S. & Berryman, K. R. 1995, 'Structural evolution along the inner forearc of the obliquely convergent Hikurangi margin, New Zealand', *Tectonics*, vol. 14, no. 1, pp. 1-18.

Kennett, J. P. & Watkins, N. D. 1974, 'Late Miocene−−Early Pliocene Paleomagnetic Stratigraphy, Paleoclimatology, and Biostratigraphy in New Zealand', *Geological Society of America Bulletin*, vol. 85, pp. 1385-1398.

King, P. R., Naish, T. R., Browne, G. H., Field, B. D. & Edbrooke, S. W. 1999, *Cretaceous to Recent sedimentary patterns in New Zealand*, *Institute of Geological & Nuclear Sciences Folio Series 1*, version 1999.1. Lower Hutt, New Zealand: Institute of Geological and Nuclear Sciences Limited.

Lees, A. 1975, 'Possible influence of salinity and temperature on modern shelf carbonate sedimentation', *Marin Geology*, vol. 19, pp. 159-198.

Lees, A. & Buller, A. T. 1972, 'Modern temperate-water and warm-water shelf carbonate sediments contrasted', *Marine Geology*, vol. 13, pp. M67-M73.

Leonard, J. E., Cameron, B., Pilkey, O. H. & Friedman, G. M. 1981, 'Evaluation of cold-water carbonates as a possible paleoclimatic indicator', *Sedimentary Geology*, vol. 28, pp. 1-28.

Lewis, K. B., Collot, J. Y., Davy, B. W., Delteil, L., Lallemand, S. E., Uruski, C. I. & team, G. (ed) 1997, *North Hikurangi GeodyNZ swath maps: depth, texture and geological interpretation*, National Institute of Water & Atmospheric Research, Wellington.

Lewis, K. B., Collot, J. Y. & Lallemand, S. E. 1998, 'The dammed Hikurangi Trough: a channel-fed trench blocked by subducting seamounts and their wake avalanches (New Zealand–France GeodyNZ Project)', *Bas. Res.*, vol. 10, pp. 441–468.

Lewis, K. B., Lallemand, S. E. & Cater, L. 2004, 'Collapse in a Quaternary shelf basin off East Cape, New Zealand: evidence for the passage of a subducted seamount inboard of the Ruatoria giant avalanche', *New Zealand Journal of Geology & Geophysics*, vol. 47, pp. 415–429.

Lewis, K. B. & Pettinga, J. R. 1993, 'The Emerging, Imbricate Frontal Wedge of the Hikurangi Margin', in P. F. Ballance (ed.), *Sedimentary Basins of the World*, Elservier, Amsterdam, pp. 413.

Marwick, J. 1965, Upper Cenozoic mollusca of Wairoa district, Hawke's Bay, *New Zealand Geological Survey Paleotological Bulletin*, vol. 39, pp. 1-83.

Mazengarb, C., Francis, D. A. & Moore, P. R. 1991, *Sheet Y16-Tauwhareparae.*, New Zealand Geological Survey. Department of Scientific and Industrial Research, Wellington.

Mazengarb, C. & Speeden, I. G. 2000, *Geology of the Raukumara Area*, Institute of Geological and Nuclear Sciences 1:250 000 geological map 6, Institute of Geological and Nuclear Sciences, Lower Hutt, New Zealand.

McInnes, B. A. 1964, *A detailed examination of microfaunas from a Miocene-Pliocene section on the Mangapoike River northern Hawkes Bay*, Ministry of Economic Development New Zealand Unpublished Petroleum Report 350.

McKay, A. 1887, 'Report on country between Cape Kidnappers and Cape Turnagain, Geological Survey of New Zealand, *Reports of geological explorations during 1874-76*, vol. 9, pp 43-53.

Moore, P. R., Francis, D. A. & Mazengarb, C. 1989, *Interim geological map of New Zealand 1:250,000. DSIR sheet QM303, Raukumara.*

Moore, P. R. & Hatton, B. A. 1985, *Limestone resources of northern and central Hawke's Bay*, New Zealand Geological Survey Record 2.

Morris, J. H. 1982, The geology of late Tertiary sediments northwest of Masterton, Wairarapa, Unpublished Thesis, Victoria University.

Mortimer, N. 1995, 'Origin if the Torlesse Terrane and coeval rocks, North Island, New Zealand', *International goelogy review*, vol. 36, pp. 891-910.

Mountjoy, J. J., Barnes, P. M. & Pettinga, J. R. 2009, 'Morphostructure of submarine canyons on an active margin: Cook Strait Canyon system, New Zealand', *Marine Geology*, vol. 260, pp. 45–68.

Nelson, C. S. 1973, 'Stratigraphy and sedimentology of the Te Kuiti Group in Waitomo country, South Auckland, Unpublished PhD thesis, University of Auckland.

Nelson, C. S. 1978, 'Temperate shelf carbonate sediments in the Cenozoic of New Zealand', *Sedimentology*, vol. 25, pp. 737-771.

Nelson, C. S. 1988, 'An introductory perspective on non-tropical shelf carbonates', *Sedimentary Geology*, vol. 60, pp. 3-12.

Nelson, C. S. & Bornhold, B. D. 1984, 'Temperate continental shelf skeletal carbonate deposits', *Geobois Mem. Spec.*, vol. 8, pp. 109-113.

Nelson, C. S. & Hancock, G. E. 1984, 'Composition and origin of temperate skeletal carbonate sediments on South Maria Ridge. northern New Zealand', *N.Z.J. Mar. Freshwater Res.*, vol. 18, pp. 221-239.

Nelson, C. S., Harris, G. J. & Young, H. R. 1988a, 'Burial dominated cementation in non-tropical carbonates of the Oligocene Te Kuiti Group, New Zealand', *Sedimentary Geology*, vol. 60, Non-Tropical Shelf Carbonates-Modern and Ancient, pp. 233-250.

Nelson, C. S., Keane, S. L. & Head, P. S. 1988b, 'Non-tropical carbonate deposits on the modern New Zealand shelf', *Sedimentary Geology*, vol. 60, no. Non-Tropical Shelf Carbonates-Modern and Ancient, pp. 71-94.

Nelson, C. S. & Smith, A. M. 1996, 'Stable oxygen and carbon isotope compositional fields for skeletal and diagenetic components in New Zealand Cenozoic nontropical carbonate sediments and limestones: a synthesis and review', *New Zealand Journal of Geology & Geophysics*, vol. 39, pp. 93-107.

Nelson, C. S., Winefield, P. R., Hood, S. D., Caron, V., Pallentin, A. & Kamp, P. J. J. 2003, 'Pliocene Te Aute limestones, New Zealand: expanding concepts for cool-water shelf carbonates', *New Zealand Journal of Geology & Geophysics*, vol. 46, pp. 407-424.

Nicol, A. & Wallace, L. M. 2007, 'Temporal stability of deformation rates : comparison of geological and geodetic observations, Hikurangi subduction margin, New Zealand', *Earth and planetary science letters*, vol. 258(3/4), pp. 397-413.

Nummedal, D. & Swift, D. J. P. 1987, *Transgressive stratigraphy at sequence-boundary unconformities: some principles derived from Holocene and Cretaceous examples*.

Ongley, M. 1928, *Wairoa Subdivision*, Annual report of the Geological Suvey Branch, Department of Scientific and Industrial Research, vol. 22, pp. 6-8.

Ongley, M. 1930, *Wairoa Subdivision*, Annual report of the Geological Suvey Branch, Department of Scientific and Industrial Research, vol. 24, pp. 7-10.

Quennell, A. M. 1940, *Geological Report of the Wairoa Area Gisborne District*, Ministry of Economic Development New Zealand Unpublished Petroleum Report 19.

Rao, C. P. 1981, 'Criteria for recognition of cold-water carbonate sedimentation: Berriedale Limestone (Lower Permian), Tasmania, Australia', *Journal of Sedimentary Petrology*, vol. 51, no. pp. 491-506.

Raymo, M. E., Mitrovica, J. X., O'Leary, M. J., DeConto, R. M., Hearty, P. J. 2011, Departure from eustasy in Pliocene sea-level records, *Nature Geoscience*, vol. 4, pp. 328-332.

Rogers, K. M., Collen, J. D., Johnston, J. H. & Elgar, N. E. 1999, 'A geochemical appraisal of oil seeps from the East Coast Basin, New Zealand', *Organic Geochemistry*, vol. 30, no. 7, pp. 593-605.

Schlager, W. 2005, 'Carbonate Sedimentology and Sequence Stratigraphy', *SEPM Concepts in Sedimentology and Paleontology*, vol. 8.

Scholle, P. A. & Ulmer-Scholle, D. S. 2003, A colour guide to the petrography of *carbonate rocks: grains, texture, porosity, diagenesis*, AAPG, Tulsa, Oklahoma.

Shackleton, N. J. 1967, 'Oxygen isotope analyses and paleotemperatures reassessed', *Nature*, vol. 215, pp. 15-17.

Smith, S. P. 1887, Sketch of the geology of the northern portion of Hawke's Bay, *Transactions and Proceedings of the New Zealand Institute*, vol. 9, pp. 565-576.

Sporli, K. B. & Pettinga, J. R. 1980, 'Mt Kahuranaki, Hawke's Bay, New Zealand, a klippe emplaced by gravity sliding from the crest of the near by Elsthorpe Anticline', *Journal of the Royal Society of New Zealand*, vol. 10, pp. 287-307.

Steineke, M. 1934, *Report on the geology and oil possiblities of the Poverty Bay district, north of Gisborne. Vacuum Oil Co.* , New Zealand Geological Survey unpublished open-file petroleum report 120.

Sutherland, R., Barnes, P. M. & Uruski, C. I. 2006, 'Miocene–Recent deformation, surface elevation, and volcanic intrusion of the overriding plate during subduction initiation, offshore southern Fiordland, Puysegur margin, southwest New Zealand', *new Zealand Journal of Geology & Geophysics*, vol. 49, pp. 131–149.

Tucker, M. E. & Wright, V. P. 1990, *Carbonate sedimentology*, Blackwell Scientific Publications, Oxford.

Vella, P. P. & Briggs, W. M. 1971, 'Lithostratigraphic names, Upper Miocene to Lower Pleistocene, northern Aorangi Range, Wairarapa', *new Zealand Journal of Geology & Geophysics*, vol. 14, pp. 253-274.

Walter, L. M. 1985, 'Relative reactivity of skeletal carbonates during dissolution: implications for diagenesis', in N. Schneidermann & P. M. Harris (ed.), *Carbonate Cements, Special publication, Society of economic paleontologists and mineralogists*, no. 36, pp. 3-16.

Wells, P. E. 1989, 'Late Neogene stratigraphy of the Carrington area, western Wairarapa, North Island, New Zealand', *Journal of the Royal Society of New Zealand*, vol. 19, pp. 283-303.

Wright, I. C. & Walcott, R. I. 1986, 'Large tectonic rotation of part of New Zealand in the last 5 Ma', *Earth and Planetary Science Letters*, vol. 80, no. 3-4, pp. 348-352.

Appendix I

Stratigraphic column sheet used in the field

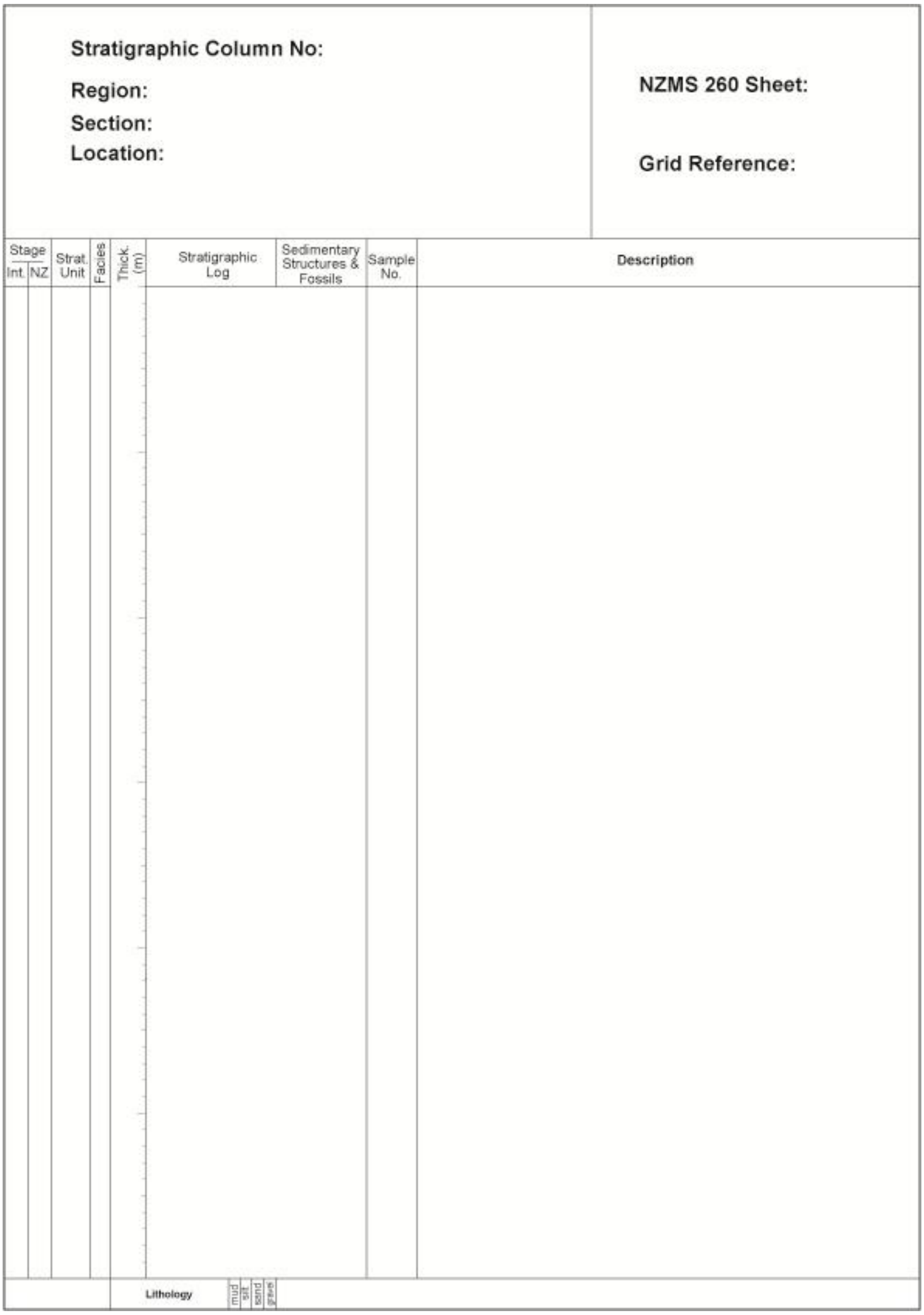
Stratigraphic Column No:
Region:
Section:
Location:
NZMS 260 Sheet:
Grid Reference:

Stage		Strat. Unit	Facies	Thick. (m)	Stratigraphic Log	Sedimentary Structures & Fossils	Sample No.	Description
Int.	NZ							
					Lithology mud silt sand gravel			

Stratigraphic column legends

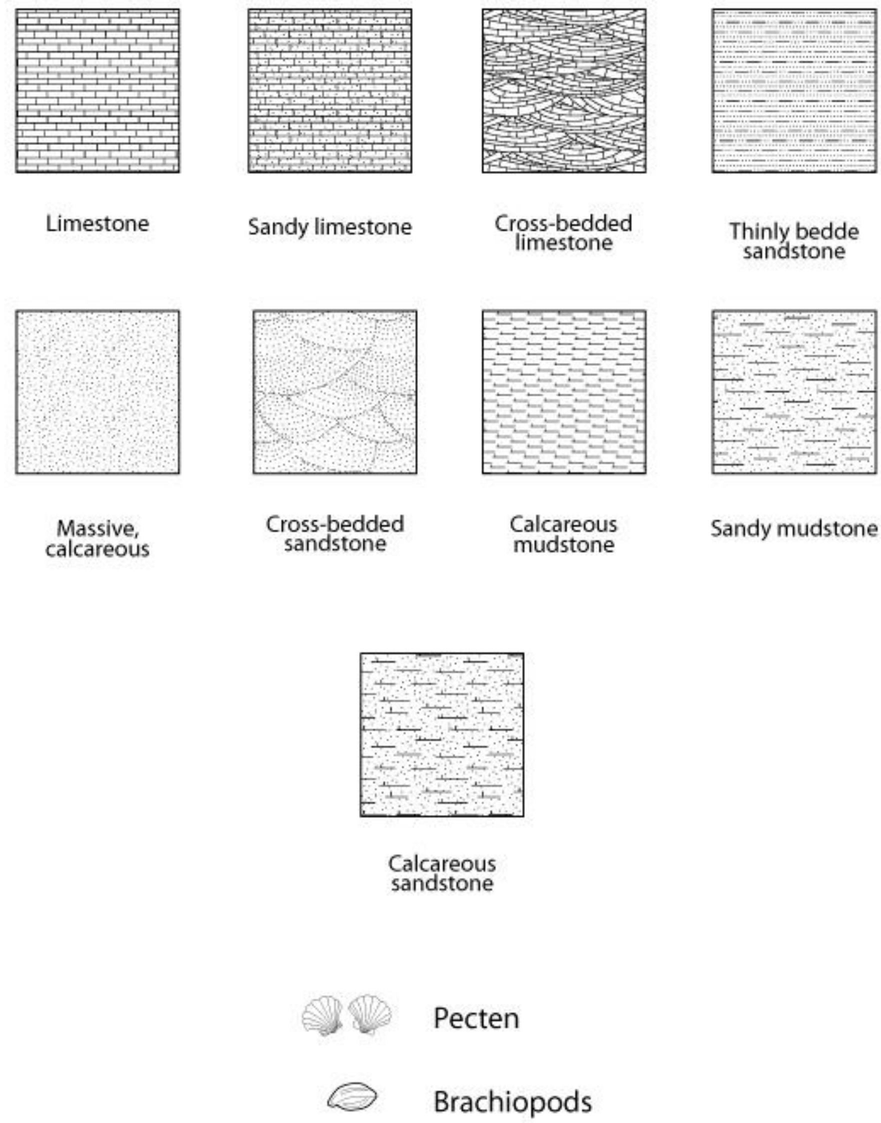

Stratigraphic Column No: 1

Region: Northern Hawke's Bay

Section:

Location: Along the Mangapoike Road, 1 km north of junction between Mangapoike Road and Hereheretau Road

NZMS 260 Sheet: X19

Grid Reference: 035425

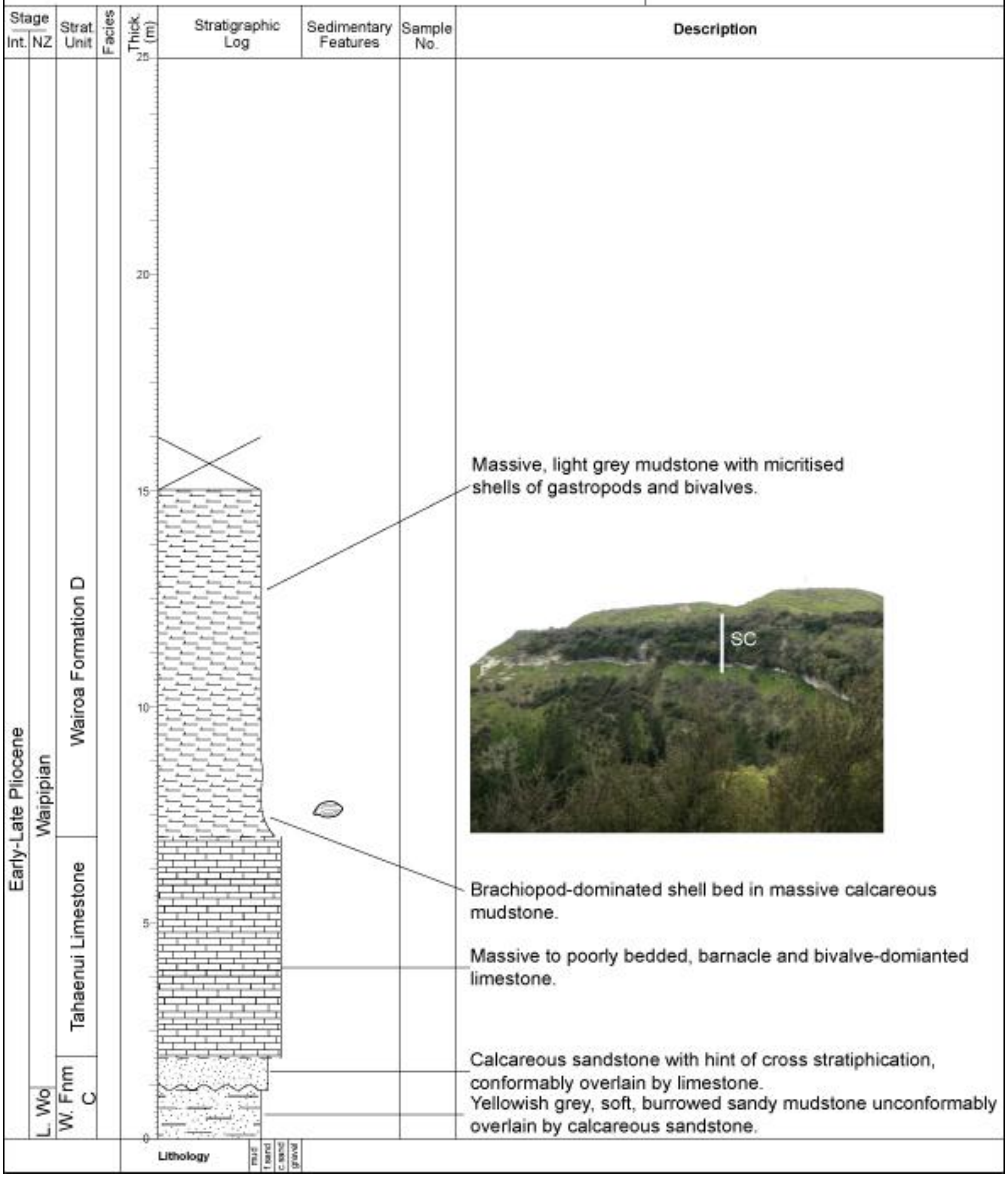

Stratigraphic Column No: 2

Region: Northern Hawke's Bay

Section:

Location: Anewa Station, along the Hereheretau Road

NZMS 260 Sheet: X19

Grid Reference: 035410

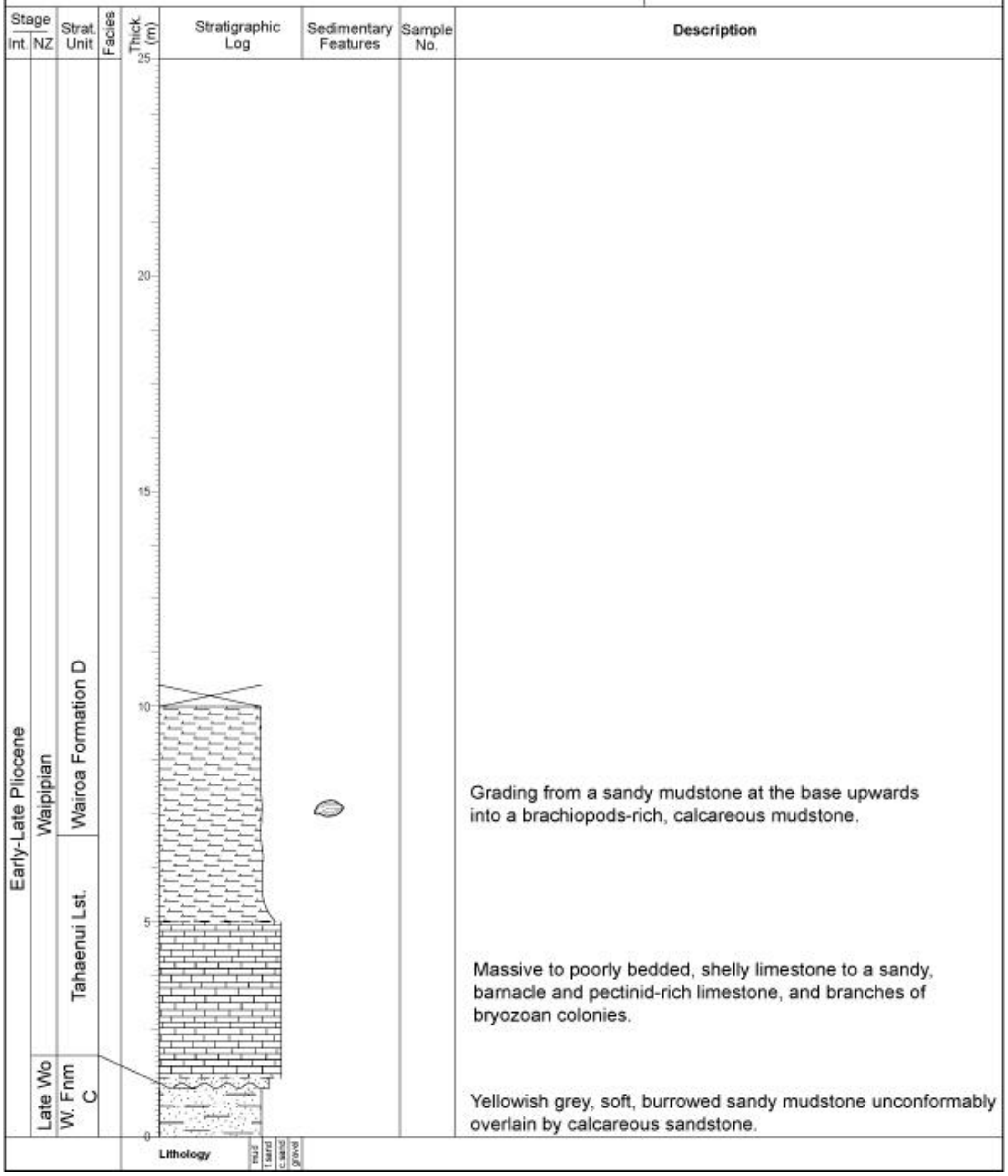

Stratigraphic Column No: 3

NZMS 260 Sheet: X18

Region: Wairoa District, Northern Hawke's Bay

Section: Hangaroa Section

Location: North of Tiniroto, roadside outcrop along the Tiniroto Road

Grid Reference: 098658

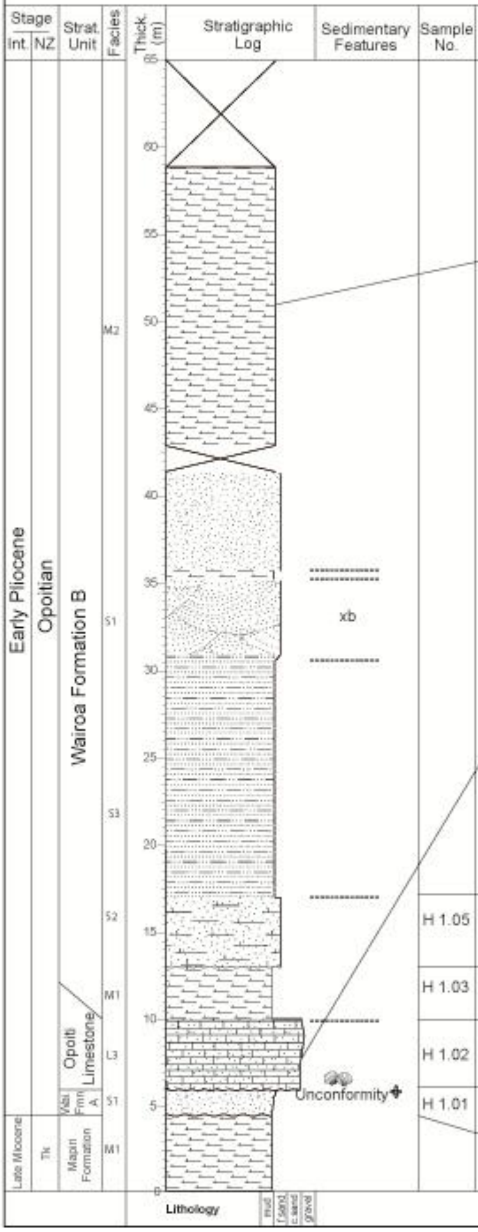

Description

Pale grey thinly bedded siltstone, the outcrop is largely inaccessible.

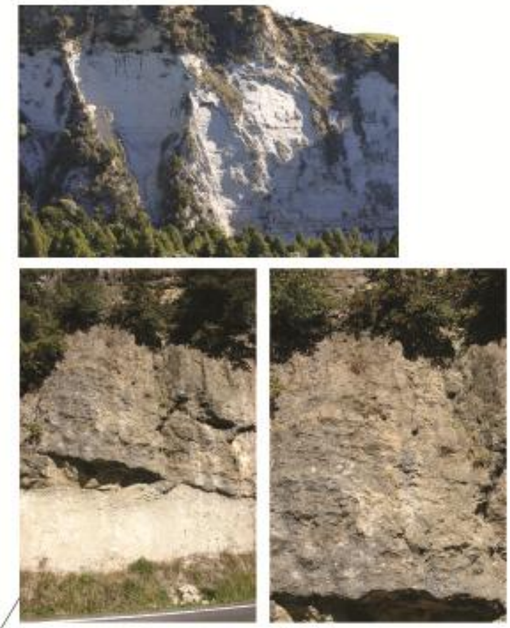

Greyish - pale grey, thinly bedded between 20-30 cm calcareous sandstone with lens-like tuff beds in upper part of the unit, and grade upwards into a slihgtly cross-bedded calcareous sandstne.

Sample No.	Description
H 1.05	A light brown to pale yellow, moderately to highly indurated, fine glauconitic and calcareous sandstone (Fig above right).
H 1.03	Massive to weakly bedded, pale grey calcareous sandstone with a gentle dip of 10 observed at the outcrop.
H 1.02	Soft greyish siliciclastic-rich limestone contains ocassional large Opoitian pectinids.
H 1.01	Light grey massive, moderatedly indurated calcareous sandstone.
	Light grey, soft to moderatedly indurated calcareous deep-marine siltstone.

Stratigraphic Column No: 4

Region: Wairoa District, Northern Hawke's Bay

Section: Hangaroa Section

Location: Roadside outcrop along the Ruakaka Rd, first bridge after Rongoio Station (farm stay)

NZMS 260 Sheet: X18

Grid Reference: 035651

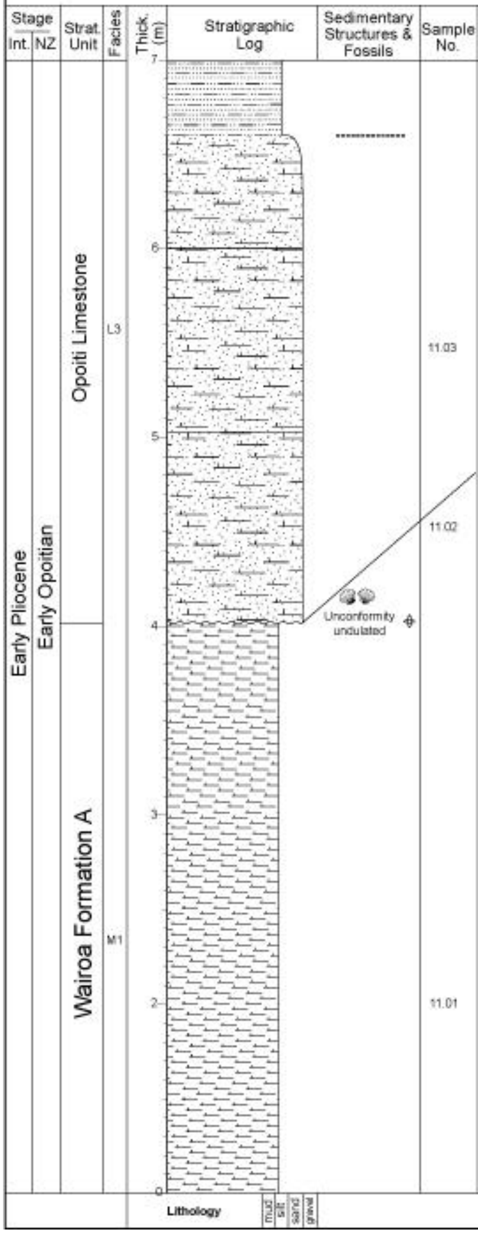

Description

Grey to light brown, massive to thickly bedded, moderately to highly indurated, glauconite and siliciclatic rich, shelly limestone, contains macrofossils (3-5 mm).

Nature of the contact is very sharp, and undulated, there is evidence of bioturbation at top of the sandstone.

Massive grey to light brown, moderately weathered, siliciclastic-bioclastic mixed, soft, calcareous fine sandstone, contain ocassional macrofossils.

Stratigraphic Column No: 5

Region: Wairoa District, Northern Hawke's Bay

Section: Hangaroa Section

Location: Along the tributary Mangapiopio Stream, 300 m upstream from Hangaroa River

NZMS 260 Sheet: X18

Grid Reference: 033652

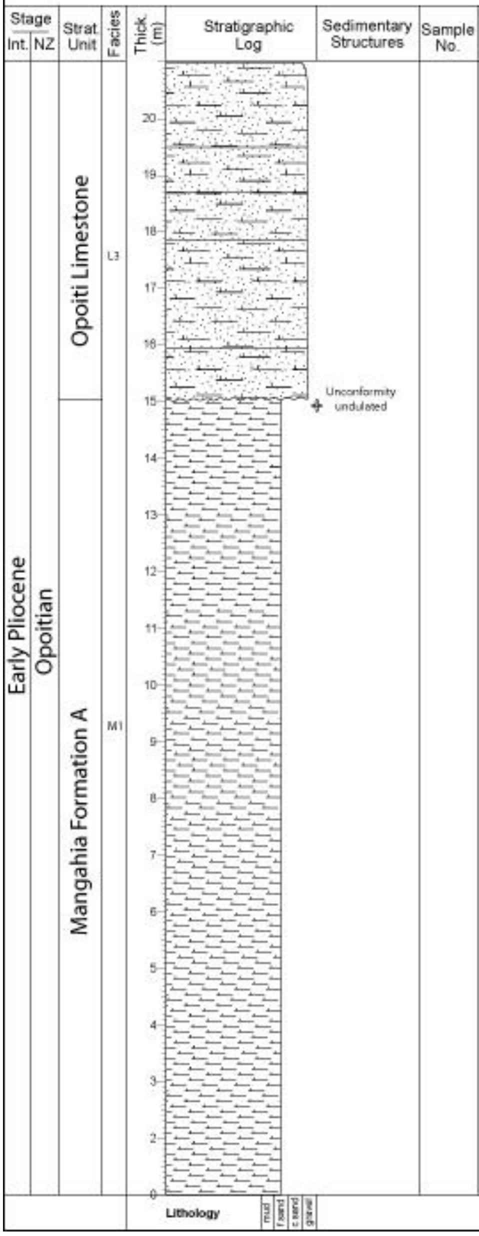

Description

Brown to dark brown, highly weathered, massive to weakly bedded calcareous sandstone.

Massive grey to light brown, moderately weathered, siliciclastic-bioclastic mixed, soft, calcareous fine sandstone, contain ocassional macrofossils.

Stratigraphic Column No: 6

Region: Wairoa District, Northern Hawke's Bay

Section: Kauhauroa Section

Location: Kauhauroa Station, Tiniroto Road

NZMS 260 Sheet: X19

Grid Reference: 958421

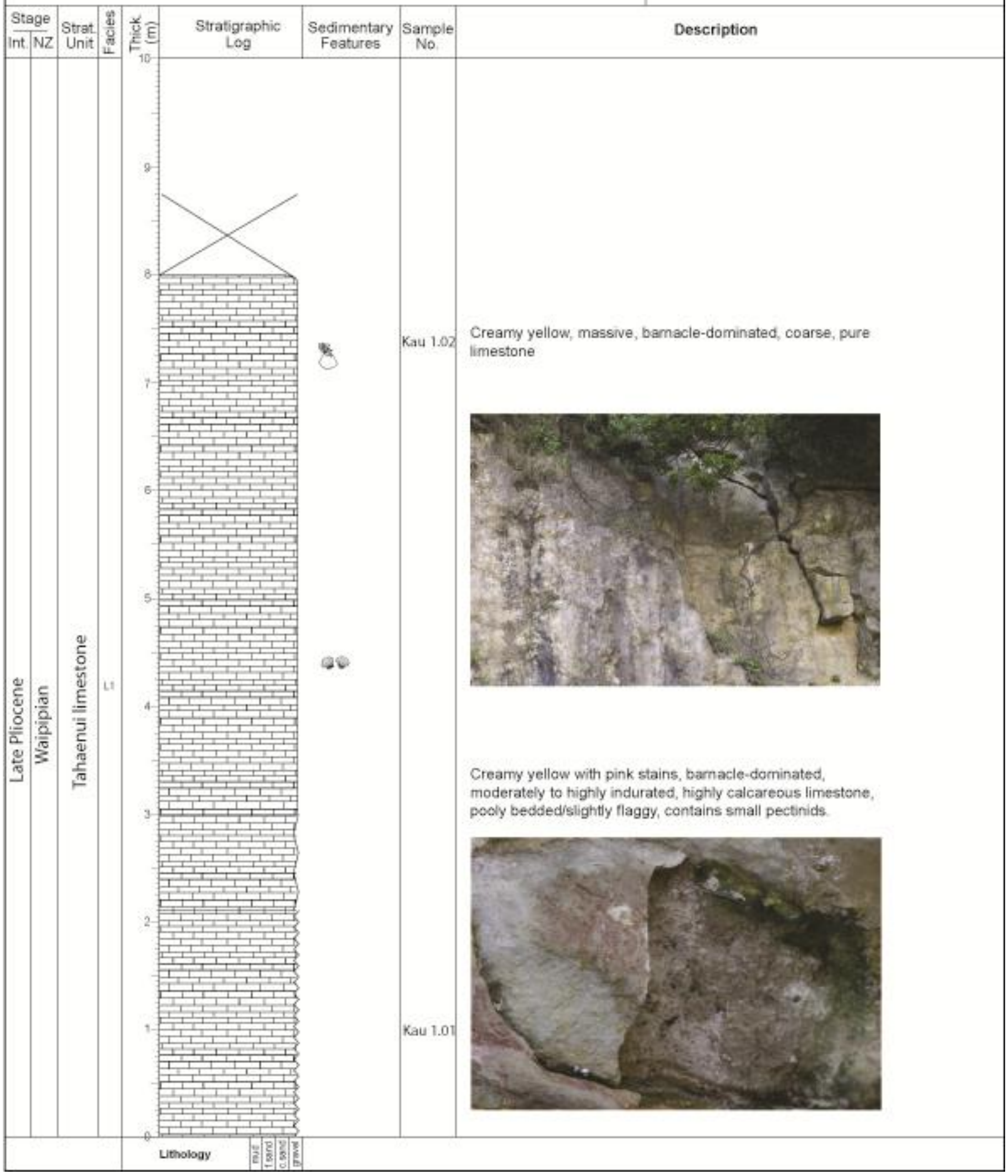

Stratigraphic Column No: 7

Region: Wairoa District, Northern Hawke's Bay

Section: Mangapoike Section

Location: Farm track at end of Kotare Road

NZMS 260 Sheet: X19

Grid Reference: 039457

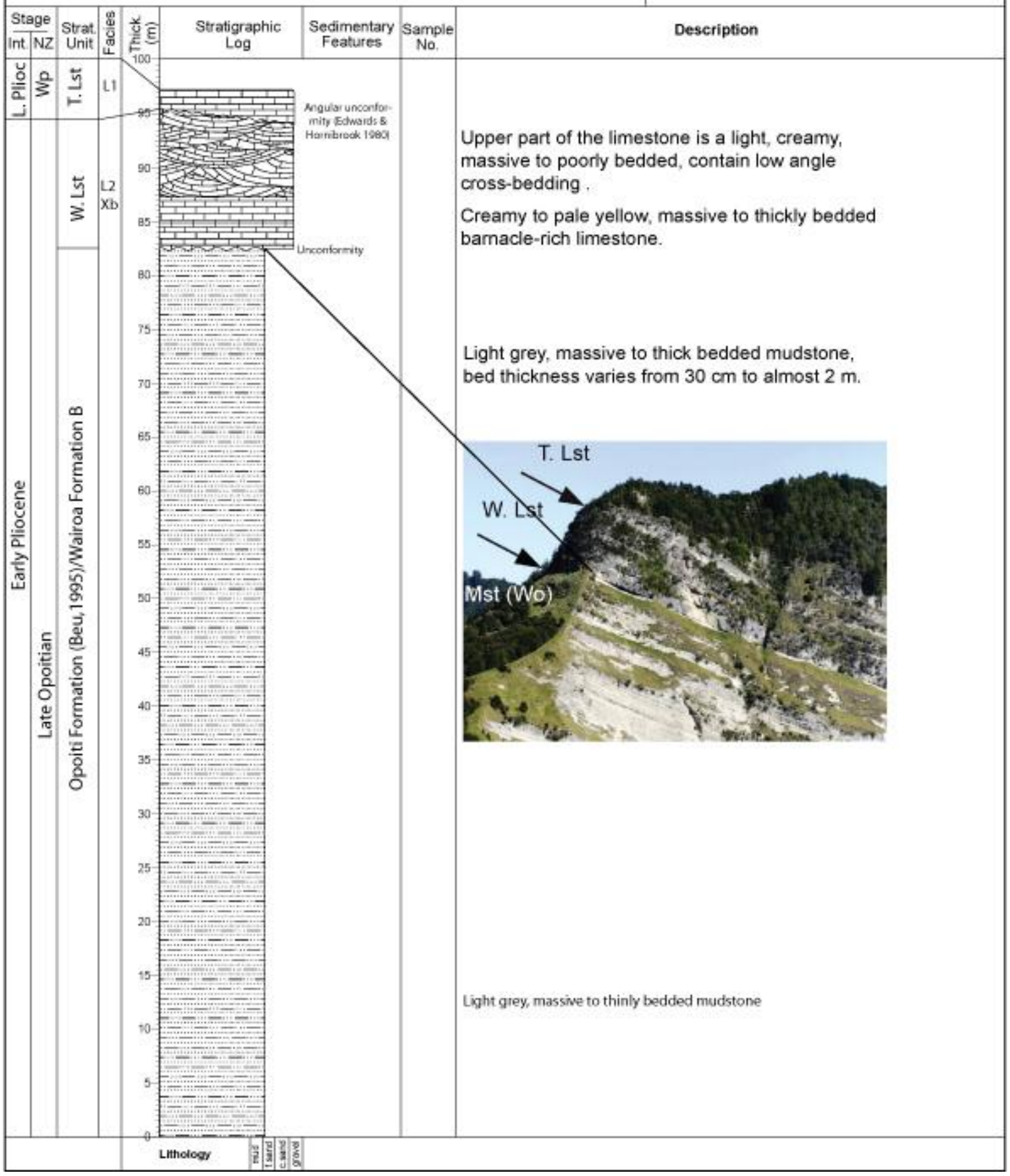

Stratigraphic Column No: 8

Region: Wairoa District, Northern Hawke's Bay

Section: Mangapoike River Section

Location: Type locality of the Whakapunake Limestone and reference section of Tahaenui Limestone, along the farm track at end of Kotare Road

NZMS 260 Sheet: X19

Grid Reference: 042468

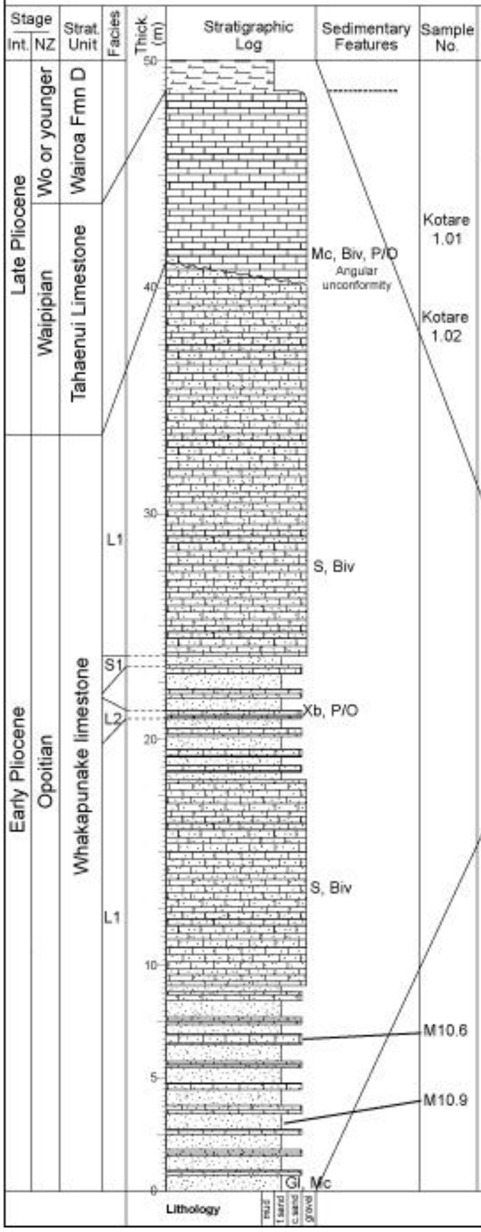

Description

Coarse, pale cream to pale yellow/brown, sandy, massive to poorly bedded, well cemented, moderately to highly indurated, barnacle and pectinid-rich limestone, contains occasional mudstone clasts (c. 2-4 mm).

Massive to weakly bedded (c. 10 m thick), sandy, coarse, light brown to creamy colour, commonly porous, moderately to highly indurated, barnacle and pectinid-dominated limestone.

Outcrop shows well-bedded, low-angle cross-bedding. The cemented interbeds are c. 20-30 cm thick, occasionally reaching half a metre thick. They are light grey to creamy colour, moderately to highly indurated, siliciclastic-rich, barnacle and pectinid-dominated beds.

The less cemented sandstone facies are light grey to light brown, relatively soft, moderately calcareous with moderate amounts of glauconite present.

Stratigraphic Column No: 9

Region: Wairoa District, Northern Hawke's Bay

Section: Mangapoike Section

Location: Outcrop is located along the Mangapoike Rd, towards Tukemokihi Station

NZMS 260 Sheet: X19

Grid Reference: 062450

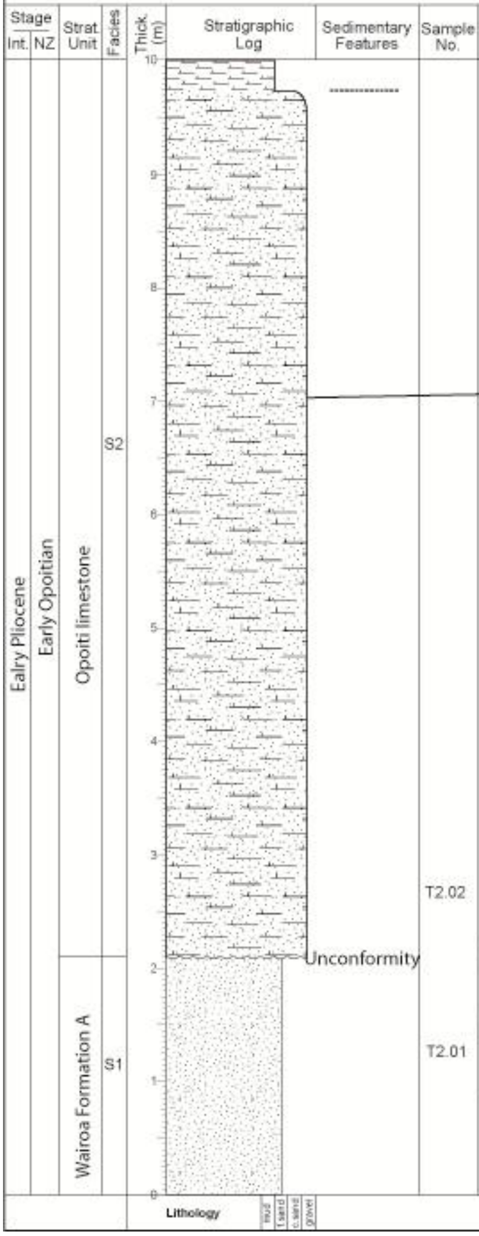

Description

Dark brown to orange-brown, sandy, fine grain, massive to poorly bedded, well sorted, moderately to highly indurated, brachiopod and glauconite-rich, calcareous sandstone.

Contact is sharp, undulates, and is strongly burrowed (see figure above).

Massive, light grey, moderately indurated, fossiliferous and highly calcareous sandstone.

Outcrop is slightly weathered.

Stratigraphic Column No: 10

Region: Wairoa District, Northern Hawke's Bay

Section: Mangapoike Section

Location: End of Kotare Road, along the farm track

NZMS 260 Sheet: X19

Grid Reference: 025465

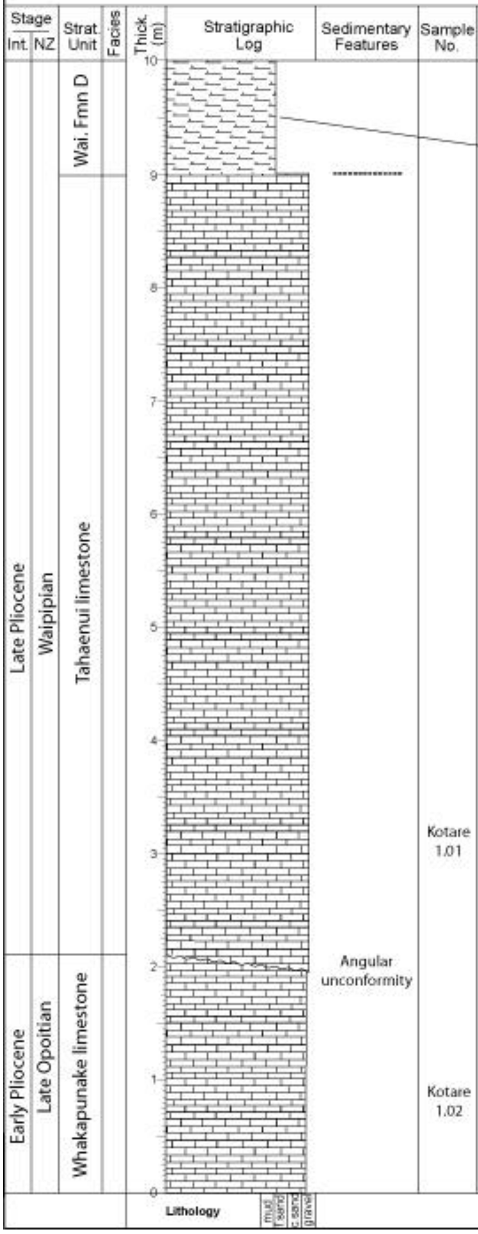

Description

Massive, thick, light grey, soft to moderately indurated calcareous mudstone.

Creamy to pale brown, massive to poorly bedded, coarse bioclasts setting in a fine sandy matrix with a few siliciclasts, soft, poorly sorted, highly calcareous limestone.

The angular unconformity is rather difficult to identify, partially due to the outcrop is covered by secondary calcite.

Creamy to pale brown, fine grain, moderately sorted, highly calcareous and indurated limestone, and weakly cross-bedded.

Stratigraphic Column No: 11

Region: Northern Hawke's Bay

Section:

Location: Te Reinga marae

NZMS 260 Sheet: X18

Grid Reference: 027536

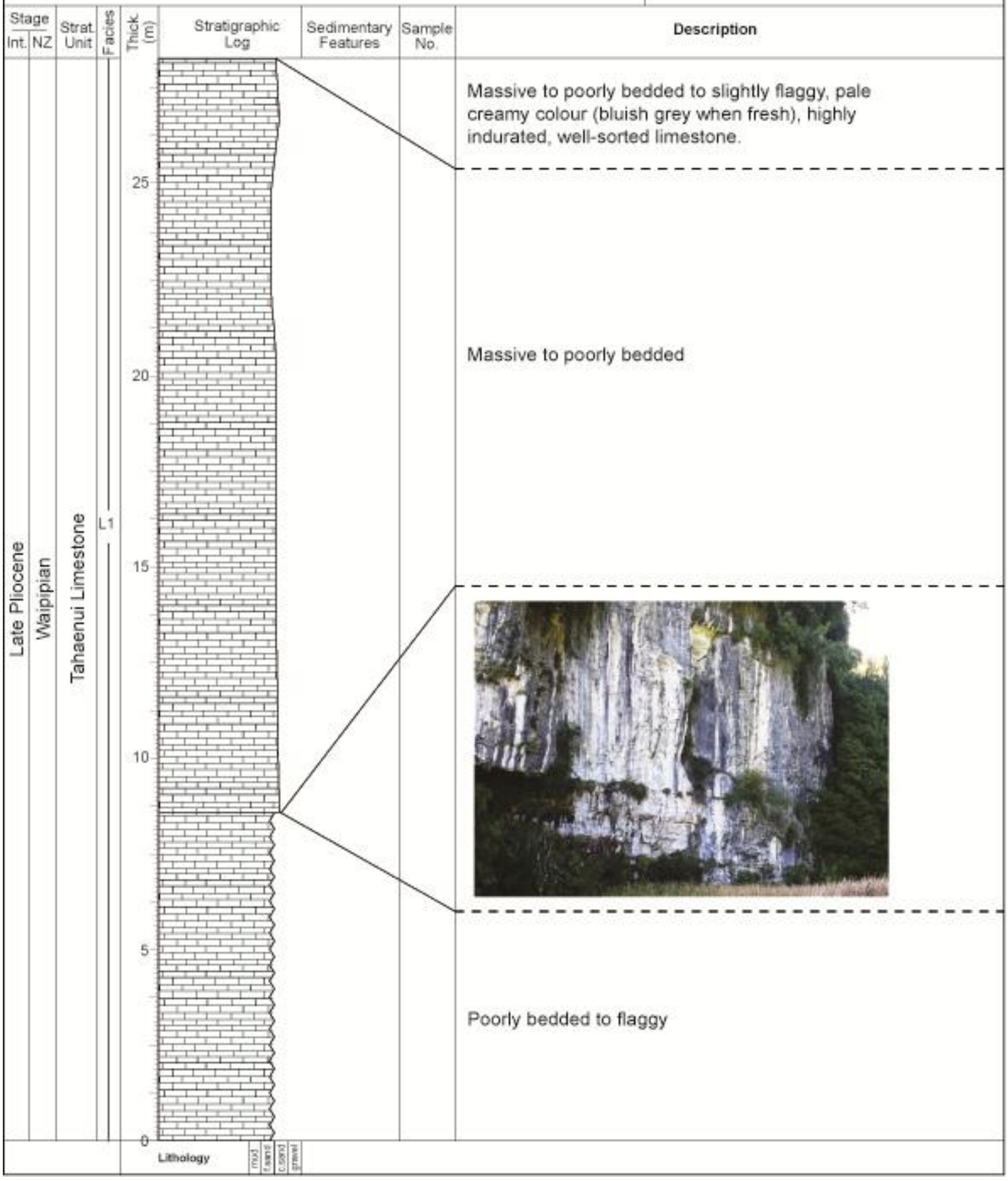

Stratigraphic Column No: 12

Region: Northern Hawke's Bay

Section:

Location: Te Reinga marae

NZMS 260 Sheet: X18

Grid Reference: 026534

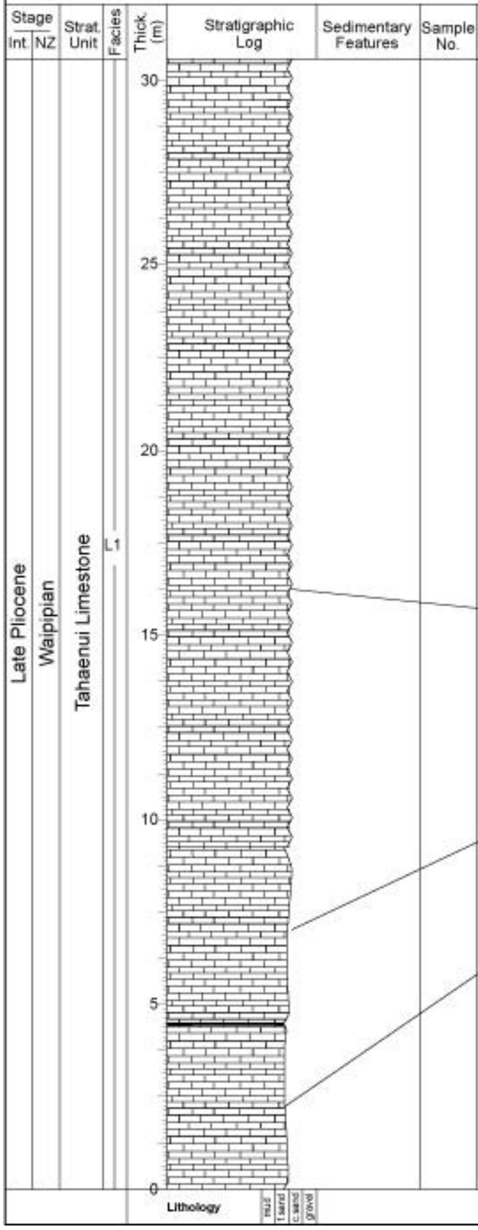

Description

Differentially cemented (15-20 cm thick), slightly crossbedded, pale yellow to creamy colour, highly indurated limestone.

Massive to poorly bedded limestone.

Massive to poorly bedded creamy colour limestone.

Stratigraphic Column No: 13

Region: Northern Hawke's Bay

Section:

Location: Whakapunake scarp, above Tiniroto Road

NZMS 260 Sheet: X18

Grid Reference: 037550

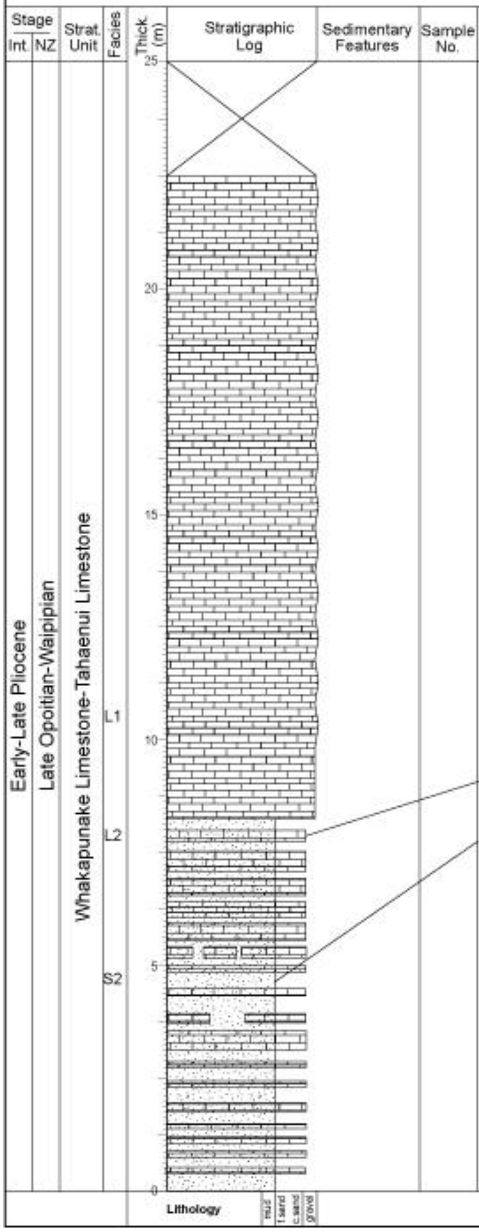

Coarse, pale cream to pale yellow/brown, sandy, massive to poorly bedded, well cemented, barnacle and pectnid-rich limestone.

Alternating siliciclastic-rich facies and coquina. The cemented interbeds are 20-30 cm thick, occasionally reaching half a metre thick. Light grey to creamy colour, highly indurated, bivalve-dominated beds. The sanstone facies are pale yellow to light brown, relatively soft, moderately calcareous with moderate amounts glauconite present.

Stratigraphic Column No: 14

Region: Northern Hawke's Bay

Section:

Location: Whakapunake repeat tower

NZMS 260 Sheet: X18

Grid Reference: 092534

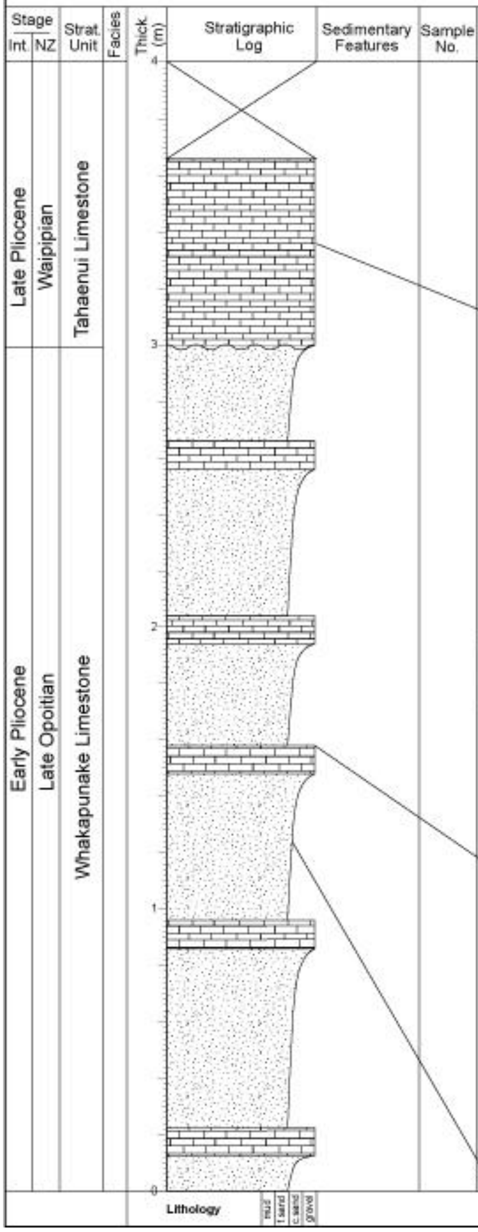

Description

Pale cream to pale yellow/brown, sandy, well cemented, barnacle and pectnid-rich limestone.

Pale cream, thin, skeletal-rich limestone facies interbeds.

Yellowish brown, massive, siliciclastic-rich facies interbeds

Appendix II

$CaCO_3$ content analysis

Sample No.	Initial weight (g)	Filter weight (g)	Dried sample+filter weigt (g)	Dried sample weight (g)	$CaCO_3$%
R1.01	5.0	2.6	7.5	4.9	3.0
11.01	5.1	2.6	7.5	4.9	3.2
Pa1.05	5.3	2.6	7.7	5.1	5.1
H1.01	5.6	2.6	7.7	5.2	7.0
P1.01	5.2	2.6	7.2	4.6	12.2
trig 1.03	5.0	2.6	6.9	4.3	14.1
Pa1.01	5.2	2.6	6.8	4.3	17.4
T1.02	5.6	2.6	6.8	4.2	24.8
T2.01	5.1	2.6	6.3	3.7	26.8
H1.02	5.7	2.6	6.4	3.8	32.5
T2.02	5.0	2.6	5.7	3.2	37.3
11.02	5.2	2.6	5.8	3.2	38.4
Ta/m	5.1	2.6	5.5	2.9	42.5
11.03	5.7	2.6	5.9	3.3	42.7
P1.03	5.1	2.6	5.5	2.9	44.0
M10.10	5.1	0.9	3.5	2.5	50.3
M10.1	5.0	0.9	3.4	2.5	50.4
P1.05	5.1	2.6	5.0	2.4	52.6
M10.6	5.0	1.0	3.3	2.3	53.9
M10.8	5.0	0.9	3.2	2.2	55.5
trig1.01	5.0	2.6	4.5	2.0	60.4
Ra/ta	5.6	2.6	4.7	2.1	61.5
Ra/op	5.1	2.6	4.3	1.7	66.7
Ko1.01	5.0	2.5	4.1	1.6	67.6
R1.02	5.6	2.6	4.3	1.8	68.5
Ma1.01	5.7	2.6	4.1	1.6	72.6
Ka1.01	5.2	2.6	3.7	1.1	78.2
M10.3	5.0	0.9	1.9	1.0	80.2
M10.4	5.0	1.0	1.8	0.9	83.0
Ko1.02	5.3	2.6	3.4	0.8	84.5

Appendix III

XRD

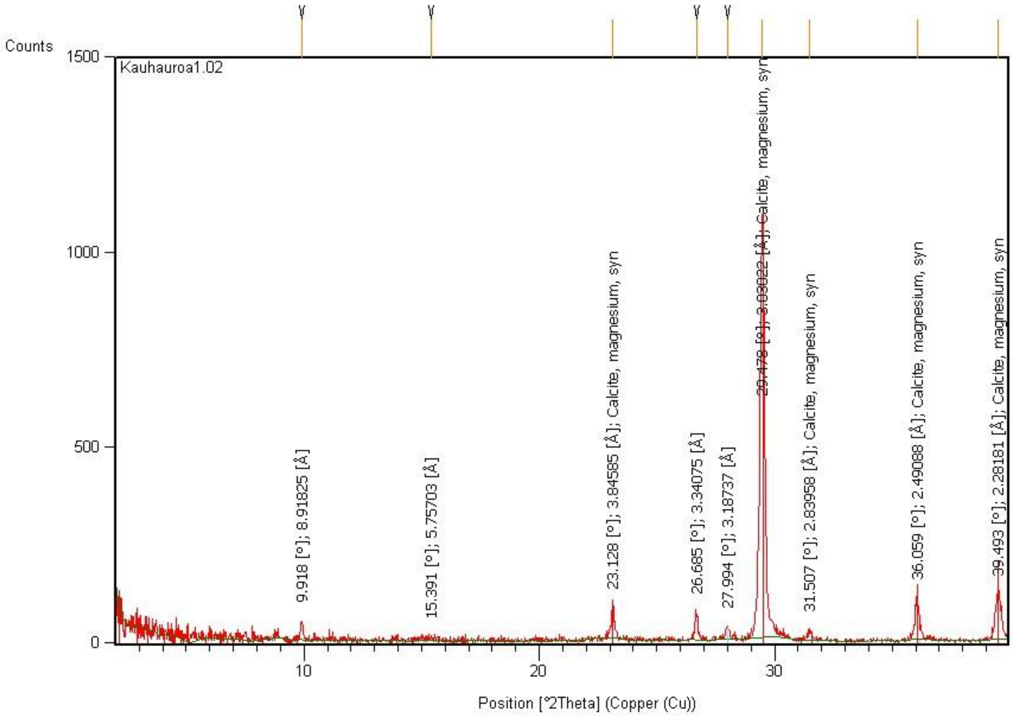
Counts
1500
1000
500
0
Kauhauroa1.02
9.918 [°]; 8.91825 [Å]
15.391 [°]; 5.75703 [Å]
23.128 [°]; 3.84585 [Å]; Calcite, magnesium, syn
26.685 [°]; 3.34075 [Å]
27.994 [°]; 3.18737 [Å]
Calcite, magnesium, syn
31.507 [°]; 2.83958 [Å]; Calcite, magnesium, syn
36.059 [°]; 2.49088 [Å]; Calcite, magnesium, syn
39.493 [°]; 2.28181 [Å]; Calcite, magnesium, syn
10
20
30
Position [°2Theta] (Copper (Cu))

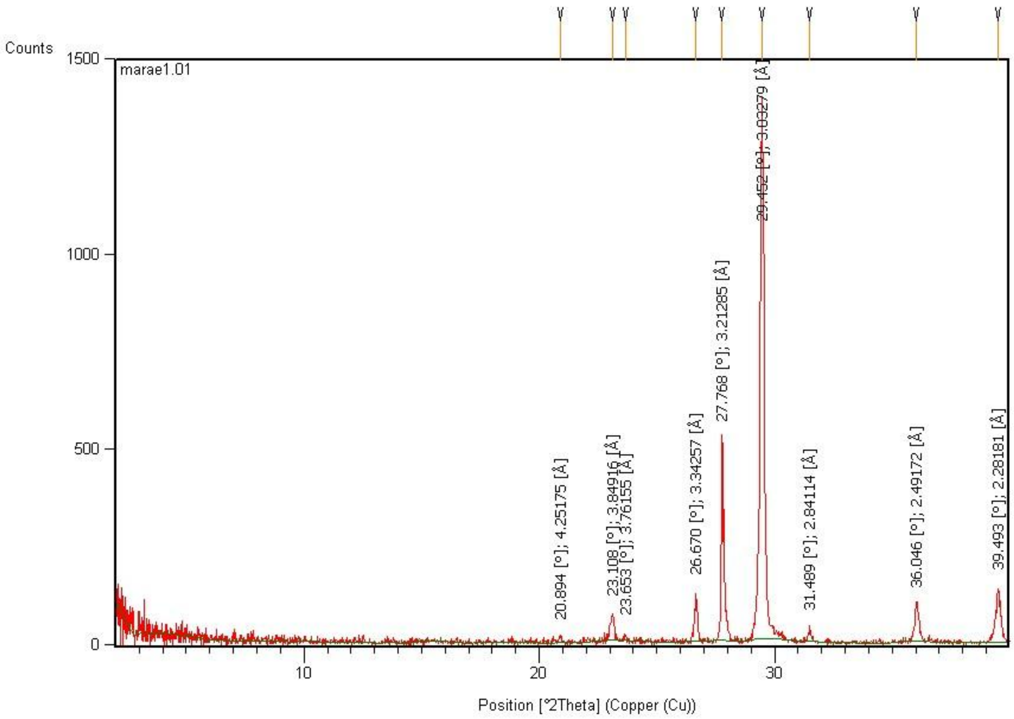
Counts
1500
1000
500
0
marae1.01
20.894 [°]; 4.25175 [Å]
23.653 [°]; 3.76155 [Å]
26.670 [°]; 3.34257 [Å]
27.768 [°]; 3.21285 [Å]
29.452 [°]; 3.03279 [Å]
31.489 [°]; 2.84114 [Å]
36.046 [°]; 2.49172 [Å]
39.493 [°]; 2.28181 [Å]
10
20
30
Position [°2Theta] (Copper (Cu))

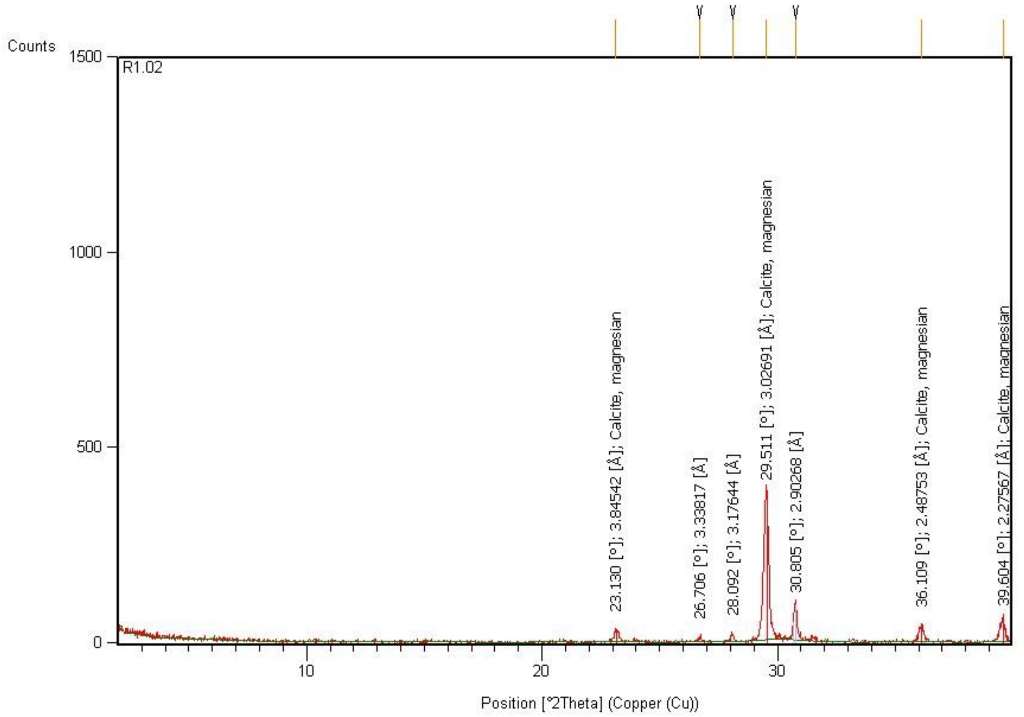
Counts
R1.02
23.130 [°]; 3.84542 [Å]; Calcite, magnesian
26.706 [°]; 3.33817 [Å]
28.092 [°]; 3.17644 [Å]
29.511 [°]; 3.02691 [Å]; Calcite, magnesian
30.805 [°]; 2.90268 [Å]
36.109 [°]; 2.48753 [Å]; Calcite, magnesian
39.604 [°]; 2.27567 [Å]; Calcite, magnesian
Position [°2Theta] (Copper (Cu))

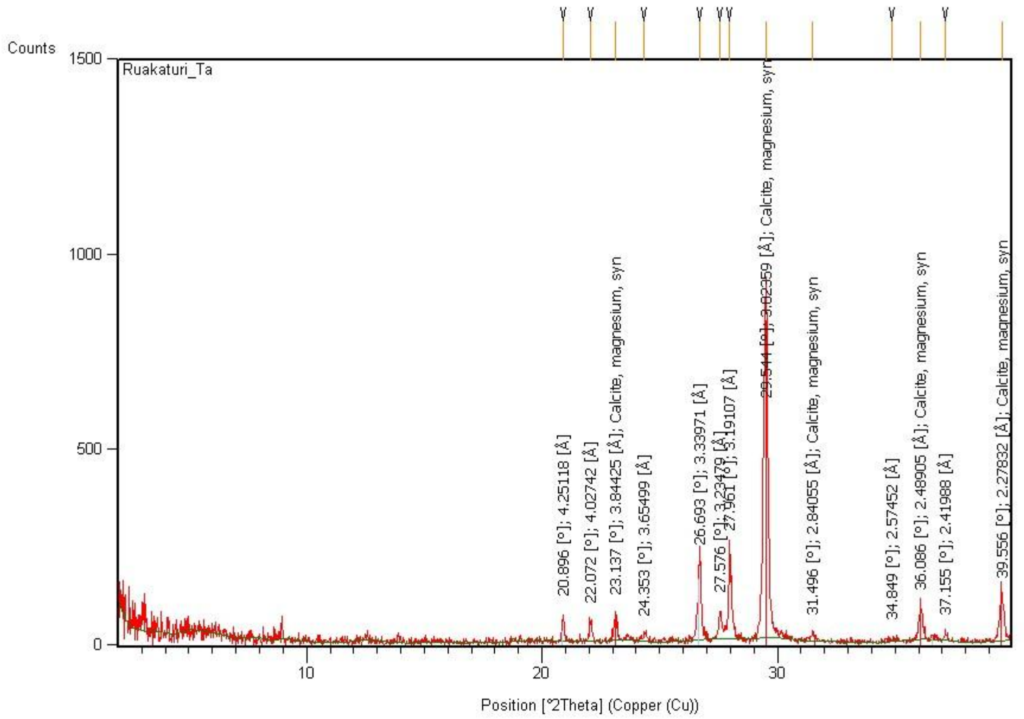
Counts
Ruakaturi_Ta
20.896 [°]; 4.25118 [Å]
22.072 [°]; 4.02742 [Å]
23.137 [°]; 3.84425 [Å]; Calcite, magnesium, syn
24.353 [°]; 3.65499 [Å]
26.693 [°]; 3.33971 [Å]
27.961 [°]; 3.19107 [Å]
29.544 [°]; 3.02359 [Å]; Calcite, magnesium, syn
31.496 [°]; 2.84055 [Å]; Calcite, magnesium, syn
34.849 [°]; 2.57452 [Å]
36.086 [°]; 2.48905 [Å]; Calcite, magnesium, syn
37.155 [°]; 2.41988 [Å]
39.556 [°]; 2.27832 [Å]; Calcite, magnesium, syn
Position [°2Theta] (Copper (Cu))

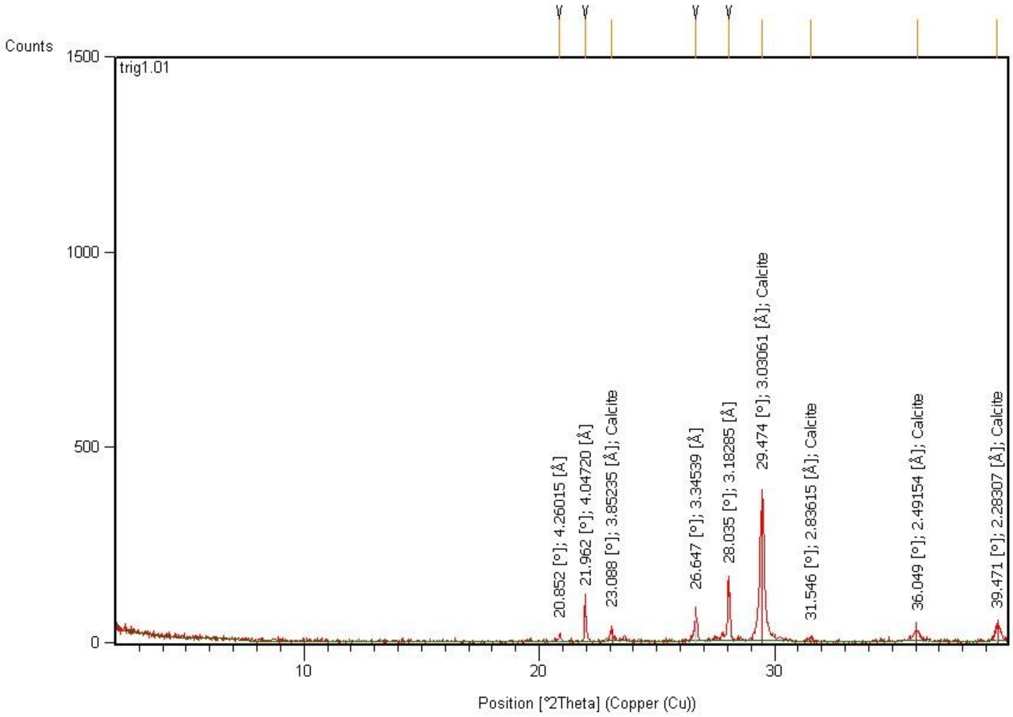
Counts
trig1.01
1500
1000
500
0
10
20
30
Position [°2Theta] (Copper (Cu))
20.852 [°]; 4.26015 [Å]
21.962 [°]; 4.04720 [Å]
23.088 [°]; 3.85235 [Å]; Calcite
26.647 [°]; 3.34539 [Å]
28.035 [°]; 3.18285 [Å]
29.474 [°]; 3.03061 [Å]; Calcite
31.546 [°]; 2.83615 [Å]; Calcite
36.049 [°]; 2.49154 [Å]; Calcite
39.471 [°]; 2.28307 [Å]; Calcite

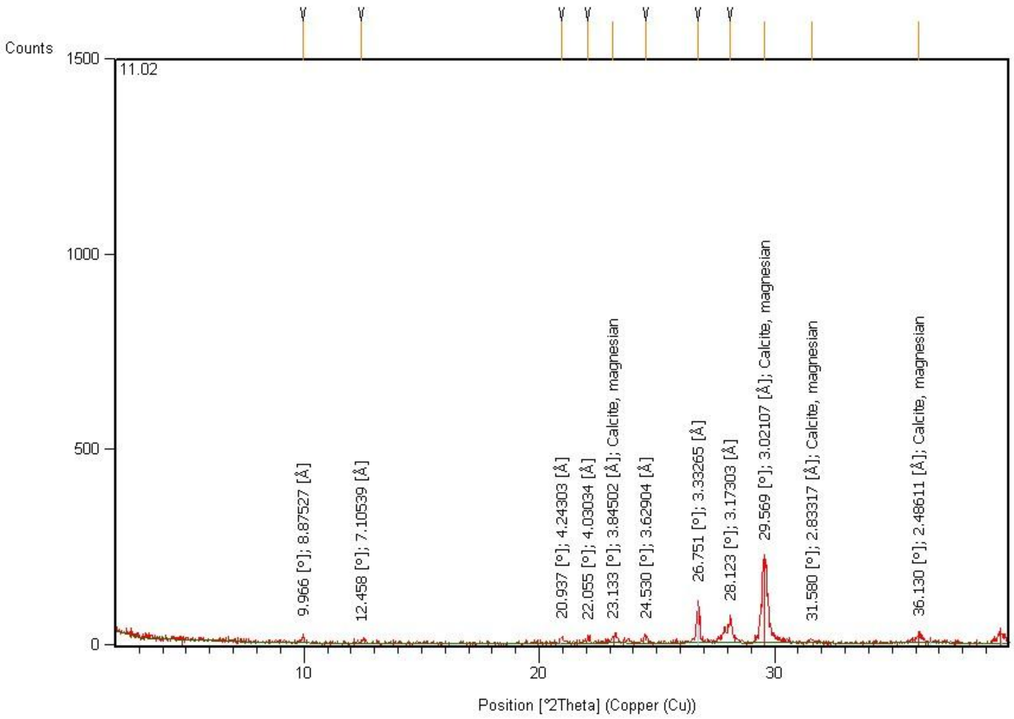
Counts
11.02
1500
1000
500
0
10
20
30
Position [°2Theta] (Copper (Cu))
9.966 [°]; 8.87527 [Å]
12.458 [°]; 7.10539 [Å]
20.937 [°]; 4.24303 [Å]
22.055 [°]; 4.03034 [Å]
23.133 [°]; 3.84502 [Å]; Calcite, magnesian
24.530 [°]; 3.62904 [Å]
26.751 [°]; 3.33265 [Å]
28.123 [°]; 3.17303 [Å]
29.569 [°]; 3.02107 [Å]; Calcite, magnesian
31.580 [°]; 2.83317 [Å]; Calcite, magnesian
36.130 [°]; 2.48611 [Å]; Calcite, magnesian

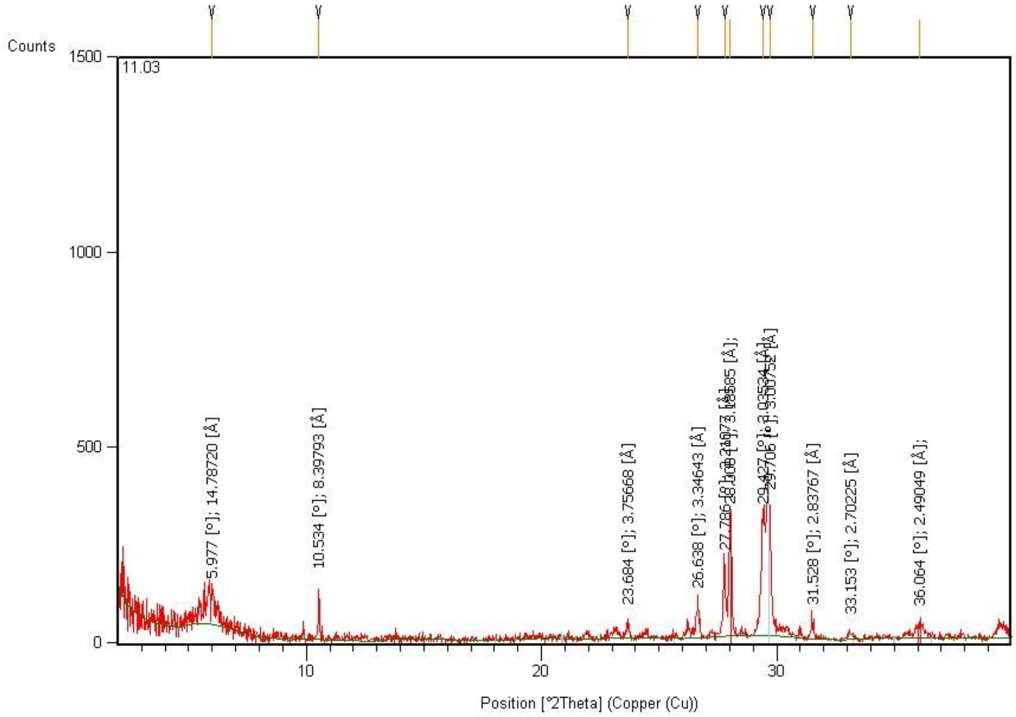

Counts
11.03
1500
1000
500
0
5.977 [°]; 14.78720 [Å]
10.534 [°]; 8.39793 [Å]
23.684 [°]; 3.75668 [Å]
26.638 [°]; 3.34643 [Å]
31.528 [°]; 2.83767 [Å]
33.153 [°]; 2.70225 [Å]
36.064 [°]; 2.49049 [Å];
10
20
30
Position [°2Theta] (Copper (Cu))

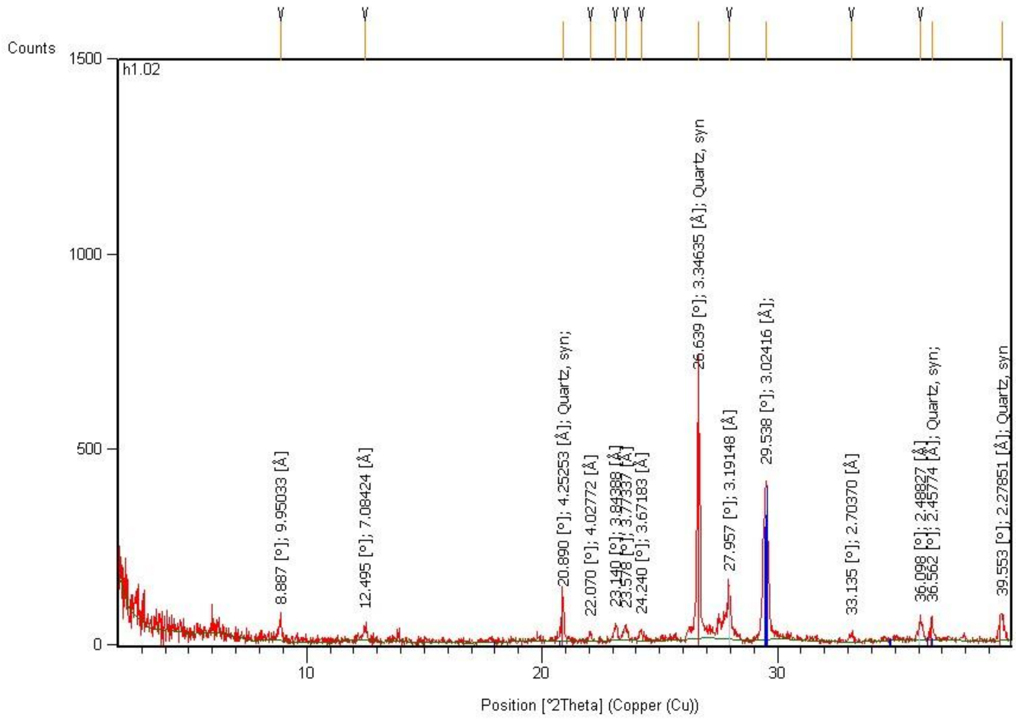

Counts
h1.02
1500
1000
500
0
8.887 [°]; 9.95033 [Å]
12.495 [°]; 7.08424 [Å]
20.890 [°]; 4.25253 [Å]; Quartz, syn;
22.070 [°]; 4.02772 [Å]
24.240 [°]; 3.67183 [Å]
26.639 [°]; 3.34635 [Å]; Quartz, syn
27.957 [°]; 3.19148 [Å]
29.538 [°]; 3.02416 [Å];
33.135 [°]; 2.70370 [Å]
39.553 [°]; 2.27851 [Å]; Quartz, syn
10
20
30
Position [°2Theta] (Copper (Cu))

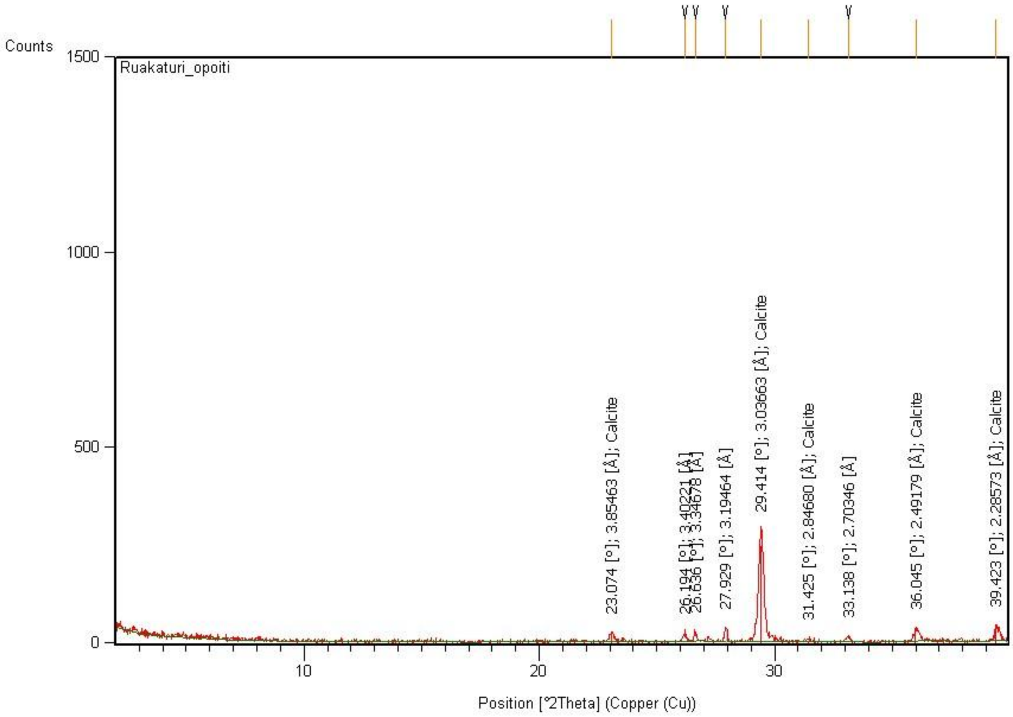
Counts
Ruakaturi_opoiti
1500
1000
500
0
10
20
30
23.074 [°]; 3.85463 [Å]; Calcite
26.194 [°]; 3.40221 [Å]
26.636 [°]; 3.34678 [Å]
27.929 [°]; 3.19464 [Å]
29.414 [°]; 3.03663 [Å]; Calcite
31.425 [°]; 2.84680 [Å]; Calcite
33.138 [°]; 2.70346 [Å]
36.045 [°]; 2.49179 [Å]; Calcite
39.423 [°]; 2.28573 [Å]; Calcite
Position [°2Theta] (Copper (Cu))

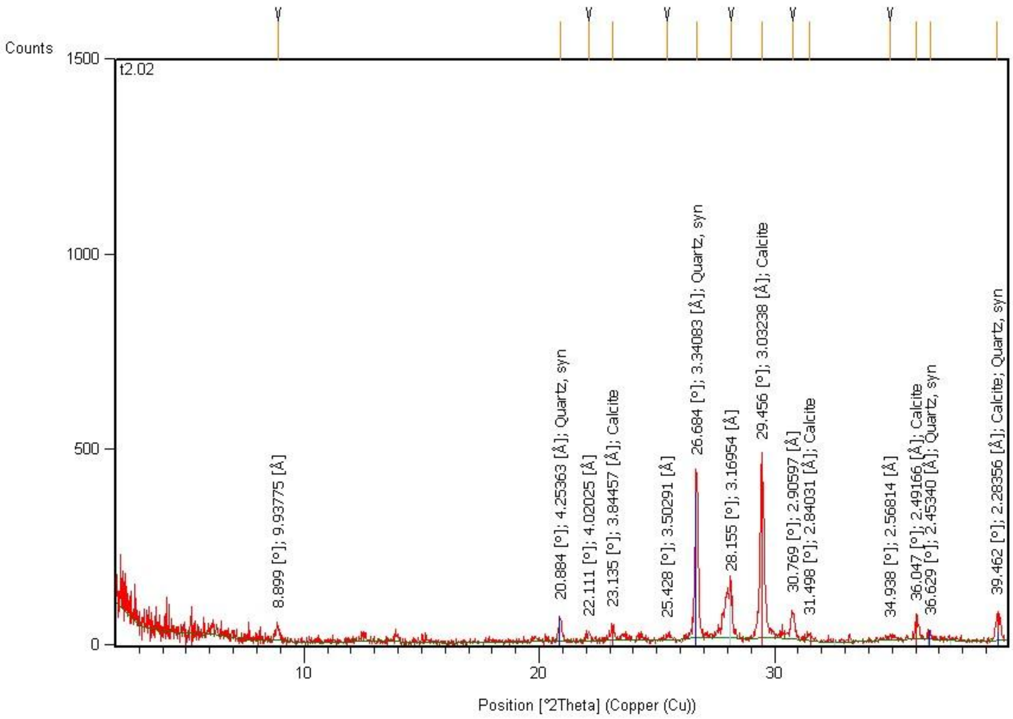
Counts
t2.02
1500
1000
500
0
10
20
30
8.899 [°]; 9.93775 [Å]
20.884 [°]; 4.25363 [Å]; Quartz, syn
22.111 [°]; 4.02025 [Å]
23.135 [°]; 3.84457 [Å]; Calcite
25.428 [°]; 3.50291 [Å]
26.684 [°]; 3.34083 [Å]; Quartz, syn
28.155 [°]; 3.16954 [Å]
29.456 [°]; 3.03238 [Å]; Calcite
30.769 [°]; 2.90597 [Å]
31.498 [°]; 2.84031 [Å]; Calcite
34.938 [°]; 2.56814 [Å]
36.047 [°]; 2.49166 [Å]; Calcite
36.629 [°]; 2.45340 [Å]; Quartz, syn
39.462 [°]; 2.28356 [Å]; Calcite; Quartz, syn
Position [°2Theta] (Copper (Cu))

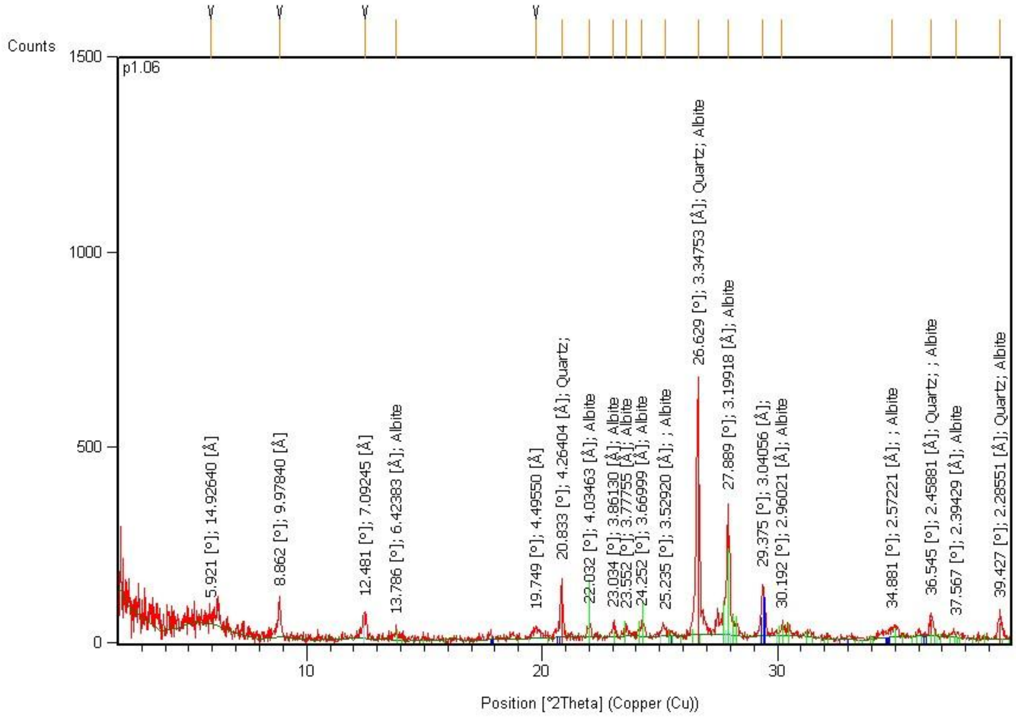
Counts
p1.06
1500
1000
500
0
10
20
30
Position [°2Theta] (Copper (Cu))
5.921 [°]; 14.92640 [Å]
8.862 [°]; 9.97840 [Å]
12.481 [°]; 7.09245 [Å]
13.786 [°]; 6.42383 [Å]; Albite
19.749 [°]; 4.49550 [Å]
20.833 [°]; 4.26404 [Å]; Quartz;
22.032 [°]; 4.03463 [Å]; Albite
23.034 [°]; 3.86130 [Å]; Albite
23.552 [°]; 3.77755 [Å]; Albite
24.252 [°]; 3.66999 [Å]; Albite
25.235 [°]; 3.52920 [Å]; ; Albite
26.629 [°]; 3.34753 [Å]; Quartz; Albite
27.889 [°]; 3.19918 [Å]; Albite
29.375 [°]; 3.04056 [Å];
30.192 [°]; 2.96021 [Å]; Albite
34.881 [°]; 2.57221 [Å]; ; Albite
36.545 [°]; 2.45881 [Å]; Quartz; ; Albite
37.567 [°]; 2.39429 [Å]; Albite
39.427 [°]; 2.28551 [Å]; Quartz; Albite

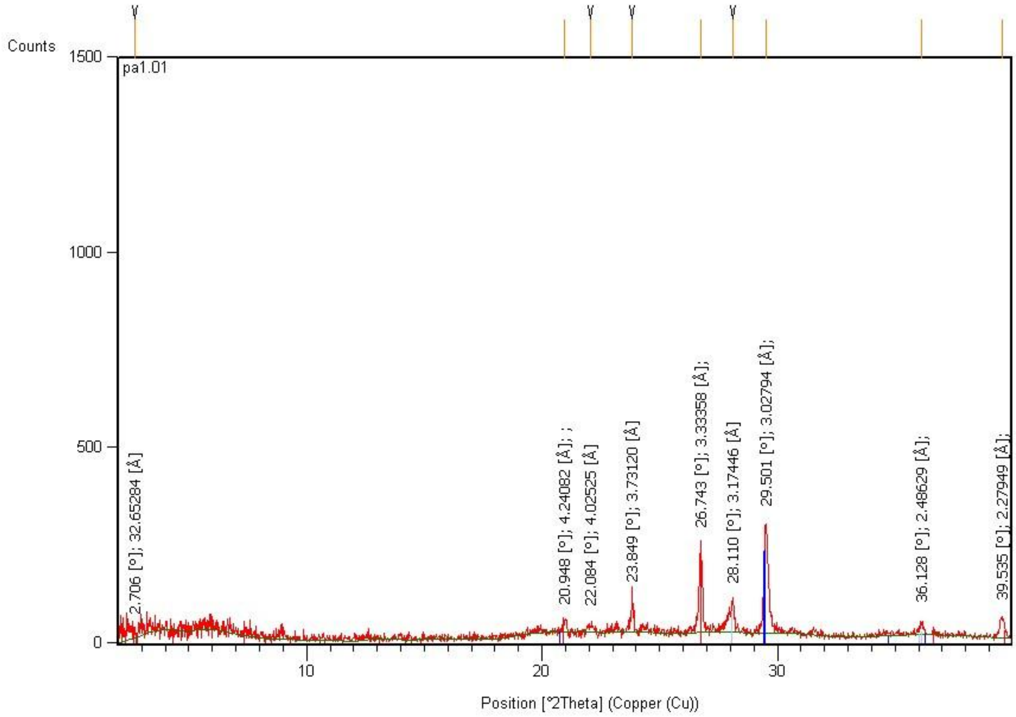
Counts
pa1.01
1500
1000
500
0
10
20
30
Position [°2Theta] (Copper (Cu))
2.706 [°]; 32.65284 [Å]
20.948 [°]; 4.24082 [Å]; ;
22.084 [°]; 4.02525 [Å]
23.849 [°]; 3.73120 [Å]
26.743 [°]; 3.33358 [Å];
28.110 [°]; 3.17446 [Å]
29.501 [°]; 3.02794 [Å];
36.128 [°]; 2.48629 [Å];
39.535 [°]; 2.27949 [Å];

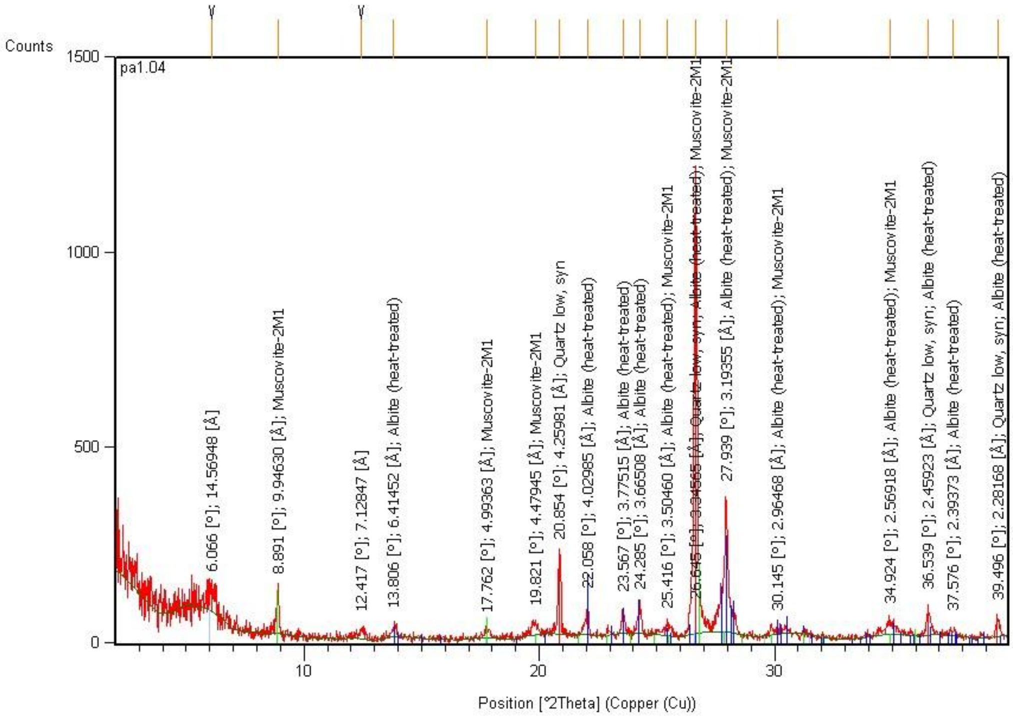
Counts
1500
1000
500
0
pa1.04
6.066 [°]; 14.56948 [Å]
8.891 [°]; 9.94630 [Å]; Muscovite-2M1
12.417 [°]; 7.12847 [Å]
13.806 [°]; 6.41452 [Å]; Albite (heat-treated)
17.762 [°]; 4.99363 [Å]; Muscovite-2M1
19.821 [°]; 4.47945 [Å]; Muscovite-2M1
20.854 [°]; 4.25981 [Å]; Quartz low, syn
22.058 [°]; 4.02985 [Å]; Albite (heat-treated)
23.567 [°]; 3.77515 [Å]; Albite (heat-treated)
24.285 [°]; 3.66508 [Å]; Albite (heat-treated)
25.416 [°]; 3.50460 [Å]; Albite (heat-treated); Muscovite-2M1
26.645 [°]; 3.34565 [Å]; Quartz low, syn; Albite (heat-treated); Muscovite-2M1
27.939 [°]; 3.19355 [Å]; Albite (heat-treated); Muscovite-2M1
30.145 [°]; 2.96468 [Å]; Albite (heat-treated); Muscovite-2M1
34.924 [°]; 2.56918 [Å]; Albite (heat-treated); Muscovite-2M1
36.539 [°]; 2.45923 [Å]; Quartz low, syn; Albite (heat-treated)
37.576 [°]; 2.39373 [Å]; Albite (heat-treated)
39.496 [°]; 2.28168 [Å]; Quartz low, syn; Albite (heat-treated)
10
20
30
Position [°2Theta] (Copper (Cu))

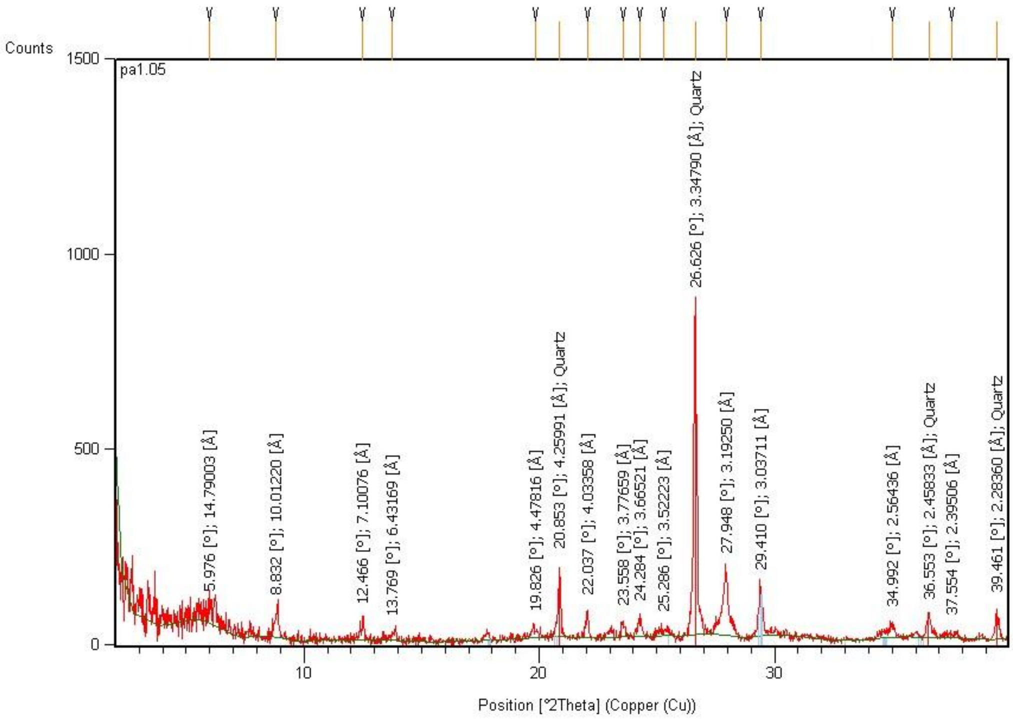
Counts
1500
1000
500
0
pa1.05
5.976 [°]; 14.79003 [Å]
8.832 [°]; 10.01220 [Å]
12.466 [°]; 7.10076 [Å]
13.769 [°]; 6.43169 [Å]
19.826 [°]; 4.47816 [Å]
20.853 [°]; 4.25991 [Å]; Quartz
22.037 [°]; 4.03358 [Å]
23.558 [°]; 3.77659 [Å]
24.284 [°]; 3.66521 [Å]
25.286 [°]; 3.52223 [Å]
26.626 [°]; 3.34790 [Å]; Quartz
27.948 [°]; 3.19250 [Å]
29.410 [°]; 3.03711 [Å]
34.992 [°]; 2.56436 [Å]
36.553 [°]; 2.45833 [Å]; Quartz
37.554 [°]; 2.39506 [Å]
39.461 [°]; 2.28360 [Å]; Quartz
10
20
30
Position [°2Theta] (Copper (Cu))

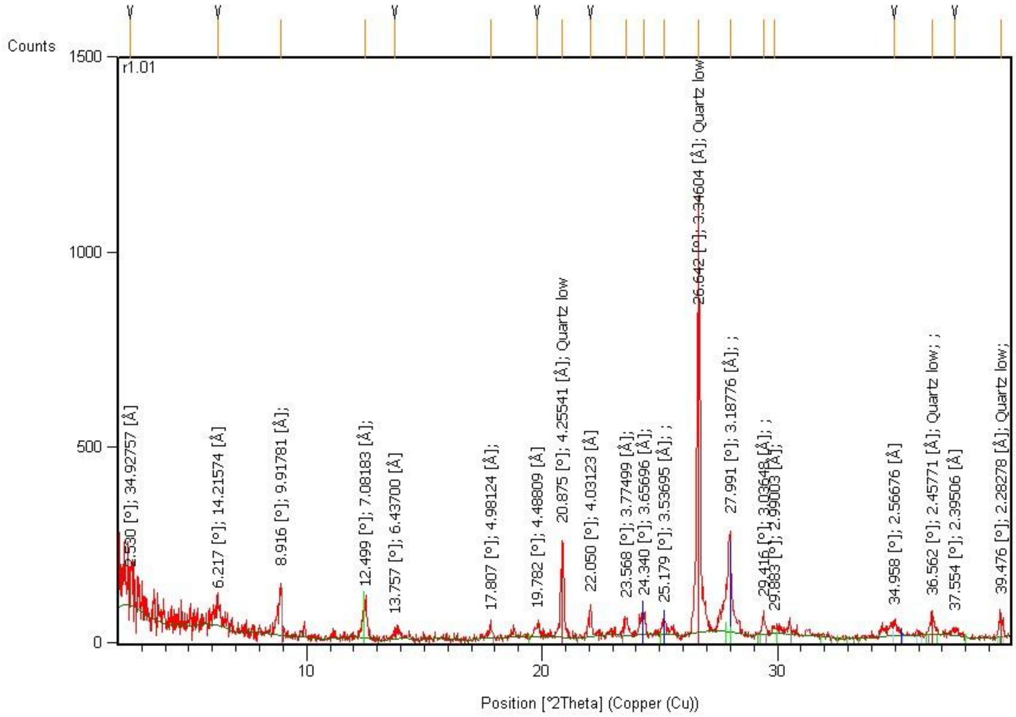
Counts
1500
1000
500
0
r1.01
2.530 [°]; 34.92757 [Å]
6.217 [°]; 14.21574 [Å]
8.916 [°]; 9.91781 [Å];
12.499 [°]; 7.08183 [Å];
13.757 [°]; 6.43700 [Å]
17.807 [°]; 4.98124 [Å];
19.782 [°]; 4.48809 [Å]
20.875 [°]; 4.25541 [Å]; Quartz low
22.050 [°]; 4.03123 [Å]
23.568 [°]; 3.77499 [Å];
24.340 [°]; 3.65696 [Å];
25.179 [°]; 3.53695 [Å]; ;
26.642 [°]; 3.34604 [Å]; Quartz low
27.991 [°]; 3.18776 [Å]; ;
29.416 [°]; 3.03648 [Å]; ;
29.883 [°]; 2.99003 [Å];
34.958 [°]; 2.56676 [Å]
36.562 [°]; 2.45771 [Å]; Quartz low; ;
37.554 [°]; 2.39506 [Å]
39.476 [°]; 2.28278 [Å]; Quartz low;
10
20
30
Position [°2Theta] (Copper (Cu))

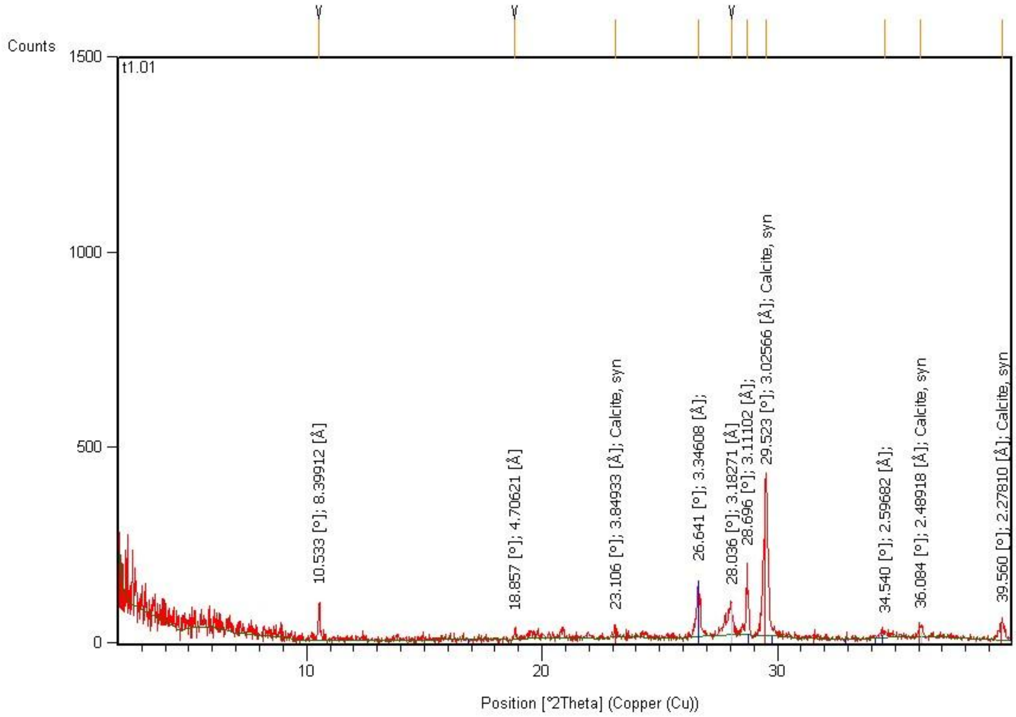
Counts
1500
1000
500
0
t1.01
10.533 [°]; 8.39912 [Å]
18.857 [°]; 4.70621 [Å]
23.106 [°]; 3.84933 [Å]; Calcite, syn
26.641 [°]; 3.34608 [Å];
28.036 [°]; 3.18271 [Å]
28.696 [°]; 3.11102 [Å];
29.523 [°]; 3.02566 [Å]; Calcite, syn
34.540 [°]; 2.59682 [Å];
36.084 [°]; 2.48918 [Å]; Calcite, syn
39.560 [°]; 2.27810 [Å]; Calcite, syn
10
20
30
Position [°2Theta] (Copper (Cu))

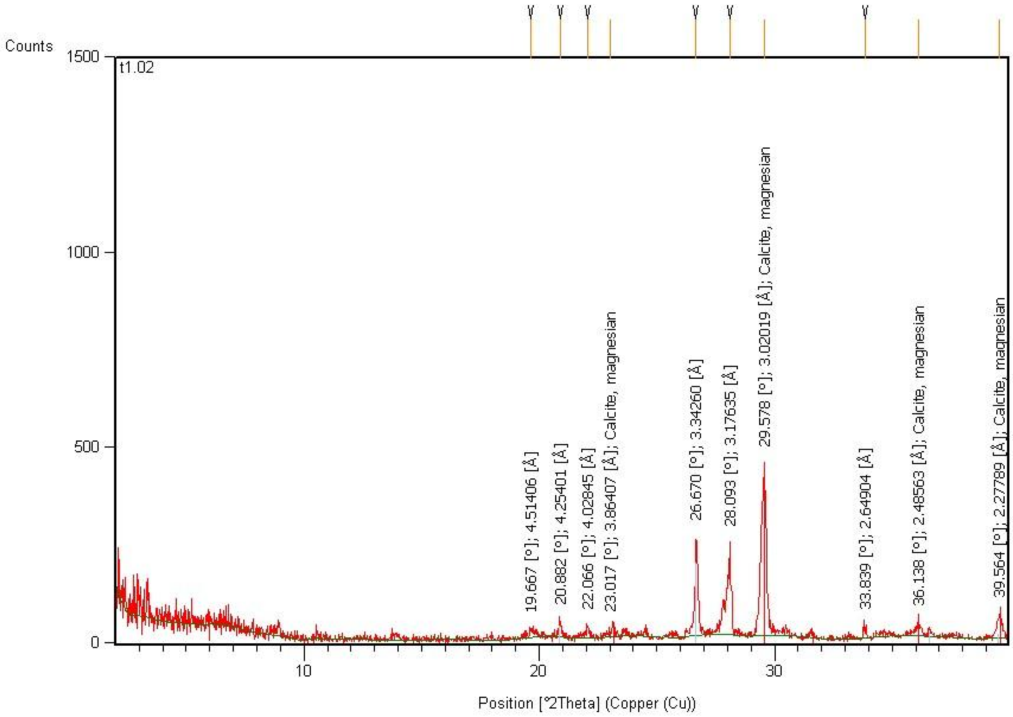
Counts
t1.02
19.667 [°]; 4.51406 [Å]
20.882 [°]; 4.25401 [Å]
22.066 [°]; 4.02845 [Å]
23.017 [°]; 3.86407 [Å]; Calcite, magnesian
26.670 [°]; 3.34260 [Å]
28.093 [°]; 3.17635 [Å]
29.578 [°]; 3.02019 [Å]; Calcite, magnesian
33.839 [°]; 2.64904 [Å]
36.138 [°]; 2.48563 [Å]; Calcite, magnesian
39.564 [°]; 2.27789 [Å]; Calcite, magnesian
Position [°2Theta] (Copper (Cu))

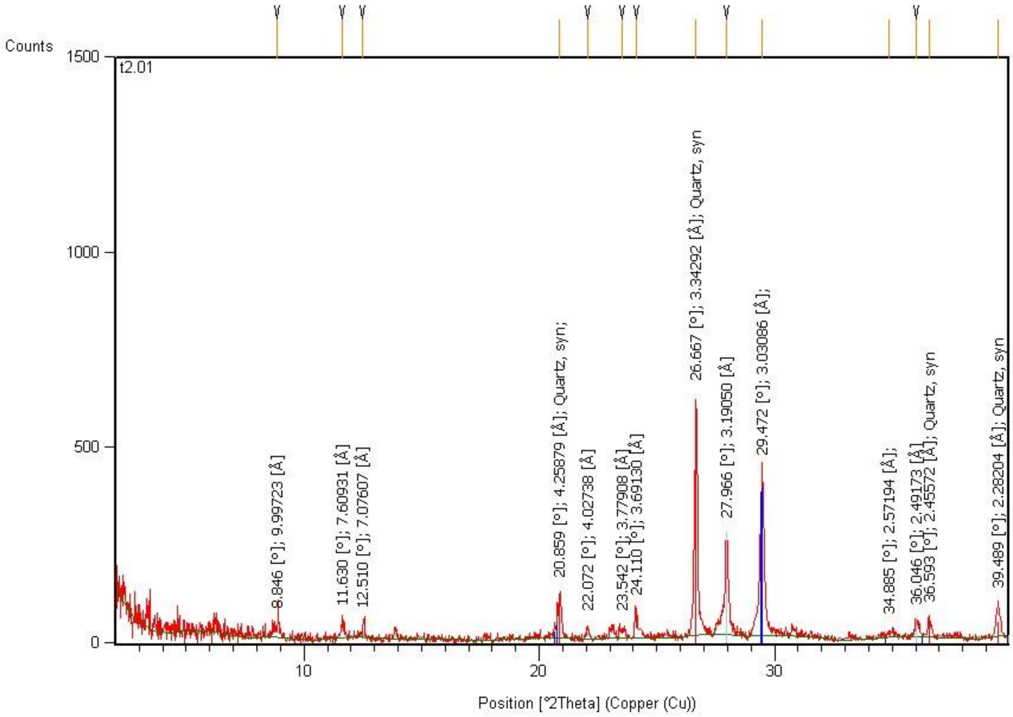
Counts
t2.01
8.846 [°]; 9.99723 [Å]
11.630 [°]; 7.60931 [Å]
12.510 [°]; 7.07607 [Å]
20.859 [°]; 4.25879 [Å]; Quartz, syn;
22.072 [°]; 4.02738 [Å]
23.542 [°]; 3.77908 [Å]
24.110 [°]; 3.69130 [Å]
26.667 [°]; 3.34292 [Å]; Quartz, syn
27.966 [°]; 3.19050 [Å]
29.472 [°]; 3.03086 [Å];
34.885 [°]; 2.57194 [Å];
36.046 [°]; 2.49173 [Å]
36.593 [°]; 2.45572 [Å]; Quartz, syn
39.489 [°]; 2.28204 [Å]; Quartz, syn
Position [°2Theta] (Copper (Cu))

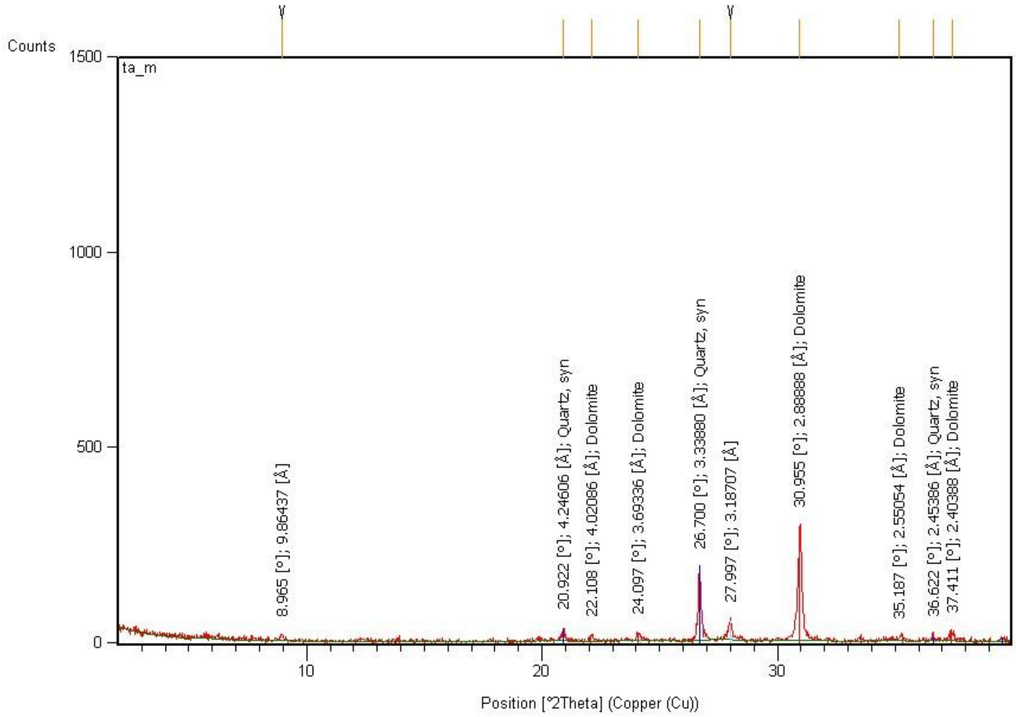
Counts
1500
1000
500
0
ta_m
8.965 [°]; 9.86437 [Å]
20.922 [°]; 4.24606 [Å]; Quartz, syn
22.108 [°]; 4.02086 [Å]; Dolomite
24.097 [°]; 3.69336 [Å]; Dolomite
26.700 [°]; 3.33880 [Å]; Quartz, syn
27.997 [°]; 3.18707 [Å]
30.955 [°]; 2.88888 [Å]; Dolomite
35.187 [°]; 2.55054 [Å]; Dolomite
36.622 [°]; 2.45386 [Å]; Quartz, syn
37.411 [°]; 2.40388 [Å]; Dolomite
10
20
30
Position [°2Theta] (Copper (Cu))

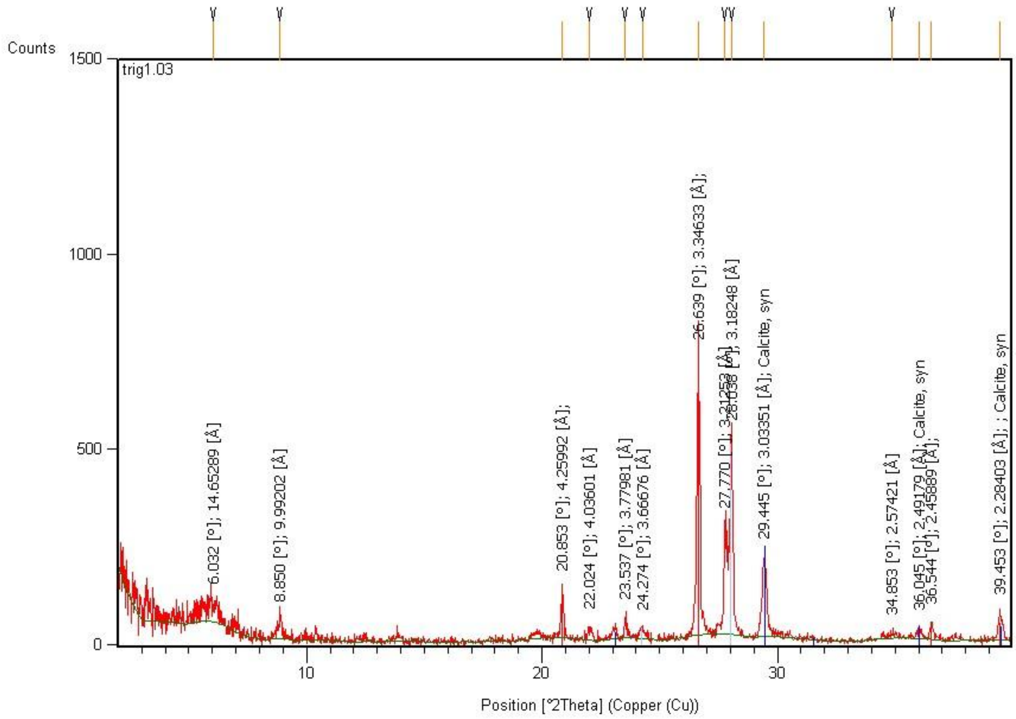
Counts
1500
1000
500
0
trig1.03
6.032 [°]; 14.65289 [Å]
8.850 [°]; 9.99202 [Å]
20.853 [°]; 4.25992 [Å];
22.024 [°]; 4.03601 [Å]
23.537 [°]; 3.77981 [Å]
24.274 [°]; 3.66676 [Å]
26.639 [°]; 3.34633 [Å];
27.770 [°]; 3.21253 [Å]
3.18248 [Å]
29.445 [°]; 3.03351 [Å]; Calcite, syn
34.853 [°]; 2.57421 [Å]
Calcite, syn
39.453 [°]; 2.28403 [Å]; ; Calcite, syn
10
20
30
Position [°2Theta] (Copper (Cu))

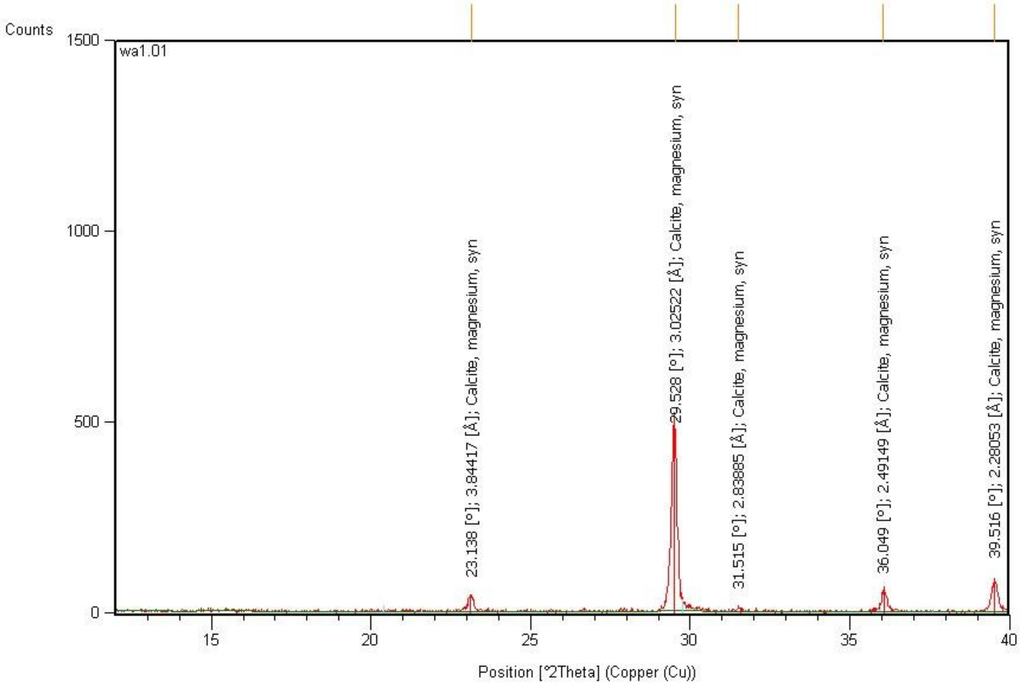
Counts
wa1.01
23.138 [°]; 3.84417 [Å]; Calcite, magnesium, syn
29.528 [°]; 3.02522 [Å]; Calcite, magnesium, syn
31.515 [°]; 2.83885 [Å]; Calcite, magnesium, syn
36.049 [°]; 2.49149 [Å]; Calcite, magnesium, syn
39.516 [°]; 2.28053 [Å]; Calcite, magnesium, syn
Position [°2Theta] (Copper (Cu))

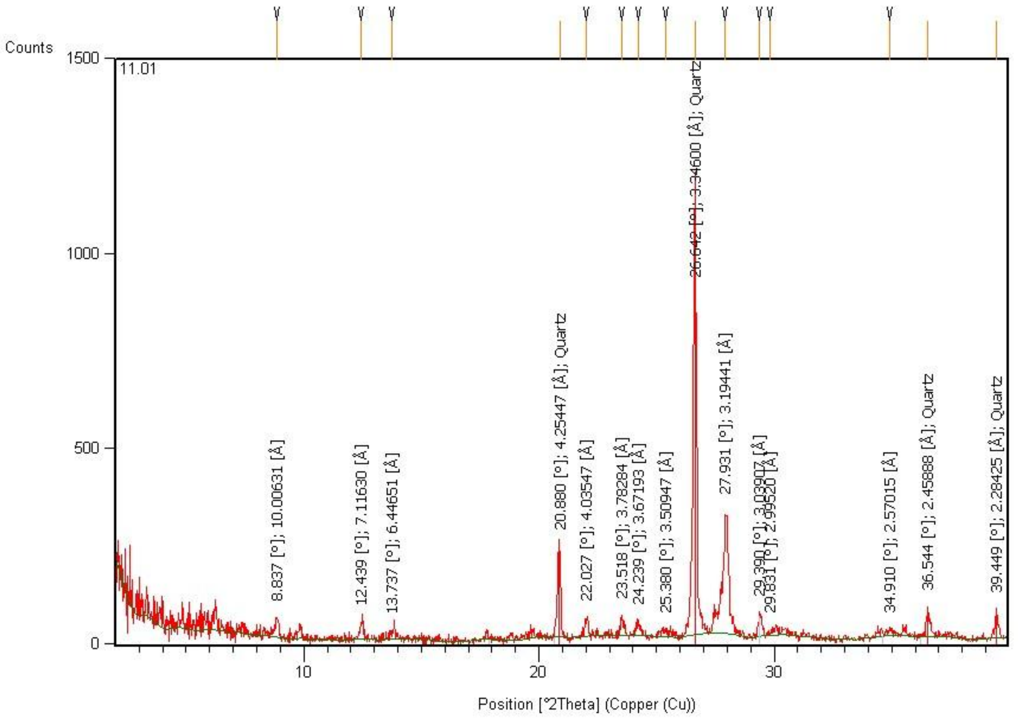
Counts
11.01
8.837 [°]; 10.00631 [Å]
12.439 [°]; 7.11630 [Å]
13.737 [°]; 6.44651 [Å]
20.880 [°]; 4.25447 [Å]; Quartz
22.027 [°]; 4.03547 [Å]
23.518 [°]; 3.78284 [Å]
24.239 [°]; 3.67193 [Å]
25.380 [°]; 3.50947 [Å]
26.642 [°]; 3.34600 [Å]; Quartz
27.931 [°]; 3.19441 [Å]
34.910 [°]; 2.57015 [Å]
36.544 [°]; 2.45688 [Å]; Quartz
39.449 [°]; 2.28425 [Å]; Quartz
Position [°2Theta] (Copper (Cu))

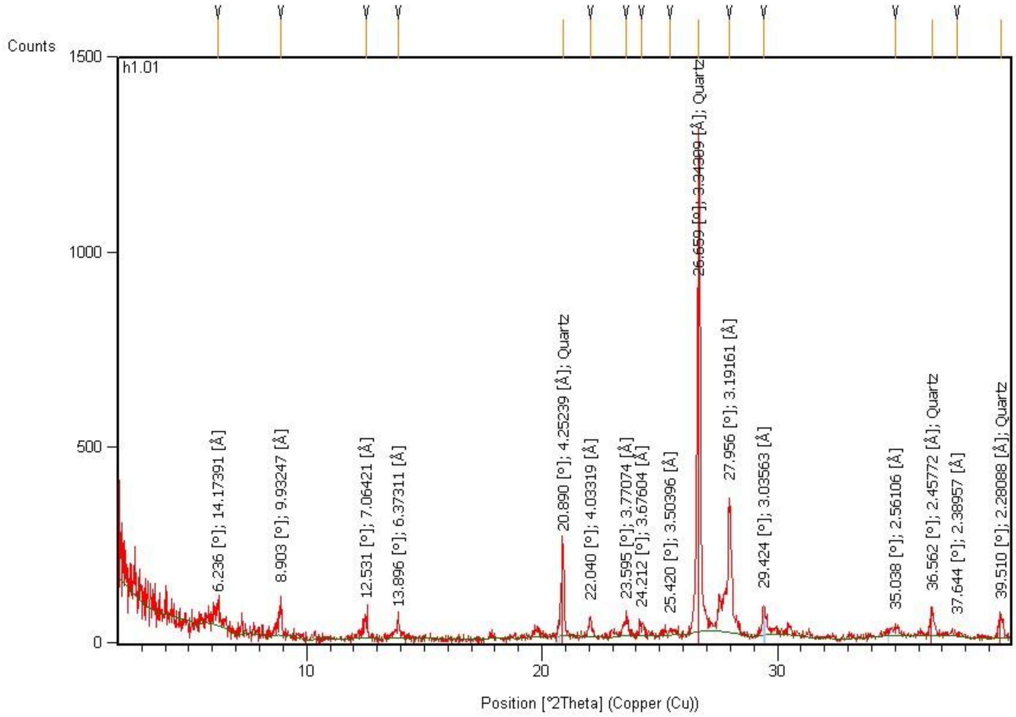

Counts
h1.01
Position [°2Theta] (Copper (Cu))

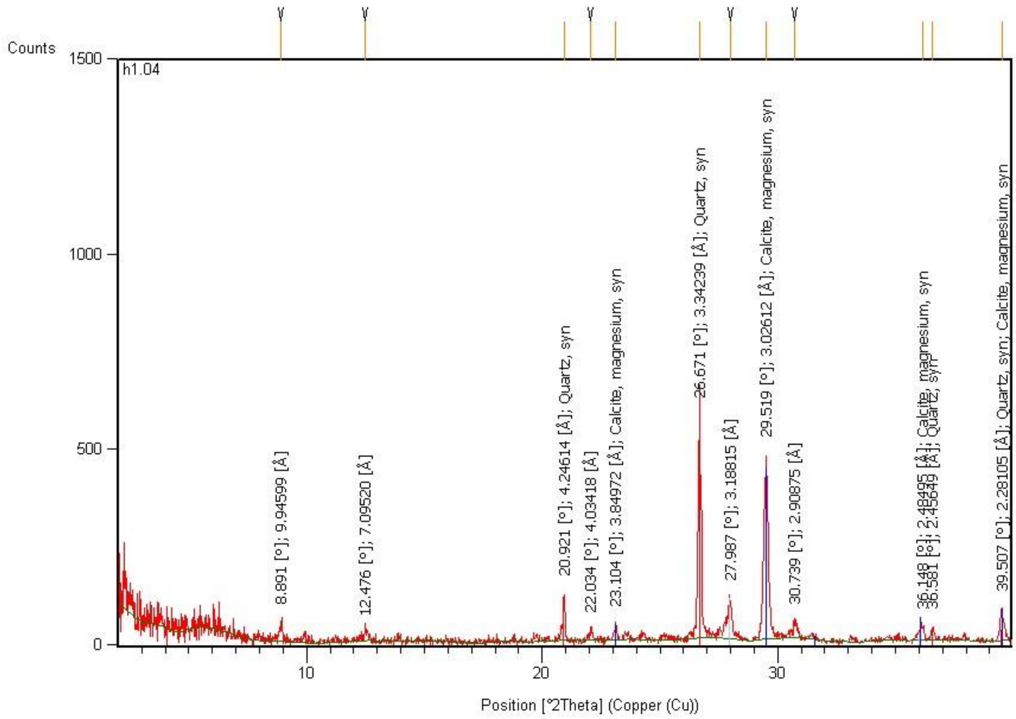

Counts
h1.04
Position [°2Theta] (Copper (Cu))

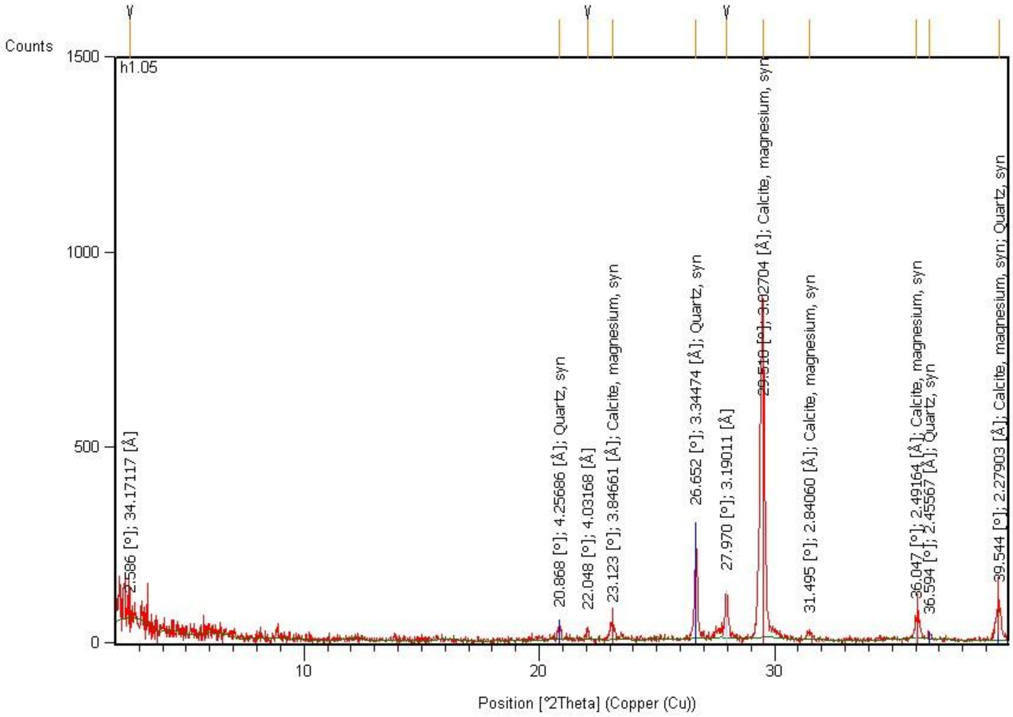
Counts
h1.05
1500
1000
500
0
10
20
30
Position [°2Theta] (Copper (Cu))
2.586 [°]; 34.17117 [Å]
20.868 [°]; 4.25686 [Å]; Quartz, syn
22.048 [°]; 4.03168 [Å]
23.123 [°]; 3.84661 [Å]; Calcite, magnesium, syn
26.652 [°]; 3.34474 [Å]; Quartz, syn
27.970 [°]; 3.19011 [Å]
29.510 [°]; 3.02704 [Å]; Calcite, magnesium, syn
31.495 [°]; 2.84060 [Å]; Calcite, magnesium, syn
36.047 [°]; 2.49164 [Å]; Calcite, magnesium, syn
36.594 [°]; 2.45567 [Å]; Quartz, syn
39.544 [°]; 2.27903 [Å]; Calcite, magnesium, syn; Quartz, syn

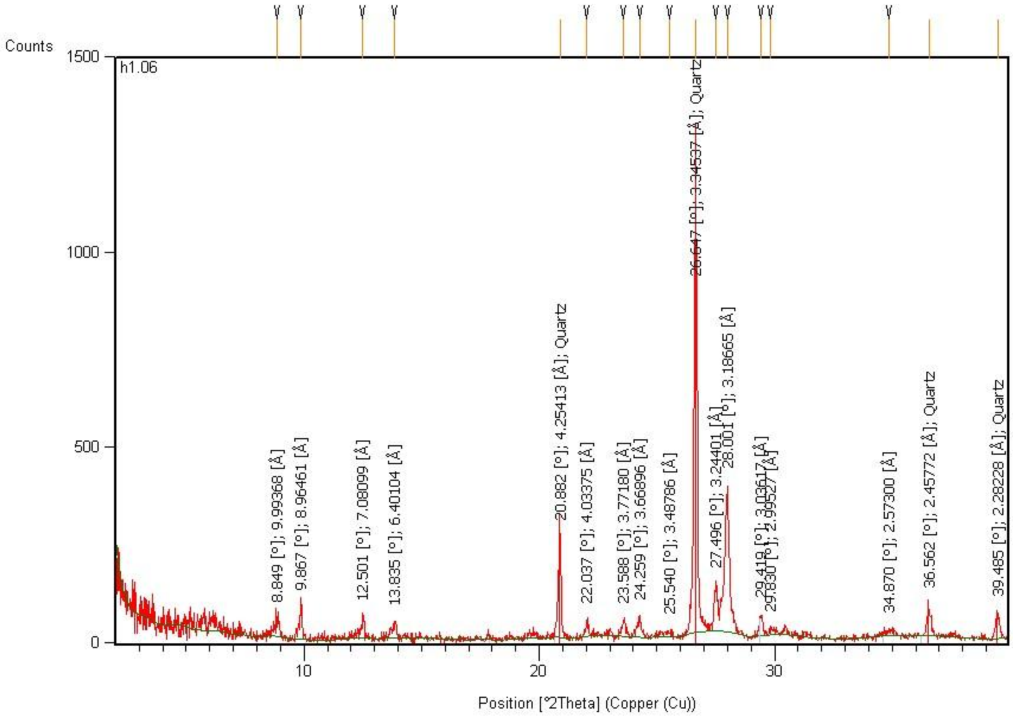
Counts
h1.06
1500
1000
500
0
10
20
30
Position [°2Theta] (Copper (Cu))
8.849 [°]; 9.99368 [Å]
9.867 [°]; 8.96461 [Å]
12.501 [°]; 7.08099 [Å]
13.835 [°]; 6.40104 [Å]
20.882 [°]; 4.25413 [Å]; Quartz
22.037 [°]; 4.03375 [Å]
23.588 [°]; 3.77180 [Å]
24.259 [°]; 3.66896 [Å]
25.540 [°]; 3.48786 [Å]
26.647 [°]; 3.34537 [Å]; Quartz
27.496 [°]; 3.24401 [Å]
28.001 [°]; 3.18665 [Å]
29.419 [°]; 3.03617 [Å]
29.830 [°]; 2.99527 [Å]
34.870 [°]; 2.57300 [Å]
36.562 [°]; 2.45772 [Å]; Quartz
39.485 [°]; 2.28228 [Å]; Quartz

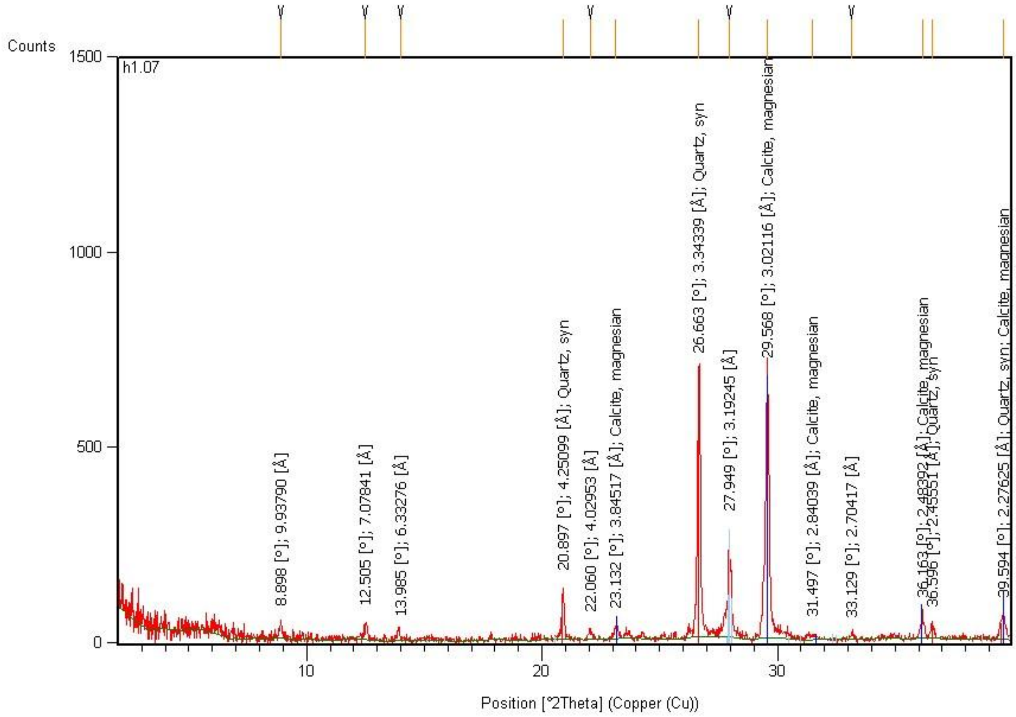
Counts
h1.07
Position [°2Theta] (Copper (Cu))
8.898 [°]; 9.93790 [Å]
12.505 [°]; 7.07841 [Å]
13.985 [°]; 6.33276 [Å]
20.897 [°]; 4.25099 [Å]; Quartz, syn
22.060 [°]; 4.02953 [Å]
23.132 [°]; 3.84517 [Å]; Calcite, magnesian
26.663 [°]; 3.34339 [Å]; Quartz, syn
27.949 [°]; 3.19245 [Å]
29.568 [°]; 3.02116 [Å]; Calcite, magnesian
31.497 [°]; 2.84039 [Å]; Calcite, magnesian
33.129 [°]; 2.70417 [Å]
39.594 [°]; 2.27625 [Å]; Quartz, syn; Calcite, magnesian

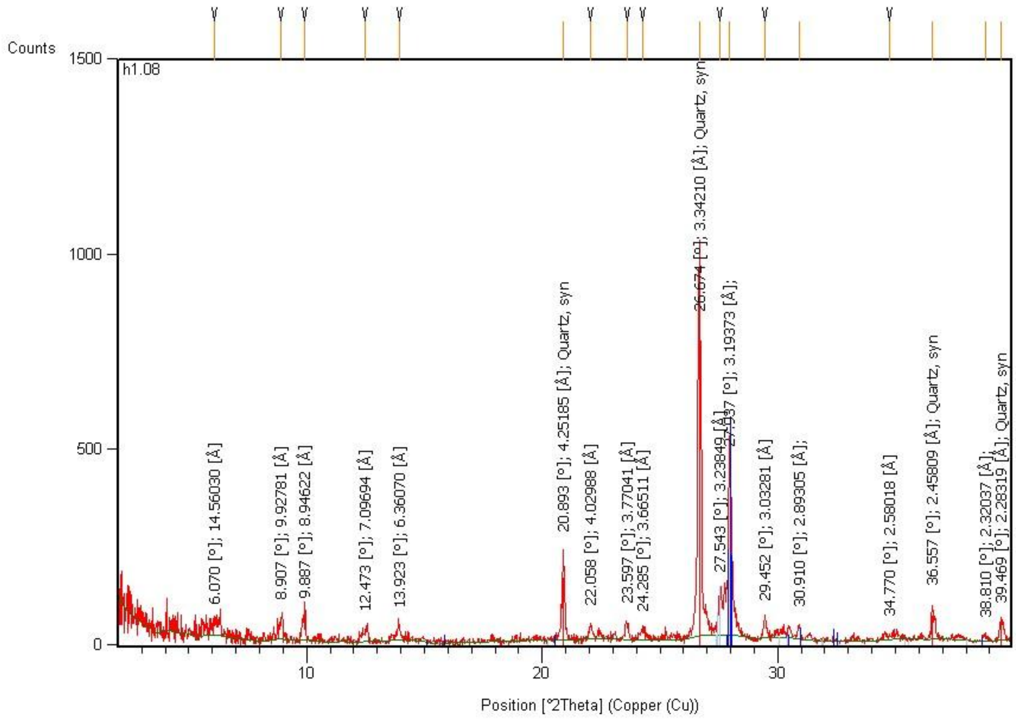
Counts
h1.08
Position [°2Theta] (Copper (Cu))
6.070 [°]; 14.56030 [Å]
8.907 [°]; 9.92781 [Å]
9.887 [°]; 8.94622 [Å]
12.473 [°]; 7.09694 [Å]
13.923 [°]; 6.36070 [Å]
20.893 [°]; 4.25185 [Å]; Quartz, syn
22.058 [°]; 4.02988 [Å]
23.597 [°]; 3.77041 [Å]
24.285 [°]; 3.66511 [Å]
26.674 [°]; 3.34210 [Å]; Quartz, syn
29.452 [°]; 3.03281 [Å]
30.910 [°]; 2.89305 [Å];
34.770 [°]; 2.58018 [Å]
36.557 [°]; 2.45809 [Å]; Quartz, syn

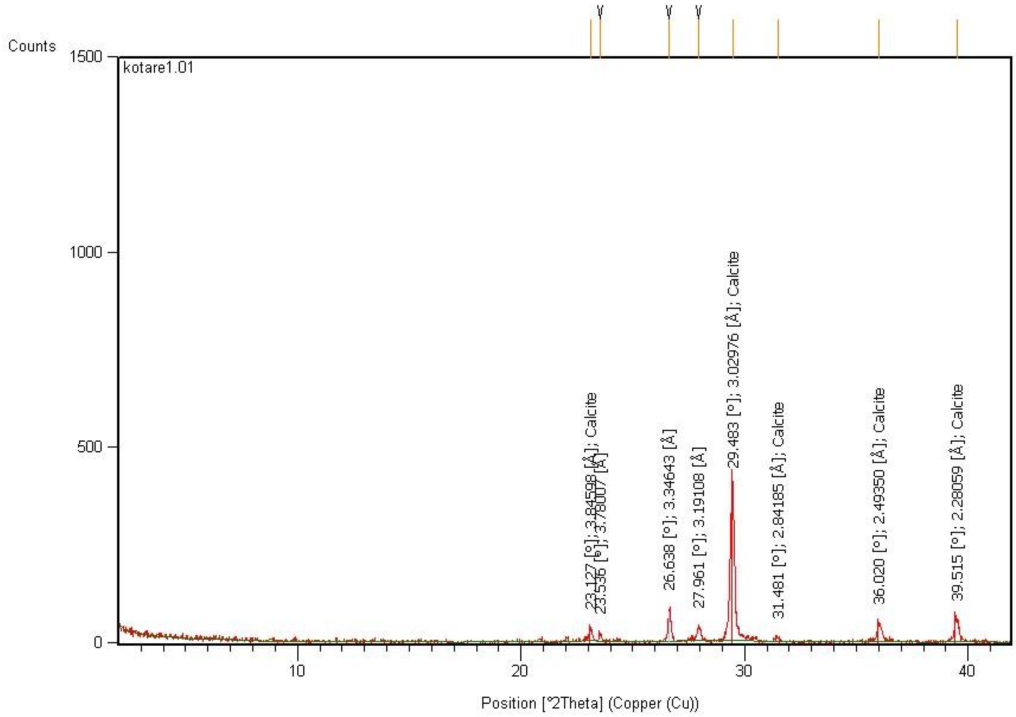
Counts
1500
1000
500
0
kotare1.01
23.127 [°]; 3.84598 [Å]; Calcite
23.536 [°]; 3.78007 [Å]
26.638 [°]; 3.34643 [Å]
27.961 [°]; 3.19108 [Å]
29.483 [°]; 3.02976 [Å]; Calcite
31.481 [°]; 2.84185 [Å]; Calcite
36.020 [°]; 2.49350 [Å]; Calcite
39.515 [°]; 2.28059 [Å]; Calcite
10
20
30
40
Position [°2Theta] (Copper (Cu))

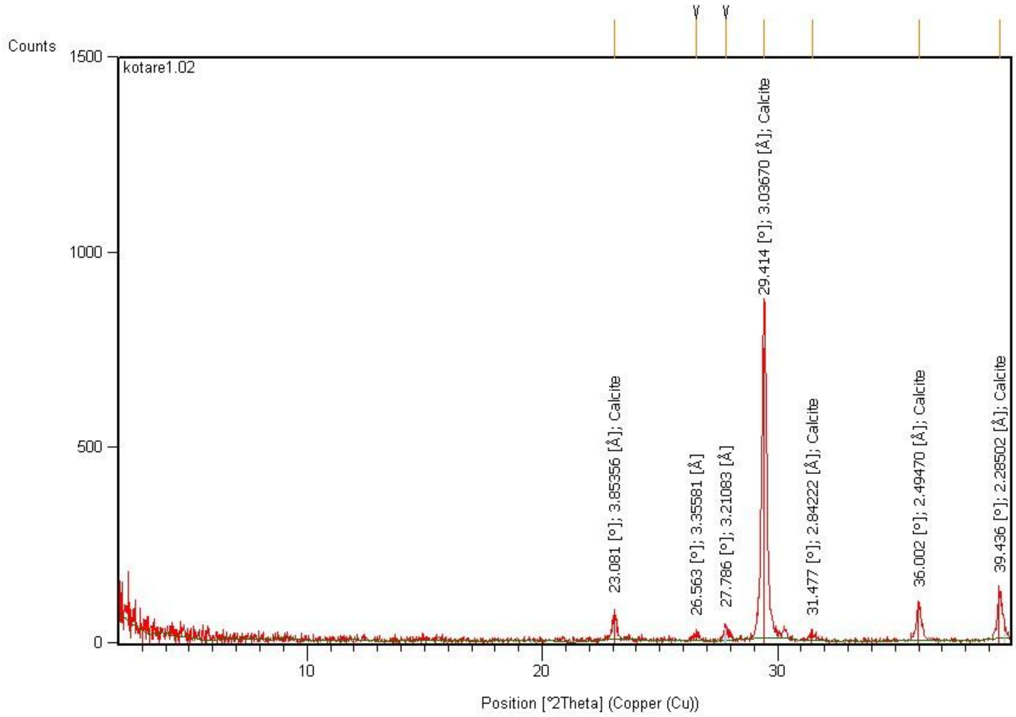
Counts
1500
1000
500
0
kotare1.02
23.081 [°]; 3.85356 [Å]; Calcite
26.563 [°]; 3.35581 [Å]
27.786 [°]; 3.21083 [Å]
29.414 [°]; 3.03670 [Å]; Calcite
31.477 [°]; 2.84222 [Å]; Calcite
36.002 [°]; 2.49470 [Å]; Calcite
39.436 [°]; 2.28502 [Å]; Calcite
10
20
30
Position [°2Theta] (Copper (Cu))

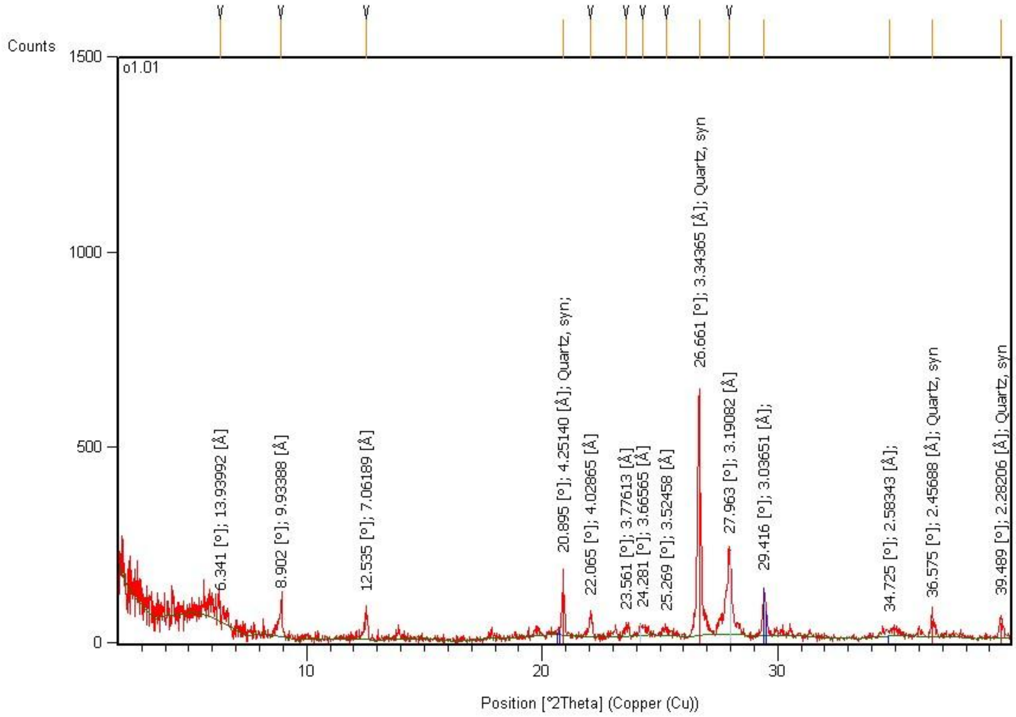
Counts
o1.01
6.341 [°]; 13.93992 [Å]
8.902 [°]; 9.93388 [Å]
12.535 [°]; 7.06189 [Å]
20.895 [°]; 4.25140 [Å]; Quartz, syn;
22.065 [°]; 4.02865 [Å]
23.561 [°]; 3.77613 [Å]
24.281 [°]; 3.66565 [Å]
25.269 [°]; 3.52458 [Å]
26.661 [°]; 3.34365 [Å]; Quartz, syn
27.963 [°]; 3.19082 [Å]
29.416 [°]; 3.03651 [Å];
34.725 [°]; 2.58343 [Å];
36.575 [°]; 2.45688 [Å]; Quartz, syn
39.489 [°]; 2.28206 [Å]; Quartz, syn
Position [°2Theta] (Copper (Cu))

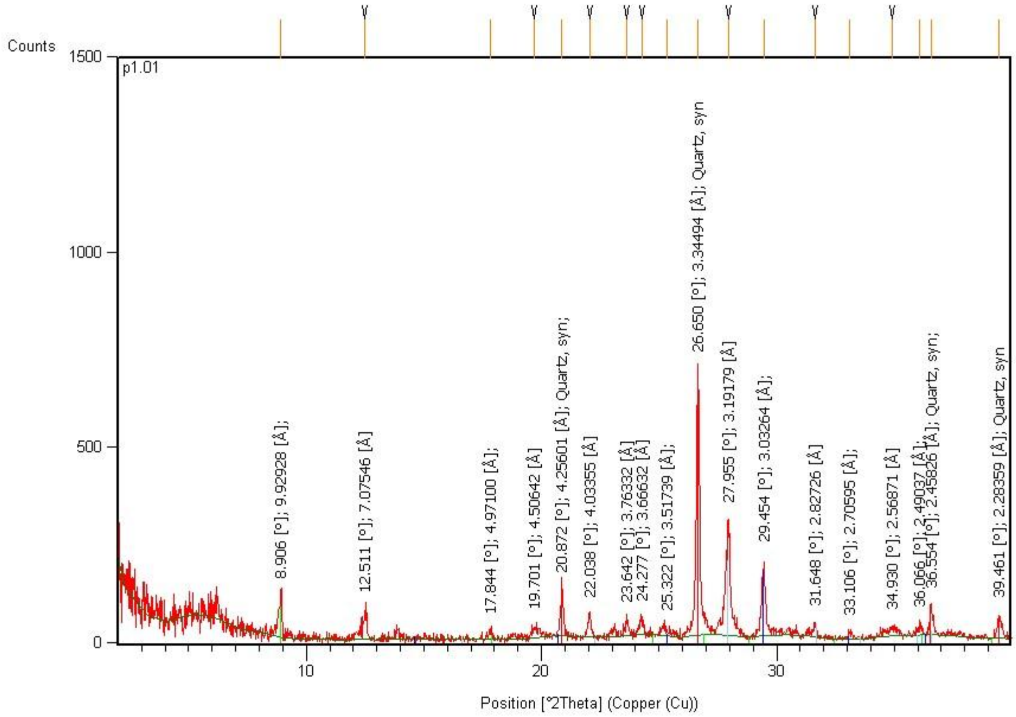
Counts
p1.01
8.906 [°]; 9.92928 [Å];
12.511 [°]; 7.07546 [Å]
17.844 [°]; 4.97100 [Å];
19.701 [°]; 4.50642 [Å]
20.872 [°]; 4.25601 [Å]; Quartz, syn;
22.038 [°]; 4.03355 [Å]
23.642 [°]; 3.76332 [Å]
24.277 [°]; 3.66632 [Å]
25.322 [°]; 3.51739 [Å];
26.650 [°]; 3.34494 [Å]; Quartz, syn
27.955 [°]; 3.19179 [Å]
29.454 [°]; 3.03264 [Å];
31.648 [°]; 2.82726 [Å]
33.106 [°]; 2.70595 [Å];
34.930 [°]; 2.56871 [Å]
36.066 [°]; 2.49037 [Å];
36.554 [°]; 2.45826 [Å]; Quartz, syn;
39.461 [°]; 2.28359 [Å]; Quartz, syn
Position [°2Theta] (Copper (Cu))

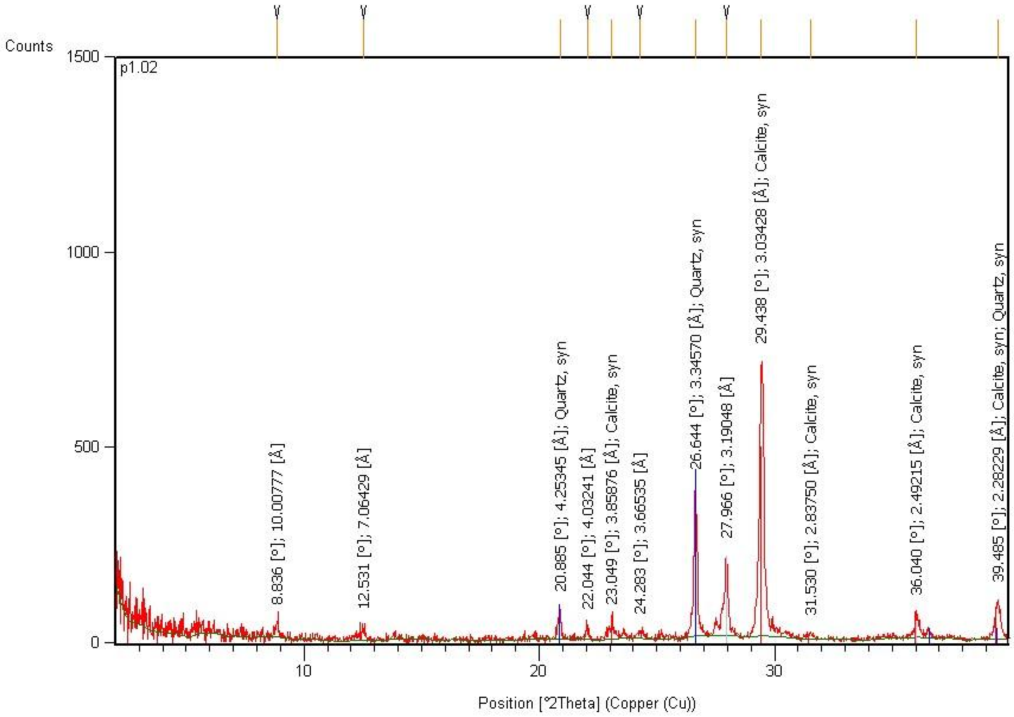
Counts
1500
1000
500
0
p1.02
8.836 [°]; 10.00777 [Å]
12.531 [°]; 7.06429 [Å]
20.885 [°]; 4.25345 [Å]; Quartz, syn
22.044 [°]; 4.03241 [Å]
23.049 [°]; 3.85876 [Å]; Calcite, syn
24.283 [°]; 3.66535 [Å]
26.644 [°]; 3.34570 [Å]; Quartz, syn
27.966 [°]; 3.19048 [Å]
29.438 [°]; 3.03428 [Å]; Calcite, syn
31.530 [°]; 2.83750 [Å]; Calcite, syn
36.040 [°]; 2.49215 [Å]; Calcite, syn
39.485 [°]; 2.28229 [Å]; Calcite, syn; Quartz, syn
10
20
30
Position [°2Theta] (Copper (Cu))

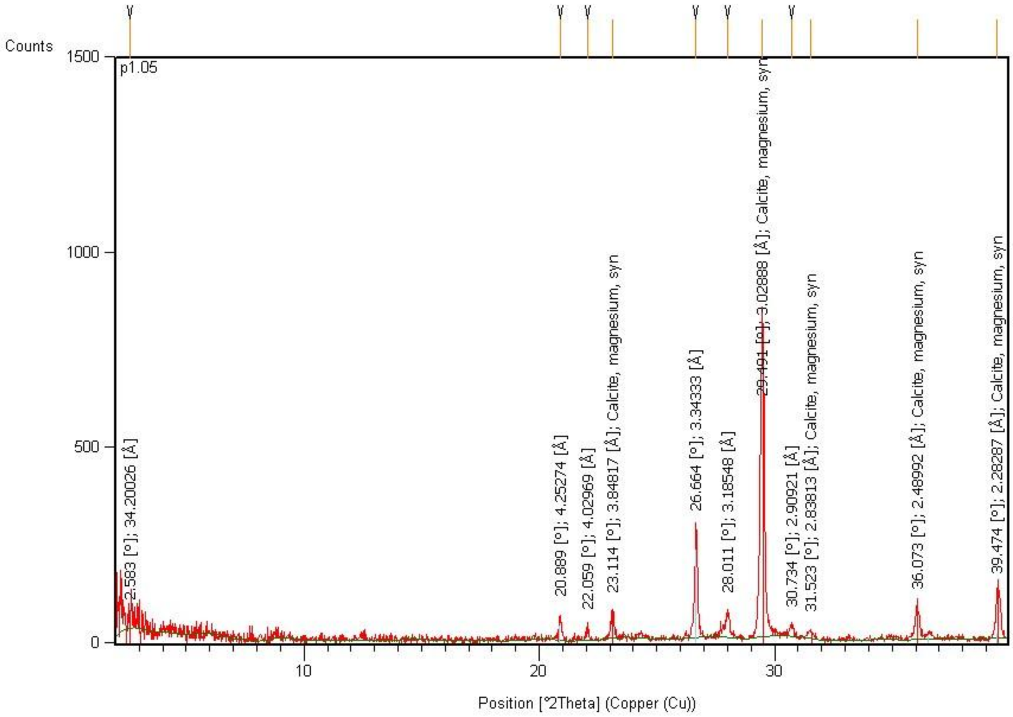
Counts
1500
1000
500
0
p1.05
2.583 [°]; 34.20026 [Å]
20.889 [°]; 4.25274 [Å]
22.059 [°]; 4.02969 [Å]
23.114 [°]; 3.84817 [Å]; Calcite, magnesium, syn
26.664 [°]; 3.34333 [Å]
28.011 [°]; 3.18548 [Å]
29.491 [°]; 3.02888 [Å]; Calcite, magnesium, syn
30.734 [°]; 2.90921 [Å]
31.523 [°]; 2.83813 [Å]; Calcite, magnesium, syn
36.073 [°]; 2.48992 [Å]; Calcite, magnesium, syn
39.474 [°]; 2.28287 [Å]; Calcite, magnesium, syn
10
20
30
Position [°2Theta] (Copper (Cu))

Appendix IV

Oxygen and carbon isotope data

Limestone Samples Waikato (May 2010)

1. Precision of Measurements

All values reported relative to vPDB, where $\delta^{13}C$ has a value of +1.95‰ and $\delta^{18}O$ has a value of -2.20‰ for NBS19 calcite

Additional NBS18 standard, due to material submitted, where $\delta^{13}C$ has a value of -5.014‰ and $\delta^{18}O$ has a value of -23.20‰

Internal precision of measurements is 0.02-0.08‰ for $\delta^{18}O$ and 0.01-0.06‰ for $\delta^{13}C$, external precision is 0.03‰ for $\delta^{18}O$ and 0.02‰ for $\delta^{13}C$, relative to vPDB

Samples were reacted with 3 drops of H_3PO_4 at 75°C in an automated individual-carbonate reaction (Kiel IV) device coupled with a Finnigan MAT253 mass spectrometer

	Precision	$\delta^{18}O$	$\delta^{13}C$
NBS19	Run 1	0.04	0.02
NBS19	Run 2	0.05	0.02
NBS18	Run 1	0.04	0.03

Balance is used as an indicator of result reliability, values approaching or less than 0.80 should be used with

caution if they are associated with a single point or outlier

Voltages below 1.2 are usually considered unreliable irrespective of balance.

2 . Results

Limestone

	Run	Sample	$\delta^{13}C$	$\delta^{18}O$	SA44[V]	ST44[V]	Balance	<1.2 volts
	Opoiti limestone							
1	1	11.02	1.18	-2.50	1.38	1.49	0.93	
2	1	11.03	0.43	-2.26	1.69	1.84	0.92	
3	2	H1.02	0.52	-0.12	1.80	1.97	0.91	
4	1	T2.02	-0.82	-0.69	2.07	2.50	0.83	
5	1	Ra/op	1.01	-1.66	2.53	2.82	0.90	
6	1	H10.03	0.95	-2.36	2.18	2.41	0.91	
	Whakapunake Limestone							
7	1	M10.06	0.09	-0.59	1.60	1.74	0.92	
8	1	M10.08	-8.62	-0.27	1.96	2.15	0.91	
9	1	M10.10	-6.24	-1.53	2.39	2.64	0.90	
10	1	M10.12	-0.57	-0.35	2.66	2.96	0.90	
11	1	M10.15	-0.44	-0.36	2.85	3.19	0.89	
12	2	M.Flow	1.45	-0.40	2.64	3.02	0.88	
	Tahaenui Limestone							
13	1	Ma1.01	-0.25	-0.97	1.58	1.71	0.92	
14	1	Ka1.02	0.02	0.02	1.29	1.38	0.94	
15	1	Ko1.01	0.05	-0.01	1.32	1.41	0.93	
16	1	R1.02	1.74	-0.56	2.09	2.31	0.91	
17	2	trig1.01	0.54	-3.13	1.78	1.98	0.90	
18	1	Ra/Ta	1.04	-0.88	1.69	2.02	0.84	
19	2	Pecten 1 (Tahaenui Limestone)	1.72	-0.36	2.17	2.40	0.90	
20	2	Pecten 2 (Whakapunake Limestone)	1.34	-0.03	1.48	1.60	0.93	
21	2	Pecten 3 (Opoiti Limestone)	0.75	-0.30	1.75	1.91	0.92	

	Limestone Cements								
	Run	$\delta^{13}C$	$\delta^{18}O$	Sample		SA44[mV]	ST44[mV]	Balance	<1.2 volts
1	1	1.16	0.26	L1	120.3	5212.36	5723.38	0.91	
2	1	1.56	0.37	L1	3	5580.64	7201.74	0.77	
3	2	1.43	0.15	L1	3	4606.66	5202.85	0.89	
4	1	0.57	-0.19	L1	107	7739.17	6413.22	0.83	
5	2	0.56	-0.15	L1	107	4704.69	5208.37	0.90	
6	1	0.90	0.01	L1	128.1	5041.72	5725.55	0.88	
7	1	-2.15	-0.21	L2	129.4	6255.05	6938.90	0.90	
8	1	-1.98	-0.14	L2	129.4	4383.36	4887.37	0.90	
9	1	0.63	-0.33	L2	112.1	7646.04	9439.81	0.81	
10	2	0.47	-0.62	L2	112.1	7349.91	7905.43	0.93	
11	1	0.30	-1.31	L2	129.1	7472.87	8447.11	0.88	
12	1	1.89	-0.17	L2	123.2	4164.97	4633.11	0.90	
13	2	1.80	-0.22	L2	123.2	5614.03	6413.73	0.88	
14	1	-0.11	-0.04	L3	129.6	4490.81	4934.66	0.91	
15	2	-0.05	0.06	L3	129.6	7957.92	10192.00	0.78	
16	1	1.91	-0.14	L3	61.2	5559.62	6352.17	0.88	
17	1	1.13	0.19	L3	106.2	5560.73	6107.64	0.91	
18	1	1.10	0.27	L3	108.2	3440.50	3796.24	0.91	
19	2	1.04	0.27	L3	108.2	4662.48	5168.36	0.90	
20	1	1.19	0.67	Barnacle		5530.44	5024.81	0.91	
21	2	1.19	0.63	Barnacle		4294.99	4755.78	0.90	
22	1	1.16	0.66	Pectinid		6752.23	7645.04	0.88	
23	1	1.16	-0.20	Brachiopod		3855.49	4268.99	0.90	

Appendix V

Petrographic data sheets

	Strat Col No.						
	Sample No.	W1.02	WA1.03	WA1.04	WA1.05	WA1.06	WA1.07
Bioclasts	**Tot Bioclasts %**	60	60	60	50	40	50
	Bivalves	C	C	S	C	M	C
	Barnacles	VC	VC	VC	C	VC	C
	Brachiopods	-	-	-	-	-	-
	Bryozoans	S	S	S	R	S	M
	Echinoderms	S	-	S	S	-	S
	Calc red algae	R	-	S	-	-	-
	Benthic forams	S	R	S	S	R	S
	Planktic forams	S	S	S	R	R	R
	Size: Max (mm)	4	10	5	9	4	9
	Mode 1	0.8	2	0.8	1.4	3.5	1.4
	Mode 2	4	5	1.8	0.5	0.9	0.5
	Sorting	P	P	P	M	P	M
	Abrasion	M-WA	M-WA	WA	WA	MA	WA
Siliciclasts	**Tot Terrigenous %**	1	2	2	2	7	5
	Quartz	S	S	S	S	M	S
	Feldspar	R	S	S	S	S	S
	Rock fragments	R	R	R	S	S	R
	Mica	-	-	-	-	-	-
	Clay	-	-	-	-	-	-
	Size: Max (mm)	0.3	0.8	0.8	0.3	1.2	0.3
	Mode 1	0.3	0.2	0.2	0.1	0.2	0.1
	Mode 2	-	-	-	0.3	-	0.3
	Sorting	W	M	W	M	P	M
	Shape	SR	SA	SA	SR-R	SR	SA-SR
Authigenic	**Tot Authigenic %**	1	3	3	7	2	<1
	Glauconite pellets	R	S	R	S	S	R
	Size (av.)	0.2	0.2	0.2	0.3	0.1	0.25
	Glauconite infills	R	S	M	S	R	R
	Pyrite grains	R	-	S	S	S	R
	Size (av.)	0.2	-	0.2	0.1	0.1	0.2
	Pyrite infills	-	-	-	-	-	-
Diagenetic	**Matrix-Cement %**	30	45	40	35	35	35
	Intrinsic material	MS	SM	SM	S	S	S
	Extrinsic material	SM	SM	MS	MS	MS	SM
	Spar cement	7	40	30	25	25	30
	Micrite	23	5	10	10	10	5
	Porosity %	8	10	10	5	15	10
	Other features	NEO	NEO	NEO	NEO	NEO	NEO
		PS	PS	PS	PS	-	-
		-	-	-	MB	MB	-
		ISO	ISO	ISO	ISO	ISO	ISO

	Strat Col No.						
	Sample No.	WA1.08	WA2.01	WA2.02	WA2.03	WA2.04	WA3.02
Bioclasts	**Tot Bioclasts %**	40	50	50	65	60	60
	Bivalves	VC	C	C	A	C	VC
	Barnacles	C	VC	VC	C	VC	C
	Brachiopods	-	-	-	-	-	R
	Bryozoans	R	-	R	-	S	R
	Echinoderms	S	S	S	-	R	S
	Calc red algae	-	-	-	-	-	-
	Benthic forams	R	R	R	S	S	S
	Planktic forams	R	R	R	R	S	S
	Size: Max	0.8	20	4	5	4	4
	Mode 1	0.8	3	0.4	1	0.8	0.5
	Mode 2	0.2	1.5	1.8	0.6	2.5	1.8
	Sorting	M-W	P	W	M-W	M	P
	Abrasion	WA	WA	WA	WA	WA	WA
Siliciclasts	**Tot Terrigenous %**	1	5	5	1	1	3
	Quartz	R	S	S	R	R	S
	Feldspar	R	S	S	R	R	S
	Rock fragments	-	-	-	-	-	-
	Mica	-	-	-	-	-	-
	Clay	-	-	-	-	-	-
	Size: Max	0.3	0.4	0.5	0.4	0.3	0.6
	Mode 1	0.2	0.3	0.2	0.1	0.2	0.2
	Mode 2	-	-	-	-	-	-
	Sorting	M	W	W	W	WA	W
	Shape	A-SA	SR-R	SR-R	R	SA-SR	SR-R
Authigenic	**Tot Authigenic %**	2	<1	5	1	1	2
	Glauconite pellets	S	R	S	R	R	S
	Size (av.)	0.3	0.3	0.3	0.3	0.3	0.3
	Glauconite infills	-	-	-	R	-	R
	Pyrite grains	S	-	R	R	R	-
	Size (av.)	0.3	-	0.2	-	0.2	-
	Pyrite infills	R	-	-	-	-	-
Diagenetic	**Matrix-Cement %**	37	25	20	28	23	25
	Intrinsic material	SM	S	S	S	S	S
	Extrinsic material	S	SM	SM	SM	SM	SM
	Spar cement	25	22	17	25	20	20
	Micrite	12	3	3	3	3	5
	Porosity %	20	20	20	5	15	10
	Other features	NEO	NEO	ISO	ISO	MB	ISO
			PS			ISO	PS
		MB	ISO				
		ISO					

	Strat Col No.						
	Sample No.	WA3.04	H1.01	H1.02	H1.05	H1.06	H1.07
Bioclasts	**Tot Bioclasts %**	60	5	30	50	5	30
	Bivalves	C	-	-		S	M
	Barnacles	VC	S	C	C	S	M
	Brachiopods	R	-	-	-	VC	-
	Bryozoans	S	-	-	-	-	-
	Echinoderms	S	R	R	R	S	R
	Calc red algae	-	-	-	-	-	R
	Benthic forams	S	S	S	S	R	R
	Planktic forams	S	R	S	S	R	R
	Gstropods		-	-	-	-	S
	Size: Max	7	3	3	10	0.9	6.6
	Mode 1	0.5	0.5	0.5	1.5	0.2	2.4
	Mode 2	1.5	0.3	0.2	0.5	-	1
	Sorting	M	P	P	P	W	M
	Abrasion	WA	WA	M-WA	WA	M-WA	M-WA
Siliciclasts	**Tot Terrigenous %**	3	50	50	15	50	50
	Quartz	S	A	VC	C	C	M
	Feldspar	S	M	C	R	VC	VC
	Rock fragments	-	R	R	R	-	M
	Mica	-	-	-	-	-	-
	Clay	-	-	-	-	-	-
	Size: Max	0.5	0.3	0.2	0.4	0.2	0.8
	Mode 1	0.3	0.1	0.1	0.1	0.1	0.1
	Mode 2	0.05	0.1	-	-	-	0.6
	Sorting	M	W	EW	W	EW	W
	Shape	SR-R	SR	SR-R	R	R	R
Authigenic	**Tot Authigenic %**	2	10	10	30	10	10
	Glauconite pellets	S	M	M	M	M	S
	Size (av.)	0.3	0.1	0.2	0.2	0.3	0.1
	Glauconite infills	R	S	S	-	S	S
	Pyrite grains	-	S	S	S	S	S
	Size (av.)	-	0.1	0.8	0.8	0.3	0.1
	Pyrite infills	-	-	-	-	S	R
Diagenetic	**Matrix-Cement %**	25	35	10	5	35	10
	Intrinsic material	SM	M	M	M	M	SM
	Extrinsic material	SM	SM	SM	M	M	SM
	Spar cement	15	5	4	-	5	8
	Micrite	10	30	6	5	30	2
	Porosity %	10	<1	<1	1	<1	<1
	Other features	MB	-	NEO	NEO	-	NEO
		ISO	-	-	PS	-	PS
		PS	MB	-	MB	-	MB
			-	-	-	-	L

	Strat Col No.						
	Sample No.	H1.08	T1.01	T1.02	T2.01	T2.02	11.01
Bioclasts	**Tot Bioclasts %**	10	20	15	10	40	10
	Bivalves	M	S	S	S	VC	-
	Barnacles	R	M	S	S	M	R
	Brachiopods	-	R	S	-	-	-
	Bryozoans	-	R	-	R	R	E
	Echinoderms	-	R	S	-	-	-
	Calc red algae	-	-	-	-	-	-
	Benthic forams	R	R	R	S	S	S
	Planktic forams	-	R	S	S	S	S
		-	-				
	Size: Max	3.7	3	1.2	1.8	2	0.3
	Mode 1	1.7	1	1	0.5	1	0.25
	Mode 2	0.8	0.4	0.5	0.2	0.5	-
	Sorting	M	P	P	P	W	W
	Abrasion	M-WA	MA	UA	M-WA	WA	W
Siliciclasts	**Tot Terrigenous %**	50	45	20	10	20	50
	Quartz	VC	S	S	M	C	M
	Feldspar	C	C	M	S	S	VC
	Rock fragments	-	M	-	-	-	-
	Mica	-	-	-	-	-	-
	Clay	-	C	-	-	-	-
	Other						
	Size: Max	0.3	1	0.6	0.3	1	0.3
	Mode 1	0.1	0.3	0.3	0.1	0.1	0.1
	Mode 2	-	0.1	0.2	0.07	0.2	0.2
	Sorting	EW	M	M	M	M-W	W
	Shape	WA	SA-SR	SA-SR	SR-R	SA-SR	SA-SR
Authigenic	**Tot Authigenic %**	20	20	40	20	10	15
	Glauconite pellets	S	M	VC	M	S	M
	Size (av.)	0.2	0.7	0.8	0.2	0.2	0.3
	Glauconite infills	S	S	S	M	S	S
	Pyrite grains	S	S	S	S	S	S
	Size (av.)	0.1	0.12	0.2	0.1	0.2	0.1
	Pyrite infills	-	S	R	S	R	-
Diagenetic	**Matrix-Cement %**	20	5	20	60	30	25
	Intrinsic material	SM	SM	MS	MS	MS	MS
	Extrinsic material	SM	SM	MS	MS	MS	-
	Spar cement	15	4	7	10	2	20
	Micrite	5	1	3	50	28	5
	Porosity %	<1	10	5	<1	<1	<1
	Other features	NEO	NEO	NEO	-	-	NEO
		PS	PS	PS	-	-	PS
		MB	MB	MB	-	-	MB
		L	L	L	L	-	L

	Strat Col No.						
	Sample No.	11.02	11.03	MA1.01	MA1.02	KO1.01	KO1.02
Bioclasts	**Tot Bioclasts %**	30	25	50	50	50	50
	Bivalves	S	M	S	S	C	C
	Barnacles	S	S	-	-	VC	VC
	Brachiopods	C	S	-	-	-	-
	Bryozoans	-	S	M	MA	S	S
	Echinoderms	S	S	S	S	S	S
	Calc red algae	-	-	-	-	-	-
	Benthic forams	C	M	M	MA	R	R
	Planktic forams	S	M	M	M	R	R
	Size: Max	4.8	4	1.5	3.8	7	5
	Mode 1	2.25	0.9	0.4	0.6	3	1
	Mode 2	0.8	1	0.2	1.6	1	2.4
	Sorting	M-P	M-W	WS	M-W	P	M-P
	Abrasion	M-WA	WA	WA	WA	M-WA	WA
Siliciclasts	**Tot Terrigenous %**	40	40	5	5	10	10
	Quartz	M	C	S	S	S	S
	Feldspar	C	C	S	S	S	S
	Rock fragments	M	-	-	-	-	-
	Mica	-	-	-	-	-	-
	Clay	-	S	-	-	-	-
			H				
	Size: Max	0.9	0.8	0.3	0.4	0.5	0.6
	Mode 1	0.3	0.5	0.1	0.3	0.2	0.3
	Mode 2	0.2	0.4	-	0.1	0.1	0.2
	Sorting	M-W	WA	WS	M-W	M-W	M-W
	Shape	SA-SR	SA-SR	A-SA	SA-SR	SR	SA-SR
Authigenic	**Tot Authigenic %**	20	30	10	10	20	10
	Glauconite pellets	S	C	M	M	C	M
	Size (av.)	0.25	C	0.2	0.3	0.3	0.4
	Glauconite infills	M	-	S	S	S	S
	Pyrite grains	S	S	R	R	R	S
	Size (av.)	0.1	0.2	0.1	0.08	0.1	0.5
	Pyrite infills	-	S	R	R	R	R
Diagenetic	**Matrix-Cement %**	10	5	35	35	10	15
	Intrinsic material	MS	M	SM	S	MS	SM
	Extrinsic material	M	M	SM	SM	MS	SM
	Spar cement	9	1	30	30	3	13
	Micrite	1	4	5	5	7	2
	Porosity %	<1	<1	<1	<1	10	15
	Other features	-	NEO	-	-	NEO	NEO
		-		-	-	PS	PS
				-	-	MB	MB
		-		-	-	-	-

	Strat Col No.						
	Sample No.	P1.02	P1.03	P1.04	P1.05	M1.01	M1.02
Bioclasts	**Tot Bioclasts %**	40	30	40	40	50	40
	Bivalves	S	S	C	C	VC	S
	Barnacles	S	S	M	M	C	C
	Brachiopods	R	-	-	-	R	-
	Bryozoans	R	R	S	S	S	S
	Echinoderms	-	R	S	S	S	R
	Calc red algae	-	-	-	-	-	-
	Benthic forams	C	M	M	M	R	R
	Planktic forams	M	M	M	M	R	R
	Size: Max	1.5	3	2	2	5	5
	Mode 1	0.4	0.3	0.2	0.2	0.6	1.6
	Mode 2	0.3	-	0.3	0.3	2	2.4
	Sorting	M-W	M-W	W	W	P	P
	Abrasion	WA	WA	WA	WA	M	M
Siliciclasts	**Tot Terrigenous %**	20	30	10	11	5	10
	Quartz	S	M	S	S	S	S
	Feldspar	M	C	S	S	S	S
	Rock fragments	-	-	-	-	R	R
	Mica	-	-	-	-	-	-
	Clay	-	-	-	-	-	-
	Size: Max	0.4	0.5	0.5	0.5	2	2.4
	Mode 1	0.2	0.2	0.2	0.2	0.2	0.3
	Mode 2	-	0.1	-	-	0.5	0.4
	Sorting	W	MW	MW	W	M	M-W
	Shape	R	SA-SR	SA-SR	SA-SR	SA-SR	SR
Authigenic	**Tot Authigenic %**	10	15	10	10	10	10
	Glauconite pellets	S	M	M	M	S	S
	Size (av.)		0.2	0.2	1.2	0.4	0.4
	Glauconite infills	M	S	R	R	S	S
	Pyrite grains	S	S	S	S	R	R
	Size (av.)	0.2	0.2	0.2	1.2	0.2	0.2
	Pyrite infills	-	-	R	R	-	-
Diagenetic	**Matrix-Cement %**	30	25	40	40	20	30
	Intrinsic material	MS	MS	S	S	SM	SM
	Extrinsic material	M	MS	SM	SM	SM	SM
	Spar cement	5	5	35	35	12	25
	Micrite	25	20	5	5	8	5
	Porosity %	-	-	-	-	15	10
	Other features	NEO	NEO	NEO	NEO	NEO	NEO
		-	PS	PS	PS	PS	PS
		-	MB	MB	MB	-	MB
		L	L			-	L

	Strat Col No.						
	Sample No.	PA1.03	TRIG1	RA/OP	RA/TA	R1.02	KA1.01
Bioclasts	**Tot Bioclasts %**	20	30	45	40	60	50
	Bivalves	-	S	S	S	VC	S
	Barnacles	-	C	S	C	C	S
	Brachiopods	-	-	VC	-	RS	-
	Bryozoans	-	S	-	S	S	S
	Echinoderms	-	S	S	R	S	S
	Calc red algae	-	-	-	-	-	-
	Benthic forams	C	S	R	S	S	S
	Planktic forams	M	S	R	S	S	C
	Size: Max	1.4	2.25	>2.5	1.3	>2.5	3.4
	Mode 1	0.2	0.7	1.5	0.5	0.4	0.3
	Mode 2	-	1	2	-	0.2	0.1
	Sorting	EW	M-W	P	W	P	W
	Abrasion	R	WA	W	WA	W	MA
Siliciclasts	**Tot Terrigenous %**	50	10	20	20	5	10
	Quartz	M	S	M	S	S	S
	Feldspar	VC	M	S	M	S	M
	Rock fragments	-	-	S	-	-	-
	Mica	-	-	-	R	-	-
	Clay	-	-	-	-	-	-
	Size: Max	0.4	0.6	0.7	0.5	0.6	0.3
	Mode 1	0.1	0.2	0.4	0.1	0.3	0.2
	Mode 2	-	0.4	0.1	0.3	-	0.1
	Sorting	EW	P	W	P	P-M	W
	Shape	WA	A-SA	SR-R	SA-SR	A	SA-SR
Authigenic	**Tot Authigenic %**	20	20	10	20	1	15
	Glauconite pellets	C	C	-	M	R	M
	Size (av.)	0.2	0.4	-	0.3	0.1	0.2
	Glauconite infills	S	S	-	M	R	R
	Pyrite grains	S	R	-	R	R	S
	Size (av.)	0.2	0.1	-	0.1	0.1	0.1
	Pyrite infills	R	R	-	-	R	R
Diagenetic	**Matrix-Cement %**	10	35	10	20	33	20
	Intrinsic material	MS	SM	M	M	MS	SM
	Extrinsic material	MS	SM	-	M	MS	SM
	Spar cement	1	30	-	<5	10	15
	Micrite	9	5	10	15	23	5
	Porosity %	<1	5	<1	-	<1	5
	Other features			H. L		BIOM	NEO
						-	-
						-	-
						-	-

	Strat Col No.						
	Sample No.	KA1.02	M10.03	M10.04	M10.05	M10.06	M10.11
Bioclasts	**Tot Bioclasts %**	51	55	45	40	50	30
	Bivalves	S	C	C	C	S	M
	Barnacles	S	C	C	C	R	C
	Brachiopods	-	S	-	-	R	M
	Bryozoans	S	S	S	S	S	-
	Echinoderms	S	S	S	R	S	-
	Calc red algae	-	-	-	-	-	-
	Benthic forams	S	S	S	S	C	S
	Planktic forams	C	S	R	R	C	S
	Size: Max	4.4	6	5	6	0.5	3
	Mode 1	1.3	1.5	2.3	3	0.25	0.75
	Mode 2	1.1	0.8	0.8	1	0.15	1.5
	Sorting	W	M	P	P	M-W	M
	Abrasion	MA	WA	M-WA	WA	WA	WA
Siliciclasts	**Tot Terrigenous %**	11	10	5	10	20	28
	Quartz	S	M	S	M	M	M
	Feldspar	M	S	S	S	S	M
	Rock fragments	-	-	-	-	-	R
	Mica	-	R	-	-	R	R
	Clay	-	-	-	R	-	-
	Size: Max	1.3	0.5	0.2	0.5	0.2	0.5
	Mode 1	1.2	0.3	0.1	0.25	0.13	0.2
	Mode 2	1.1	0.13	-	0.1	0.08	0.1
	Sorting	W	M	W	M	M	W
	Shape	SA-SR	SA-SR	SA-SR	SA-SR	SA-SR	SA-SR
Authigenic	**Tot Authigenic %**	16	10	15	5	5	20
	Glauconite pellets	M	M	S	S	S	M
	Size (av.)	1.2	0.4	0.2	0.2	0.3	0.25
	Glauconite infills	R	R	M	R	R	M
	Pyrite grains	S	R	S	-	R	S
	Size (av.)	1.1	0.25	0.01	-	0.18	0.12
	Pyrite infills	R	-	-	-	-	R
Diagenetic	**Matrix-Cement %**	21	15	25	20	25	20
	Intrinsic material	SM	SM	MS	S	SM	SM
	Extrinsic material	SM	SM	SM	S	SM	SM
	Spar cement	16	12	15	20	20	15
	Micrite	6	3	10	0	5	5
	Porosity %	6	10	10	25	<1	2
	Other features	NEO					
		-					
		-					
		-					

	Strat Col No.						
	Sample No.	M10.12	M10.14	M10.15	M10.18	H10.02	H10.03
Bioclasts	**Tot Bioclasts %**	60	25	20	60	40	30
	Bivalves	C	S	S	VC	M	M
	Barnacles	VC	-	S	C	M	M
	Brachiopods	M	-	-	S	M	M
	Bryozoans	M	-	R	S	S	S
	Echinoderms	S	-	S	S	S	S
	Calc red algae	-	-	-	-	-	-
	Benthic forams	S	M	M	S	S	S
	Planktic forams	R	M	M	S	S	S
	Size: Max	4.4	1.6	1.5	3.4		
	Mode 1	0.2	0.2	0.6	1	10	1.5
	Mode 2	0.6	-	0.1	0.25	1.25	0.5
	Sorting	M	W	W	M	P	P
	Abrasion	WA	WA	WA	WA	WA	WA
Siliciclasts	**Tot Terrigenous %**	5	45	50	5	30	40
	Quartz	S	C	VC	S	C	C
	Feldspar	S	C	C	S	S	M
	Rock fragments	-	-	-	-	-	-
	Mica	R	S	S	R	R	R
	Clay	-	-	-	-	-	-
	Size: Max	1.2	0.25	0.3	0.25	0.4	0.3
	Mode 1	0.5	0.12	0.18	0.13	0.25	0.12
	Mode 2	0.12	0.08	0.1	0.8	0.12	0.05
	Sorting	M	W	M-W	W	M	M-W
	Shape	SA-SR	SA-SR	SA-SR	SA-SR	SA-SR	SA-SR
Authigenic	**Tot Authigenic %**	5	20	15	15	5	10
	Glauconite pellets	S	S	M	M	S	S
	Size (av.)	0.7	0.12	0.25	0.25	0.4	0.12
	Glauconite infills	S	M	M	S	S	M
	Pyrite grains	R	M	R	S	-	R
	Size (av.)	0.12	0.08	0.1	0.12	-	0.8
	Pyrite infills	-	-	-	-	-	-
Diagenetic	**Matrix-Cement %**	15	10	15	20	25	20
	Intrinsic material	SM	M	SM	SM	MS	MS
	Extrinsic material	SM	M	-	SM	MS	MS
	Spar cement	12	1	12	15	5	1
	Micrite	3	9	3	5	20	9
	Porosity %	15	<1	<1	<1	<1	<1
	Other features						

Field sample No.	University of Waikato sample No.	Grid reference NZMG
W1.02	W2011 1100	X19/981449
W1.03	W2011 1101	X19/981449
W1.04	W2011 1102	X19/981449
W1.05	W2011 1103	X19/981449
W1.06	W2011 1104	X19/981449
W1.07	W2011 1105	X19/981449
W1.08	W2011 1106	X19/981449
W2.01	W2011 1107	X19/981448
W2.02	W2011 1108	X19/981448
W2.03	W2011 1109	X19/981448
W2.04	W2011 1110	X19/981448
W3.02	W2011 1111	X19/981448
W3.04	W2011 1112	X19/981448
H1.01	W2011 1113	X18/099658
H1.02	W2011 1114	X18/099658
H1.05	W2011 1115	X18/099658
H1.06	W2011 1116	X18/099658
H1.07	W2011 1117	X18/099658
H1.08	W2011 1118	X18/099658
T1.01	W2011 1119	X19/062452
T1.02	W2011 1120	X19/062452
T2.01	W2011 1121	X19/061451
T2.02	W2011 1122	X19/061451
11.01	W2011 1123	X18/033651
11.02	W2011 1124	X18/033651
11.03	W2011 1125	X18/033651
MA1.01	W2011 1126	X18/026539
MA1.02	W2011 1127	X18/026539
KO1.01	W2011 1128	X19/041468
KO1.02	W2011 1129	X19/041468
P1.02	W2011 1130	X18/037550
P1.03	W2011 1131	X18/037550
P1.04	W2011 1132	X18/037550
P1.05	W2011 1133	X18/037550
M1.01	W2011 1134	X19/041468
M1.02	W2011 1135	X19/041468
PA1.03	W2011 1136	X18105588
TRIG1	W2011 1137	X18/090528
RA/OP	W2011 1138	X18/958577
RA/TA	W2011 1139	X18/996545
R1.02	W2011 1140	X19/029429
KA1.01	W2011 1141	X19/959421
KA1.02	W2011 1142	X19/959421
M10.03	W2011 1143	X19/041468
M10.04	W2011 1144	X19/041468
M10.05	W2011 1145	X19/041468
M10.06	W2011 1146	X19/041468
M10.11	W2011 1147	X19/041468
M10.12	W2011 1148	X19/041468
M10.14	W2011 1149	X19/041468
M10.15	W2011 1150	X19/041468
M10.18	W2011 1151	X19/041468
H10.02	W2011 1152	X18/099658
H10.03	W2011 1153	X18/099658